Investigating Changes in Mercury Concentrations in Small-Bodied Fishes Following Mine-Related Flooding in the Canadian Arctic

by

Noel Soogrim

A thesis

presented to the University of Waterloo

in fulfilment of the

thesis requirements for the degree of

Master of Science

in

Biology

Waterloo, Ontario, Canada, 2025

© Noel Soogrim 2025

Author's Declaration

I hereby declare that I am the sole author of this thesis. This is a true copy of the thesis, including required final revisions, as accepted by my examiners. I understand that my thesis may be made electronically available to the public.

Abstract

Mercury (Hg) is a globally distributed contaminant that, in its methylated form (methyl mercury (MeHg)), is a potent neurotoxin that bioaccumulates and biomagnifies in aquatic food webs. At high enough exposures, Hg can pose risks to wildlife and human health. While Hg concentrations in aquatic ecosystems have been relatively well-studied in boreal systems, less research has been conducted in Arctic freshwater ecosystems, particularly in Barrenland tundra lakes that are increasingly affected by industrial activity and climate-driven change. This thesis examined the effects of a mine-related flooding event at the Amaruq project site in Nunavut, Canada, on aqueous and biological concentrations of Hg in a series of shallow Arctic lakes. Concentrations of total mercury (THg) and methyl mercury (MeHg) in water, indicators of organic matter (OM) quantity and quality in water, including concentrations of dissolved organic carbon (DOC), humification index (HIX), and specific ultraviolet absorbance (at 254 nm; SUVA) and concentrations of Hg in the tissues of Slimy Sculpin (*Cottus cognatus*) and Ninespine Stickleback (*Pungitius pungitius*), were compared: 1) before and after flooding in impacted lakes; and, 2) between flooded and reference lakes in the post-flood years. A series of potential covariates of fish Hg concentrations, including fish age, condition, C: N, $\delta^{13}C$, and $\delta^{15}N$, were also compared between pre- and post-flood years and between flooded and reference lakes.

Aqueous concentrations of THg and MeHg were significantly higher in flooded lakes compared to reference lakes (THg filtered: $p = 0.01$; MeHg filtered: $p < 0.001$) in post-flood years. In flooded lakes, concentrations of THg and MeHg were significantly higher in post-flood years compared to pre-flood years ($p < 0.05$) whereas there were no significant differences among years in reference lakes ($p > 0.28$). Concentrations of DOC were significantly higher in flooded lakes than in reference lakes in post-flood years ($p < 0.001$), suggesting increased terrestrial OM inputs. Higher MeHg concentrations and higher % MeHg in water in flooded lakes relative to reference lakes in post-flood years may indicate that terrestrial OM inputs increased net Hg methylation rates, but there was no difference in % MeHg between pre- and post-flood years in the flooded lakes ($p < 0.05$). Evidence for enhanced methylation post-flood is thus mixed, and more research is necessary.

Fish tissue Hg concentrations were significantly higher in flooded lakes than in reference lakes in the post-flood years for both Slimy Sculpin ($p < 0.001$ in 2020 and 2021) and Ninespine Stickleback ($p = 0.002$ in 2021). Within flooded lakes, tissue Hg concentrations in both species were significantly higher in the post-flood years relative to pre-flood years (Slimy Sculpin: $F_{3,261.71} = 14.53$, $p < 0.001$; Ninespine Stickleback: $F_{3,11.06} = 33.96$, $p < 0.001$). Flooding-induced increases in fish Hg concentrations appeared to be most closely related to concomitant decreases in $\delta^{13}C$; $\delta^{13}C$ ratios were significantly more depleted in post-flood years (Slimy Sculpin: $F_{3,315.28} = 20.11$, $p < 0.0001$; Ninespine Stickleback: $F_{3,367.33} = 5.38$, $p =$

0.001) compared to pre-flood years, and were negatively correlated with fish Hg concentrations (Slimy Sculpin: r = -0.72; Ninespine Stickleback: r = -0.63). These results suggest a shift in basal carbon sources, likely reflecting increased reliance on terrestrially derived, allochthonous OM. The strong correlation between $\delta^{13}C$ and Hg concentrations indicates that OM dynamics played a central role in driving Hg bioaccumulation in the food web. Other potential covariates of fish Hg concentrations, including relative condition, C:N ratio, and length-at-age, explained less variation in Hg concentrations and/or did not appear to be affected by flooding, although weak negative correlations between Hg concentrations and condition were observed.

While the general patterns observed in this study align with findings from boreal systems subjected to flooding, it is possible that Arctic lakes are uniquely vulnerable to flooding-induced Hg mobilization and increases in fish Hg concentrations due to their low productivity and catchments with permafrost. These characteristics may increase the release of OM and Hg during flooding and increase bioaccumulation of newly released Hg. Despite limitations in sampling design and data availability, results of this study provide the first empirical evidence linking industrial flooding to increases in Hg concentrations in Arctic lakes. Results underscore the need for long-term contaminant monitoring in remote tundra regions where climate warming, industrial development, and permafrost degradation are expected to intensify. Given the cultural importance of fish for northern communities, understanding how environmental disturbances affect Hg bioaccumulation is critical for protecting both ecosystem and human health in the Arctic.

Acknowledgements

I would first like to express my deepest gratitude to my supervisor and mentor, Dr. Heidi Swanson, for her unwavering support, guidance, and belief in me throughout the course of this thesis. Her mentorship has been instrumental in the success and formation of this project, and I am truly grateful for the encouragement she provided during both the high points and the inevitable challenges that arose along the way. I am also sincerely thankful to my graduate committee members, Dr. Mark Servos and Dr. Mark Hanson, for their thoughtful insights, valuable feedback, and continued guidance. Their expertise greatly enriched the quality and direction of this research. Special thanks are owed to Kirsten Nikel, whose tireless organization, technical skill, and steadfast support were critical during every phase of this project. I am incredibly appreciative of the effort and care she put into helping make this research possible. I would like to thank Bronte McPhedran for their years of dedicated assistance in collecting field data in the demanding and remote conditions of the high Arctic. Their commitment and perseverance were fundamental to the success of the field program. Thank you to Amy Nguyen for her invaluable assistance with data management, responding to data inquiries, overseeing lab operations, and supporting numerous last-minute requests. I am grateful for everything you did to help make this work possible. To the members of the Swanson Lab, thank you for your encouragement, and the collaborative spirit that made this journey both productive and enjoyable. I also gratefully acknowledge Agnico Eagle Mines Limited (Meadowbank Mine) for their collaboration and support in facilitating project implementation, including logistical coordination and site access. Heartfelt thanks to my family and friends for their constant encouragement and kind words throughout all the challenges, your support helped keep me grounded and moving forward. Finally, I extend my appreciation to the broader community of researchers, staff, and colleagues who contributed to the development and execution of this work. This thesis would not have been possible without the combined efforts and generosity of many. Funding for this project was provided by Agnico Eagle Mines Ltd, Natural Sciences and Engineering Research Council (CRD to Jamieson, DG and NRS to Swanson), Northern Scientific Training Program, Canada First Research Excellence Fund (Northern Water Futures), and University of Waterloo.

Table of Contents

Author's Declaration ..... **ii**
Abstract ..... **iii**
Acknowledgements ..... **v**
Table of Contents ..... **vi**
List of Figures ..... **viii**
List of Tables ..... **x**
List of Abbreviations ..... **xi**
Chapter 1: Introduction **1**
1.1 Background 1
1.2 Effects of Flooding on Mercury in Aquatic Ecosystems 2
1.3 Factors that Influence Mercury Concentrations in Fish 5
1.4 Industrial Development in the Arctic 6
1.4.1 Monitoring Industrial Impacts in Aquatic Environments 8
1.5 Local Context and Study Area 9
1.6 Study Objectives 10
Chapter 2: Methods **12**
2.1 Study Area 12
2.1.1 Industrial Development and Flooding 14
2.1.2 Study Constraints 15
2.2 Sample Collection 16
2.3 Sample Preparation 17
2.4 Laboratory Analysis 18
2.5 Data Analysis 19
2.5.1 Analyses of Fish Tissue - Mercury 20
2.5.2 Analysis of Fish Tissue – Covariates 21
2.5.3 Water Chemistry 23
Chapter 3: Results **24**
3.1 Water Chemistry 24
3.1.1 Comparisons of [Hg] in water among years and between flooded and reference lakes 24
3.2 Analyses of Fish Tissue 25
3.2.1 Slimy Sculpin 26

3.2.2 Ninespine Stickleback 33
3.3 Additional Water Chemistry Analyses 39
Chapter 4: Discussion 41
4.1 Conclusions 49
4.2. Future Directions 50
References 52
Appendices 61
Appendix A: Water Chemistry Sample Preparation 61
Appendix A: Figures 62
Appendix A: Tables 86

List of Figures

Figure 1: The location of Agnico's two gold mining facilities relative to Baker Lake, located in the Kivalliq District, Nunavut, Canada. The well-established, operational Meadowbank facility and the now operational Amaruq Satellite Deposit are shown in brown. The location of the Whale Tail Pit Project is within the Amaruq Mine facility. 13

Figure 2: Outline of the waterbodies impacted by the Whale Tail Pit Project. The flooded lakes are outlined with a yellow dotted line, representing the pre-flood (2018) conditions. The lakes outlined with a green dotted line are the reference lakes. The orange solid line represents the flood zone following the construction of the Whale Tail Dam (which is represented by a white bar), representing the post-flood (2019 to 2021) conditions. The brown outlined areas indicate the locations of industrial infrastructure. Blue arrows indicate flow direction. 14

Figure 3: Log_{10} dry Hg concentrations for Slimy Sculpin and Ninespine Stickleback collected at flooded and reference lakes from 2018 to 2021. Boxplots indicate the median, 25^{th} and 75^{th} percentiles, and minimum and maximum values within 1.5x the interquartile range. All individual data points are plotted. Flooding occurred in 2019. (Note, one Slimy Sculpin with very low Hg concentration was removed from Lake B03, 2021). 26

Figure 4: Log_{10} dry Hg concentrations in (a) flooded and (b) reference lakes from 2018 to 2021. Boxplots show data for each waterbody. Black diamonds and error bars depict estimated marginal mean Hg concentrations ± standard error at a fork length of 48 mm in each exposure category. Significant pairwise differences are indicated by dissimilar letters. 27

Figure 5: Log_{10} dry Hg concentrations in Slim Sculpin at flooded and reference lakes in (a) 2020 and (b) 2021. Boxplots show data for each waterbody. Black diamonds and error bars depicted estimated marginal mean Hg concentrations ± standard error at a fork length of 48 mm for each exposure category. Hg concentration was significantly higher in flooded lakes than reference lakes in both 2020 and 2021 (2020: $F_{1,132.5}$=25.89, $p < 0.001$; 2021: $F_{1,90.9} = 37.89$, $p < 0.001$). 29

Figure 6: $\delta^{13}C$ in Slimy Sculpin at (a) flooded lakes and (b) reference lakes from 2018 to 2021. Boxplots show data for each waterbody. Black diamonds and error bars depict estimated marginal mean for $\delta^{13}C$ ± standard error for each year. Significant pairwise differences between years are indicated by different letters. 30

Figure 7: Relative condition in Slimy Sculpin at (a) flooded lakes and (b) reference lakes from 2018 to 2021. Boxplots show data for each waterbody. Black diamonds and error bars depict estimated marginal mean relative condition ± standard error for each year. Significant pairwise difference between years are

indicated by different letters. (Note, flooded lakes were analyzed with a LMEM, whereas reference lakes could not be analyzed with a LMEM so were analyzed with an ANCOVA without random effects). 32
Figure 8: $\delta^{13}C$ in Slimy Sculpin from flooded and reference lakes in post-flood years (a) 2020 and (b) 2021. Boxplots show data for each waterbody. Black diamonds and error bars depict estimated marginal mean $\delta^{13}C \pm$ standard error for each year at a fork length of 48 mm. $\delta^{13}C$ was significantly more depleted in flooded lakes ($F_{>1,3.99} > 13.662$, $p < 0.019$) in 2020. In 2021, the omnibus test showed a significant difference in $\delta^{13}C$ between flooded and reference lakes, but at a fork length of 48 mm, there was no significant difference..... 33
Figure 9: Log_{10} dry Hg concentrations for Ninespine Stickleback between 2018 and 2021 in flooded lakes. Black diamonds and error bars show estimated marginal means ± standard error calculated at a fork length of 50 mm. 34
Figure 10: Log_{10} dry Hg concentration for Ninespine Stickleback at flooded and reference lakes in 2021. Boxplots show data for each lake. Black diamonds and error bars show estimated marginal means ± standard error calculated at a fork length of 50 mm. Mercury concentrations in Ninespine Stickleback from flooded lakes were significantly higher than Hg concentrations in Ninespine Stickleback from reference lakes ($F_{1,4.13} = 45.14$, $p = 0.002$)..... 35
Figure 11: $\delta^{13}C$ for Ninespine Stickleback between 2018 and 2021 in flooded lakes. Black diamonds and error bars show estimated marginal means $\delta^{13}C \pm$ standard error calculated at a fork length of 50 mm. .. 37
Figure 12: Relative condition for Ninespine Stickleback between 2018 and 2021 at flooded lakes. Boxplots show data for each lake. Black diamonds and error bars show estimated marginal mean relative condition factor ± standard error calculated at a fork length of 50 mm..... 38

List of Tables

Table 1: Summary of sampling that occurred pre – (2018) and post-flooding (2019 to 2021) at each of the study lakes. “C” and green shading indicate samples were collected. “NC” and blue shading indicate samples that were not collected. 16

Table 2: Mean values for [MeHg], %MeHg, and [THg] categorized by pre-flood (2018) and post-flood (2020 and 2021) years, and by exposure type (reference or flooded) of the study lakes. Data are presented as mean (standard deviation). Units are ng/L. NA indicates data is not available. No data were available for any parameter listed in 2019 (contamination issue). 25

Table 3: Results of Pearson’s correlation analyses between [Hg] Slimy Sculpin tissue and each of several statistically significant covariates in flooded lakes (all years of data included)..... 29

Table 4: Results of Pearson’s correlation analyses between [Hg] in Ninespine Stickleback tissue and each of several statistically significant covariates in flooded lakes (all years of data included). 36

Table 5: Mean water chemistry values for DOC, HIX 1999, HIX 2002, and SUVA, categorized by pre-flood (2018) and post-flood (2020 to 2021) years, and by the exposure type (reference or flooded) of the study lakes. Data are presented as mean (standard deviation). NA indicates data is not available. No data were available for any parameter listed in 2019 (contamination issue). 40

List of Abbreviations

A20 – Lake A20

A44 – Lake A44

A63 – Lake A63

A65 – Lake A65

AAE – AAE Tech Incorporated

Agnico Eagle – Agnico Eagle Mines Limited

ALTER – Arctic Long-Term Ecological Research

AMAP – Arctic Monitoring Assessment Program

ANCOVA – Analysis of Covariance

B03 – Lake B03

BACI – Before-After-Control-Impact

CALA – Canadian Association for Laboratory Accreditation

CFIRMS – Continuous Flow Isotope Ratio Mass Spectrometer

C: N – Carbon-to-Nitrogen Ratio

CREMP – Core Receiving Environmental Monitoring Program

CPUE – Catch-Per-Unit-Effort

DOC – Dissolved Organic Carbon

[DOC] – Dissolved Organic Carbon Concentration

DOM – Dissolved Organic Matter

Dw – Dry weight

EEM – Environmental Effects Monitoring

EPA – Environmental Protection Agency

G – Grams

HCl – Hydrochloric Acid

Hg (0) – Gaseous Elemental Mercury

Hg^{2+} – Oxidized Mercury

Hg – Mercury

[Hg] – Mercury Concentration

$HgCl^2$ – Mercuric Chloride

HgO – Mercuric Oxide

HgS – Mercuric Sulfide

HIX – Humification Indices

HSD – Honestly Significant Difference

Kn – Relative Condition

L – Length

LK8 – Lake 8

LMEM – Linear Mixed Effects Model

Mbar – Millibar

MDMER – Metal and Diamond Mining Effluent Regulations

MeHg – Methyl Mercury

[MeHg] – Methyl Mercury Concentration

mL – Milliliter

mm – Millimeter

OM – Organic Matter

PETG – Polyethylene Terephthalate Glycol-modified

QA/QC – Quality Assurance / Quality Control

REML – Restricted Maximum Likelihood

RPD – Relative Percent Difference

SUVA – Specific Ultraviolet Absorbance

USA – United States of America

VPDB – Vienna Pee Dee Belemnite

W – Weight

WTL – Whale Tail Lake South

α – Alpha

δ – Delta

δ^{13}C – Stable Isotope Ratios of Carbon

δ^{15}N – Stable Isotope Ratios of Nitrogen

‰ – Per Mill

%C – Percent Carbon

%N – Percent Nitrogen

Chapter 1: Introduction

1.1 Background

Mercury (Hg) is a naturally occurring metal that can be released into the atmosphere through both natural processes (e.g., volcanic eruptions) and human activities (e.g., cement production, small-scale gold mining) (AMAP, 2019; Burke, 2019; Lewis, 2018; Schroeder, 1998). Once in the atmosphere, gaseous elemental Hg (Hg (0)) has a long residence time (0.7 to 1.4 years), which allows it to travel vast distances, including to remote areas (AMAP, 2011; Burke, 2019; Schroeder, 1998). Atmospherically transported Hg can be deposited on landscapes and waterbodies, often after oxidation to Hg^{2+} (AMAP, 2011; Burke, 2019; Schroeder 1998). Gaseous elemental Hg can also be absorbed directly by plants (Obrist et al., 2017).

The Arctic acts as a "sink" for atmospheric Hg (Fitzgerald et al., 2005; French et al., 2014). Atmospheric transport accounts for nearly half of the annual Hg inputs to Arctic ecosystems (AMAP, 2011), though ocean currents, river discharge, and erosion also contribute (AMAP, 2011, Fitzgerald et al., 2005; French et al., 2014). It is primarily the oxidized form of Hg (Hg^{2+}) that is deposited on snow, ice, water, vegetation, and soils, where it can be transformed into methyl mercury (MeHg), the toxic, biomagnifying, and bioaccumulative form (AMAP, 2011). The microbial transformation of inorganic Hg (i.e., mercuric chloride [$HgCl_2$], mercuric sulfide [HgS], and mercuric oxide [HgO]) into MeHg is primarily mediated by sulfate-reducing bacteria, iron-reducing bacteria, methanogens, and some algae (Bravo et al., 2017; Hall et al., 2009; Johnston et al., 1991). Previously, methylation was thought to occur mainly in anoxic bottom sediments, but recent research suggests it can also occur in nearshore aquatic environments, terrestrial sediments (i.e., in catchments), and wetlands, where anoxic conditions and sufficient organic matter (OM) support methylating microbes (AMAP, 2011; Bravo et al., 2017; Moslemi-Aqdam et al., 2022).

Once in aquatic systems, MeHg bioconcentrates from water into lower trophic level organisms, bioaccumulates in individual organisms, and biomagnifies through food webs (e.g., Atwell et al., 1998; Boening, 2000; Clarkson, 2002; Clayden et al., 2015; Depew et al., 2013; Hammerschmidt & Fitzgerald, 2006; Kidd et al., 1995). This leads to high Hg concentrations ([Hg]) in long-lived, slow-growing, top predators, including certain fish species (Atwell et al., 1998; Boening, 2000; Clarkson, 2002; Clayden et al., 2015; Depew et al., 2013; Hammerschmidt & Fitzgerald, 2006; Kidd et al., 1995). Notably, MeHg biomagnification rates increase with latitude (see Sumner et al., 2020), making Arctic ecosystems particularly vulnerable to Hg accumulation in aquatic food webs. Studies highlight concerns over Hg contamination in Arctic fish species, particularly in lakes and rivers influenced by thawing permafrost, which can release additional Hg into aquatic ecosystems (AMAP, 2021; Schaefer et al., 2020). In Arctic freshwater food webs, fish often occupy the highest trophic level, leading to elevated [Hg] (e.g., Bilodeau

et al., 2016; Morris et al., 2022; Wheatley & Paradis 1995). Since fish are the primary food source for Indigenous communities (e.g., Moslemi-Aqdam et al., 2022) and Arctic wildlife, understanding the spatial and temporal variability of [Hg] is critical for assessing ecological and human health risks. Exposure to MeHg poses risks to both wildlife and human health. MeHg is a neurotoxin and endocrine disruptor that can impair neurological function. At high enough concentrations, exposure to MeHg can cause immunotoxic effects and fetal mortality (Tan et al., 2009). Arctic populations of humans are among the most exposed to Hg globally, due to reliance on traditional foods that can be high in MeHg (AMAP, 2021).

Climate change and industrial development are altering Hg transport and biogeochemistry in the Arctic. Melting sea ice increases Hg exchange between the ocean and atmosphere, and permafrost thaw releases previously stored "legacy" Hg (AMAP, 2011; Atwell et al., 1998; Boening, 2000; Depew et al., 2013; Laske et al., 2022; Poissant et al., 2008; Willacker et al., 2016). Permafrost soils contain significantly more Hg than non-permafrost soils; northern Canadian permafrost is estimated to store ~ 1,656 grams (g) of Hg (Schuster et al., 2018), which can be mobilized by warming temperatures and development-related disturbance. Researchers conducting studies that contribute to the Arctic Monitoring Assessment Program (AMAP) have raised concerns about increasing [Hg] in terrestrial and aquatic biota (Morris et al., 2022), and the concomitant potential health risks posed by climate change and other environmental disturbances (AMAP, 2011; Poissant et al., 2008).

1.2 Effects of Flooding on Mercury in Aquatic Ecosystems

Flooding can result from natural processes, such as heavy rainfall, melting snow, and coastal storms, as well as anthropogenic activities, including industrial operations, dam construction, and urban development. Flooding inundates vegetation, soil, woody debris, and other forms of OM. When flooded, terrestrially derived OM, including decomposing plant material, microbial biomass, and humic substances, breaks down into smaller, water-soluble organic molecules that contribute to dissolved organic carbon (DOC) in downstream aquatic ecosystems (Boening, 2000; Bravo et al., 2017; Letourneur et al., 2013; Li et al., 2020; St. Louis et al., 2004). DOC is transported via surface runoff, groundwater flow, and flooding into lakes, rivers, and wetlands (Bravo et al., 2017; Li et al., 2020; St. Louis et al., 2004). Hg, particularly in its inorganic form (Hg^{2+}), has a strong affinity for DOC (Fitzgerald et al., 2005; Fitzgerald et al., 2007; French et al., 2014; Poissant et al., 2008; St. Louis et al., 2004). Key functional groups involved in Hg-DOC binding include carboxyl (-COOH) groups in humic and fulvic acids, phenolic (-OH) groups from plant material and lignin, and sulfhydryl (-SH) groups, which have the strongest binding affinity for Hg, and which play a critical role in forming Hg-DOC complexes (Fitzgerald et al., 2005; Fitzgerald et al., 2007; French et al., 2014; Poissant et al., 2008; St. Louis et al., 2004). As OM decomposes, it releases DOC enriched with these functional groups, allowing Hg^{2+} to form soluble Hg-DOC complexes and increasing

Hg mobility in water (French et al., 2014; St. Louis et al., 2004). Once bound to DOC, Hg remains more soluble and is transported through hydrological processes such as flooding and runoff (Bravo et al., 2018; French et al., 2014; Li et al., 2020; St. Louis et al., 2004).

The microbial conversion of inorganic Hg into MeHg is strongly influenced by DOC and OM. Sulfate-reducing and iron-reducing bacteria, which mediate methylation, depend on OM as an energy source (French et al., 2014; Poissant et al., 2008). Additionally, OM decomposition consumes oxygen, creating anoxic conditions that favor Hg methylation (Boening, 2000; Fitzgerald et al., 2005; French et al., 2014; Kelly et al., 1997). The role of Hg-DOC complexes in methylation is complex; labile DOC facilities microbial uptake, enhancing methylation, whereas strong Hg binding to refractory DOC may reduce bioavailability and methylation (French et al., 2014). Hg bound to DOC can ultimately enter aquatic food webs through multiple direct and indirect pathways: 1) direct uptake by microbes and phytoplankton can be followed by conversion to MeHg; 2) adsorption onto particulate OM can be followed by ingestion by zooplankton and small fish; and, 3) desorption, where bound Hg is released from DOC (under certain environmental conditions), which increases uptake by aquatic organisms (Boening, 2000; Bravo et al., 2017; French et al., 2014). Overall, OM acts as both a source of DOC and a key binding agent for Hg, and regulates mobility, transformation, and bioavailability of Hg in aquatic environments. The relationship between DOC and Hg is crucial for understanding how flooding affects Hg cycling and ultimately can increase potential risks to aquatic ecosystems and fish populations.

Anthropogenic flooding occurs when human-driven activities, such as industrial, agricultural, and/or infrastructure-related projects, intentionally submerge terrestrial environments. Flooding releases nutrients and Hg into the environment (Talbot et al., 2021; Ullrich et al., 2001). Studies in the Northwest Territories and Alaska have shown that nutrient concentrations are enhanced and affect community richness, growth, and abundance of lower trophic level organisms in the initial years after flooding, and [Hg] increase due to enhanced availability and bioaccumulation (Gough et al., 2016; Hershey, 1992; Jorgenson et al., 1992; Lienesch et al., 2005; Lougheed et al., 2015). Effects on productivity can reverse within years as nutrient levels decline due to depletion and competitive exclusion, while Hg continues to bioaccumulate and biomagnify, posing long term ecological risks (Gough et al., 2016; Grimard & Jones, 1982; Hershey, 1992; Jorgenson et al., 1992; Lougheed et al., 2015; Ostrofsky & Duthie, 1980; Paterson et al., 1997).

Previous research has shown that flooding events significantly increase [Hg] in fish tissue. Research in temperate and boreal reservoirs indicates that flooding enhances Hg bioaccumulation, with [MeHg] rising within 1 to 3 years after flooding (St. Louis et al., 2004). This early increase is driven by the rapid influx/decomposition of OM, which fuels microbial methylation of Hg. [Hg] in tissue can peak approximately 3 to 4 years post-flooding (Verdon et al., 1991). Hg accumulation in fish tissue continues,

however, and peaks ~ 4 to 11 years after flooding (Bilodeau et al., 2016; St. Louis et al., 2004; Verdon et al., 1991). In most cases, elevated [Hg] persist for up to 30 years before returning to background levels (Hall et al., 2009; Verdon et al., 1991; Willacker et al., 2016). A meta-analysis of [Hg] in freshwater fishes across Canada (1967-2010; representing 104 species; the majority large-bodied fishes) from 5,000 locations found that high [Hg] in fish tissue were frequently linked to reservoirs (i.e., flooded areas) and/or contaminated sites (Depew et al., 2013). In the Arctic, flooding-induced increases in fish [Hg] may be especially prolonged. Model simulations based on lakes impacted by the Churchill River diversion in northern Manitoba suggest that [Hg] in high-latitude reservoirs remain elevated longer than in lower latitudes (Johnston et al., 1991).

Despite extensive research on Hg bioaccumulation in other regions, no studies have directly examined the effects of flooding on [Hg] in Arctic freshwater fishes. Long-term monitoring in the Northwest Territories, Yukon, Nunavut, northern Quebec, Alaska, and Greenland has shown that total [Hg] and/or [MeHg] in fish tissue frequently exceed government-established guidelines for human health consumptions (see AMAP, 2011; Poissant et al., 2008), or surpass baseline levels (Atwell et al., 1998). The highest [Hg] occurs in top predatory fish that occupy the highest trophic levels (see AMAP, 2011). No clear geographic patterns in fish [Hg] have been observed in the Arctic, indicating variability between lake systems and food webs (Poissant et al., 2008). Elevated [Hg] in northern fish species is especially concerning because many Arctic communities rely on traditionally harvested wild foods, including fish, for sustenance, cultural practices, and spiritual wellness (Hughson, 2010). In northern Canada, activities such as fishing for Arctic Char (*Salvelinus alpinus*), hunting for caribou (*Rangifer tarandus*), and gathering berries or eggs are vital traditions, reflecting Indigenous peoples' deep connection to their ancestral lands (Hughson, 2010; Newell et al., 2020). Land-use changes in the Arctic increasingly disrupt these traditions, with residents expressing concerns about the potential health impacts associated with environmental alterations (Grigorieva, 2024).

While flooding in Arctic lakes may influence [Hg] in fish tissue similarly to boreal lakes, the distinct landscape and climate in Arctic systems introduce additional complexities. The region experiences extreme seasonality, with periods of continuous darkness in winter and 24-hour daylight in summer (AMAP, 2021). These conditions affect key hydrological and biogeochemical processes, including the timing and extent of spring freshet, biological production, and photo-active transformations, all of which influence Hg delivery and methylation in aquatic systems (AMAP, 2011). Additionally, although the tundra lacks trees, plant growth is significant, and Arctic greening is expanding vegetative cover, increasing the surface area available for Hg sequestration (AMAP, 2021). The Arctic is warming at more than twice the global average rate due to climate feedback mechanisms, making it particularly vulnerable to environmental change (Kiovurova et al., 2016). Permafrost soils act as long-term sinks for both carbon and Hg; both elements are

sequestered for centuries under cold, stable conditions that prevent microbial breakdown and release (Jin & Ma, 2021). However, flooding of permafrost destabilizes these conditions, with significant but poorly understood implications for Hg dynamics in Arctic freshwater systems. As the climate warms, permafrost thaw is expected to increase Hg release, raising concentrations in aquatic systems and fish (Kiovurova et al., 2016). While thaw-induced permafrost slumps mobilize metals and carbon into downstream ecosystems (MacDonald et al., 2000), flooding represents a distinct hydrological process that may further alter Hg mobilization. The active layer, the uppermost permafrost region subject to annual freeze/thaw cycles, contains high levels of recalcitrant OM (Schnurr, 2019). This OM is resistant to microbial breakdown but strongly binds to Hg, facilitating its transport into aquatic systems and promoting Hg methylation by creating anoxic conditions favorable to methylating microbes (Schnurr, 2019). Thus, flooding in the Arctic may enhance Hg and carbon mobilization, with potentially significant consequences for downstream aquatic ecosystems and food webs.

1.3 Factors that Influence Mercury Concentrations in Fish

Mercury concentrations in fish are affected by many interacting biotic and abiotic factors. Biotic factors include trophic ecology and growth rates of individual fish species, and food web ecology (e.g., Atwell et al., 1998; Clayden et al., 2015; St Louis et al., 2004), which are in turn affected by primary and secondary productivity, and composition of lower trophic level communities. Flooding influences trophic dynamics in aquatic ecosystems by enhancing primary productivity and MeHg production, as terrestrial carbon inputs stimulate microbial activity (Wang et al., 2024). This, in turn, affects species richness, growth, abundance, and [Hg] across all trophic levels (Boening, 2000; Gough et al., 2016; Hershey, 1992; Jorgenson et al., 1992; Lougheed et al., 2015; Moslemi-Aqdam et al., 2022; St Louis et al., 2004). In fish, [Hg] is primarily derived from diet (Hall et al., 2009), making trophic position, foraging habitat (i.e., carbon source), and [Hg] in prey critical factors in understanding Hg accumulation (e.g., Kidd et al., 1995; Power et al., 2002). Physicochemical variables, including nutrient concentrations, primary productivity, water quality and clarity, and dissolved OM (DOM), influence these biotic factors as well as other aspects of Hg cycling, availability, and biomagnification within food webs (see Moslemi-Aqdam et al., 2022). Physicochemical variables are in turn shaped by catchment characteristics, such as area, elevation, slope, soil type, vegetation cover, and proximity to anthropogenic disturbances, which ultimately regulate DOM levels and primary productivity, and thus affect Hg methylation and bioaccumulation (see Moslemi-Aqdam et al., 2022).

Stable isotope ratios are commonly used to help assess trophic position and foraging habitat, and to provide insights into food web structure and Hg bioaccumulation. Stable isotope ratios of Nitrogen ($\delta^{15}N$) are used to estimate trophic position, as $\delta^{15}N$ increases by approximately 3-5‰ with each trophic transfer

(e.g., Post, 2002). Higher $\delta^{15}N$ values typically indicate higher trophic positions, which correlate with increased Hg accumulation (Minigwa & Wada, 1984). Stable isotopes of Carbon ($\delta^{13}C$) trace energy sources and can be used to distinguish between littoral and pelagic carbon sources (Peterson & Fry, 1987; Post et al., 2000; Post, 2002; Tiselius & Fransson, 2016). Fish feeding on pelagic-derived carbon sources generally have higher [Hg] than those relying on benthic-derived carbon sources (Power et al., 2002). Analyses of stable isotope ratios before and after flooding, or between flooded and reference systems, can help researchers evaluate how flooding alters trophic interactions and Hg dynamics in fish populations.

In addition to trophic position and carbon source, fish growth rates significantly influence [Hg] in tissues, with growth efficiency shaped by lake physiochemical conditions and catchment characteristics (see Moslemi-Aqdam et al., 2022). For example, in an Arctic Long-Term Ecological Research (ALTER) Project study in Alaska, flooding induced eutrophic conditions led to increased body size and population density in Lake Trout (*Salvelinus namaycush*) (Lienesch et al., 2005). Growth rates doubled in the initial years post-flooding (Gough et al., 2016), but recruitment declined a decade later as nutrient depletion and low dissolved oxygen levels negatively affected embryos and eggs, particularly in oxygen-sensitive bottom substrates (Gough et al., 2016; Hershey, 1992; Lienesch et al., 2005; Stekoll et al., 2009). Fish, occupying the highest trophic levels in aquatic ecosystems, typically have higher [Hg] than lower trophic level organisms due to biomagnification (Kidd et al., 2003; Power et al., 2002; Hall et al., 2009). A well-documented inverse relationship, known as “somatic growth dilution”, has also been observed, with faster growing fish having lower [Hg], as observed in Northern Pike (*Esox lucius*) (Moslemi-Aqdam et al., 2022; Ward et al., 2010). Increased [DOC], which are commonly associated with flooding, can impair fish growth by reducing visual performance in sight-dependent predators and lowering dissolved oxygen levels, impacting metabolism and feeding efficiency (Creed et al., 2018; Lindmark et al., 2022; Moslemi-Aqdam et al., 2022; Niklitschek & Secor, 2009; Solomon et al., 2015). Thus, flooding may not only affect fish [Hg] through increased loading and net methylation rates, but also indirectly through effects on trophic ecology and fish growth rates.

1.4 Industrial Development in the Arctic

The growing global demand for natural resources continues to drive mineral exploration and development in resource-rich regions, including the Arctic (Bidgood & Hall, 2024; Koivurova et al., 2016; Southcott et al., 2019; Tolvanen et al., 2019). Initially, industrial development in the Arctic focused on extracting high-value metals, such as gold and silver. While early efforts were constrained by high transportation costs, the region’s vast mineral wealth was recognized in the 20th century, sparking increased investment and expansion (Southcott et al., 2019). Climate change is further facilitating Arctic resource extraction by improving access to previously remote areas (Southcott et al., 2019). However, it is also

amplifying the environmental impacts of industrial activities, often to a greater extent than in other regions (Tolvanen et al., 2019). Negative consequences of industrial development include soil erosion, contamination, pollution of local water bodies, increased noise and emissions, and habitat fragmentation due to infrastructure expansion (Haddaway et al., 2019).

Mining, a major industrial activity in the Arctic, can cause long-term environmental damage. Studies monitoring mining impacts in the Canadian Arctic have shown that tailings, residual materials left after metal and mineral extraction, can lead to metal accumulation in aquatic sediments and biota, including elevated [Hg] in fish tissue (Tolvanen et al., 2019). Disruptions to microbial communities, which play a crucial role in ecosystem stability and nutrient cycling, have also been observed (see Tolvanen et al., 2019). Mining operations frequently involve intentional alterations to water flow, including dewatering, the removal of water from mineral rich areas, and the creation of tailings ponds (Tubis et al., 2020). These activities can trigger industrial-related flooding, where water is diverted or released, impacting downstream aquatic ecosystems (Tubis et al., 2020).

Industrial-related flooding has multifaceted and long-term consequences on aquatic systems, which can be categorized into four key areas: 1) chemical contamination: industrial facilities store hazardous chemicals, fuels, heavy metals, and other pollutants. When released due to flooding, intentional discharges, waste/sewage outflows, or spills, these contaminants degrade water quality, can bioaccumulate in aquatic organisms, and enter the food web, posing risks to both wildlife and humans consuming contaminated fish (Bashir et al., 2020; Mateo-Sagasta et al., 2017); 2) increased turbidity and eutrophication: flooding mobilizes sediment, nutrients, and debris from industrial sites, and increases turbidity in waterbodies (Bashir et al., 2020). The influx of nutrients and OM can drive eutrophication, fostering algal blooms, depleting oxygen levels, and leading to fish kills and ecosystem imbalances (Bashir et al., 2020; Mateo-Sagasta et al., 2017); 3) habitat destruction and species displacement: floodwaters physically alter aquatic habitats through erosion, sediment deposition, and changes in waterbody structure. These disruptions can displace native species, degrade breeding and feeding grounds, and destabilize food webs, ultimately reducing biodiversity (Bashir et al., 2020); and 4) altered hydrology and flow: industrial flooding can significantly alter water temperature and flow patterns, impacting survival, reproduction, and migratory behavior of aquatic species (Bain et al., 1988). Changes in flow rates can disrupt critical biological processes, such as spawning and feeding cycles (Bain et al., 1988). Long-term ecological impacts can result from the consequences of industrial flooding and can persist for decades. Contaminated sites often take years to recover, and habitat destruction may lead to permanent population declines or local extinctions due to cumulative stressors (Bashir et al., 2020; Ghani, 2015).

Fragile ecosystems in the Arctic are particularly vulnerable to long-term effects of industrial activities, including flooding. Flooding events can exacerbate Hg mobilization by introducing terrestrially derived carbon and microbial communities that enhance Hg methylation and result in increasing [MeHg] in aquatic food webs. Given the high trophic position of many Arctic fish species, Hg bioaccumulation poses a significant risk to both wildlife and Indigenous communities relying on traditional subsistence fisheries. Thus, as industrial activities continue to expand in the Arctic, understanding their ecological consequences, particularly in relation to Hg cycling, is crucial for environmental management and the protection of Arctic aquatic ecosystems.

1.4.1 Monitoring Industrial Impacts in Aquatic Environments

Monitoring the effects of mining on aquatic ecosystems is essential. In Canada, the Metal and Diamond Mining Effluent Regulations (MDMER) and the Environmental Effects Monitoring (EEM) programs play key roles in the regulatory framework that is applied to mineral developments. The MDMER governs mining effluent discharges, setting limits on harmful substances (e.g., Hg) to protect water quality and aquatic life (Government of Canada, 2025). The EEM program, which is part of the MDMER, evaluates broader ecological impacts by monitoring aquatic species, including fish, benthic invertebrates, and aquatic plants (Government of Canada, 2025). A critical aspect of the EEM program is the use of small-bodied fish species, such as fathead minnows (*Pimephales promelas*), as sentinel organisms. These species are sensitive to water quality changes and provide early indicators of contamination through measurable effects on growth, reproduction, and behavior (Government of Canada, 2025; Rozon-Ramilo, 2011). Their position near the base of aquatic food webs makes them effective for assessing ecosystem health (Fausch et al., 1990). In the Canadian Arctic, Slimy Sculpin (*Cottus cognatus*) and Ninespine Stickleback (*Pungitius pungitius*) are abundant and widespread (Richardson et al., 2001; Scott and Crossman, 1973) small-bodied fishes, which makes them ideal for monitoring the ecological impacts of mine-induced flooding and other environmental disturbances.

1.4.1.1 Slimy Sculpin as an Indicator Species

Slimy Sculpin are widely distributed across Canada, inhabiting freshwater lakes and streams with gravel, rock, or mud substrates where they shelter under rocks and submerged debris (Arciszewski et al. 2015; Mansfield 2004; Scott and Crossman 1973). They are non-migratory with high site fidelity and are thought to maintain small home ranges (~ 10 meters (m)) - rarely dispersing beyond 50 m (Arciszewski et al., 2015; Craig & Wells, 1976; Power et al., 2022). Their limited movement makes them effective for detection of localized environmental changes. As benthic-dwelling, nocturnal ambush predators, Slimy Sculpin primarily feed on benthic invertebrates (e.g., *Chironomidae*) but also consume terrestrial insects, crustaceans, fish eggs, and small fish, with their diet reflecting prey availability (Arciszewski et al., 2015;

Mansfield, 2004; Power et al., 2022). Due to their small size and lack of swim bladder, which limits their swimming ability, they are a common prey item for larger predators, including Burbot (*Lota lota*) and Lake Trout (Arciszewski et al., 2015; Mansfield, 2004). Slimy Sculpin links benthic and pelagic food webs and serves as sentinel species for environmental monitoring due to their sensitivity to contaminants and habitat alterations (see Arciszewski et al., 2015). They reach sexual maturity at ~ 2 years and have a lifespan of ~ 5 years (Mansfield, 2004).

1.4.1.2 Ninespine Stickleback as an Indicator Species

Ninespine Stickleback are a small-bodied, euryhaline fish with a circumpolar distribution found in in freshwater, brackish, and marine environments (Aldohoven et al., 2010; Hammerson, 1994; Von Hippel et al., 2016). Ninespine Stickleback exhibit both anadromous and freshwater resident life histories, which contributes to substantial variation in morphology, behavior, and physiology and makes them valuable models for comparative genetics and evolution (Aldohoven et al., 2010). Although data on home range size for Ninespine Sticklebacks are limited, research on related species (e.g., Three-spined Stickleback (*Gasterosteus aculeatus*)), suggests high site fidelity, particularly during the spawning season (Ivanova et al., 2019; Ward et al., 2013). Due to their abundance at northern latitudes, Ninespine Stickleback are emerging as a key indicator species for assessing environmental effects (Von Hippel et al., 2016; Wootton, 2023). They prefer cool, quiet waters, and inhabit lakes, ponds, streams, and estuaries, often in shallow vegetated areas or over sand (see Hammerson, 1994). As mostly nocturnal predators, they consume small crustaceans, aquatic insects, fish eggs, and fry, and are preyed upon by large fish and piscivorous birds (see Hammerson, 1994). Despite displaying adaptability, Ninespine Stickleback may still experience habitat-related stresses from industrial activities (Von Hippel et al., 2016). They reach sexual maturity between 1 to 2 years and rarely live beyond 3 years (see Hammerson, 1994).

1.5 Local Context and Study Area

A unique opportunity to investigate the effects of flooding on Hg dynamics in Arctic aquatic ecosystems arose from an industrial development in Nunavut, Canada. As part of a gold mining project, a lake (surface area:1.67 kilometers squared (km^2)) was dewatered to create a new mining pit, while several smaller downstream lakes (combined surface area: ~ 1.5 km^2) were flooded as a result. This event had the potential to provide valuable insights into how flooding influenced Hg transport, methylation, and bioaccumulation in Arctic freshwater systems.

The industrial development and study area is located ~ 160 kilometers (km) north of Baker Lake, Nunavut, (64.32ºN, 96.02ºW), within the Kivalliq District. The region has been subject to mineral resource development due to the presence of two major gold deposits: Meadowbank (~ 110 km north of Baker Lake) and Amaruq (~ 160 km north of Baker Lake). Both deposits are owned and operated by Agnico Eagle Mines

Limited (Agnico Eagle), an open-pit gold mining company. The mine is situated within Barrenland tundra, an extreme environment characterized by low temperatures, permafrost, and a brief growing season. Following the discovery of the Amaruq mineral deposit in 2018, landscape modifications were required to accommodate mining operations. One of these projects, the Whale Tail Pit Project, involved the dewatering of northern Whale Tail Lake and the construction of a dam to redirect water downstream, which flooded adjacent waterbodies. By 2019, this new flooded area had significantly altered downstream aquatic habitats.

The impacted flood zone covered ~ 3.3 km^2, that contained numerous small- to medium-sized lakes interspersed among rolling lowlands, boulder fields, eskers, bedrock outcrops, and uplands (Azimuth 2018, Smith et al. 1998). These lakes are predominantly oligotrophic (Azimuth, 2018), meaning they exhibit low productivity and nutrient-poor conditions (Wetzel, 2001). The drainage system in the study area is indistinct and complex, which is typical of Barrenland tundra systems. Small chain-lake systems exist, where interconnected lakes are linked by ephemeral streams, but overland flow is also common (Azimuth, 2018). Hydrological connectivity is generally low to non-existent most of the year, except during spring freshet, when high flows temporarily enhance connectivity (Azimuth, 2018). Given these seasonally constrained hydrological pathways, fish movement between lakes is likely limited (Azimuth, 2018).

1.6 Study Objectives

The primary objective of this study was to assess how flooding associated with mining development affected [Hg] in small Barrenland tundra lakes. Specifically, this study aimed to answer the question "*How are [Hg] and [DOC] in water and [Hg] in fish in Barrenland tundra lakes impacted by flooding?".* Small-bodied fish were chosen as focal species for several reasons: 1) limited home range: compared to larger fish, small-bodied species have smaller home ranges (Schoener, 1971), making them less likely to migrate between study lakes; 2) faster physiological response: due to their shorter lifespans and higher metabolic rates, small-bodied fish experience faster growth and flesh turnover, making them more responsive to environmental changes (Fausch et al., 1990); and 3) widespread distribution: in the Canadian Arctic, small-bodied fish are more widely distributed across small, shallow lakes than larger-bodied fishes. Slimy Sculpin and Ninespine Stickleback, both abundant in the study area, were selected as indicator species.

My first study objective was to compare [Hg] and key OM indicators in water: 1) before and after flooding in impacted lakes; and 2) between reference and impacted lakes after flooding. The following variables were measured: total [THg] and [MeHg], indicators of Hg mobilization and net methylation; [DOC]; Humification Indices (HIX), a measure of humic substance content (e.g., humic and fulvic acids); and Specific Ultraviolet Absorbance (SUVA) at 254 nm, an indicator of DOM composition, particularly humic content (Weishaar et al., 2003). I hypothesized for these water chemistry parameters that flooding

would alter OM (as measured by DOC, HIX, and SUVA) and [Hg] (THg and MeHg) via mobilization of terrestrially stored Hg and OM. Specifically, my hypotheses were that aqueous [THg], [MeHg], [DOC] and indices of HIX and SUVA would differ 1) before and after flooding in impacted lakes; and, 2) between reference and impacted lakes after flooding.

Following water chemistry, my second objective was to compare [THg], and covariates of [Hg] (e.g., trophic position, carbon source, growth rate), in forage fish tissue between flooded and reference lakes (post-flooding) and between pre-and-post flood years. Flooding was expected to mobilize terrestrially stored Hg and increase net methylation rates, which could both act to increase fish [Hg]. Trophic ecology, carbon sources, and growth dynamics were also expected to be influenced by flooding and differ between both flooded and reference lakes and between pre- and post-flood years in ways that could influence [Hg]. I hypothesized that [Hg] in forage fish tissue would differ 1) between reference and impacted lakes after flooding; and 2) before and after flooding in impacted lakes.

Chapter 2: Methods

2.1 Study Area

The study area is located within the Southern Arctic Ecozone and is situated above the tree line on the northwestern side of Hudson Bay, within the Thelon River basin, which drains into Hudson Bay (Government of Canada, 2022). The terrain has been shaped by glaciations, and features thick continuous permafrost underlain by granite bedrock, overlain with glacial till, glaciofluvial deposits, and shallow organic material (Smith et al., 1998). Soils in the region are Cryosolic and support a terrestrial vegetation community that is dominated by dwarf shrubs such as birch (*Betula spp.*) and willow (*Salix spp.*), as well as heath (*Erica spp.*), mosses (*Bryophyta spp.*), lichens (*Cryptothele spp.*), and sedge-moss (*Carex spp.*) (Smith et al., 1998). The climate is marked by moist, cool summers and extremely cold winters, resulting in a short growing season of approximately four months (Smith et al., 1998). Based on climate data from 1981 to 2010, the region has a mean annual temperature of -12.2°C (ranging from -34.8°C to 17.0°C) and mean monthly precipitation of 22.7 mm (ranging from 6.2 mm to 52 mm) (Government of Canada, 2024). The ice-free season is brief and typically extends from late-June to mid-July until late-September to early-October (Azimuth, 2018).

The nearest community to the study site is Baker Lake, Nunavut (64.32ºN, 96.02ºW), which is located ~ 160 km south (Figure 1). The region is home to two major gold deposits, Meadowbank (~ 110 km north of Baker Lake) and Amaruq (~ 160 km north of Baker Lake), both owned and operated by Agnico Eagle. Development of the Amaruq deposit required substantial landscape modifications to facilitate mining operations, including the construction of an access road connecting the mine site to the community, an uncommon feature in the territorial context of Nunavut.

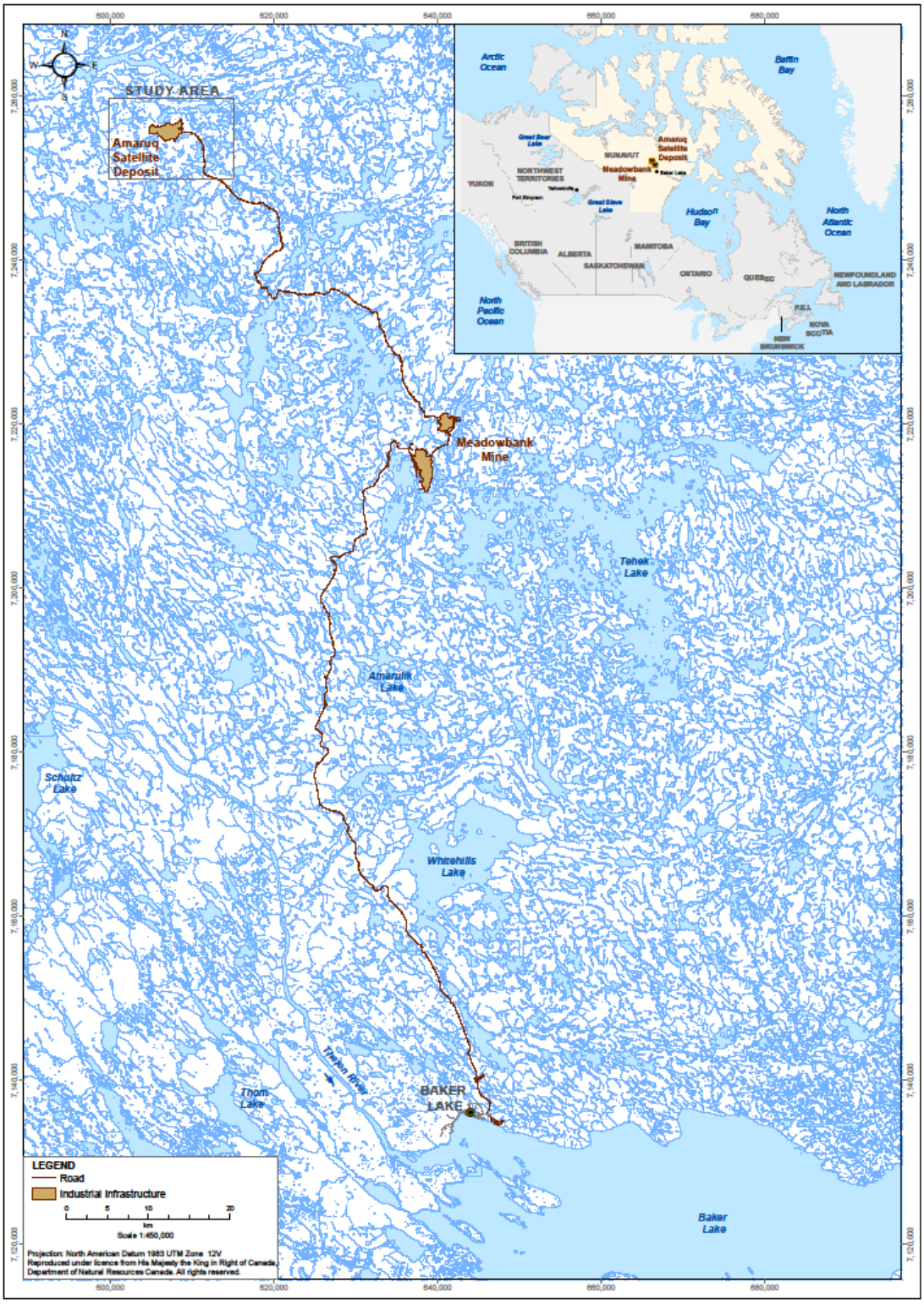


Figure 1: ***The location of Agnico Eagle's two gold mining facilities relative to Baker Lake, located in the Kivalliq District, Nunavut, Canada. The well-established, operational Meadowbank facility and the now operational Amaruq Satellite Deposit are shown in brown. The location of the Whale Tail Pit Project is within the Amaruq Mine facility.***

2.1.1 Industrial Development and Flooding

In 2019, development of the Whale Tail Pit (Amaruq Project, Agnico Eagle Mines Ltd.) involved constructing a dam in the center of Whale Tail Lake, followed by the removal and diversion of water from the northern part of the lake into the southern part of the lake (Figure 2). A total of seven lakes near or within the Amaruq mine development site were sampled in August of 2018 (i.e., pre-flood), 2019, 2020, and 2021 (i.e., post-flood). During each sampling period, water, Slimy Sculpin, and Ninespine Stickleback were collected.

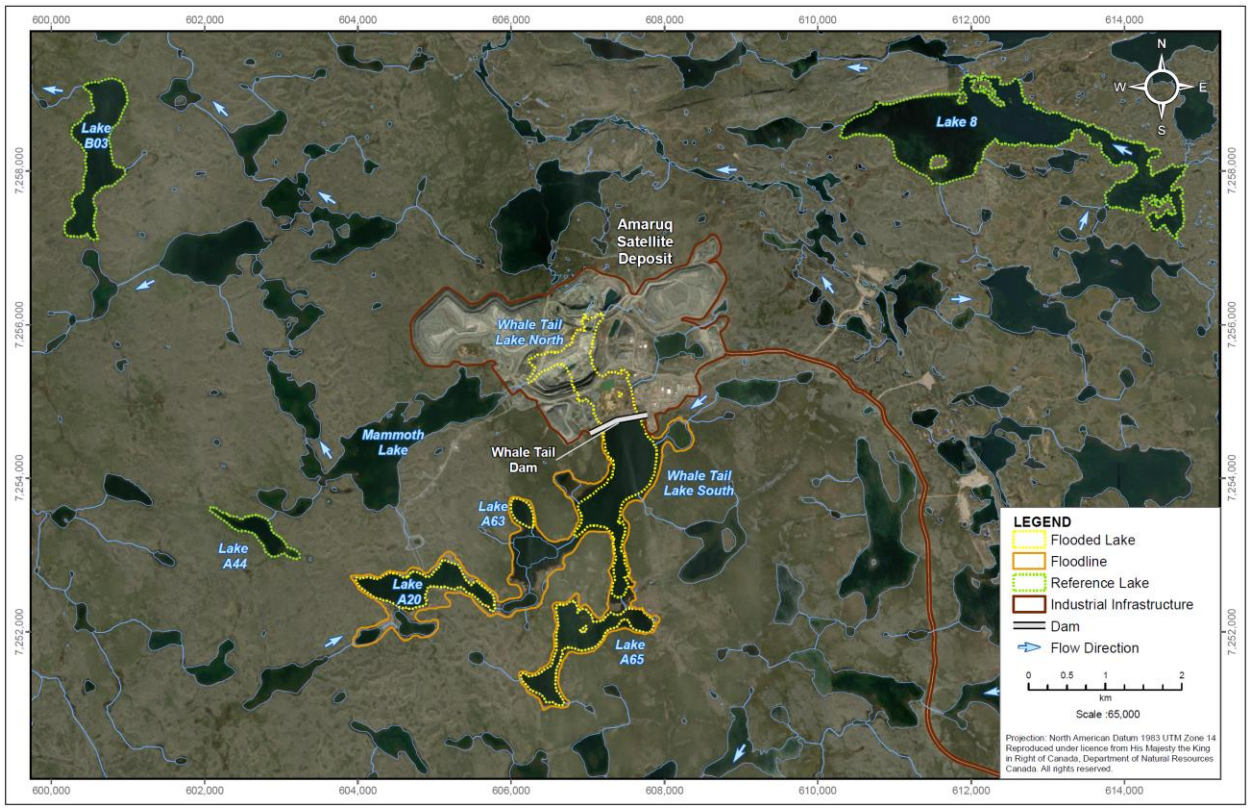


***Figure 2:* Outline of the waterbodies impacted by the Whale Tail Pit Project. The flooded lakes are outlined with a yellow dotted line, representing the pre-flood (2018) conditions. The lakes outlined with a green dotted line are the reference lakes. The orange solid line represents the flood zone following the construction of the Whale Tail Dam (which is represented by a white bar), representing the post-flood (2019 to 2021) conditions. The brown outlined areas indicate the locations of industrial infrastructure. Blue arrows indicate flow direction.**

Four lakes were directly impacted by flooding from the Whale Tail Pit Project and are referred to as the flooded lakes: Whale Tail Lake South (WTL), Lake A20 (A20), Lake A63 (A63), and Lake A65 (A65) (Figure 2). In addition to these, three reference lakes, chosen based on similar habitat and morphology to the flooded lakes, were also sampled: Lake A44 (A44), Lake B03 (B03), and Lake 8 (LK8) (Figure 2). These reference lakes were not selected specifically for this thesis but were predetermined to support

regulatory sampling requirements associated with mine permitting. They were, however, chosen based on general similarity in habitat and morphology to the flooded lakes to allow for comparative analyses. A44 is within the same watershed as the flooded lakes but is located outside the downstream flow path, approximately 4.4 km northwest of WTL. In contrast, B03 and LK8 are in a different watershed, positioned approximately 5.5 km northeast and 7.8 km northwest of WTL, respectively (Figure 2).

Prior to flooding, baseline data indicated that WTL, including its northern section, had a surface area of 1.67 km^2 and a maximum depth of 18.3 m. Lake A20 had a surface area of 0.56 km^2 with a maximum depth of 25 m, while A63 measured 0.084 km^2 in surface area and 5.7 m in depth. Lake A65 covered 0.63 km^2 and had a maximum depth of 11.2 m, whereas A44, the reference lake, had a surface area of 0.22 km^2 and a maximum depth of 12.3 m. Following the flooding event, significant hydrological changes were observed. The surface area of WTL expanded by 3.59%, increasing from 1.67 km^2 to 1.73 km^2. A63, which had previously been a separate waterbody, merged with WTL, increasing 38% from 0.079 km^2 to 0.116 km^2. Lake A20 experienced the most substantial increase, expanding by 46.43% from 0.56 km^2 to 0.82 km^2. Similarly, A65 increased in size by 19%, increasing in surface area from 0.63 km^2 to 0.75 km^2. In contrast, the surface area of A44, which is within the same watershed but was not directly affected by flooding. Depths also increased across the flooded lakes, with WTL becoming approximately 2.2 m deeper than baseline measurements, while A20 and A63 showed increases of 30 to 50 cm in depth.

Both Slimy Sculpin and Ninespine Stickleback were present in all study lakes, making them key species for assessing the ecological effects of flooding on small-bodied fish. Additional fish species were also recorded in the study lakes, as outlined in Table A2.1. Lake Trout were present in all lakes, while Arctic Char (*Salvelinus alpinus*), Round Whitefish (*Prosopium cylindraceum*), and Burbot (*Lota lota*) were found in a subset of lakes. While flooding caused many of the lakes to become more hydrologically connected than they were prior to flooding, the study species, Slimy Sculpin and Ninespine Stickleback, have small home ranges and exhibit limited movement (Power et al., 2022; Von Hippel et al., 2016). I therefore assumed that the lake where they were collected reflected their primary habitat.

2.1.2 Study Constraints

This study was originally designed following a Before-After-Control-Impact (BACI) approach. However, logistical constraints impacted data collection throughout the life of field sampling activities. Due to the remote nature of the study site, lake access was limited to helicopter transport, and regulatory programs, such as the EEM and Core Receiving Environmental Monitoring Program (CREMP), were prioritized over this research project. As a result, LK8 was the only reference lake where data were consistently collected both before and after the flooding event (Table 1). The prioritization of regulatory programs, particularly access to helicopter time, was beyond my control and not a decision within the scope

of this study, resulting in inconsistences in data collection that limited the type of statistical analyses that could be conducted.

***Table 1:** Summary of sampling that occurred pre – (2018) and post-flooding (2019 to 2021) at each of the study lakes. "C" and green shading indicate samples were collected. "NC" and blue shading indicate samples that were not collected.*

Type	Waterbody	Water Sampling				Fish Sampling			
		Pre-Flood	Post-Flood			Pre-Flood	Post-Flood		
		2018	2019	2020	2021	2018	2019	2020	2021
Flooded	Whale Tail South	C	C	C	C	C	C	C	C
	Lake A63	C	C	C	C	C	C	C	C
	Lake A65	C	C	C	C	C	C	C	C
	Lake A20	C	C	C	C	C	C	C	C
Reference	Lake 8	C	C	C	C	C	NC	C	C
	Lake A44	C	NC	C	C	NC	C	C	C
	Lake B03	NC	NC	C	C	NC	NC	C	C

2.2 Sample Collection

Water samples were collected for various analyses, some of which extended beyond the scope of this study. I focused on analyses of total Hg, MeHg, DOC, HIX, and SUVA.

Water sampling occurred annually in August from 2018 to 2021 in all flooded lakes and in LK8 (reference lake). Samples were also collected from A44 in all years except 2019, and from B03 in 2020 and 2021 only (Table 1). For total metal and nutrient analysis, grab samples were collected from the approximate center of each lake near the surface (approximately 0.5 m depth), using new, sterile Nalgene bottles.

Unfiltered water samples designated for ultra-trace Hg analyses were collected following the clean hands/dirty hands method (USEPA, 1996), a specialized technique designed to minimize contamination. These samples were stored in new, double-bagged 250 milliliter (mL) Polyethylene Terephthalate Glycol-modified (PETG) bottles. For the analysis of dissolved ultra-trace Hg, the clean hands/dirty hands method was again employed, using a peristaltic pump and acid-washed Teflon tubing. Water was filtered through an acid-washed filter cartridge and muffled quartz QMA filters (2.2. µm pore size; e.g., USEPA, 1996) before being transferred into double-bagged 250 mL PETG bottles. Between samples, quartz QMA filters and tubing were replaced to prevent cross-contamination. Samples designated for Hg analysis were preserved with trace metal-grade hydrochloric acid (HCl; Omnitract ®, Supelco) to a final concentration of 0.5% v/v.

For DOC, HIX, and SUVA, 60 mL of near-surface water were pumped directly from the lake surface through muffled quartz QMA filters using a peristaltic pump and stored in amber glass bottles. As with Hg sampling, quartz QMA filters were renewed between samples. All water samples for nutrient and Hg analysis were kept cool until they could be stored at 4ºC in a refrigerator and subsequently shipped to a Canadian Association for Laboratory Accreditation (CALA) certified laboratory for chemical analysis.

Fish sampling was conducted using a backpack electrofisher (Smith-Root Inc., Vancouver, British Columbia) in accordance with University of Waterloo Animal Use Permit 41176. The sampling team aimed to collect 30 individuals of each target species, Slimy Sculpin and Ninespine Stickleback, from each study lake in each sampling year, although actual capture numbers varied. The number of fish collected per lake and year is detailed in Tables A2.2 and A2.3. Captured fish were euthanized using a blow to the head and/or cervical dislocation, then placed on ice in a cooler until further processing. Within hours of collection, each fish was measured for fork length (millimeter (mm)) and weight (g), before being placed in a clean, labeled, polyethylene Whirl-Pak™ bag and frozen for subsequent processing at the University of Waterloo Fish Laboratory. Summarized backpack electrofishing catch records are presented in Tables A2.2 and A2.3, while detailed fish measurements are available in Table A2.4.

2.3 Sample Preparation

Water samples were shipped to the Biotron Center for Experimental Climate Change Research at Western University for analyses of total Hg and MeHg, and to the Branfireun Lab at Western University (London, Ontario) for analyses of DOC, HIX, and SUVA. Water samples were also shipped to the University of Alberta Biogeochemical Analytical Service Laboratory for analyses of nutrients and other parameters not specifically addressed in this thesis (Edmonton, Alberta; see Appendix A).

Frozen fish samples were shipped to the University of Waterloo Fish Laboratory (Waterloo, Ontario) for processing. At the Fish Laboratory, sagittal otoliths and viscera were extracted from each fish. The otoliths were cleaned, dried, and placed in microcentrifuge tubes, while the viscera, except for the livers, which were archived, were discarded. The remaining whole "dressed" fish, excluding viscera and otoliths, were then individually placed in a 0.5 mL sterile glass or polyethylene vials and freeze-dried using a Labconco® FreeZone (United States of America (USA)) freeze dryer. The freeze-drying process lasted a minimum of 48 hours at 0.04 millibar (mbar) and -48˚C. Once freeze-dried, samples were homogenized using ultra-fine scissors. Following homogenization, fish tissue was weighed to 0.30 mg using a Mettler Toledo Analytical Balance to support carbon and stable isotope analysis. Remaining freeze-dried fish tissue was submitted to the Biotron Center for Experimental Climate Change Research for analysis of [THg]. The sagittal otoliths were submitted to AAE Tech Incorporated (AAE) in La Salle, Manitoba for aging. Otoliths were prepared and examined under a compound microscope using transmitted light, with age and edge condition recorded alongside a confidence rating for each age determination. To ensure Quality Assurance/Quality Control (QA/QC), over 25% of samples were reassessed by a second individual at the laboratory to verify accuracy.

2.4 Laboratory Analysis

At the Biotron Center for Experimental Climate Change Research, water samples (n = 300) were analyzed for [THg] and [MeHg]. Cold vapour atomic fluorescence spectrophotometry was used to conduct [THg] analyses. Analyses for [THg] were conducted using a Tekran® 2600 automated THg Analysis System (Canada) in accordance with EPA method 1631 (Lab Method ID - TM.0811). Analyses for [MeHg] were conducted using a Tekran® 2700 automated MeHg Analysis System (Canada) in accordance with EPA method 1630 (Lab Method ID - TM.0812) (USEPA, 2007). Concentrations of DOC (n = 96) were determined using phosphoric acid digestion followed by persulphate oxidation on an Aurora® 1030 W total organic carbon analyzer (USA). Fluorescence and absorbance measures were used to determine the SUVA index (n = 58), with appropriate corrections applied using a Horiba Aqualog® spectrofluorometer (Japan). Specific UV absorbance at 254 nanometers (nm; SUVA), an indicator of the degree of aromaticity of DOM, was calculated as absorbance at 254 nm divided by [DOC] (Weishaar et al. 2003). The HIX index (n = 117) was determined using fluorescence spectroscopy, where fluorescence intensity was measured at specific wavelength ranges (435-480 nm for humic-like material and 480-510 nm for fulvic-like material) to calculate HIX. QA/QC was performed in strict compliance with the laboratory's ISO 17025 accreditation.

Freeze-dried and homogenized tissue samples of Slimy Sculpin (n = 715) and Ninespine Stickleback (n = 452) were also analyzed at Biotron Center for Experimental Climate Change Research for [THg] using a Milestone® DMA-80 Direct Mercury Analyzer (Italy), following Environmental Protection

Agency (EPA) Methods 7473 (USEPA, 2007). QA/QC procedures were conducted according to the lab's ISO 17025 accreditation, and results are provided in Tables A2.5 to A2.7.

At the University of Waterloo Environmental Isotope Laboratory, freeze-dried and weighed whole-body Slimy Sculpin (n = 694) and Ninespine Stickleback (n = 451) were analyzed for stable carbon and nitrogen isotope ratios. Isotope analysis was conducted using a 4010 Elemental Analyzer (Costech Instruments, Italy), coupled to a Delta Plus XL (Thermo-Finnigan, Germany) continuous flow isotope ratio mass spectrometer (CFIRMS). Stable isotope ratios for each sample were determined using the following formula:

$$\delta^{13}C \text{ or } \delta^{15}N = [(R_{sample} - R_{standard})/R_{standard}] * 1000$$

where R represents $^{15}N/^{14}N$ or $^{13}C/^{12}C$ ratio. Corrected delta (δ) value, reported in per mill (‰) units, were compared against the Vienna Pee Dee Belemnite (VPDB) scale for $\delta^{13}C$ and Atmospheric AIR for $\delta^{15}N$. Precision was assessed by calculating the relative percent difference (RPD) between duplicate samples. Duplicates were analyzed for approximately 10% of Slimy Sculpin (n = 72) and 9% of Ninespine Stickleback (n = 40), with results detailed in Table A2.6. The mean differences between duplicate samples were 0.03‰ for $\delta^{13}C$ for both species, 0.02‰ for $\delta^{15}N$ in Slimy Sculpin $\delta^{15}N$, and 0.06‰ for $\delta^{15}N$ in Ninespine Stickleback (Table A2.4). Accuracy was ensured using international reference materials (IAEA-N1 & N2, IAEA-CH3 & CH6, USGS-40 & 41) and in-house reference materials (EIL-72, EIL-3, JSEC-0).

At AAE, sagittal otoliths were prepared and analyzed for age determination in Slimy Sculpin (n = 693) and Ninespine Stickleback (n = 449). Sagittal otoliths were aged by AAE using whole otoliths viewed under reflected light microscopy. Standard protocols included cleaning and air-drying otoliths, followed by placement in black-bottomed trays with immersion oil to enhance growth zone visibility. Otoliths were examined at multiple magnifications to identify and count annual growth zones (annuli). A minimum of two readings were taken by independent readers, with a 25% random subsample re-aged in duplicate to evaluate precision. Discrepancies in duplicate or initial readings were reviewed by a senior age reader and resolved through consensus. Results of the ageing analyses are provided in Table A2.4.

2.5 Data Analysis

For the data analysis conducted in this thesis, which included both fish and water data, two primary approaches were used to address the research objectives. First, data from pre-flood years (2018 and 2019) were compared with data from the post-flood years (2020 and 2021) in both flooded and reference lakes. Second, differences between flooded and reference lakes were examined during the post-flood years (2020 and 2021). The year 2019 was categorized as a pre-flood year for the fish data analysis, as changes in fish tissue were expected to occur with a delay following flooding (e.g., French et al. 1998, St Louis et al., 2004,

Verdon et al., 1991). Lakes A20, A63, A65, and WTL were classified as flooded/exposed lakes, while B03, LK8, and A44 served as reference lakes. One Slimy Sculpin with very low [Hg] was identified as a statistical outlier and removed from the dataset (Lake B03, 2021). Due to inconsistent sampling across lakes from 2018 to 2021, Linear Mixed Effects Models (LMEMs) were applied, as the dataset did not meet the requirement for a standard BACI statistical approach. All data analyses were conducted in R Studio (R version 4.3.0, R Core Team, 2023) using packages tidyverse, lme4, lmerTest, car, and emmeans. For all statistical tests, alpha (α) was set to 0.05, unless otherwise specified. Exploratory data analyses were conducted to identify potential data entry errors and assess normality using histograms and QQ plots. Residuals were tested for normality where applicable (i.e., for parametric statistical tests) through visual assessments, Shapiro-Wilk tests, and Kolmogorov-Smirnov tests. When necessary, data were $\log_{10}$ transformed to meet normality assumptions.

2.5.1 Analyses of Fish Tissue - Mercury

LMEMs were fitted using the "lmer" function from the "lme4" package (Bates et al., 2009), employing restricted maximum likelihood (REML), which provides unbiased estimates of variance and covariance parameters. If random effect variance estimates approached zero and model singularity was detected, the model was deemed over-parameterized. In such cases, the relationship between the response variable and fixed effect was instead examined using a linear model without a random effect (Zurr et al., 2009). Fork length, a measure of fish size, was consistently included as a fixed effect in all LMEMs or as a predictor variable in linear models, as fish [Hg] are often significantly and positively related to body size (e.g., Wang & Wang 2012). A summary of all models used, including fixed and random effects, is provided in Table A2.8.

To assess differences in tissue [Hg] in Slimy Sculpin and Ninespine Stickleback between pre-flood (2018 and 2019) and post-flood (2020 and 2021) years within the flooded lakes (approach #1), LMEM were used with [Hg] as the response variable. The model was structured to examine the effects of year and fork length on [Hg], while accounting for variability in intercepts and slopes across different year-waterbody combinations (see Table A2.8 for further details). In this analysis, year and fork length were treated as fixed effects, and their interaction was also assessed. The random effect consisted of the combination of an individual waterbody (lakes) and individual year, which allowed the model to account for random variation in intercepts for each waterbody as well as random variation in waterbody*year interactions (see Table A2.8). This hierarchical approach is particularly useful when data are nested within multiple levels, such as measurements within waterbodies, that are further grouped by year (Gelman & Hill, 2006). For Slimy Sculpin in reference lakes, a similar model structure was used; however, only waterbody was included as a random effect with random intercepts (Table A2.8). Due to data limitations, no comparisons could be made

for Ninespine Stickleback [Hg] between pre-and-post flood years in reference lakes. To compare Ninespine Stickleback between pre- and post-flood years in flooded lakes, a model similar to that applied for Slimy Sculpin was used, but with an additional random effect for fork length, allowing for exploration of random slopes (Table A2.8).

To compare differences in tissue [Hg] between flooded and reference lakes in post-flood years (2020 and 2021; approach #2), an additional LMEM was used. Mercury concentration was the response variable. In this model, exposure type (flooded vs. reference) and fork length were included as fixed effects, with interactions assessed, while waterbody was included as a random effect with random intercepts. This model was applied separately for each post-flood year (2020 and 2021) for each species.

For both approaches, the significance of fixed effects terms in the final model was assessed using an analysis of covariance (ANCOVA) with Type III sums of squares (car package; Fox et al., 2019). If the interaction was not significant, it was removed from the model. When a significant interaction between variables was detected, post-hoc comparisons and contrasts were conducted using estimated marginal means (emmeans package; Lenth R, 2023), calculated at a fork length most representative of the dataset. If no significant interaction was observed, pairwise comparisons were conducted using Tukey's Honestly Significant Difference (HSD) method via the emmeans package.

2.5.2 Analysis of Fish Tissue – Covariates

To investigate the potential drivers of increases in length-adjusted [Hg] in Slimy Sculpin and Ninespine Stickleback following flooding, several ecological covariates were examined, including stable carbon isotopes ($\delta^{13}C$), carbon-to-nitrogen (C: N) ratio, age-at-length, and relative condition. The C: N ratio was calculated by dividing the percent carbon (%C) by the percent nitrogen (%N) in tissue samples, as reported in stable isotope laboratory analyses results.

Fish condition was estimated by first modelling weight (W) as a function of length (L), using the equation:

$$W=aL^{b}$$

where W represented fish weight (g), L is fish length (cm), a is the regression intercept, and b is an exponential parameter describing the relationship between length and weight. Both Slimy Sculpin and Ninespine Stickleback exhibited allometric growth, requiring the use of the Relative Condition (Kn) equation to estimate individual fish condition:

$$Kn=w/W$$

where w is the observed weight of a fish at a given length, and W is the expected weight, which is derived from the length-weight regression. Fish ecological variables that were significantly related to tissue [Hg] (see below) were compared between pre- and post-flood years, as well as between flooded and reference lakes in post-flood years only, using the LMEM approach applied for Hg analysis.

For each species, Pearson correlation tests were conducted to assess relationships between [Hg] and each potential covariate, including $\delta^{15}N$, $\delta^{13}C$, age-at-length, C: N ratio, and relative condition. Because most Ninespine Stickleback were aged at one year, age-at-length analyses were not performed for this species. Normality was tested using the Shapiro-Wilk test. As baseline nitrogen stable isotope ($\delta^{15}N$) data were unavailable, a multi-lake correlation analysis between [Hg] and $\delta^{15}N$ was not conducted. However, given the well-established positive relationships between [Hg] and $\delta^{15}N$ in the literature (e.g., Kidd et al., 1995), a positive relationship was assumed. Instead of a full Hg-nitrogen correlation analysis, therefore, $\delta^{15}N$ ratios in Slimy Sculpin were compared across years within each lake using ANCOVA, and pairwise differences were interpreted in the context of pre- vs. post-flooding conditions.

To compare pre-and post-flood years in both flooded and reference lakes for each species (approach #1), a LMEM was constructed for each covariate of interest (relative condition, C: N ratio, $\delta^{13}C$, age). The covariate of interest was treated as the response variable, while year and fork length were included as fixed effects. Waterbody and year were included as random effects to account for inter-annual and site-specific variability. One exception occurred when examining pre-and post-flood years in reference lakes for relative condition in Slimy Sculpin, where a linear model (ANCOVA) was used instead, due to convergence issues with the LMEM (Table A2.8). In this case, relative condition served as the response variable, while year and fork length were included as predictor variables. For $\delta^{15}N$, individual linear models (ANCOVAs) were applied for each species and each lake, with $\delta^{15}N$ as the response variable and year and fork length as the predictor variables. Due to data limitations, no comparisons of pre-and post-flood years in reference lakes were conducted for Ninespine Stickleback. The final model assessments for the covariates followed the same approach as outlined for [Hg].

To compare covariates of fish [Hg] between flooded and reference lakes in each post-flood year (2020 and 2021; approach #2), LMEMs were again applied with relative condition, C: N ratio, $\delta^{13}C$, $\delta^{15}N$, or age as the response variable. Exposure type (flooded vs. reference) and fork length were treated as fixed effects, while waterbody was included as a random effect. This model was applied to both Slimy Sculpin and Ninespine Stickleback for each individual post-flood year. Exceptions to this model included the 2021 relative condition analysis for both species, where a linear model (ANCOVA) was used instead (Table A2.8). In this case, exposure type and fork length were treated as fixed predictor effects, and relative

condition was the response variable. Additionally, in 2020, C: N in Slimy Sculpin was modeled using fork length in the random effects term of the model to account for random slopes (Table A2.8).

2.5.3 Water Chemistry

To complement analyses conducted on fish tissue, the percentage of MeHg (% MeHg) relative to total Hg in water, along with [THg], [MeHg], and [DOC], were analyzed using non-parametric Mann-Whitney U tests. These tests were performed using the "wilcox.test()" function in R. A non-parametric approach was selected due to the non-normal distribution of the data and the small sample size, ensuring that all comparisons followed a consistent analytical method. The Mann-Whitney U test is particularly suited for comparing differences between two independent groups when the assumptions required for parametric tests, such as normality, are not met.

Comparisons were made between the pre-flood year (2018) and each post-flood year (2020 and 2021) for both flooded and reference lakes (approach #1). For Hg, analyses were conducted on both filtered and unfiltered samples; however, only the filtered data are included in the results (Chapter 3), while the remaining data are available in the appendices. Filtered water samples were prioritized because they are considered more ecologically relevant in assessing the bioavailability of contaminants such as Hg. The dissolved fraction of Hg, captured in filtered samples, is more readily available for uptake by aquatic organisms (Eckley et al. 2022), making it the most meaningful measure for evaluating contaminant exposure. Unfortunately, water [Hg] data for 2019 were unavailable due to a contamination issue. Further comparisons of [THg], [MeHg], and [DOC], and % MeHg (for both unfiltered and filtered samples) were conducted between flooded and reference lakes for 2020 and 2021 (approach #2). In these post-flood years, data for two indices of DOC quality, SUVA and HIX, were available and were also compared between flooded and reference lakes to assess differences in DOC composition and potential influences of Hg transport and bioavailability.

Chapter 3: Results

3.1 Water Chemistry

As outlined previously, two analytical approaches were employed to address the objectives of this thesis. The first approach compared pre-flood (2018) and post-flood (2020 to 2021) data for both flooded and reference lakes. The second examined differences between flooded and reference lakes specifically during the post-flood years (2020 to 2021). These results of these analyses are presented below, and descriptive statistics for [THg], [MeHg], and % MeHg in water samples are provided in Table A3.1.

3.1.1 Comparisons of [Hg] in water among years and between flooded and reference lakes

Mercury concentrations in water appeared to increase after flooding, but evidence for flooding-induced increases in net methylation rates was mixed. When comparing concentrations between the pre-flood year (2018) and post-flood years (2019 to 2021) for the flooded lakes (approach #1), both [THg] (Mann-Whitney U test; W = 32, *p*-value = 0.00404) and [MeHg] (W = 32, *p*-value = 0.00836) were significantly higher in post-flood years than in the pre-flood year (Figures A3.2a and A3.3a, see supplementary Figures A3.1 and A3.4 for unfiltered results). However, the % of MeHg in filtered water samples from the flooded lakes did not show a significant difference between pre-and-post flood years (W = 27, *p*-value = 0.0727) (Figure A3.5a, see supplementary Figure A3.6 for unfiltered results). In the reference lakes, neither [THg] (W = 6, *p*-value = 0.286) nor [MeHg] (W = 4, *p*-value = 0.857) exhibited significant differences between pre-and post-flood years (Figure A3.2b and A3.3b, see supplementary Figures A3.7 and A3.8 for unfiltered results). Similarly, % MeHg in water from reference lakes remained unchanged among years (W = 0, *p*-value = 0.286) (Figure A3.5b, see supplementary Figure A3.9 for unfiltered results).

When comparing flooded and reference lakes during post-flood years (2020 to 2021; approach #2), filtered samples from flooded lakes had significantly higher [THg] (W = 43, *p*-value = 0.0127), [MeHg] (W = 48, *p*-value = 0.000666) and % MeHg (W = 48, *p*-value = 0.000666) compared to reference lakes (Figures A3.10, A3.11, A3.12, see supplementary Figures A3.13, A3.14, A3.15 for unfiltered results).

Overall, comparisons across years within both flooded and reference lakes, as well as comparisons between the flooded and reference lakes in post-flood years, indicate that flooding increased [THg] and [MeHg] in water. However, % MeHg was only significantly impacted by flooding when comparing flooded and reference lakes post-flooding, rather than over time within flooded lakes alone.

Table 2: Mean values for filtered [MeHg], % MeHg, and [THg] categorized by pre-flood (2018) and post-flood (2020 and 2021) years, and by exposure type (reference or flooded) of the study lakes. Data are presented as mean (standard deviation). Units are ng/L. NA indicates data is not available due to low sample size. No data was available for any parameter listed in 2019 (contamination issue).

Years	Exposure Type	n	% MeHg	MeHg	THg
Pre-Flood	Reference	1	2.918 (NA)	0.007 (NA)	0.281 (NA)
Pre-Flood	Flooded	4	5.227 (2.828)	0.009 (0.004)	0.217 (0.119)
Post-Flood	Reference	6	1.326 (0.193)	0.01 (0.005)	0.744 (0.338)
Post-Flood	Flooded	8	13.976 (8.409)	0.21 (0.169)	1.603 (0.594)

3.2 Analyses of Fish Tissue

Fish data were analyzed using the same two broad approaches applied to the water analysis to address the objectives of this thesis. The first approach compared pre-flood years (2018 and 2019) with post-flood years (2020 and 2021) for both flooded and reference lakes. The second approach examined differences between flooded and reference lakes, specifically during the post-flood years (2020 and 2021). [Hg] in both fish Slimy Sculpin and Ninespine Stickleback, across exposure types (flooded vs reference lakes), and sampling years, are illustrated in Figure 3.

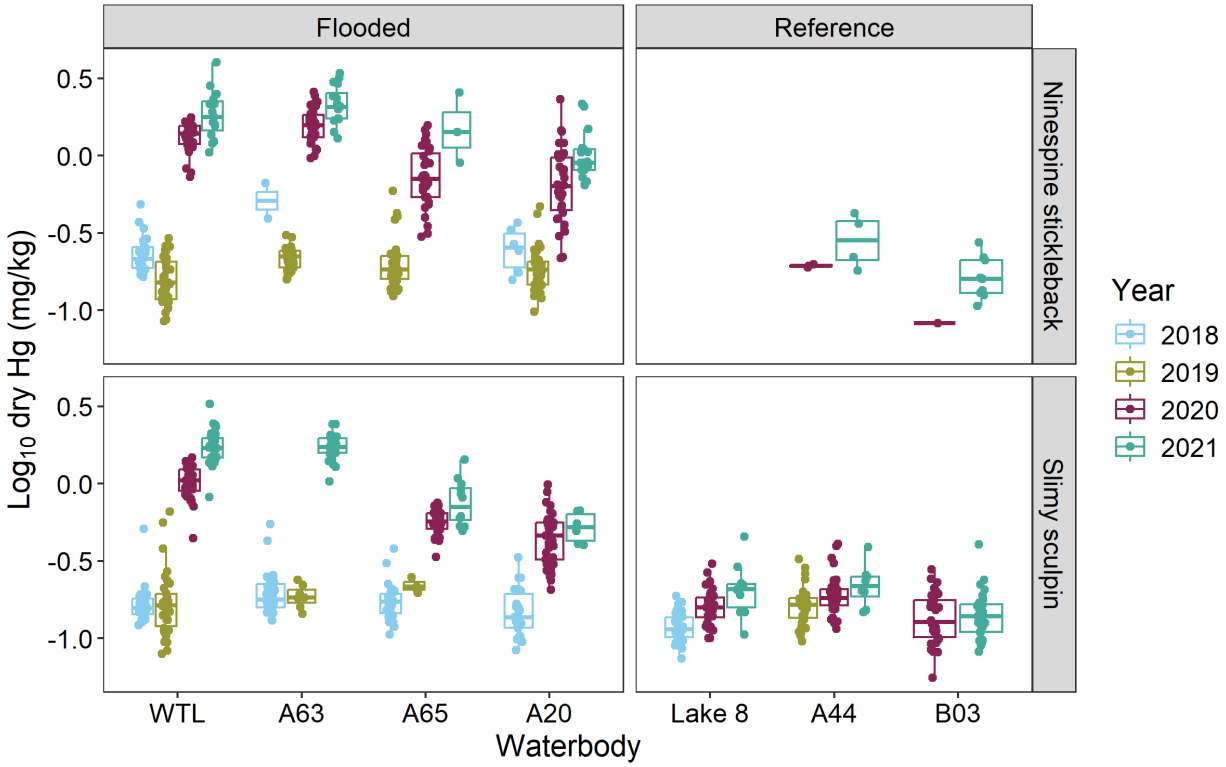


***Figure 3:** Log₁₀ dry Hg concentrations for Slimy Sculpin and Ninespine Stickleback collected at flooded and reference lakes from 2018 to 2021. Boxplots indicate the median, 25th and 75th percentiles, and minimum and maximum values within 1.5x the interquartile range. All individual data points are plotted. Flooding occurred in 2019.*

3.2.1 Slimy Sculpin

3.2.1.1 [Hg] Comparisons Among Years

In flooded lakes, lake-specific mean [THg] in Slimy Sculpin was higher in post-flood years than in pre-flood years and ranged from 0.18 to 1.8 mg/kg dry weight (dw) in 2020 and 2021, compared to 0.16 to 0.22 mg/kg dw in 2018 and 2019. [Hg] were higher in 2021 than in 2020 (Table A3.2), with the higher concentrations observed in WTL and A63, and lower concentrations observed in A65 and A20 (Figure 3). Results from a mixed model, which included year and fork length as fixed factors and lake as a random effect, indicated that [Hg] differed significantly among years (LMEM; $F_{3,261.71}$,=14.53, $p < 0.001$). [Hg] were also significantly and positively related to fork length across all years of the study (LMEM; $F_{1,333.07}$ = 22.66, $p < 0.001$)), with a significant interaction between year and fork length (LMEM; $F_{3,332.35}$ = 5.40, p = 0.001). Due to the significant interaction between year and fork length, post-hoc pairwise comparisons were conducted at a standardized fork length of 48 mm (the mean value for the dataset). At this fork length, [Hg]

in Slimy Sculpin muscle tissue did not differ significantly between the two pre-flood years (2018 and 2019) or between the two post-flood years (2020 and 2021). However, all other pairwise comparisons between pre-flood and post-flood years were significant, indicating a clear increase in [Hg] following flooding (Figure 2a).

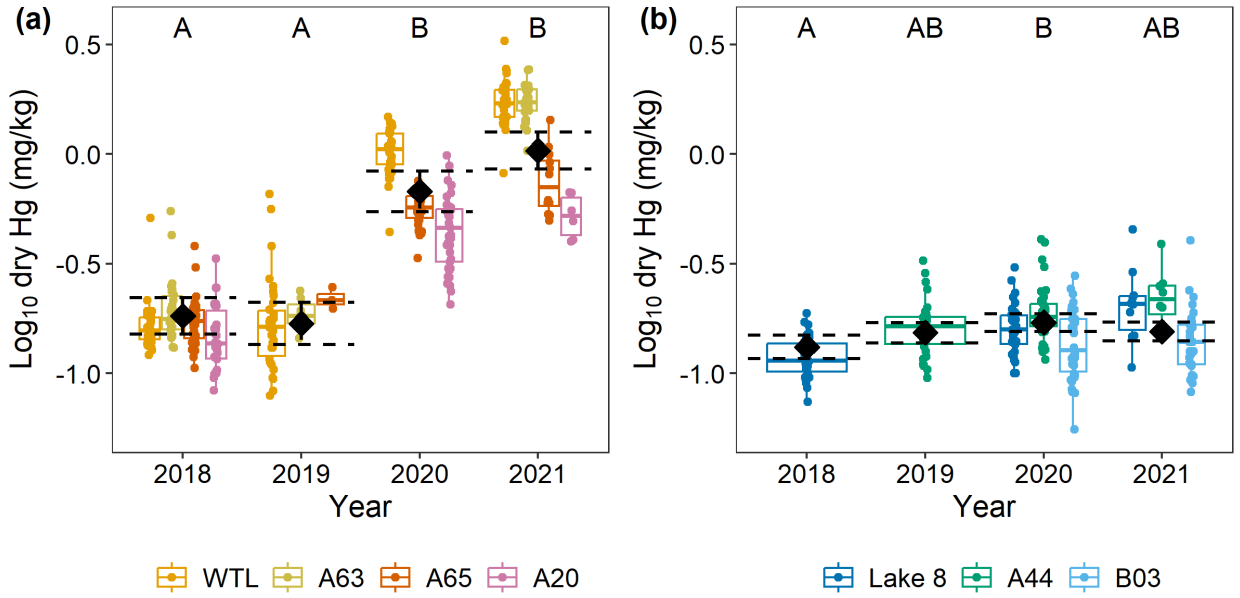


***Figure 4:** Log_{10} dry Hg concentrations in (a) flooded and (b) reference lakes from 2018 to 2021. Boxplots show data for each waterbody. Black diamonds and error bars (dashed line) depict estimated marginal mean Hg concentrations ± standard error at a fork length of 48 mm in each exposure category. Significant pairwise differences are indicated by dissimilar letters.*

In reference lakes (A44, B03, LK8), mean muscle [THg] were 0.12 mg/kg in 2018, and 0.17 mg/kg in 2019 (pre-flood years), increasing to 0.16 mg/kg in 2020 and 0.22 mg/kg in 2021 (post-flood years) (Table A3.2). Similar to the patterns observed in flooded lakes, [Hg] in SLSC muscle tissue from reference lakes varied significantly among years (LMEM; $F_{3,205.71} = 3.05$, $p = 0.030$), and was significantly and positively related to fork length (LMEM; $F_{1,205.15} = 80.9$, $p < 0.0010$). A significant interaction between fork length and year was also detected (LMEM; $F_{3,205.67} = 3.11$, $p = 0.028$), prompting post-hoc pairwise comparisons adjusted to a standardized fork length of 48 mm (dataset average). Unlike the consistent post-flood increases in [Hg] observed in flooded lakes, Slimy Sculpin from reference lakes did not exhibit a clear difference between pre-and-post flood years (Figure 4b). The only significant pairwise difference occurred between 2018 and 2020 (post-hoc; t = -2.79, $p = 0.030$; Table A3.4). This difference was likely influenced, at least in part, by the smaller average fish sizes captured in 2018 compared to the other years (Figure A3.16). Although [Hg] values were length-adjusted, these adjustments were based on year-specific slopes between [Hg] and fork length, which are influenced by the size distribution of sampled fish in that

year. Because the range of sizes in 2018 was narrower than in other years, the estimated slope was shallower, resulting in a lower length-adjusted mean (Figure A3.16).

3.2.1.2 [Hg] comparisons between flooded and reference lakes in the post-flood years (2020 and 2021)

In the post-flood years (2020 and 2021), mean [Hg] in Slimy Sculpin were significantly higher in flooded lakes than in reference lakes (Figure 3 bottom, Table A2.4). The highest lake-specific mean [Hg] observed in flooded lakes was 1.0 mg/kg dw in 2020 and 1.8 mg/kg dw in 2021, whereas in reference lakes, mean [Hg] remained below 0.25 mg/kg dw in both years (Table A3.2). Mixed-effect models conducted separately for 2020 and 2021, with exposure (flooded vs. reference) and fork length as fixed factors and lake as a random factor, confirmed that [Hg] was significantly higher in flooded lakes than in reference lakes (LMEM; 2020: $F_{1,132.5} = 25.9$, $p < 0.0010$; 2021: $F_{1,90.9} = 37.9$, $p < 0.0010$) (Figure 5a, 5b). Mercury concentrations also increased significantly with fork length in both years ($F_{>1,118.0} \geq 24.8$, $p < 0.00010$), and a significant interaction between fork length and exposure type was detected (LMEM; 2020: $F_{1,200.20} = 11.7$, $p < 0.0010$, 2021: $F_{1,118.0} = 21.8$, $p < 0.0010$). Given the significant interaction between fork length and exposure, post-hoc comparisons were conducted at a standardized fork length of 48 mm, which closely matched the dataset mean and minimized extrapolation. At this standardized length, [Hg] in Slimy Sculpin was significantly higher in flooded lakes than in reference lakes in both post-flood years (Tukey's test; 2020: $t = 5.24$, $p = 0.0060$; 2021: $t = 5.07$, $p = 0.0050$).

Overall, comparisons between flooded and reference lakes in post-flood years, as well as among-year comparisons within each exposure type, indicate that flooding significantly increased [Hg] in Slimy Sculpin.

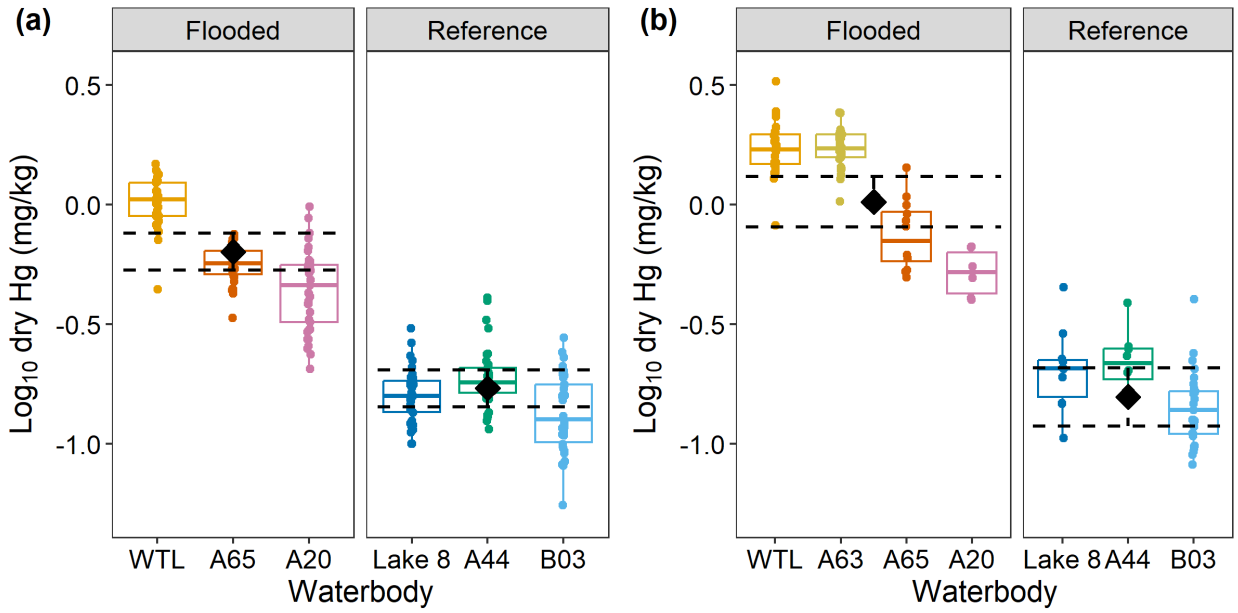


Figure 5: ***Log_{10} dry Hg concentrations in Slim Sculpin at flooded and reference lakes in (a) 2020 and (b) 2021. Boxplots show data for each waterbody. Black diamonds and error bars (dashed line) depicted estimated marginal mean Hg concentrations ± standard error at a fork length of 48 mm for each exposure category. Hg concentration was significantly higher in flooded lakes than reference lakes in both 2020 and 2021 (2020: $F_{1,132.5}$=25.9, p <0.0010; 2021: $F_{1,90.9}$ = 37.9, p < 0.0010).***

3.2.1.3 Relationships between fish [Hg] and covariates

In flooded lakes, [Hg] in Slimy Sculpin were significantly correlated with $\delta^{13}C$, C: N ratio, age, and relative condition (Table 3), with the strongest relationship observed between [Hg] and $\delta^{13}C$ (Table 3). As anticipated, [Hg] was negatively correlated with both $\delta^{13}C$ and relative condition, indicating that fish relying on more pelagic and/or terrestrially derived carbon sources tended to have higher [Hg] and those in better condition tended to have lower [Hg]. Conversely, [Hg] was positively correlated with age, consistent with the expected pattern of Hg bioaccumulation over time. Unexpectedly, a positive correlation was also observed between [Hg] and C: N ratio (Table 3), suggesting that fish with higher lipid content or greater carbon accumulation relative to nitrogen exhibited higher [Hg].

Table 3: ***Results of Pearson's correlation analyses between [Hg] in Slimy Sculpin tissue and each of several statistically significant covariates in flooded lakes (all years of data included).***

Variable 1	Variable 2	Pearson's r	*p*	n
logdryHg	$\delta^{13}C$	-0.72612	<0.0001	345
logdryHg	C: N	0.22203	<0.0001	345
logdryHg	Age	0.12360	0.02205	343
logdryHg	Relative Condition	-0.17729	0.00094	345

Results from mixed-effects models and post-hoc analyses suggest that flooding-induced changes in carbon source, as indicated by $\delta^{13}C$, may have contributed to the observed increase in [Hg] in Slimy Sculpin between pre- and post-flood years. As previously reported, [Hg] in Slimy Sculpin was significantly higher in post-flood years than in pre-flood years, and [Hg] was negatively correlated with $\delta^{13}C$ in flooded lakes. $\delta^{13}C$ ratios differed significantly among years (LMEM; $F_{3,315.28} = 20.1$, $p < 0.00010$), with values in post-flood years being more depleted than those in pre-flood years (Figure 6a). Because $\delta^{13}C$ was significantly related to fork length ($F_{1,334.09} = 8.49$, $p = 0.0040$) and there was a significant interaction between fork length and year ($F_{3,333.3} = 18.7$, $p < 0.0010$), post-hoc pairwise comparisons were conducted at a standardized fork length of 48 mm (dataset mean). Most pairwise comparisons between years were significant, including 2018 vs. 2019 (t = 3.25, $p = 0.050$), 2018 vs. 2020 (t = 8.31, $p < 0.0010$), 2018 vs. 2021 (t = 9.26, $p = 0.0020$), 2019 vs. 2020 (t = 3.92, $p = 0.022$), and 2019 vs. 2021 (t = 4.56, $p = 0.0080$), but there was no significant difference between the two post-flood years, 2020 and 2021 (t= 0.390, $p = 0.98$), suggesting that $\delta^{13}C$ depletion may have stabilized after the initial flood impact. In reference lakes, $\delta^{13}C$ also exhibited significant variation across years (LMEM; $F_{3,197.79} = 4.72$, $p = 0.0030$), but unlike in flooded lakes, no significant pairwise differences among years were detected at the standardized fork length of 48 mm ($|t| < 1.54$, $p > 0.49$) (Figure 6b). As declines in $\delta^{13}C$ were not observed in reference lakes after flooding, the results suggest that flooding led to a shift toward more depleted $\delta^{13}C$ in Slimy Sculpin.

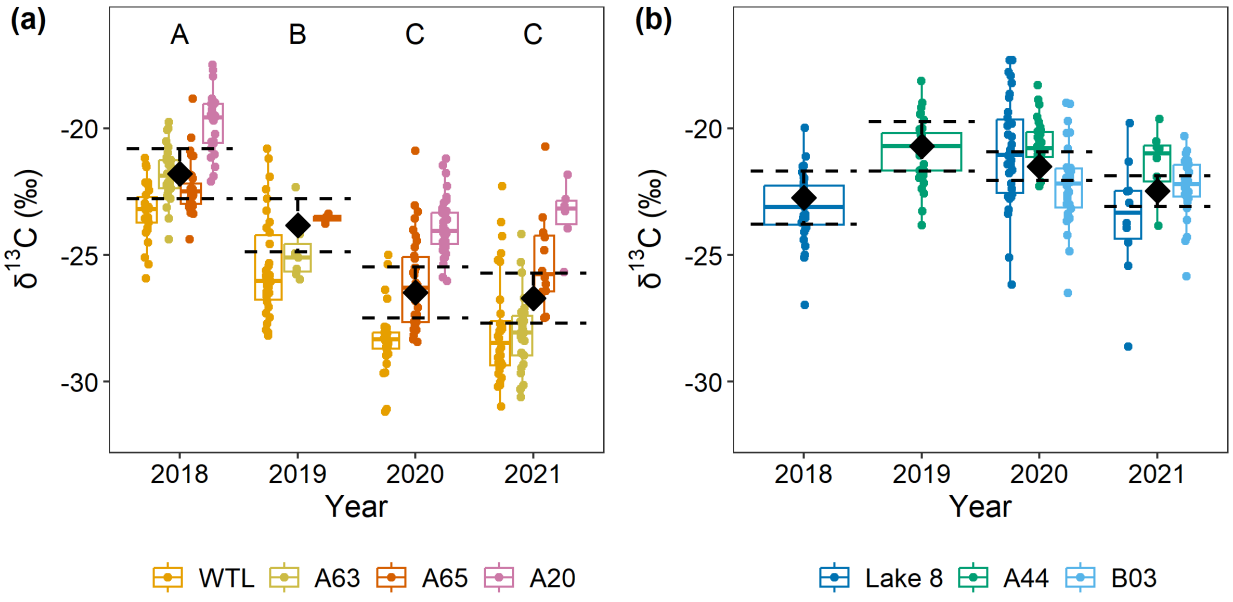


Figure 6: ***$\delta^{13}C$ in Slimy Sculpin at (a) flooded lakes and (b) reference lakes from 2018 to 2021. Boxplots show data for each waterbody. Black diamonds and error bars (dashed line) depict estimated marginal mean for $\delta^{13}C$ ± standard error for each year. Significant pairwise differences between years are indicated by different letters.***

Age, C: N ratio, and relative condition were also (in addition to $\delta^{13}C$) all significantly correlated with [Hg] in Slimy Sculpin from flooded lakes; however, mixed model analyses comparing these variables across years suggest that only a decline in relative condition may be linked to the observed increase in [Hg] post-flooding.

When Slimy Sculpin age was modeled as a function of length, year, and their interaction, the interaction term was significant (LMEM; $F_{3,332.56} = 2.99$, $p = 0.031$), indicating that the age-length relationship varied significantly among years. Pairwise comparisons at a standardized length of 48 mm (dataset average) revealed significant differences in age between 2018 and 2021 and between 2019 and 2021 ($t > 3.36$, p-value < 0.025). However, the estimated age-at-length for 48 mm fish was significantly younger in 2021 compared to 2018 and 2019 (Table A3.5). Given that the correlation between age and [Hg] was positive, the observed increase in [Hg] post-flooding cannot be explained by slower growth rates. Additionally, in both post-flood years, mean age (adjusted for length) did not differ significantly between flooded and reference lakes (LMEM; 2020: $F_{1,3.98} = 2.17$, $p = 0.21$; 2021: $F_{1,4.82} = 1.18$, $p = 0.33$).

Although C N ratios differed significantly among years in an overall comparison (LMEM; $F_{3,321.68} = 5.52$, $p = 0.0010$), pairwise differences between individual years were not significant when tested at a standardized fork length of 48 mm ($t < -0.29$, $p > 0.18$). For C:N ratios to explain the increase in [Hg] in Slimy Sculpin post-flooding, C: N values would have needed to increase after flooding, given that the relationship between [Hg] and C: N was positive (Table 3). However, no such increase was observed, even when assessed qualitatively (Figure A3.17).

Relative condition was significantly and negatively correlated with [Hg] in Slimy Sculpin and differed significantly among years (LMEM, $F_{3,325.768} = 5.56$, $p = 0.0010$). Post-hoc pairwise comparisons at a standardized fork length of 48 mm revealed significant differences between 2021 and each of the other years ($t \geq 3.33$, $p = 0.033$; Figure 7a), while no other pairwise differences were significant ($|t| < 1.04$, $p \geq 0.81$). Although it is possible that flooding led to a delayed decrease in relative condition (by one year), which in turn contributed to increased [Hg], this explanation seems unlikely because a similar decline in relative condition was also observed in reference lakes in 2021 (Figure 7b). In reference lakes, relative condition differed significantly among years (LMEM; $F_{3,208} = 9.30$, $p < 0.00010$), and post hoc comparisons at a standardized size of 48 mm showed that, similar to trends in the flooded lakes, the only significant pairwise differences were between 2021 and each of the other years ($t \geq 2.94$, $p \leq 0.019$), whereas no other pairwise differences were significant ($|t| \leq 1.43$, $p \geq 0.48$).

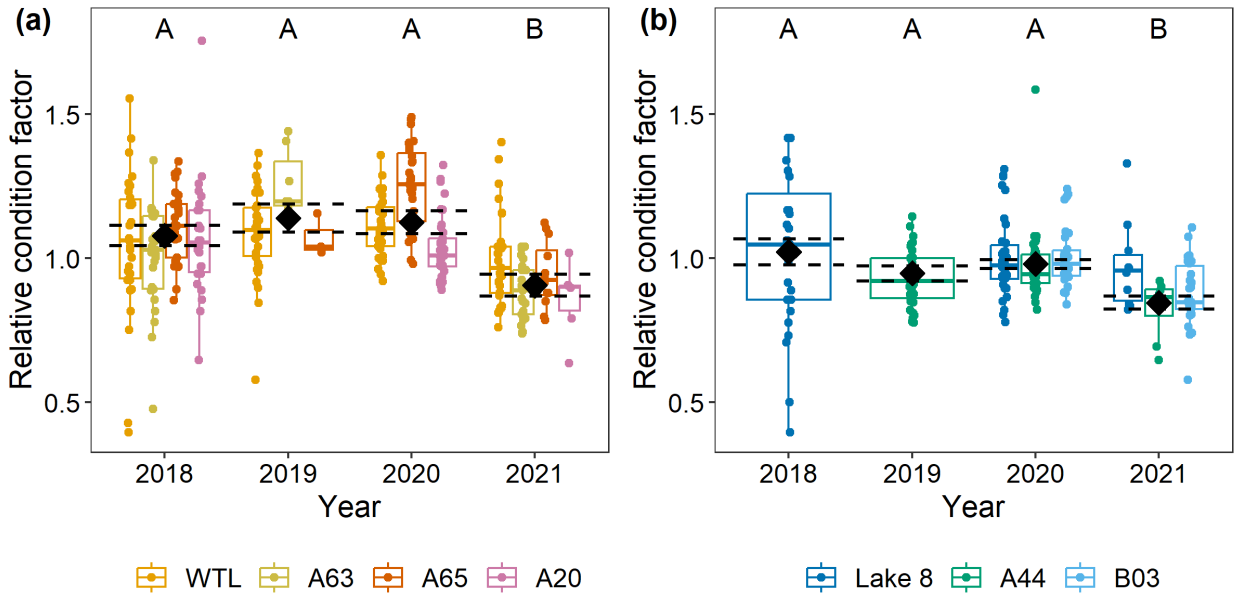


Figure 7: ***Relative condition in Slimy Sculpin at (a) flooded lakes and (b) reference lakes from 2018 to 2021. Boxplots show data for each waterbody. Black diamonds and error bars (dashed line) depict estimated marginal mean relative condition ± standard error for each year. Significant pairwise differences between years are indicated by different letters. (Note, flooded lakes were analyzed with a LMEM, whereas reference lakes could not be analyzed with a LMEM so were analyzed with an ANCOVA without random effects).***

Post-flood increases in [Hg] in Slimy Sculpin did not appear to be driven by flooding-induced changes in $\delta^{15}N$. While $\delta^{15}N$ differed among years in some lake-specific ANCOVAs (Table A3.3), pairwise comparisons of length-adjusted $\delta^{15}N$ did not indicate a consistent or significant increase in $\delta^{15}N$ across all or most flooded lakes in post-flood years (Table A3.4). The only lake where a clear pattern of higher $\delta^{15}N$ post-flood was observed was A63 (Figure A3.18; Table A3.4).

Among the covariates examined, $\delta^{13}C$ appears to be most strongly linked to flooding-induced increases in [Hg]. [Hg] in Slimy Sculpin were significantly and negatively correlated with $\delta^{13}C$ in flooded lakes (Table 3), and $\delta^{13}C$ values in Slimy Sculpin generally declined after flooding in flooded lakes, but remained unchanged in reference lakes (Figure 6a, 6b). Additionally, $\delta^{13}C$ in Slimy Sculpin was significantly more depleted in flooded lakes than in reference lakes during post-flood years (2020 and 2021) (LMEM; $F_{\geq 1,3.99} \geq 13.7$, $p \leq 0.019$; Figure 8a, 8b).

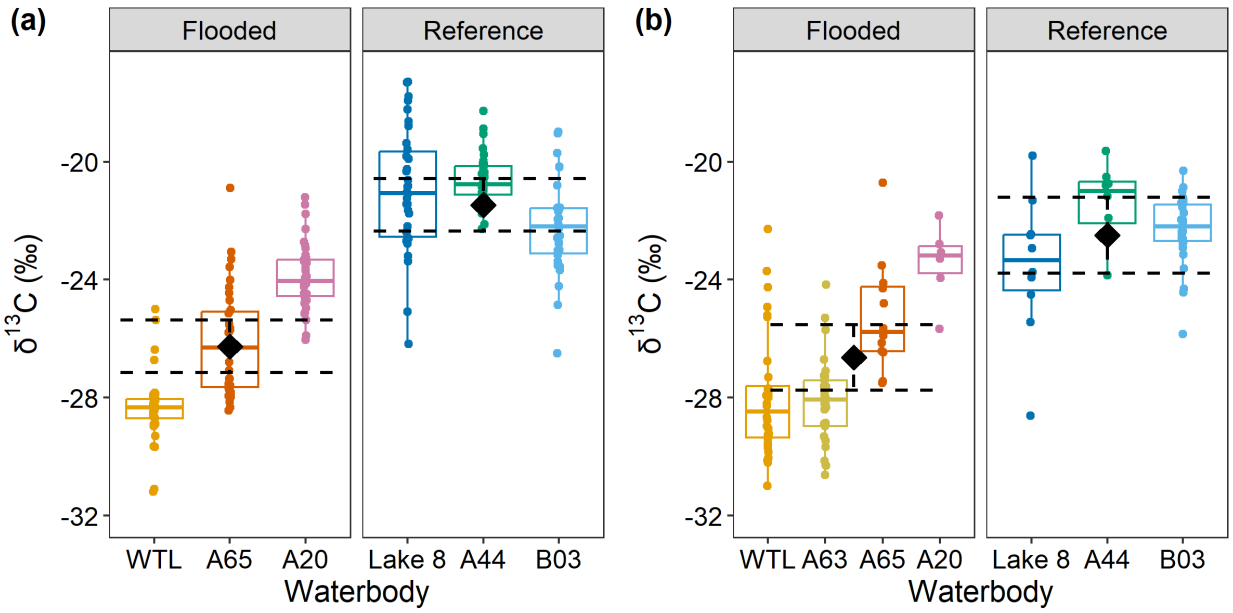


Figure 8: ***δ ^{13}C in Slimy Sculpin from flooded and reference lakes in post-flood years (a) 2020 and (b) 2021. Boxplots show data for each waterbody. Black diamonds and error bars (dashed line) depict estimated marginal mean δ^{13}C ± standard error for each year at a fork length of 48 mm. δ^{13}C was significantly more depleted in flooded lakes (F>1,3.99 > 13.662, p < 0.019) in 2020. In 2021, the omnibus test showed a significant difference in δ ^{13}C between flooded and reference lakes, but at a fork length of 48 mm, there was no significant difference.***

3.2.2 Ninespine Stickleback

3.2.2.1 [Hg] Comparisons Among Years

In flooded lakes (A20, A63, A65, WTL), mean [Hg] in Ninespine Stickleback were well below 0.1 mg/kg dw in pre-flood years (2018 and 2019), and ranged from 0.1 to 0.4 mg/kg dw in post-flood years (2020 and 2021) (Table A3.2). Similar to the patterns observed for Slimy Sculpin, the highest [Hg] were found in WTL and A63, while lower concentrations were observed in A65 and A20 (Figure 3). Results from an LMEM, which included year and fork length as fixed factors and lake as a random factor, indicated that [Hg] differed significantly among years (LMEM; $F_{3,11.06}$ = 34.0, p < 0.0010). However, unlike Slimy Sculpin, [Hg] in Ninespine Stickleback was not significantly correlated with fork length ($F_{1,10.70}$ = 3.21, p = 0.10). Post-hoc comparisons showed significant differences in [Hg] between pre-flood and post-flood years, with increases observed between 2018 and 2020 (t = -4.61, p = 0.0030), 2018 and 2021 (t = -6.66, p < 0.0010), 2019 and 2020 (t = -6.54, p < 0.0010), and 2019 and 2021 (t = -9.05, p < 0.0010), indicating that [Hg] levels were significantly higher in post-flood years (Figure 9). Pairwise comparisons between the two pre-flood years (2018 and 2019) and the two post-flood years (2020 and 2021) were not significant (Figure 9), suggesting that [Hg] remained consistently elevated in post-flood years. Since [Hg] data for Ninespine

Stickleback from reference lakes were not available prior to flooding, pre-vs. post-flood comparisons could not be conducted for reference lakes.

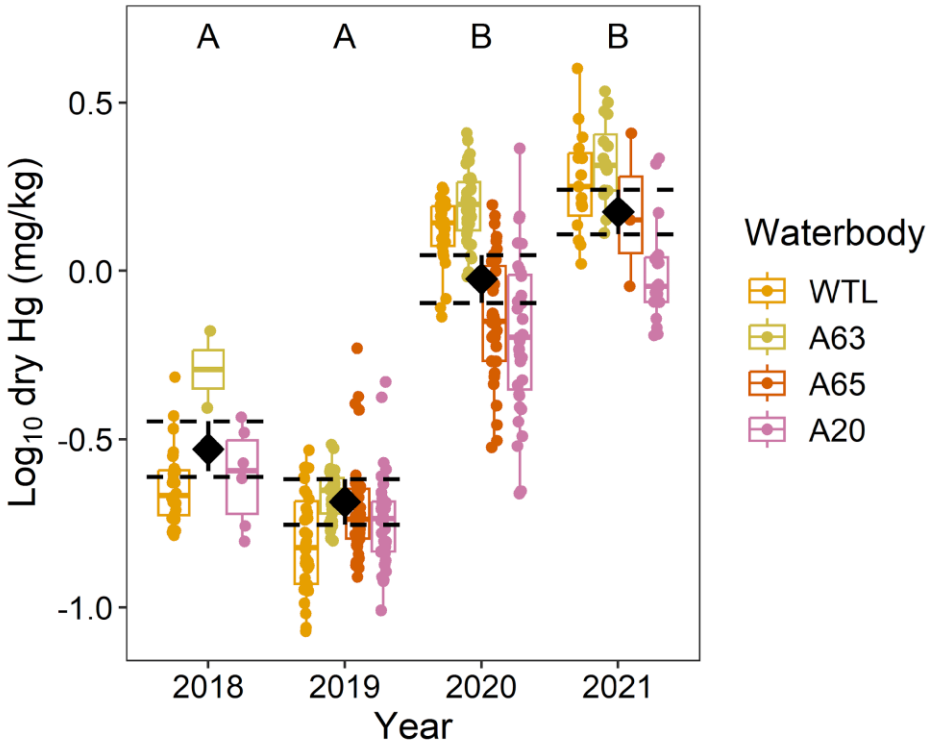


***Figure 9:** Log_{10} dry Hg concentrations for Ninespine Stickleback between 2018 and 2021 in flooded lakes. Black diamonds and error bars (dashed line) show estimated marginal means ± standard error calculated at a fork length of 50 mm. Significant pairwise differences between years are indicated by different letters.*

3.2.2.2 [Hg] Comparisons between flooded and reference lakes in the post-flood years (2020 and 2021)

Sample sizes for Ninespine Stickleback from reference lakes were very limited, restricting the scope of statistical analysis. In 2020, [Hg] data were only available for two reference lakes (A44 and B03), with sample sizes of just one and three fish, respectively. A qualitative, visual assessment suggests that mean [Hg] were higher in flooded lakes than in reference lakes in both 2020 and 2021 (Table A3.2; Figure 3), but due to low sample sizes, statistical analyses were only conducted on 2021 data. Results from LMEM for 2021 indicated that [Hg] in Ninespine Stickleback was significantly higher in flooded lakes than in reference lakes (LMEM; $F_{1,4.13} = 45.1$, $p = 0.0020$; Figure 10). Additionally, [Hg] was significantly related to fork length (LMEM; $F_{1,59.55} = 7.01$, $p = 0.010$), suggesting that larger fish exhibited higher [Hg].

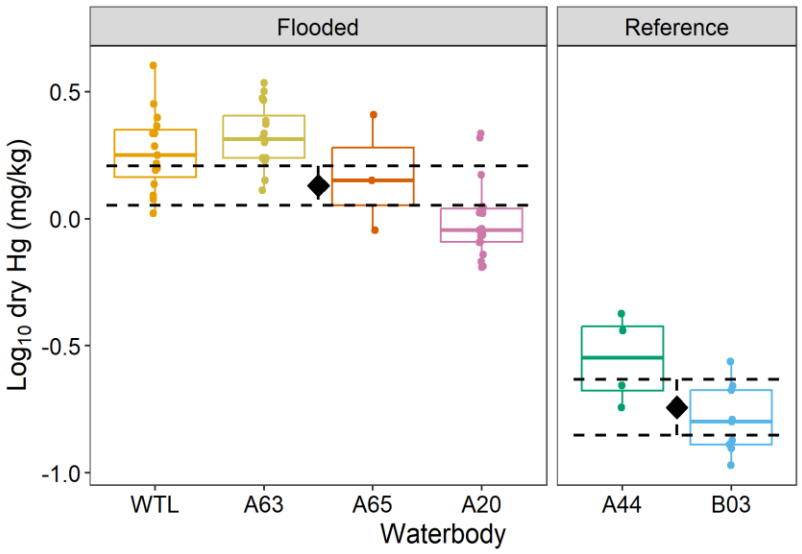


Figure 10: ***Log$_{10}$ dry Hg concentration for Ninespine Stickleback at flooded and reference lakes in 2021. Boxplots show data for each lake. Black diamonds and error bars (dashed line) show estimated marginal means ± standard error calculated at a fork length of 50 mm. Mercury concentrations in Ninespine Stickleback from flooded lakes were significantly higher than Hg concentrations in Ninespine Stickleback from reference lakes ($F_{1,4.13}$ = 45.1, p = 0.0020).***

Overall, comparisons between flooded and reference lakes in post-flood years, as well as among-year differences in flooded lakes, indicate that flooding contributed to increases [Hg] in Ninespine Stickleback.

3.2.2.3 Correlations between fish [Hg] and covariates

In the flooded lakes, [Hg] in Ninespine Stickleback was significantly correlated with $\delta^{13}C$, C: N ratio, and relative condition (Table 4). Due to limited sample sizes, analyses involving age could not be conducted. As observed in Slimy Sculpin, the strongest correlation was between [Hg] and $\delta^{13}C$ (Table 4). Correlations between [Hg] and each of $\delta^{13}C$ and relative condition were negative, whereas similar to what was observed for Slimy Sculpin, the correlation between [Hg] and C: N was unexpectedly positive (Table 4). Results of mixed model and post-hoc analyses suggest that, similar to Slimy Sculpin, differences in Ninespine Stickleback [Hg] pre- vs. post-flooding may be associated with flooding-induced shifts in carbon source (as indicated by $\delta^{13}C$) and changes in relative condition. However, the evidence for Ninespine Stickleback is not as strong as for Slimy Sculpin, likely due to more limited data for this species.

Table 4: ***Results of Pearson's correlation analyses between [Hg] in Ninespine Stickleback tissue and each of several statistically significant covariates in flooded lakes (all years of data included).***

Variable 1	Variable 2	Pearson's r	*p*	n
logdryHg	$\delta^{13}C$	-0.63730	<0.0001	382
logdryHg	C: N	0.14760	0.00384	382
logdryHg	Age	0.04091	0.42953	375
logdryHg	Relative condition	-0.24095	<0.0001	380

$\delta^{13}C$ in Ninespine Stickleback differed significantly among years in flooded lakes (LMEM; $F_{3,367.33} = 5.38$, $p = 0.0010$), with more depleted values in post-flood years compared to pre-flood years (Figure 11). Because $\delta^{13}C$ was significantly related to fork length ($F_{1,337.48} = 4.36$, $p = 0.038$) and there was a significant interaction between fork length and year ($F_{3,369.61} = 7.80$, $p < 0.0010$), post-hoc comparisons were conducted at a standardized fork length of 50 mm (dataset mean). At this standardized size, all pairwise comparisons among years were significant ($|t| > 3.23$, $p \leq 0.040$). Size-standardized $\delta^{13}C$ ratios were more similar within pre-flood (2018-2019) and post-flood (2020-2021) years than across pre-flood and post-flood year comparisons, with post-flood years consistently showing more depleted $\delta^{13}C$ values (Figure 11). Since $\delta^{13}C$ data for Ninespine Stickleback were not available from reference lakes prior to flooding, pre- vs. post-flood comparisons were not possible for reference lakes. Unlike what was observed for Slimy Sculpin, $\delta^{13}C$ in Ninespine Stickleback did not differ significantly between flooded and reference lakes in 2021, the only year for which comparative data were available (LMEM; $F_{1,4.23} = 0.40$ $p = 0.56$). While it is thus possible that flooding-induced declines in $\delta^{13}C$ contributed to increased [Hg] in Ninespine Stickleback, the evidence for this correlation and mechanism is weaker than what was observed for Slimy Sculpin.

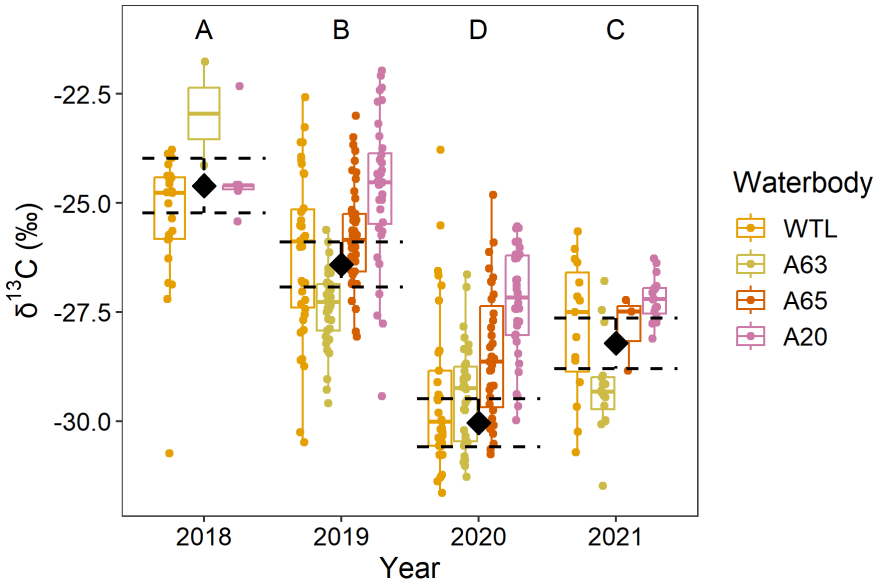


Figure 11: ***$\delta^{13}C$ for Ninespine Stickleback between 2018 and 2021 in flooded lakes. Black diamonds and error bars (dashed line) show estimated marginal means $\delta^{13}C \pm$ standard error calculated at a fork length of 50 mm. Significant pairwise differences between years are indicated by different letters.***

C: N ratio and relative condition were both significantly correlated with [Hg] in Ninespine Stickleback from flooded lakes (Table 4). However, mixed model analyses comparing these variables across years suggest that, similar to Slimy Sculpin, only a decline in relative condition may be associated with the observed increase in [Hg] post-flooding. C: N ratios in Ninespine Stickleback differed significantly among years (LMEM; $F_{3,371,79} = 8.80$, $p < 0.0010$). Post-hoc comparisons at a standardized fork length of 50 mm (minimizing extrapolation) revealed that C: N ratios in 2018 were significantly lower than in all other years ($|t| \geq 4.73$, $p \leq 0.0010$), but no other pairwise differences were significant ($|t| \leq 0.28$, $p \geq 0.99$) (Figure A3.19). This pattern does not align with expectations for flooding-induced changes in C: N and therefore does not explain the increase in [Hg] in Ninespine Stickleback post-flooding. Following a major flooding event, we would typically expect C: N ratios to increase due to a dietary shift toward more carbon-rich, terrestrial organic matter and/or reductions in protein-rich autochthonous food sources (Lau et al. 2009; Wilcox et al. 2011). Additionally, because the correlation between [Hg] and C: N was positive, flooding-related increases in [Hg] would require a corresponding increase in C: N ratios post-flood, which was not consistently observed. In 2021, the only year for which a direct comparison between flooded and reference lakes was possible, C: N ratios did not differ significantly between exposure types at the standardized fork length of 50 mm ($t = 0.0060$, $p = 0.99$) (Figure A3.20). Therefore, flooding-induced increases in [Hg] in Ninespine Stickleback do not appear to be mediated by changes in C: N ratios.

The correlation between [Hg] and relative condition for Ninespine Stickleback was negative (Table 4) and may have contributed to flooding-induced increases in [Hg], though the evidence remains limited. Relative condition varied significantly among years (LMEM; $F_{3,371.02} = 5.56$, $p = 0.0010$), with higher values observed in the two pre-flood years (2018 and 2019) compared to the two post-flood years (2020 and 2021) (Figure 12, Table A3.5). At a standardized fork length of 50 mm (minimizing extrapolation), pairwise comparisons indicated significant differences in relative condition between 2019 and each of 2020 and 2021 ($t \geq 3.62$, $p \leq 0.010$). However, comparisons between 2018 and the post-flood years were not significant ($t \leq 1.55$, $p \geq 0.43$). Significant differences were also not observed between the two pre-flood years or between the two post-flood years ($|t| \leq 2.22$, $p \geq 0.16$) (Figure 12). In 2021, the only year for which a direct comparison between flooded and reference lakes was available, relative condition did not significantly differ between exposure types (ANCOVA; $F_{1,62} = 0.020$, $p = 0.88$) (Figure A3.21).

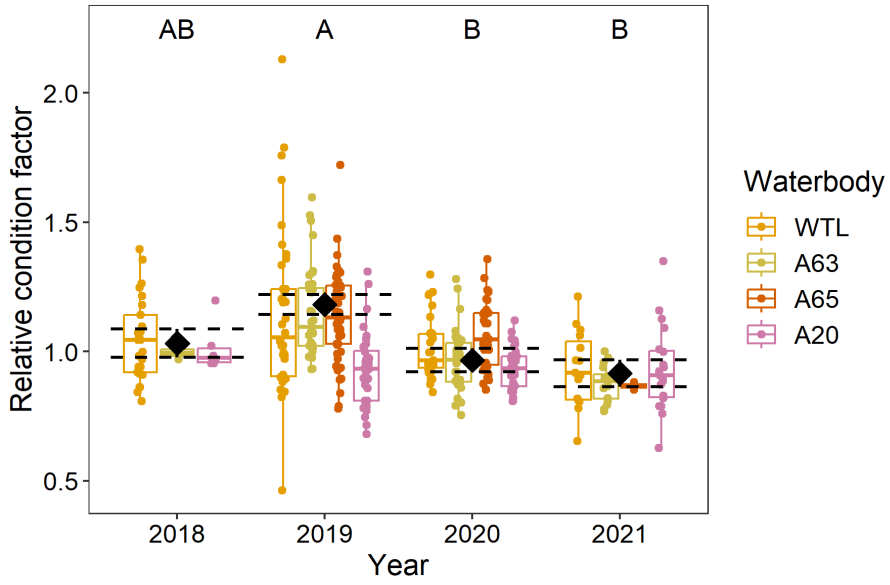


***Figure 12:** Relative condition for Ninespine Stickleback between 2018 and 2021 at flooded lakes. Boxplots show data for each lake. Black diamonds and error bars (dashed line) show estimated marginal mean relative condition factor ± standard error calculated at a fork length of 50 mm. Significant pairwise differences between years are indicated by different letters.*

There was little evidence to suggest that post-flood increases in [Hg] in Ninespine Stickleback were linked to elevated $\delta^{15}N$. While $\delta^{15}N$ differed significantly among years in three of the four flooded lakes (A20, A63, and A65; ANCOVA; $F_{>2,80} \geq 3.97$, $p \leq 0.0040$); there was no significant variation in $\delta^{15}N$ across years in WTL (ANCOVA; $F_{3,105} = 1.96$, $p = 0.12$). Post-hoc comparisons at a standardized fork length of 50 mm (minimizing extrapolation) showed that $\delta^{15}N$ ratios were not consistently or significantly higher in post-flood years compared to pre-flood years (Table A3.5). While some significant differences were detected between specific pre- and post-flood years in A20, A63, and A65, similar differences were also

observed between the two post-flood years. In some cases, $\delta^{15}N$ ratios were actually higher in pre-flood years than in post-flood years (Table A3.5), suggesting no clear post-flood increase in trophic position.

Among the covariates analyzed, $\delta^{13}C$ appears to be the most likely factor associated with flooding-induced increases in [Hg]. [Hg] in Ninespine Stickleback were significantly and negatively correlated to $\delta^{13}C$ in flooded lakes (Table 4), and $\delta^{13}C$ values in Ninespine Stickleback generally declined after flooding (Figure 11). However, unlike Slimy Sculpin, $\delta^{13}C$ in Ninespine Stickleback did not differ significantly between flooded and reference lakes in the only year with comparative data available (2021; LMEM; $F_{1,4.23} = 0.40$ $p = 0.56$). While it is possible that flooding-induced declines in $\delta^{13}C$ contributed to increased [Hg] in Ninespine Stickleback, the evidence supporting this correlation is weaker that what was observed for Slimy Sculpin.

3.3 Additional Water Chemistry Analyses

Because $\delta^{13}C$, a key indicator of changes in carbon changes (Post et al., 2000; Post, 2002), was the most likely covariate affecting increased [Hg] in Slimy Sculpin and, to a lesser extent, Ninespine Stickleback following the flooding event, analyses of additional water quality parameters related to carbon quantity and quality were conducted. Concentrations of DOC, HIX, and SUVA were examined to further investigate potential shifts in carbon sources due to flooding. When comparing [DOC] in water between pre-flood (2018) and post-flood years (2020 to 2021) in flooded lakes, no significant difference was detected (W = 27, *p*-value = 0.073) (Figure A3.22a). Similarly, no significant difference in [DOC] was observed in reference lakes over the same period (W = 1, *p*-value = 0.57) (Figure A3.22b). However, when comparing flooded and reference lakes during post-flood years (2020 to 2021), [DOC] was significantly higher in flooded lakes than in reference lakes (W = 48, *p*-value = 0.00066) (Figure A3.23). Comparisons of HIX and SUVA between pre-flood and post-flood years were not possible, as pre-flood data for these parameters were unavailable. HIX1999 (W = 34, *p*-value = 0.23), HIX2002 (W = 43, *p*-value = 0.23) (Figure A3.24), and SUVA (W = 36, *p*-value = 0.14) (Figure A3.25) did not differ significantly between flooded and reference lakes in post-flood years.

Overall, [DOC] in water appeared to be influenced by flooding in post-flood years, whereas HIX and SUVA did not show significant changes. This indicates that the amount of DOC increased in lakes, likely as a result of flooding, but that the quality of that carbon (i.e., labile vs. recalcitrant) did not change.

Table 5: Mean water chemistry values for [DOC], HIX 1999, HIX 2002, and SUVA, categorized by pre-flood (2018) and post-flood (2020 to 2021) years, and by the exposure type (reference or flooded) of the study lakes. Data are presented as mean (standard deviation). NA indicates data were not collected. No data was available for any parameter listed in 2019 (contamination issue).

Years	Exposure Type	N	DOC (mg/L)	HIX 1999	HIX 2002	SUVA
Pre-Flood	Reference	1	2.29 (NA)	NA	NA	NA
Pre-Flood	Flooded	4	2.60 (0.275)	NA	NA	NA
Post-Flood	Reference	6	1.87 (0.344)	0.508 (0.116)	0.334 (0.0520)	1.77 (0.386)
Post-Flood	Flooded	8	3.16 (0.544)	0.585 (0.0540)	0.368 (0.0220)	2.14 (0.459)

Chapter 4: Discussion

I aimed to assess changes in [Hg] following a mine-related flooding event by comparing pre- and post-flood years in both flooded and reference lakes, as well as evaluating differences between flooded and reference lakes in post-flood years. Results indicate that in this Barrenland tundra system, flooding did increase loading of both inorganic and MeHg into affected lakes, as evidenced by significantly elevated [THg] and [MeHg] in water samples from flooded lakes during the post-flood years. While [Hg] in freshwater lakes vary due to factors such as geographic location, environmental conditions, and biological interactions, post-flood [THg] and [MeHg] observed in this study were within or at the higher end of ranges reported elsewhere in the Arctic, including sites such as Cornwallis Island, Devon Island, Somerset Island, Ellesmere Island, the Mackenzie River Basin, Iqaluit, and Resolute Bay (AMAP, 2021). Thus, while flooding increased [Hg] in lake water, these concentrations were still within the expected range for Arctic freshwater lakes (AMAP, 2021). The increased aqueous [Hg] observed in flooded lakes were likely facilitated by mobilization of OM and an increase in DOC, which facilitates the formation of Hg-DOC complexes and enhances Hg mobility in water (e.g., Johnston et al.,1991, St Louis et al., 2004). Indeed, I did find evidence that flooding increased [DOC] in water.

Tundra vegetation, including heath, moss, lichens, willows (Smith et al., 1998), and soils in the study area are known to sequester atmospheric Hg (Obrist et al., 2017). The disruption of these terrestrial Hg pools due to flooding likely contributed to increased loading of Hg to systems located downstream of flooding. Additionally, the proximity of the gold mine to the study lakes and the alteration of natural water flow due to dam construction may have further increased Hg input via overland runoff and sediment transport. The elevated [DOC] in flooded lakes compared to the reference lakes in post-flood years, suggests an increased flux of allochthonous, terrestrially derived carbon (see Moslemi-Aqdam et al., 2022) following the flooding event. This flux of external OM, combined with higher [Hg] in water, can create conditions that are favorable for microbial methylation and subsequent MeHg production (see Bravo et al., 2017, Moslemi-Aqdam et al., 2022), although % MeHg, and thus inferred net methylation rates, in water did not appear to be affected by flooding.

Elevated aqueous [MeHg] in flooded lakes likely provided the foundation for increased bioaccumulation and biomagnification of Hg through flooded ecosystems, which ultimately resulted in higher [Hg] in the two small-bodied fish species that were studied. All four lakes affected by the flooding event (A20, A63, A65, WTL) exhibited elevated [Hg] in the muscle tissue of Slimy Sculpin and Ninespine Stickleback in the years following flooding. While species-specific studies on Hg accumulation in these fish within Arctic environments are limited, available literature suggests that Ninespine Stickleback muscle [Hg] observed in this study exceeded some previously reported values (Burke, 2019). For Slimy Sculpin,

[Hg] in this study fall within, or slightly exceed, the range observed in Arctic and sub-Arctic literature (MacFarlane & Olegario, 2008; Matz et al., 2017).

The higher fish [Hg] observed after flooding in this study align with findings presented in existing literature. Several previous researchers have shown that fish exposed to flooding events experience significant increases in tissue [Hg] (see Bilodeau et al., 2016). The rapid response of Slimy Sculpin and Ninespine Stickleback to increased Hg loading (i.e., within two years post-flood) suggests that forage fish in this system were highly responsive to increased Hg inputs. This may be partly due to the fact that both species may feed directly on flooded terrestrial material, where DOC-Hg complexes likely maintain Hg in a mobile and bioavailable form, and where anoxic conditions (due to decomposition of terrestrial OM) promote the activity of methylating microbes. It is possible that [Hg] in these forage fish species have not yet reached peak concentrations, as studies in boreal flood-affected environments indicate that [Hg] can continue rising for several years (Bilodeau et al., 2016). Continuing increases in [Hg] could also be exacerbated by climate-induced mobilization of Hg from permafrost (e.g., Schuster et al., 2018). Although Hg mobilization into aquatic ecosystems is already difficult to predict due to climate change (see Burke, 2019), it is possible that [Hg] in Slimy Sculpin and Ninespine Stickleback will continue to increase due to compounding effects of mine-related flooding and ongoing climate-driven changes in Hg cycling.

In this study, the elevated [Hg] observed in the muscle tissue of Slimy Sculpin and Ninespine Stickleback likely reflects similar changes at both lower and higher trophic levels within the exposed lakes (see Bilodeau et al., 2016, Morris et al., 2022, Scheuhammer et al., 2015). There is extensive research indicating that species occupying higher trophic levels, such as Lake Trout and Northern Pike, tend to accumulate higher [Hg] in their muscle tissue (e.g., Barst et al., 2022, Depew et al., 2013). In piscivorous fish, Hg accumulation is influenced by food web length and ontogenetic dietary shifts, often leading to a 2- to 3-fold increase in [Hg] compared to their prey (e.g., Jessen et al., 2010). Therefore, larger-bodied predatory fish may exhibit an even greater increase in [Hg] in response to flooding. Consequently, large-bodied predatory fish present in the study lakes, such as Lake Trout, Arctic Char, Round Whitefish, and Burbot, would also be expected to have increased [Hg] in their tissuespost-flooding. Many of these larger fish species are important diet items for Arctic communities and wildlife, making increased Hg accumulation and concentrations particularly concerning. The lack of data on large-bodied fish in this study is a key limitation, as their longer lifespans and higher trophic positions mean that they are likely to experience greater Hg bioaccumulation over time. Further research should explore Hg dynamics in these species and assess potential risks to subsistence fishers and wildlife in the area.

Most Hg studies in the Arctic, as well as studies of impacts of flooding on Hg, have occurred in boreal environments and have focused on large-bodied fish species, including Arctic Char, Northern Pike,

Lake Trout, Dolly Varden (*Salvelinus malma*), Burbot, Atlantic Salmon (*Salmo salar*), Yellow Perch (*Perca flavescens*), Arctic Grayling (*Thymallus arcticus*), and Walleye (*Sander vitreus*; e.g., Chételat et al., 2015, Keva et al., 2017, Power et al., 2002, Swanson et al., 2011). However, small-bodied fishes, including Slimy Sculpin and Ninespine Stickleback, offer unique advantages for environmental monitoring. Due to their smaller home ranges and shorter life spans, these species can respond more rapidly to environmental changes compared to larger fish (Schoener, 1971). In addition, their broad distribution across various lake types further enhances their suitability as indicator species. While smaller-bodied species such as those used in this study may offer valuable early indications of disturbance-induced changes in Hg dynamics, the absence of data from large-bodied fish species limits the ability to fully quantify effects. Expanding future monitoring efforts to include larger-bodied fish species would strengthen the understanding of the full impact of mine-related flooding on Arctic aquatic food webs.

Mining activities other than flooding may have also played a role in the elevated [Hg] observed in Slimy Sculpin and Ninespine Stickleback. Activities including road building, dam building and use of roads have no doubt increased soil erosion and contamination and resulted in pollution from dust and emissions (Haddaway et al., 2019), all of which may have introduced additional pathways for Hg to enter the aquatic environment. Literature suggests that proximity to point-source contamination is associated with elevated [Hg] in fish tissue (Barst et al., 2022). In addition to altering lake morphology, ongoing water management activities associated with mining operations, such as water intake to support mining activities and effluent discharge (Golder, 2018), likely influenced and will continue to influence hydrology and biogeochemistry of the study lakes. Going forward, fluctuations in water levels driven by mine operations may cause repeated wetting and drying of sediments, which can promote activity of methylating microbes and increase sulphate availability for sulphate-reducing bacteria, enhance the production of MeHg (St Louis et al., 2004, Willacker et al., 2016), and further increase Hg uptake and accumulation in biota. Future research should consider all aspects of mine-related activities and consequent effects on Hg biogeochemistry and accumulation in proximate aquatic systems.

In addition to increases in [Hg] in water, increases in [DOC] were also noted. Increases in [DOC] may have both direct and indirect effects on Hg biogeochemistry, bioavailability, and bioaccumulation (see Ravichandran, 2004). The elevated [DOC] observed in the flooded lakes during this study supports the hypothesis that terrestrial inputs from the surrounding catchment increased as a result of flooding. The study lakes thus likely received greater inputs of allochthonous carbon, which is generally of lower nutritional quality than autochthonous carbon (see Moslemi-Aqdam et al., 2022). Shifts in the relative importance of allochthonous and autochthonous carbon, as well as effects of [DOC] on fish growth rates, can impact fish [Hg] (Moslemi-Aqdam et al., 2022). In addition, flooding-induced changes in lake morphology and

shoreline/nearshore habitat likely impacted habitat availability and habitat use for both Slimy Sculpin and Ninespine Stickleback.

Although not the focus of this thesis, data on catch-per-unit-effort (CPUE), a standardized measure of fish abundance per unit of sampling effort, revealed contrasting trends between Slimy Sculpin and Ninespine Stickleback in post-flood years across all flooded lakes (C. Portt, personal communication). Slimy sculpin CPUE declined immediately after flooding, likely because slimy sculpin moved from newly flooded littoral zones (where electrofishing took place) into deeper areas where preferred cobble and boulder habitats were more available; Slimy Sculpin were more difficult to capture via shoreline electrofishing under high water levels (J. Ellenor and C. Portt, personal communication). In contrast, Ninespine Stickleback CPUE increased after flooding, which is consistent with their preference for vegetated habitats used for both feeding and nesting; field crews frequently observed Ninepsine Stickleback using flooded tundra habitats. These species-specific shifts in habitat use may have contributed to observed changes in Hg bioaccumulation, $\delta^{13}C$, and relative condition, as changes in diet and habitat availability can significantly influence contaminant exposure and energy balance. Long-term monitoring of water levels and fish habitat use, as well as ongoing monitoring of chemical analytes, will lend more insight into the mechanisms that regulate impacts of water level fluctuations on fish [Hg].

Of the potential covariates influencing elevated [Hg] in Slimy Sculpin and Ninespine Stickleback tissue, $\delta^{13}C$ was the most strongly correlated to flooding-induced increases in [Hg] for both species. As $\delta^{13}C$ in fish tissue reflects long-term dietary sources, it serves as a key tracer of energy flow through the food web (Post et al., 2000, Post, 2002, Tiselius and Fransson, 2016, Weidel et al., 2011) and has also been shown to influence [Hg] in fish (Power et al., 2002). The finding that $\delta^{13}C$ values in Slimy Sculpin and Ninespine Stickleback generally decreased in post-flood years compared to pre-flood years is consistent with results of previous research. An influx of terrestrially derived OM into an aquatic system can result in lower $\delta^{13}C$ values in fish (Letourneur et al., 2013). This shift likely reflects an increased reliance on carbon sources from newly flooded terrestrial OM, which has a more depleted isotopic signature than pre-existing aquatic carbon sources (Hiltunen et al., 2019, Lau et al., 2009). The significant negative correlation between [Hg] and $\delta^{13}C$ in flooded lakes suggests that fish relying more on terrestrially derived carbon sources accumulated higher [Hg], likely due to the lower quality of this source of OM, as well as enhanced bioavailability of Hg in flooded environments.

Arctic freshwater ecosystems typically exhibit low autochthonous primary productivity. Allochthonous plant material from terrestrial sources, such as leaves from willows, dwarf birch, juniper, lichens, and mosses, are known to support energy dynamics and carbon cycling in Arctic aquatic systems

(Brittan & Bjornstad, 2010). While spring snowmelt and its associated high discharge rates drive natural influxes of allochthonous material into aquatic systems, incorporating plant debris from the previous year into catchment systems (Brittan & Bjornstad, 2010, Medeiros & Arthington, 2011), mine-induced flooding can change both the quantity and quality of OM entering the system. Allochthonous OM is generally nutritionally inferior to autochthonous OM, possessing lower-quality fatty acids (Hiltunen et al., 2019, Lau et al., 2009). The quality of carbon sources entering aquatic ecosystems plays a crucial role in regulating fish trophic level, foraging habitat, growth rate, and [Hg] accumulation (Moslemi-Aqdam et al., 2022). Enhanced transport of terrestrial nutrients into downstream aquatic systems can thus influence trophic interactions, productivity, and ultimately, contaminant concentrations across all levels of the food web. $\delta^{13}C$ was the strongest predictor of [Hg] in fish muscle tissue in flooded lakes during post-flood years, explaining 72% of variation in Slimy Sculpin and 63% of variation in Ninespine Stickleback. The negative correlation between $\delta^{13}C$ and [Hg] aligns with previous findings, where about half of total Hg variation has been attributed to seasonally variable factors, such as $\delta^{13}C$ (Keva et al., 2017). However, in this study, $\delta^{13}C$ explained even greater variation in [Hg] than reported in literature, likely due to flooding-induced shifts in carbon-availability and the higher sensitivity of this Arctic system to environmental disturbances.

The sources and extent of run-off, along with hydrologic conditions, have been linked to $\delta^{13}C$ values due to their influence on OM dynamics (Letourneur et al., 2013). Changes in OM type can directly impact primary productivity (i.e., energy flow) at the lowest trophic levels by altering species composition, abundance, and growth rates (Duda et al., 2011), which in turn affects higher trophic-level species, such as fish. A study by Moslemi-Aqdam et al. (2022) on drivers of among-lake variation in fish [Hg] in the Dehcho Region of Northwest Territories, Canada, found that $\delta^{13}C$ values were more depleted in slow-growing Northern Pike compared to their faster-growing counterparts. Their study suggested that the importance of terrestrial OM sources (allochthonous vs. autochthonous) influenced both fish growth rates and [Hg] accumulation (Moslemi-Aqdam et al., 2021) in the study systems. The results of Moslemi-Aqdam et al. (2022) align with this study's findings, as lower $\delta^{13}C$ values observed in post-flood years and the negative relationship between [Hg] and $\delta^{13}C$, support previously reported correlations among $\delta^{13}C$, OM, and [Hg] in fish (Duda et al., 2011; Letourneur et al., 2013). Further reinforcing these connections, Moslemi-Aqdam et al. (2021) found positive correlations between $\delta^{13}C$ values in Northern Pike and benthic invertebrates from littoral lake areas, suggesting that prey selection and habitat use influence $\delta^{13}C$ signatures in predatory fish. Given that Hg contamination increases with trophic position (Power et al., 2002), it is possible that similar correlations between $\delta^{13}C$ and [Hg] exist between the target forage fish species of this study and the benthic invertebrate community in the study lakes, though this was not directly examined due to absence of benthic invertebrate data. Future research should include not only higher trophic level large-bodied

fishes, but also lower trophic level organisms, including benthic invertebrates, and intentionally collected hydrologic data.

In this study, decreases in $\delta^{13}C$ could have been driven by changes in the quality of OM following the flooding event, as indicated by elevated [DOC] in flooded lakes in post flood years. However, it is important to consider that fish habitat use may also have changed in response to flooding; specifically, fish may have fed more on pelagic carbon sources than on littoral carbon sources in post-flood years. Mercury contamination in fish has been reported to be inversely correlated to $\delta^{13}C$, with benthic-feeding species typically exhibiting lower [Hg] than pelagic-feeding fish (Power et al., 2002). As discussed above, future studies should include consideration of habitat availability and habitat use, which would further inform inferences regarding the mechanism(s) driving the observed negative correlation between fish [Hg] and $\delta^{13}C$. For example, it is possible that the inferred flooding-induced decrease in $\delta^{13}C$ observed for Slimy Sculpin was due to a shift to deeper waters where preferred substrate (i.e., cobbles) was available. There was no significant difference in $\delta^{13}C$ values between flooded and reference lakes in post-flood years for Ninespine Stickleback. This could be due to low sample size and consequently low power to detect differences induced by increases in terrestrially derived OM. It could also be due to the fact that Ninespine Stickleback did not appear to change their nearshore habitat use after flooding; Ninespine Stickleback were observed using flooded tundra (i.e., vegetation) habitats to a greater degree than Slimy Sculpin (J. Ellenor and C. Portt, pers. comm) in post-flood years. It is also important to consider that some researchers have found no significant differences in MeHg exposure between nearshore and offshore feeding fish (Rohonczy et al., 2020). Additional research that includes consideration of habitat use and collection of multiple trophic levels, is necessary.

C: N ratios are commonly used as proxy for lipid content (or fatty acid composition) in fish tissue, can provide insights into fish condition (Fagan et al., 2011), and serve as a correction factor for the effect of lipid content on stable isotopes, such as $\delta^{13}C$ (Post et al., 2007). In this study, the C: N ratio accounted for only a small portion of the variation in Slimy Sculpin [Hg] (22%), and no significant differences in C: N were detected between pre-and post-flood years or between flooded and reference lakes. Following a flooding event, an increase in C: N ratio might be expected, particularly in fish relying more heavily on terrestrial OM, which tends to be higher in carbon-rich structural compounds (e.g., lignin, cellulose) and lower in nitrogen-rich proteins (Fagan et al., 2011). However, the absence of a detectable change in C: N ratio may reflect a relatively stable lipid content in fish muscle tissue despite habitat and dietary shifts, or it may suggest that changes in carbon quality did not significantly alter lipid accumulation in the short term. Additionally, the timing of sampling relative to fish growth or spawning cycles, species-specific metabolic responses, or compensatory dietary adjustments may have masked subtle shifts in tissue C: N ratios. Given

that total lipid concentrations in muscle tissue are generally expected to correlate positively with C: N ratios (Fagan et al., 2011, Post et al., 2007), this suggests that lipid content in Slimy Sculpin tissue was not significantly altered by the flooding event. Given the complexity of Hg dynamics in aquatic ecosystems, however, additional studies incorporating direct lipid analyses and trophic biomarkers (e.g., fatty acids) could help further elucidate the relationship between dietary carbon sources, lipid metabolism, and Hg accumulation in Arctic freshwater fishes. Further, sex should be considered in future studies of effects of flooding on fish [Hg]. Sex-related physiological differences, including differences in lipid content, reproductive investment, and metabolic rate, can influence Hg dynamics. Females often exhibit lower muscle [Hg] compared to males, potentially due to the depuration of Hg through egg production or differences in energy allocation toward reproduction versus growth (Madenjian et al. 2014). Males, particularly during spawning, may experience increased metabolic mobilization of Hg from tissue stores (McKinley et al. 2012). Incorporating sex as a variable in future studies may improve the resolution of observed patterns and predictors of [Hg], particularly in species where reproductive status strongly affects proximate composition of tissues and contaminant storage.

In this study, relative condition (or condition) was significantly and negatively correlated with [Hg] in both Slimy Sculpin and Ninespine Stickleback; however, the amount of variation explained by this covariate was minimal. Relative condition is a commonly used metric that integrates fish length and body weight to assess overall "health" by comparing an individual's body size to that of conspecifics within the same population and age class. Several factors can influence fish condition, including exposure to contaminants, fish age (Bilodeau et al., 2016), nutritional status, and energy reserves (Fagan et al., 2011). Given this complexity, the correlation between Hg exposure and fish condition can potentially be confounded by multiple ecological and physiological factors. Condition has been identified in the literature as a "seasonally variable factor" with declines associated with starvation, which many fish experience during the winter months, as well with spawning activity and growth dilution (Keva et al., 2017). The observed negative correlation between [Hg] and fish condition in this study is consistent with previous findings in European Whitefish (*Coregonus lavaretus*; Keva et al., 2017), Walleye, and Northern Pike (Bilodeau et al., 2016). The negative correlation is often interpreted as evidence for starvation and growth dilution effects, where fish in poorer condition may have higher [Hg] due to increased metabolic mobilization of contaminants from tissue reserves or reduced growth rates that limit somatic dilution of Hg (Keva et al., 2015). These processes may be particularly relevant in Arctic environments, where short growing seasons and limited food availability can exacerbate energetic constraints and affect contaminant dynamics. Additionally, seasonal variability in condition can influence Hg dynamics, and sampling fish at different times of the year (e.g., winter vs. summer) could yield different correlations between fish condition and [Hg]. Flooding may further compound these seasonal stressors by altering food web structure, reducing

prey availability, or increasing competition, all of which could influence condition and thereby affect [Hg]. Despite the observed negative correlations, and in addition to the fact that condition explained only a small portion of variation in [Hg], no significant differences were detected between post-flood years or between flooded and reference lakes. These findings indicate that relative condition was not substantially impacted by the flooding event and likely not a major driver of Hg accumulation in Slimy Sculpin and Ninespine Stickleback. However, future studies examining seasonal variability, metabolic rates, and energy allocation in fish from flooded versus reference lakes may provide further insight into the potential role of condition in influencing Hg dynamics in Arctic freshwater fish.

It is well established that faster growing fish (measured as length-at-age in this study) often have lower [Hg] due to somatic growth dilution (e.g., Trudel & Rasmussen, 2006). However, in this study, length-at-age data explained only a small portion of the variation in [Hg] for Slimy Sculpin (12%). Interestingly, an increase in length-at-age was observed in both flooded and reference lakes during the post-flood years, suggesting that fish grew larger relative to their age, which should result in lower [Hg]. The fact that length-at-age was higher in both flooded and reference lakes in post-flood years suggests that larger-scale (i.e., regional) climate factors could have been influencing primary productivity, food availability, and/or other growing conditions within the study systems. For instance, longer ice-free seasons, warmer summer temperatures, or shifts in invertebrate prey communities could enhance growth rates in Arctic freshwater fish by extending foraging opportunities and increasing metabolic efficiency. These broader environmental changes may partially mask or override localized flood-related stressors, complicating the interpretation of Hg accumulation trends and emphasizing the need for future studies to account for both regional climate drivers and site-specific disturbance events.

The effects of flooding on [Hg] in fish have primarily been studied in lower-latitude boreal environments, which may not fully represent how Arctic aquatic systems, particularly those in Barrenland tundra, respond to similar disturbances. While the observed increase in [Hg] and its correlation with $\delta^{13}C$ in this study align with patterns documented in large-bodied fish from boreal environments, Arctic environments are uniquely vulnerable to environmental change, suggesting that flooding-induced impacts may be more pronounced over time. The short growing seasons, low primary productivity, and cool temperatures in Arctic systems, which together result in relatively slow fish growth rates and also affect trophic ecology, likely mean that [Hg] in fishes are affected by flooding in ways that are distinct from more southerly systems. Additionally, permafrost underlies much of the tundra landscape. Unlike boreal ecosystems, where soils are richer in OM and support a more rapid carbon cycle, Arctic systems store vast amounts of carbon and Hg in permafrost and peat-rich soils (Schnurr, 2019). The lower quality of allochthonous carbon entering Arctic lakes during flooding, compared to boreal systems, may influence

energy transfer through the food web and enhance the bioavailability of Hg. Flooding and permafrost thaw may work synergistically to mobilize not only large quantities of carbon but also previously sequestered Hg into Arctic aquatic systems. When permafrost thaws, Hg that has been stored for millennia can be reintroduced into the environment (Schnurr, 2019), increasing aqueous [Hg] and providing more substrate for methylating microbes to produce MeHg. This process is further compounded by shifts in microbial communities, changes in oxygen availability, and altered nutrient dynamics associated with permafrost degradation that could be mediated by flooding (Ernakovich et al., 2022; Wu et al., 2021). Moreover, Arctic vegetation acts as a significant Hg reservoir (Schnurr, 2019). Peat-rich soils, when disturbed by flooding, can release substantial amounts of Hg into aquatic environments. While the findings of this study resemble patterns observed in boreal systems, the distinct characteristics of Arctic ecosystems, including slower fish growth rates, lower nutrient availability, and the presence of permafrost, suggest that the long-term effects of flooding on Hg dynamics may be more severe and persistent in Arctic lakes, and these may be exacerbated as climate change accelerates permafrost thaw and increases the frequency of extreme weather events. Future research should further explore how the interplay between permafrost, OM mobilization, and Hg cycling interacts in flooded Arctic environments.

4.1 Conclusions

The results of this study largely support the hypotheses outlined for both objectives. I hypothesized that aqueous [Hg] would differ before and after flooding in impacted lakes, as well as between reference and impacted lakes after flooding, and my results were consistent with this hypothesis. [THg] and [MeHg] in water were significantly higher in the flooded lakes during post-flood years compared to pre-flood years, while no such increases were observed in the reference lakes. Additionally, when comparing flooded lakes to reference lakes in post-flood years, aqueous [Hg] was significantly elevated in the flooded lakes. These results indicate that the flooding event mobilized previously sequestered Hg from terrestrial sources into the aquatic system, a well-documented phenomenon in flood-impacted environments (e.g., Bilodeau et al., 2016; St. Louis et al., 2004). The increased [DOC] observed in the flooded lakes further supports this hypothesis, as DOC has been shown to enhance Hg mobility and bioavailability by forming Hg-DOC complexes (Johnston et al., 1991). While aqueous [Hg] increased as expected, humic content indicators (HIX and SUVA) were not significantly different between flooded and reference lakes in post-flood years, suggesting that while OM quantity increased, its quality (in terms of humic vs non-humic fractions) was similar. Data for indicators for OM quality were limited, however, and effects of flooding on OM quality in tundra lakes warrants further study.

I hypothesized that the flooding of terrestrial environments would change fish [Hg], and my results were consistent with this hypothesis. In flooded lakes, [Hg] in Slimy Sculpin and Ninespine Stickleback

were significantly higher in post-flood years compared to pre-flood years. Furthermore, comparisons between flooded and references lakes in post-flood years showed consistently higher [Hg] in the flooded lakes, confirming that the flooding event had a measurable impact on Hg bioaccumulation in forage fishes. The strong negative correlation between $\delta^{13}C$ and [Hg] suggested that altered carbon sources in the flooded lakes influenced Hg dynamics; fish in flooded environments appeared to rely more on allochthonous, terrestrially derived carbon and have higher [Hg]. While results confirmed that flooding increased [Hg] in forage fish and appeared to be related to flooding-induced changes in $\delta^{13}C$, the observed relationship between [Hg] and other covariates, such as fish condition and C:N ratio, was weaker than expected. This may be due to inter-individual variability, seasonal influences, or the short time frame between the flooding event and sample collection, which may have limited detectable changes in physiological metrics. Additionally, the lack of data on large-bodied fishes remains a limitation, as these species often occupy higher trophic levels, accumulate greater Hg burdens over time, and are relied on as traditional food sources by Arctic Indigenous communities. Future research should explore longer-term effects of mine-induced flooding on higher trophic levels and assess whether [Hg] in forage fish will continue to increase or stabilize over time.

4.2. Future Directions

Future research should focus on assessing the long-term impacts of mine-induced flooding on Hg dynamics in Arctic aquatic ecosystems, particularly given the increasing presence of industrial activities in the region. While this study provided valuable insight into how flooding influenced Hg accumulation in water and forage fish, it remains unclear how these changes will propagate through the broader food web, especially in higher trophic-level species, such as Lake Trout, Arctic Char, and Burbot. Given that large-bodied fishes often exhibit greater Hg bioaccumulation due to their longer lifespans and higher trophic positions, continued monitoring of these species is critical for assessing potential risks to both ecosystem health and human consumption. Fish are a staple subsistence food source for local Inuit communities, and the bioaccumulation of Hg poses significant health concerns. Ongoing research should prioritize studying how these changes in fish [Hg] might impact northern food security and how alternative food sources or mitigation strategies could protect traditional harvesting practices.

Additionally, the findings of this study indicate that increases in fish [Hg] were related to decreases in $\delta^{13}C$. This relationship was likely driven by an influx of allochthonous following flooding, but no differences in quality of DOC were observed between reference and flooded lakes in post-flood years. However, mechanisms underlying the relationship between [Hg] and $\delta^{13}C$ are complex and require further exploration. Future work should investigate how changes in DOM composition influence Hg methylation rates, particularly in relation to microbial communities that drive methylation processes. The potential

release of contaminants from permafrost due to industrial activities and climate change is also a growing concern. With rising temperatures and thawing of cryospheric soils expected to increase flooding frequency in the Arctic, Hg and other contaminants previously sequestered into frozen soils could become more bioavailable, exacerbating Hg-related effects in aquatic food webs. Given that Arctic permafrost contains vast reservoirs of organic material and Hg, further research should assess interactions between flooding and permafrost thaw.

Finally, expanding research efforts to include lower trophic levels, such as benthic invertebrates, zooplankton, and piscivorous birds or mammals, as well as higher trophic levels, would provide a more comprehensive understanding of Hg transfer through the ecosystem. Ultimately, this study serves as an important foundation for future research, highlighting the need for continued monitoring and interdisciplinary approaches to assess the long-term consequences of both industrial development and climate-induced flooding on Arctic aquatic systems. These efforts will be critical for informing environmental management strategies and safeguarding the ecological integrity of northern freshwater resources.

References

Aldenhoven, J. T., Miller, M. A., Corneli, P. S., & Shapiro, M. D. (2010). Phylogeography of ninespine sticklebacks (*Pungitius pungitius*) in North America: Glacial refugia and the origins of adaptive traits. *Molecular Ecology*, *19*(18), 4061–4076. https://doi.org/10.1111/j.1365-294X.2010.04801.x

APHA. (2017). *Standard methods for the examination of water and wastewater* (23rd ed.). American Public Health Association, American Water Works Association, & Water Environment Federation.

Arciszewski, T., Reist, J. D., Gray, M. A., Hrenchuk, C., Cott, P. A., & Mochnacz, N. J. (2015). *Fish life history, diets, and habitat use in the Northwest Territories: Freshwater sculpin species*. Fisheries and Oceans Canada, Central and Arctic Region.

Arctic Monitoring and Assessment Programme. (2011). Mercury in the Arctic. Arctic Monitoring and Assessment Programme (AMAP), Oslo, Norway. xiv. 191.

Arctic Monitoring and Assessment Programme (AMAP)/United Nations Environment Programme (UNEP). (2019). Global Mercury Assessment 2018. Oslo, Norway/UNEP Chemicals Branch, Geneva, Switzerland.

AMAP. (2021). AMAP Assessment 2021: Mercury in the Arctic. Arctic Monitoring and Assessment Programme (AMAP), Tromsø, Norway. 324.

Atwell, L., Hobson, K. A., & Welch, H. E. (1998). Biomagnification and bioaccumulation of mercury in an Arctic marine food web: nsights from stable nitrogen isotope analysis. *Canadian Journal of Fisheries and Aquatic Sciences*, *55*(5), 1114-1121. https://doi.org/10.1139/cjfas-55-5-1114

Azimuth Consulting Group. (2018). Whale Tail Pit Core Receiving Environment Monitoring Program (CREMP): 2014-2017 Baseline Studies.

Bain, M. B., Finn, J. T., & Booke, H. E. (1988). Streamflow regulation and fish community structure. *Ecology*, *69*(2), 382-392. https://doi.org/10.2307/1940436

Barst, B. D., Chételat, J., & Basu, N. (2022). Toxicological risk of mercury for fish and invertebrate prey in the Arctic. *The Science of the Total Environment*, *836*, 155702. https://doi.org/10.1016/j.scitotenv.2022.155702

Bashir, I., Lone, F. A., Bhat, R. A., Mir, S. A., Dar, Z. A., & Dar, S. A. (2020). Concerns and threats of contamination on aquatic ecosystems. *Bioremediation and biotechnology: Sustainable approaches to pollution degradation* (pp. 1–26). Springer. https://doi.org/10.1007/978-3-030-35691-0_1

Bates, D., Maechler, M., Bolker, B., Walker, S., Christensen, R. H. B., Singmann, H., Dai, B., Scheipl, F., Grothendieck, G., & Green, P. (2009). *Package 'lme4'*. R package version 0.999375-32. https://cran.r-project.org/package=lme4

Bidgood, A. K., & Hall, J. (2024). We need to talk about mining in the Arctic. *Earth Science, Systems and Society*, *4*, Article 10117. https://doi.org/10.3389/esss.2024.10117

Bilodeau, F., Schetagne, R., Therrien, J., & Verdon, R. (2016). Absence of noticeable mercury effects on fish populations in boreal reservoirs despite threefold to sevenfold increases in mercury concentrations. *Canadian Journal of Fisheries and Aquatic Sciences*, *73*(7), 1104-1125. https://doi.org/10.1139/cjfas-2015-0035

Boening, D. W. (2000). Ecological effects, transport, and fate of mercury: A general review. *Chemosphere*, *40*(12), 1335-1351. https://doi.org/10.1016/S0045-6535(99)00283-0

Bravo, A. G., Bouchet, S., Tolu, J., Björn, E., Mateos-Rivera, A., & Bertilsson, S. (2017). Molecular composition of organic matter controls methylmercury formation in boreal lakes. *Nature Communications*, *8*(1), 14255. https://doi.org/10.1038/ncomms14255

Brittan, J. E., & Bjørnstad, H. E. (2010). A long-term study of catchment inputs of 137Cs to a subalpine lake in the form of allochthonous terrestrial plant material. *Hydrobiologia*, *654*(1), 101-106. https://doi.org/10.1007/s10750-010-0163-5

Burke, S. (2019). An integrative study on the controls of mercury (Hg) in the sediments and food webs of

thermokarst lakes on the Arctic Coastal Plain of Alaska. (Doctoral Dissertation). University of Waterloo, Waterloo, Ontario.
Chételat, J., Amyot, M., Arp, P., Blais, J. M., Depew, D., Emmerton, C. A., Evans, M., Gamberg, M., Gantner, N., Girard, C., Graydon, J., Kirk, J., Lean, D., Lehnherr, I., Muir, D., Nasr, M., Poulain, A. J., Power, M., Roach, P., Stern, G., Swanson, H., & van der Velden, S. (2015). Mercury in freshwater ecosystems of the Canadian Arctic: Recent advances on its cycling and fate. *Science of The Total Environment*, *509–510*, 41–66. https://doi.org/10.1016/j.scitotenv.2014.05.151
Clarkson, T. W. (2002). The three modern faces of mercury. *Environmental Health Perspectives*, *110*(1), 11-23. https://doi.org/10.1289/ehp.02110s111
Clayden, M. G., Arsenault, L. M., Kidd, K. A., O'Driscoll, N. J., & Mallory, M. L. (2015). Mercury bioaccumulation and biomagnification in a small Arctic polynya ecosystem. *The Science of the Total Environment*, *509-510*, 206-215. https://doi.org/10.1016/j.scitotenv.2014.07.087
Craig, P. C., & Wells, J. (1976). Life history notes for a population of slimy sculpin (*Cottus cognatus*) in an Alaskan Arctic stream. *Canadian Journal of Fisheries and Aquatic Sciences*, *33*(7), 1639-1642. https://doi.org/10.1139/f76-206
Creed, I. F., Bergström, A.-K., Trick, C. G., Grimm, N. B., Hessen, D. O., Karlsson, J., Kidd, K. A., Kritzberg, E. S., McKnight, D. M., Freeman, E. C., Senar, O. E., Andersson, A., Ask, J., Berggren, M., Cherif, M., Giesler, R., Hotchkiss, E. R., Kortelainen, P., Palta, M. M., & Weyhenmeyer, G. A. (2018). Global change-driven effects on dissolved organic matter composition: Implications for food webs of northern lakes. *Global Change Biology*, *24*(8), 3692–3714. https://doi.org/10.1111/gcb.14129
Depew, D. C., Burgess, N. M., Anderson, M. R., Baker, R., Bhavsar, S. P., Bodaly, R. A., Eckley, C. S., Evans, M. S., Gantner, N., Graydon, J. A., Jacobs, K., LeBlanc, J. E., St. Louis, V. L., & Campbell, L. M. (2013). An overview of mercury concentrations in freshwater fish species: A national fish mercury dataset for Canada. *Canadian Journal of Fisheries and Aquatic Sciences*, *70*(3), 436–451. https://doi.org/10.1139/cjfas-2012-0338
Duda, J. J., Coe, H. J., Morley, S. A., & Kloehn, K. K. (2011). Establishing spatial trends in water chemistry and stable isotopes (δ15N and δ13C) in the Elwha River prior to dam removal and salmon recolonization. *River Research and Applications*, *27*, 1169-1181. https://doi.org/10.1002/rra.1413
Eckley, C. S., Luxton, T. P., Knightes, C. D., & Shah, V. (2022). Methylmercury production and degradation under light and dark conditions in the water column of the Hells Canyon reservoirs, USA. *Environmental Toxicology and Chemistry*, *40*(7), 1829-1839. https://doi.org/10.1002/etc.5041
Ernakovich, J. G., Barbato, R. A., Rich, V. I., Schädel, C., Hewitt, R. E., Doherty, S. J., Whalen, E. D., Abbott, B. W., Barta, J., Biasi, C., Chabot, C. L., Hultman, J., Knoblauch, C., Lau, M. C. Y., Leewis, M.-C., Liebner, S., Mackelprang, R., Onstott, T. C., Richter, A., Schütte, U. M. E., Siljanen, H. M. P., Taş, N., Timling, I., Vishnivetskaya, T. A., Waldrop, M. P., & Winkel, M. (2022). Microbiome assembly in thawing permafrost and its feedbacks to climate. *Global Change Biology*, *28*(17), 5007–5026. https://doi.org/10.1111/gcb.16231
Fagan, K., Koops, M. A., Arts, M. T., & Power, M. (2011). Assessing the utility of C:N ratios for predicting lipid content in fishes. *Canadian Journal of Fisheries and Aquatic Sciences*, *68*(3), 374–385. https://doi.org/10.1139/F10-119
Fausch, K. D., Lyons, J., Karr, J. R., & Angermeier, P. L. (1990). Fish communities as indicators of environmental degradation. *Biological indicators of stress in fish* (pp. 123–144). American Fisheries Society.
Fitzgerald, W. F., Engstrom, D. R., Lamborg, C. H., Tseng, C.-M., Balcom, P. H., & Hammerschmidt, C. R. (2005). Modern and historic atmospheric mercury fluxes in northern Alaska: Global sources and Arctic depletion. *Environmental Science & Technology*, *39*(2), 557-568. https://doi.org/10.1021/es049128x
Fitzgerald, W. F., Lamborg, C. H., & Hammerschmidt, C. R. (2007). Marine biogeochemical cycling of

mercury. *Chemical Reviews*, *107*(2), 641-662. https://doi.org/10.1021/cr050353m
Fox, J., & Weisberg, S. (2019). *An R Companion to Applied Regression* (3rd ed.). Sage Publications. https://www.john-fox.ca/Companion/
French, K. J., Anderson, M. R., Scruton, D. A., Ledrew, L. J., Rudd, J. W. M., Gilmour, C. C., & Bodaly, R. A. (1998). Fish mercury levels in relation to characteristics of hydroelectric reservoirs in Newfoundland, Canada. *Biogeochemistry*, *40*(2/3), 217-233. https://doi.org/10.1023/A:1005975714493
French, T. D., Houben, A. J., Desforges, J.-P. W., Kimpe, L. E., Kokelj, S. V., Poulain, A. J., Smol, J. P., Wang, X., & Blais, J. M. (2014). Dissolved organic carbon thresholds affect mercury bioaccumulation in Arctic lakes. *Environmental Science & Technology*, *48*(6), 3162-3168. https://doi.org/10.1021/es403849d
Gelman, A., & Hill, J. (2006). Data analysis using regression and multilevel/hierarchical models (1st ed.). Cambridge University Press.
Ghani, S. A. A. (2015). Trace metals in seawater, sediments, and some fish species from Marsa Matrouh beaches in north-western Mediterranean coast, Egypt. *The Egyptian Journal of Aquatic Research*, *41*(2), 145–154. https://doi.org/10.1016/j.ejar.2015.02.006
Golder Associates Limited (Golder). (2018). Project Description FEIS Addendum Whale Tail Pit – Expansion Project.
Gough, L., Bettez, N. D., Slavik, K. A., Bowden, W. B., Giblin, A. E., Kling, G. W., Laundre, J. A., & Shaver, G. R. (2016). Effects of long-term nutrient additions on Arctic tundra, stream, and lake ecosystems: Beyond NPP. *Oecologia*, *182*(3), 653–665. https://doi.org/10.1007/s00442-016-3716-0
Government of Canada. (2022). Drainage Basins (Nunavut). Natural Resources Canada. https://open.canada.ca/data/en/dataset/e6c2539e-8893-11e0-ab4b-6cf049291510
Government of Canada. (2024). Canadian Climate Normals 1981–2010: Baker Lake A station data. Environment and Climate Change Canada. https://climate.weather.gc.ca/climate_normals/results_1981_2010_e.html?SearchType=Contains&StationName=Baker+Lake&dCode=1&dispBack=1&lang=e&stnID=1709
Government of Canada. (2025). Metal and Diamond Mining Effluent Regulations (SOR/2002-222). Fisheries Act. https://laws-lois.justice.gc.ca/eng/regulations/sor-2002-222/
Grigorieva, E. A. (2024). Climate change and human health in the Arctic: A review. *Climate*, *12*(7), 89. https://doi.org/10.3390/cli12070089
Grimard, Y., & Jones, H. G. (1982). Trophic upsurge in new reservoirs: A model for total phosphorus concentrations. *Canadian Journal of Fisheries and Aquatic Sciences*, *39*(11), 1473-1483. https://doi.org/10.1139/f82-199
Haddaway, N. R., Cooke, S. J., Lesser, P., Macura, B., Nilsson, A. E., Taylor, J. J., & Raito, K. (2019). Evidence of the impacts of metal mining and the effectiveness of mining mitigation measures on social-ecological systems in Arctic and boreal regions: A systematic map protocol. *Environmental Evidence*, *8*(1), 1-11. https://doi.org/10.1186/s13750-019-0152-8
Hall, B. D., Cherewyk, K. A., Paterson, M. J., & Bodaly, R. A. (2009). Changes in methyl mercury concentrations in zooplankton from four experimental reservoirs with differing amounts of carbon in the flooded catchments. *Canadian Journal of Fisheries and Aquatic Sciences*, *66*(11), 1910-1919. https://doi.org/10.1139/F09-123
Hammerschmidt, C. R., & Fitzgerald, W. F. (2006). Methylmercury in freshwater fish linked to atmospheric mercury deposition. *Environmental Science & Technology*, *40*(24), 7764-7770. https://doi.org/10.1021/es061480i
Hammerson, G. (1994). Ninespine stickleback. U.S. Fish and Wildlife Service, Region 7. Retrieved from https://www.adfg.alaska.gov/static/species/speciesinfo/_aknhp/ninespine_stickleback.pdf
Hershey, A. E. (1992). Effects of experimental fertilization on the benthic macroinvertebrate community of an Arctic lake. *Journal of the North American Benthological Society*, *11*(2), 204-217. https://doi.org/10.2307/1467386

Hiltunen, M., Peltomaa, E., Brett, M. T., Aalto, S. L., Strandberg, U., Oudenampsen, J., Rajala, S., Vehmaa, A., & Taipale, S. J. (2019). Terrestrial organic matter quantity or decomposition state does not compensate for its poor nutritional quality for *Daphnia*. *Freshwater Biology*, *64*(10), 1769–1786. https://doi.org/10.1111/fwb.13368

Hughson, P. K. (2010). Our homeland for the past, present and future: Akulliqpaaq Qamaniq (Aberdeen Lake) and Qamaniq Tugliqpaaq (Schultz Lake) landscapes described by Elder John Killularк (Unpublished manuscript). University of Manitoba, Winnipeg, Manitoba.

Ivanova, T. S., Ivanov, M. V., Bakhvalova, A. E., Polyakova, N. V., Golovin, P. V., Kucheryavyy, A. V., Yurtseva, A. O., Smirnova, K. A., & Lajus, D. L. (2019). Homing ability and site fidelity of marine threespine stickleback on spawning grounds. *Evolutionary Ecology Research*, *20*(3), 297–315.

Jenssen, M. T. S., Borgstrøm, R., Salbu, B., & Rosseland, B. O. (2010). The importance of size and growth rate in determining mercury concentrations in European minnow (*Phoxinus phoxinus*) and brown trout (*Salmo trutta*) in the subalpine lake, Øvre Heimdalsvatn. *The subalpine lake ecosystem, Øvre Heimdalsvatn, and its catchment: Local and global changes over the last 50 years* (pp. 115–126). Springer. https://doi.org/10.1007/978-90-481-9388-2_12

Jin, H., & Ma, Q. (2021). Impacts of permafrost degradation on carbon stocks and emissions under a warming climate: A review. *Atmosphere*, *12*(11), 1425. https://doi.org/10.3390/atmos12111425

Johnston, T. A., Bodaly, R. A., & Mathias, J. A. (1991). Predicting fish mercury levels from physical characteristics of boreal reservoirs. *Canadian Journal of Fisheries and Aquatic Sciences*, *48*(8), 1468-1475. https://doi.org/10.1139/f91-174

Jorgenson, J. K., Welch, H. E., & Curtis, M. F. (1992). Response of Amphipoda and Trichoptera to lake fertilization in the Canadian Arctic. *Canadian Journal of Fisheries and Aquatic Sciences*, *49*(11), 2354-2362. https://doi.org/10.1139/f92-259

Kelly, C. A., Rudd, J. W. M., Bodaly, R. A., Roulet, N. P., St. Louis, V. L., Heyes, A., Moore, T. R., Schiff, S., Aravena, R., Scott, K. J., Dyck, B., Harris, R., Warner, B., & Edwards, G. (1997). Increases in fluxes of greenhouse gases and methyl mercury following flooding of an experimental reservoir. *Environmental Science & Technology*, *31*(5), 1334–1344. https://doi.org/10.1021/es9604931

Keva, O., Hayden, B., Harrod, C., & Kahilainen, K. K. (2017). Total mercury concentrations in liver and muscle of European whitefish (*Coregonus lavaretus* (L.)) in a subarctic lake - Assessing the factors driving year-round variation. *Environmental Pollution*, *231*, 1518. https://doi.org/10.1016/j.envpol.2017.09.012

Kidd, K. A., Bootsma, H. A., Hesslein, R. H., Lockhart, W. L., & Hecky, R. E. (2003). Mercury concentrations in the food web of Lake Malawi, East Africa. *Journal of Great Lakes Research*, *29*(2), 258-266. https://doi.org/10.1016/S0380-1330(03)70553-X

Kidd, K. A., Hesslein, R. H., Fudge, R. J. P., & Hallard, K. A. (1995). The influence of trophic level as measured by δ15N on mercury concentrations in freshwater organisms. *Water, Air, & Soil Pollution*, *80*(1–4), 1011–1015. https://doi.org/10.1007/BF01189756

Koivurova, T., & Lesser, P. (2016). Environmental impact assessment in the Arctic: A guide to best practice. Edward Elgar Publishing. https://doi.org/10.4337/9781784711580

Laske, S. M., Burke, S. M., Carey, M. P., Swanson, H. K., & Zimmerman, C. E. (2022). Investigating effects of climate-induced changes in water temperature and diet on mercury concentrations in an Arctic freshwater forage fish. *Environmental Research*, *218*, 114851. https://doi.org/10.1016/j.envres.2022.114851

Lau, D. C. P., Leung, K. M. Y., & Dudgeon, D. (2009). Are autochthonous foods more important than allochthonous resources to benthic consumers in tropical headwater streams? *Journal of the North American Benthological Society*, *28*(2), 426-439. https://doi.org/10.1899/07-079.1

Lenth, R. (2023). *emmeans: Estimated Marginal Means, aka Least-Squares Means* (R package version 1.8.7). https://CRAN.R-project.org/package=emmeans

Letourneur, Y., Lison De Loma, T., Richard, P., Harmelin-Vivien, M. L., Cresson, P., Banaru, D.,

Fontaine, M.-F., Gref, T., & Planes, S. (2013). Identifying carbon sources and trophic position of coral reef fishes using diet and stable isotope ($\delta^{15}N$ and $\delta^{13}C$) analyses in two contrasted bays in Moorea, French Polynesia. *Coral Reefs*, *32*(4), 1091–1102. https://doi.org/10.1007/s00338-013-1073-6

Lewis, J. B. (2018). Comparing habitat use and mercury accumulation in Arctic grayling (*Thymallus arcticus*) from two northern ecosystems (Masters Thesis). University of Waterloo, Waterloo, Ontario, Canada.

Li, Q., Tang, L., Qiu, G., & Liu, C. (2020). Total mercury and methylmercury in the soil and vegetation of a riparian zone along a mercury-impacted reservoir. *The Science of the Total Environment*, *738*, 139794. https://doi.org/10.1016/j.scitotenv.2020.139794

Lienesch, P. W., McDonald, M. E., Hershey, A. E., O'Brien, W. J., & Bettez, N. D. (2005). Effects of a whole-lake, experimental fertilization on lake trout in a small oligotrophic Arctic lake. *Hydrobiologia*, *548*(1), 51-66. https://doi.org/10.1007/s10750-005-3620-9

Lindmark, M., Audzijonyte, A., Blanchard, J. L., & Gårdmark, A. (2022). Temperature impacts on fish physiology and resource abundance lead to faster growth but smaller fish sizes and yields under warming. *Global Change Biology*, *28*(21), 6239–6253. https://doi.org/10.1111/gcb.16341

Lougheed, V. L., Hernandez, C., Andresen, C. G., Miller, N. A., Alexander, V., & Prentki, R. (2015). Contrasting responses of phytoplankton and benthic algae to recent nutrient enrichment in Arctic tundra ponds. *Freshwater Biology*, *60*(10), 2169-2186. https://doi.org/10.1111/fwb.12644

Luis Marrugo-Negrete, J., Urango-Cardenas, I., Burgos Nunez, S. M., & Diez, S. (2014). Atmospheric deposition of heavy metals in the mining area of the San Jorge river basin, Colombia. *Air Quality, Atmosphere & Health*, *7*(4), 577-588. https://doi.org/10.1007/s11869-014-0260-0

Macdonald, R. W., Barrie, L. A., Bidleman, T. F., Diamond, M. L., Gregor, D. J., Semkin, R. G., Strachan, W. M., Li, Y. F., Wania, F., Alaee, M., Alexeeva, L. B., Backus, S. M., Bailey, R., Bewers, J. M., Gobeil, C., Halsall, C. J., Harner, T., Hoff, J. T., Jantunen, L. M., Lockhart, W. L., Mackay, D., Muir, D. C., Pudykiewicz, J., Reimer, K. J., Smith, J. N., Stern, G. A., Schroeder, W. H., Wagemann, R., & Yunker, M. B. (2000). Contaminants in the Canadian Arctic: 5 years of progress in understanding sources, occurrence, and pathways. *Science of the Total Environment*, *254*(2–3), 93–234. https://doi.org/10.1016/S0048-9697(00)00434-4

MacFarlane, B., & Olegario, A. (2008). *Mercury concentrations in fish and sediment in Resurrection Creek, Alaska, July 2008*. U.S. Department of Agriculture, Forest Service, Chugach National Forest.

Madenjian, C. P., Stapanian, M. A., Rediske, R. R., & O'Keefe, J. P. (2014). Sex differences in mercury contamination of fish: A synthesis. *Biology of Sex Differences*, 5(1), 1–7. https://doi.org/10.1186/s13293-014-0020-0

Mansfield, K. (2004). *Alaska Department of Fish & Game: Slimy Sculpin*. Alaska Department of Fish and Game. Retrieved from https://www.adfg.alaska.gov/static/education/wns/slimy_sculpin.pdf

Mateo-Sagasta, J., Zadeh, S. M., Turral, H., & Burke, J. (2017). Water pollution from agriculture: A global review – Executive summary (35 pages). Food and Agriculture Organization of the United Nations (FAO); International Water Management Institute (IWMI).

Matz, A., Varner, M., Albert, M., & Wuttig, K. (2017). Mercury, arsenic, and antimony in aquatic biota from the Middle Kuskokwim River Region, Alaska, 2010–2014 (BLM Technical Report 61). U.S. Department of the Interior, Bureau of Land Management.

McKinley, A. C., Taylor, M. D., Johnston, E. L., & Taylor, K. E. (2012). Strong links between mercury accumulation and reproductive investment in a wild fish population. *Environmental Pollution*, 160, 116–122. https://doi.org/10.1016/j.envpol.2011.09.021

Medeiros, E. S. F., & Arthington, A. H. (2011). Allochthonous and autochthonous carbon sources for fish in floodplain lagoons of an Australian dryland river. *Environmental Biology of Fishes*, *90*(1), 1–17. https://doi.org/10.1007/s10641-010-9706-x

Minagawa, M., & Wada, E. (1984). Stepwise enrichment of 15N along food chains: Further evidence and the relation between δ15N and animal age. *Geochimica et Cosmochimica Acta*, *48*(5), 1135–

1140. https://doi.org/10.1016/0016-7037(84)90204-7
Morris, A. D., Wilson, S. J., Fryer, R. J., Thomas, P. J., Hudelson, K., Andreasen, B., Blévin, P., Bustamante, P., Chastel, O., Christensen, G., Dietz, R., Evans, M., Evenset, A., Ferguson, S. H., Fort, J., Gamberg, M., Grémillet, D., Houde, M., Letcher, R. J., … Rigét, F. F. (2022). Temporal trends of mercury in Arctic biota: 10 more years of progress in Arctic monitoring. *Science of the Total Environment*, *839*, 155803. https://doi.org/10.1016/j.scitotenv.2022.155803
Moslemi-Aqdam, M., Baker, L. F., Baltzer, J. L., Branfireun, B. A., Evans, M. S., Laird, B. D., Low, G., Low, M., & Swanson, H. K. (2022). Understanding among-lake variability of mercury concentrations in Northern Pike (*Esox lucius*): A whole-ecosystem study in subarctic lakes. *Science of The Total Environment*, *822*, 153430. https://doi.org/10.1016/j.scitotenv.2022.153430
Moslemi-Aqdam, M., Low, G. C., Low, M., Branfireun, B. A., & Swanson, H. K. (2021). Catchments affect growth rate of Northern Pike (*Esox lucius*) in subarctic lakes. *Aquatic Sciences*, *83*(3), Article 59. https://doi.org/10.1007/s00027-021-00817-4
Newell, S. L., Doubleday, N. C., & Community of Chesterfield Inlet, Nunavut. (2020). Sharing country food: Connecting health, food security and cultural continuity in Chesterfield Inlet, Nunavut. *Polar Research*, *39*, 3755. https://doi.org/10.33265/polar.v39.3755
Niklitschek, E. J., & Secor, D. H. (2009). Dissolved oxygen, temperature and salinity effects on the ecophysiology and survival of juvenile Atlantic sturgeon in estuarine waters: I. Laboratory results. *Journal of Experimental Marine Biology and Ecology*, *381*(Supplement), S150–S160. https://doi.org/10.1016/j.jembe.2009.07.018
Obrist, D., Agnan, Y., Jiskra, M., Olson, C. L., Colegrove, D. P., Hueber, J., Moore, C. W., Sonke, J. E., & Helmig, D. (2017). Tundra uptake of atmospheric elemental mercury drives Arctic mercury pollution. *Nature*, *547*(7662), 201–204. https://doi.org/10.1038/nature22997
Ostrofsky, M. L., & Duthie, H. C. (1980). Trophic upsurge and the relationship between phytoplankton biomass and productivity in Smallwood Reservoir, Canada. *Canadian Journal of Botany*, *58*(10), 1174–1180. https://doi.org/10.1139/b80-146
Paterson, M. J., Findlay, D. L., Beaty, K. G., Findlay, W. J., Schindler, E. U., Stainton, M. P., & McCullough, G. K. (1997). Changes in the planktonic food web of a new experimental reservoir. *Canadian Journal of Fisheries and Aquatic Sciences*, *54*(5), 1088–1102. https://doi.org/10.1139/f97-018
Peterson, B. J., & Fry, B. (1987). Stable isotopes in ecosystem studies. *Annual Review of Ecology and Systematics*, *18*, 293–320. https://doi.org/10.1146/annurev.es.18.110187.001453
Poissant, L., Zhang, H. H., Canário, J., & Constant, P. (2008). Critical review of mercury fates and contamination in the Arctic tundra ecosystem. *Science of The Total Environment*, *400*(1–3), 173–211. https://doi.org/10.1016/j.scitotenv.2008.06.050
Post, D. M. (2002). Using stable isotopes to estimate trophic position: Models, methods, and assumptions. *Ecology*, *83*(3), 703–718. https://doi.org/10.1890/0012-9658(2002)083[0703:USITET]2.0.CO;2
Post, D. M., Layman, C. A., Arrington, D. A., Takimoto, G., Quattrochi, J., & Montaña, C. G. (2007). Getting to the fat of the matter: Models, methods and assumptions for dealing with lipids in stable isotope analyses. *Oecologia*, *152*(1), 179–189. https://doi.org/10.1007/s00442-006-0630-x
Post, D. M., Pace, M. L., & Hairston, N. G. Jr. (2000). Ecosystem size determines food-chain length in lakes. *Nature*, *405*(6790), 1047–1049. https://doi.org/10.1038/35016565
Power, M., Klein, G. M., Guiguer, K. R. R. A., & Kwan, M. K. H. (2002). Mercury accumulation in the fish community of a sub-Arctic lake in relation to trophic position and carbon sources. *Journal of Applied Ecology*, *39*(5), 819–830. https://doi.org/10.1046/j.1365-2664.2002.00758.x
R Core Team. (2023). *R: A language and environment for statistical computing*. R Foundation for Statistical Computing. https://www.R-project.org/
Ravichandran, M. (2004). Interactions between mercury and dissolved organic matter—a review. *Chemosphere*, *55*(3), 319–331. https://doi.org/10.1016/j.chemosphere.2003.11.011
Richardson, E. S., Reist, J. D., & Minns, C. K. (2001). Life history characteristics of freshwater fishes occurring in the Northwest Territories and Nunavut, with major emphasis on lake habitat

requirements (Canadian Manuscript Report of Fisheries and Aquatic Sciences No. 2569). Fisheries and Oceans Canada. https://waves-vagues.dfo-mpo.gc.ca/library-bibliotheque/261275.pdf

Rohonczy, J., Cott, P. A., Benwell, A., Forbes, M. R., Robinson, S. A., Rosabal, M., Amyot, M., & Chételat, J. (2020). Trophic structure and mercury transfer in the subarctic fish community of Great Slave Lake, Northwest Territories, Canada. *Journal of Great Lakes Research*, *46*(2), 402–413. https://doi.org/10.1016/j.jglr.2019.12.009

Rozon-Ramilo, L. D. (2011). Examination of the exposure pathways and effects of metal mining mixtures in fathead minnow (*Pimephales promelas*) (Master's thesis). University of Saskatchewan, Saskatoon, Saskatchewan.

Schaefer, K., Elshorbany, Y., Jafarov, E., Schuster, P. F., Striegl, R. G., Wickland, K. P., & Sunderland, E. M. (2020). Potential impacts of mercury released from thawing permafrost. *Nature Communications*, *11*, 4650. https://doi.org/10.1038/s41467-020-18398-5

Scheuhammer, A. M., Braune, B. M., Chan, H. M., Frouin, H., Krey, A., Letcher, R. J., Loseto, L. L., Noël, M., Ostertag, S. K., Ross, P. S., & Wayland, M. (2015). Recent progress on our understanding of the biological effects of mercury in fish and wildlife in the Canadian Arctic. *Science of The Total Environment*, *509–510*, 91–103. https://doi.org/10.1016/j.scitotenv.2014.05.142

Schuur, E. A. G. (2019). Permafrost and the global carbon cycle. Arctic Report Card 2019. National Oceanic and Atmospheric Administration. https://arctic.noaa.gov/report-card/report-card-2019/permafrost-and-the-global-carbon-cycle/

Schoener, T. W. (1971). Theory of feeding strategies. *Annual Review of Ecology and Systematics*, *2*(1), 369–404. https://doi.org/10.1146/annurev.es.02.110171.002101

Schroeder, W. H., Munthe, J., Lindberg, S. E., Keeler, G. J., & Petersen, G. (1998). Atmospheric mercury—An overview. *Atmospheric Environment*, *32*(5), 809–822. https://doi.org/10.1016/S1352-2310(97)00293-8

Schuster, P. F., Schaefer, K. M., Aiken, G. R., Antweiler, R. C., DeWild, J. F., Gryziec, J. D., Gusmeroli, A., Hugelius, G., Jafarov, E., Krabbenhoft, D. P., Liu, L., Herman-Mercer, N., Mu, C., Roth, D. A., Schaefer, T., Striegl, R. G., Wickland, K. P., & Zhang, T. (2018). Permafrost stores a globally significant amount of mercury. *Geophysical Research Letters*, *45*(3), 1463–1471. https://doi.org/10.1002/2017GL075571

Scott, W. B., & Crossman, E. J. (1973). *Freshwater fishes of Canada* (Bulletin 184). Fisheries Research Board of Canada. https://publications.gc.ca/site/eng/9.870340/publication.html

Smith, R. E., Veldhuis, H., Mills, G. F., Eilers, R. G., Fraser, W. R., & Lelyk, G. W. (1998). *Terrestrial ecozones, ecoregions, and ecodistricts of Manitoba: An ecological stratification of Manitoba's natural landscapes* (Technical Bulletin 1998-9E). Agriculture and Agri-Food Canada, Research Branch, Brandon Research Centre. https://sis.agr.gc.ca/cansis/publications/manuals/1998-9e/Ecostrat%20southern%20arctic.pdf

Solomon, C. T., Jones, S. E., Weidel, B. C., Buffam, I., Fork, M. L., Karlsson, J., Larsen, S., Lennon, J. T., Read, J. S., Sadro, S., & Saros, J. E. (2015). Ecosystem consequences of changing inputs of terrestrial dissolved organic matter to lakes: Current knowledge and future challenges. *Ecosystems*, *18*(3), 376–389. https://doi.org/10.1007/s10021-015-9848-y

Southcott, C., Abele, F., Natcher, D. C., & Parlee, B. (Eds.). (2019). Resources and sustainable development in the Arctic. Routledge. https://doi.org/10.4324/9781351019101

St. Louis, V. L., Rudd, J. W. M., Kelly, C. A., Bodaly, R. A., Paterson, M. J., Beaty, K. G., Hesslein, R. H., Heyes, A., & Majewski, A. R. (2004). The rise and fall of mercury methylation in an experimental reservoir. *Environmental Science & Technology*, *38*(5), 1348–1358. https://doi.org/10.1021/es034424f

Stekoll, M. S., Smoker, W. W., Failor-Rounds, B., Wang, I. A., & Joyce, V. J. (2009). Response of the early developmental stages of hatchery reared salmonids to major ions in a simulated mine effluent. *Aquaculture*, *298*(1–2), 172–181. https://doi.org/10.1016/j.aquaculture.2009.10.017.

Sumner, A. W., Johnston, T. A., Lescord, G. L., Branfireun, B. A., & Gunn, J. M. (2020). Mercury bioaccumulation in lacustrine fish populations along a climatic gradient in northern Ontario, Canada. *Ecosystems*, *23*(6), 1206–1226. https://doi.org/10.1007/s10021-019-00464-9

Swanson, H. K., Gantner, N., Kidd, K. A., Muir, D. C. G., & Reist, J. D. (2011). Comparison of mercury concentrations in landlocked, resident, and sea-run fish (*Salvelinus* spp.) from Nunavut, Canada. *Environmental Toxicology and Chemistry*, *30*(6), 1459–1467. https://doi.org/10.1002/etc.517

Talbot, C. J., Paterson, M. J., Beaty, K. G., Bodaly, R. A., & Xenopoulos, M. A. (2021). Nutrient budgets calculated in floodwaters using a whole-ecosystem reservoir creation and flooding experiment. *Water Resources Research*, *57*(8), e2020WR028786. https://doi.org/10.1029/2020WR028786

Tan, S. W., Meiller, J. C., & Mahaffey, K. R. (2009). The endocrine effects of mercury in humans and wildlife. *Critical Reviews in Toxicology*, *39*(3), 228–269. https://doi.org/10.1080/10408440802233259

Tiselius, P., & Fransson, K. (2016). Daily changes in $\delta^{15}N$ and $\delta^{13}C$ stable isotopes in copepods: Equilibrium dynamics and variations of trophic level in the field. *Journal of Plankton Research*, *38*(3), 751–761. https://doi.org/10.1093/plankt/fbv048

Tolvanen, A., Eilu, P., Juutinen, A., Kangas, K., Kivinen, M., Markovaara-Koivisto, M., Naskali, A., Salokannel, V., Tuulentie, S., & Similä, J. (2019). Mining in the Arctic environment: A review from ecological, socioeconomic and legal perspectives. *Journal of Environmental Management*, *233*, 832–844. https://doi.org/10.1016/j.jenvman.2018.11.124

Trudel, M., & Rasmussen, J. B. (2006). Bioenergetics and mercury dynamics in fish: A modelling perspective. *Canadian Journal of Fisheries and Aquatic Sciences*, *63*(8), 1890–1902. https://doi.org/10.1139/f06-081

Tubis, A., Werbińska-Wojciechowska, S., & Wroblewski, A. (2020). Risk assessment methods in mining industry—A systematic review. *Applied Sciences*, *10*(15), 5172. https://doi.org/10.3390/app10155172

Ullrich, S. M., Tanton, T. W., & Abdrashitova, S. A. (2001). Mercury in the aquatic environment: A review of factors affecting methylation. *Critical Reviews in Environmental Science and Technology*, *31*(3), 241–293. https://doi.org/10.1080/20016491089226

United States Environmental Protection Agency (USEPA). (1994). *Method 200.8: Determination of trace elements in waters and wastes by ICP-MS (Revision 5.4)*. https://www.epa.gov/esam/epa-method-2008-determination-trace-elements-waters-and-wastes-icp-ms

United States Environmental Protection Agency (USEPA). (1996). *Method 1669: Sampling ambient water for trace metals at EPA water quality criteria levels* (EPA 821-R-96-008). Office of Water. https://www.epa.gov/sites/default/files/2015-10/documents/method_1669_1996.pdf

United States Environmental Protection Agency (USEPA). (2007). *Method 300.0: Determination of inorganic anions by ion chromatography*. https://www.epa.gov/sites/default/files/2015-10/documents/method_300-0_rev_2-1_1993.pdf

United States Environmental Protection Agency (USEPA). (2007). *Method 7473: Mercury in solids and solutions by thermal decomposition, amalgamation, and atomic absorption spectrophotometry* (SW-846, Revision 0). https://www.epa.gov/sites/default/files/2015-12/documents/7473.pdf

Verdon, R., Brouard, D., Demers, C., Lalumière, R., Laperle, M., & Schetagne, R. (1991). Mercury evolution (1978–1988) in fishes of the La Grande hydroelectric complex, Quebec, Canada. *Water, Air, and Soil Pollution*, *56*(1), 405–417. https://doi.org/10.1007/BF00342287

Von Hippel, F. A., Trammell, E. J., Merilä, J., Sanders, M. B., Schwarz, T., Postlethwait, J. H., Titus, T. A., Buck, C. L., & Katsiadaki, I. (2016). The ninespine stickleback as a model organism in arctic ecotoxicology. *Evolutionary Ecology Research*, *17*, 487–504.

Wang, J., Xie, Q., Xiang, Y., Xue, J., Jiang, T., Zhang, C., Li, J., Wang, Y., & Wang, D. (2024). Anthropogenic activities enhance mercury methylation in sediments of a multifunctional lake: Evidence from dissolved organic matter and mercury methylating microorganisms. *Journal of Hazardous Materials*, *466*, 133505. https://doi.org/10.1016/j.jhazmat.2024.133505

Wang, W., & Wang, J. (2012). Mercury bioaccumulation in aquatic organisms: A review of ecological

factors and modeling approaches. *Environmental Toxicology and Chemistry*, *31*(9), 1909–1919.
Ward, A. J. W., James, R., Wilson, A. D. M., & Webster, M. M. (2013). Site fidelity and localised homing behaviour in three-spined sticklebacks (*Gasterosteus aculeatus*). *Behaviour*, *150*(14), 1689–1708.
Ward, D. M., Nislow, K. H., & Folt, C. L. (2010). Bioaccumulation syndrome: Identifying factors that make some stream food webs prone to elevated mercury bioaccumulation. *Annals of the New York Academy of Sciences*, *1195*(1), 62–83. https://doi.org/10.1111/j.1749-6632.2010.05456.x
Weidel, B. C., Carpenter, S. R., Kitchell, J. F., & Vander Zanden, M. J. (2011). Rates and components of carbon turnover in fish muscle: Insights from bioenergetics models and a whole-lake 13C addition. *Canadian Journal of Fisheries and Aquatic Sciences*, *68*(3), 387–399. https://doi.org/10.1139/F10-158
Weishaar, J. L., Aiken, G. R., Bergamaschi, B. A., Fram, M. S., Fujii, R., & Mopper, K. (2003). Evaluation of specific ultraviolet absorbance as an indicator of the chemical composition and reactivity of dissolved organic carbon. *Environmental Science & Technology*, *37*(20), 4702–4708. https://doi.org/10.1021/es030360x
Wetzel, R. G. (2001). Limnology: Lake and river ecosystems (3rd ed.). Academic Press.
Wheatley, B., Paradis, S., Porcella, D., & Huckabee, J. (1995). Exposure of Canadian Aboriginal peoples to methylmercury. *Water, Air, and Soil Pollution*, *80*(1–4), 3–11. https://doi.org/10.1007/BF01189647
Wilcox, A. C., Trowbridge, W. B., & Bowker, M. A. (2011). Dynamics of vegetation and organic matter in flood-affected streams: Implications for carbon and nutrient cycling. *River Research and Applications*, 27(6), 682–693. https://doi.org/10.1002/rra.1389
Willacker, J. J., Eagles-Smith, C. A., Lutz, M. A., Tate, M. T., Lepak, J. M., & Ackerman, J. T. (2016). Reservoirs and water management influence fish mercury concentrations in the western United States and Canada. *Science of the Total Environment*, *568*, 739–748. https://doi.org/10.1016/j.scitotenv.2016.03.050
Wootton, R. J. (2023). *A functional biology of sticklebacks*. University of California Press.
Wu, M.-H., Chen, S.-Y., Chen, J.-W., Xue, K., Chen, S.-L., Wang, X.-M., Chen, T., Kang, S.-C., Rui, J.-P., Thies, J. E., Bardgett, R. D., & Wang, Y.-F. (2021). Reduced microbial stability in the active layer is associated with carbon loss under alpine permafrost degradation. *Proceedings of the National Academy of Sciences*, *118*(25), e2025321118. https://doi.org/10.1073/pnas.2025321118
Zsolnay, Á., Baigar, E., Jimenez, M., Steinweg, B., & Saccomandi, F. (1999). Differentiating with fluorescence spectroscopy the sources of dissolved organic matter in soils subjected to drying. *Chemosphere, 38*(1), 45–50. https://doi.org/10.1016/S0045-6535(98)00166-0
Zuur, A. F., Ieno, E. N., Walker, N., Saveliev, A. A., & Smith, G. M. (2009). Mixed effects models and extensions in ecology with R. Springer. https://doi.org/10.1007/978-0-387-87458-6

Appendices

Appendix A: Water Chemistry Sample Preparation

Water chemistry analyses were conducted using standardized laboratory protocols to ensure consistency and comparability across parameters. Total and dissolved metal concentrations were determined using inductively coupled plasma mass spectrometry (ICP-MS) or inductively coupled plasma optical emission spectrometry (ICP-OES), following United States (U.S) Environmental Protection Agency (EPA) Method 200.8 (USEPA, 1994). Dissolved metal samples were filtered to 0.45 µm prior to acidification, whereas total metal samples underwent acid digestion prior to analysis. Analytical results were calibrated using certified reference materials and subjected to quality assurance/quality control (QA/QC) procedures, including procedural blanks, duplicates, and matrix spikes.

Nutrient analyses included nitrate, nitrite, ammonia, orthophosphate, and total Kjeldahl nitrogen (TKN), which were quantified using colorimetric or ion chromatography methods (APHA 2017). TKN samples underwent acid digestion prior to analysis. Anion and cation concentrations (e.g., chloride, sulfate, sodium, calcium, magnesium) were determined using ion chromatography following U.S. EPA Method 300.0 (2007), with calibration against multi-point standard curves and quality control using laboratory control samples and field replicates.

Chlorophyll-a was quantified from filtered samples using fluorometric or spectrophotometric analysis after pigment extraction in acetone, as described in APHA (2017). Samples were filtered through GF/F glass fiber filters and stored frozen or in the dark until processing.

Dissolved organic carbon (DOC) was analyzed via high-temperature catalytic combustion or wet chemical oxidation using a total organic carbon analyzer. Specific ultraviolet absorbance (SUVA) was calculated by dividing the ultraviolet absorbance at 254 nm (UV254) by the DOC concentration, yielding SUVA254 in units of $L \cdot mg^{-1} \cdot m^{-1}$ (Weishaar et al., 2003). The humification index (HIX), an indicator of dissolved organic matter aromaticity and humic content, was calculated from fluorescence excitation-emission matrix (EEM) spectroscopy using emission intensities over specific wavelength ranges (Zsolnay et al., 1999).

Methylmercury (MeHg) concentrations were quantified using U.S. EPA Method 1630 (2001), which involves distillation, aqueous ethylation, purge and trap, and cold vapor atomic fluorescence spectrometry (CVAFS). Samples were analyzed under clean laboratory conditions with rigorous contamination control procedures, including method blanks, matrix spikes, and use of ultra-clean reagents and containers.

Appendix A: Figures

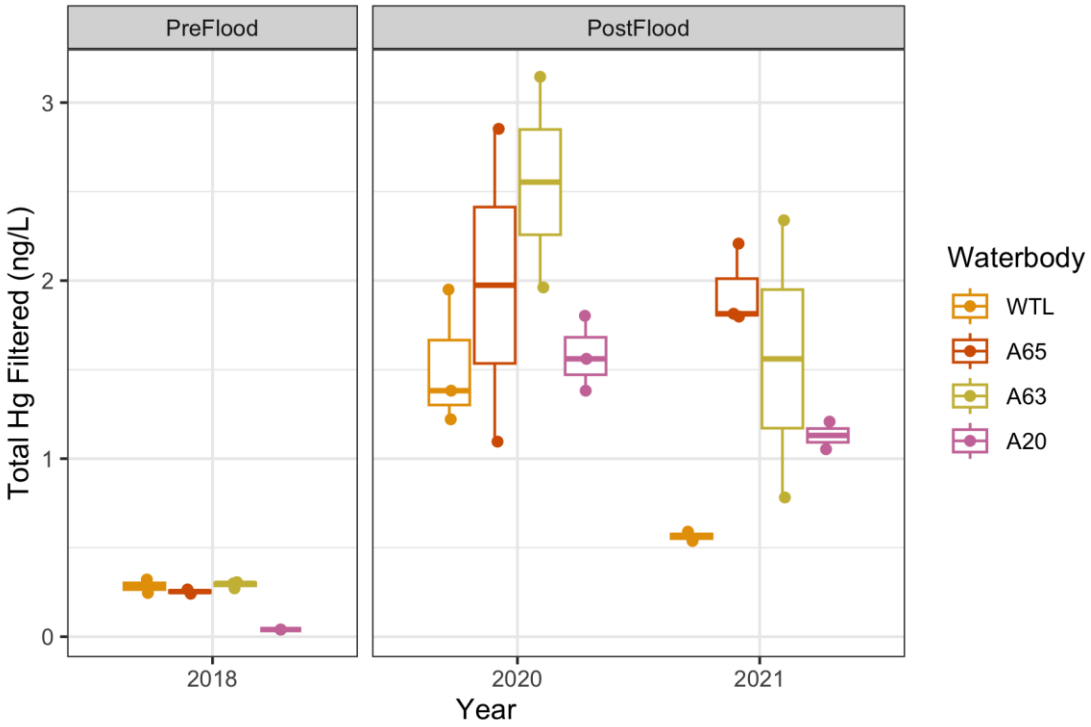


Figure A3.1: *Total aqueous mercury (Hg) concentrations (ng/L) in filtered water chemistry samples collected at flooded lakes during pre-flood (2018) and post-flood (2020 and 20212) years. Box plots indicate the mean, 25th, and 75th percentiles, minimum and maximum values with 1.5x the interquartile range. Individual mean values are plotted. Mercury data from 2019 was contaminated, therefore it was not used in these analyses.*

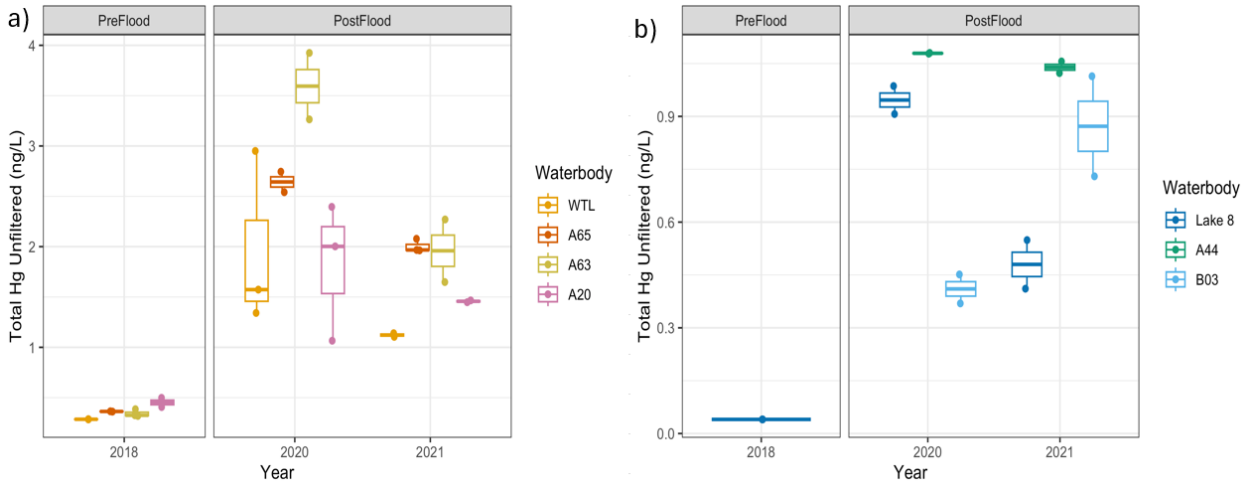


Figure A3.2: *Total aqueous mercury (Hg) concentrations (ng/L) in unfiltered water chemistry samples collected at flooded lakes (a) and reference lakes (b) during pre-flood (2018) and post-flood (2020 and 20212) years. Box plots indicate the mean, 25th, and 75th percentiles, minimum and maximum values with 1.5x the interquartile range. Individual mean values are plotted. Mercury data from 2019 was contaminated, therefore it was not used in these analyses.*

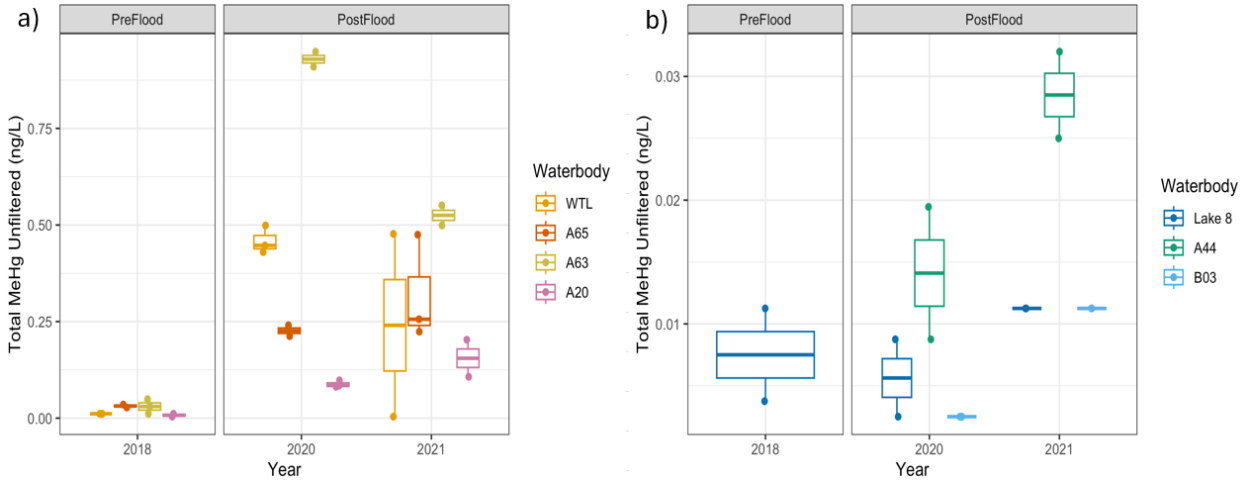


Figure A3.3: *Total aqueous methyl-mercury (MeHg) concentrations (ng/L) in unfiltered water chemistry samples collected at flooded lakes (a) and reference lakes (b) during pre-flood (2018) and post-flood (2020 and 2021) years. Box plots indicate the mean, 25th, and 75th percentiles, minimum and maximum values with 1.5x the interquartile range. Individual mean values are plotted. Mercury data from 2019 was contaminated, therefore it was not used in these analyses.*

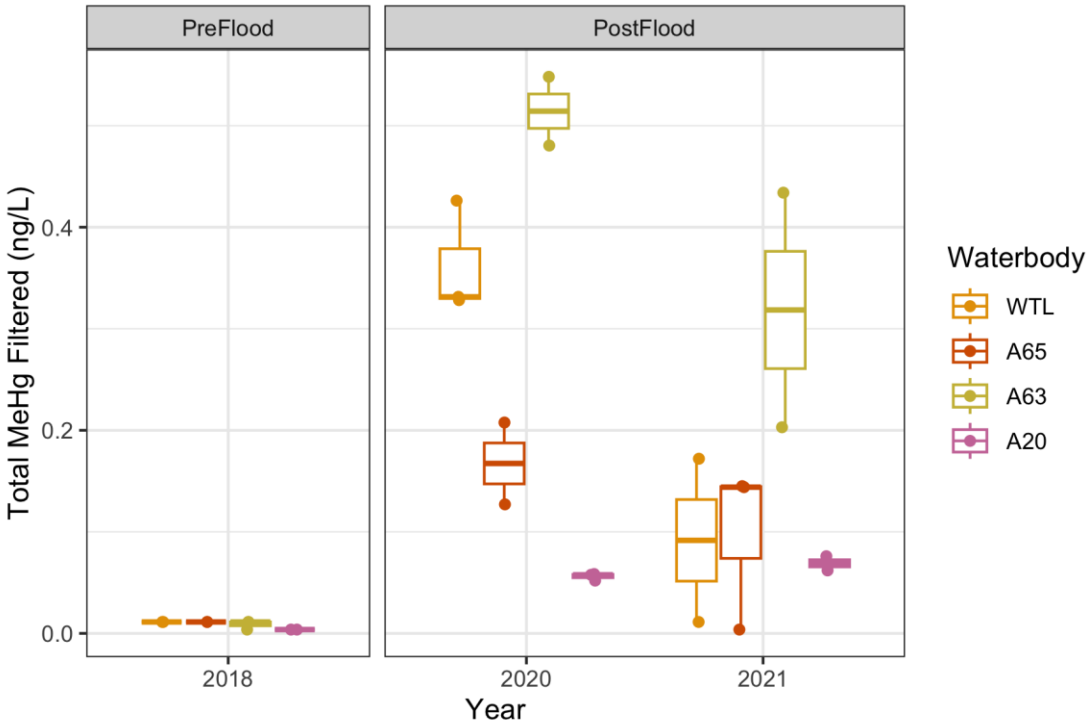


Figure A3.4: *Total aqueous methyl-mercury (MeHg) concentrations (ng/L) in filtered water chemistry samples collected at flooded lakes during pre-flood (2018) and post-flood (2020 and 2021) years. Box plots indicate the mean, 25th, and 75th percentiles, minimum and maximum values with 1.5x the interquartile range. Individual mean values are plotted. Mercury data from 2019 was contaminated, therefore it was not used in these analyses.*

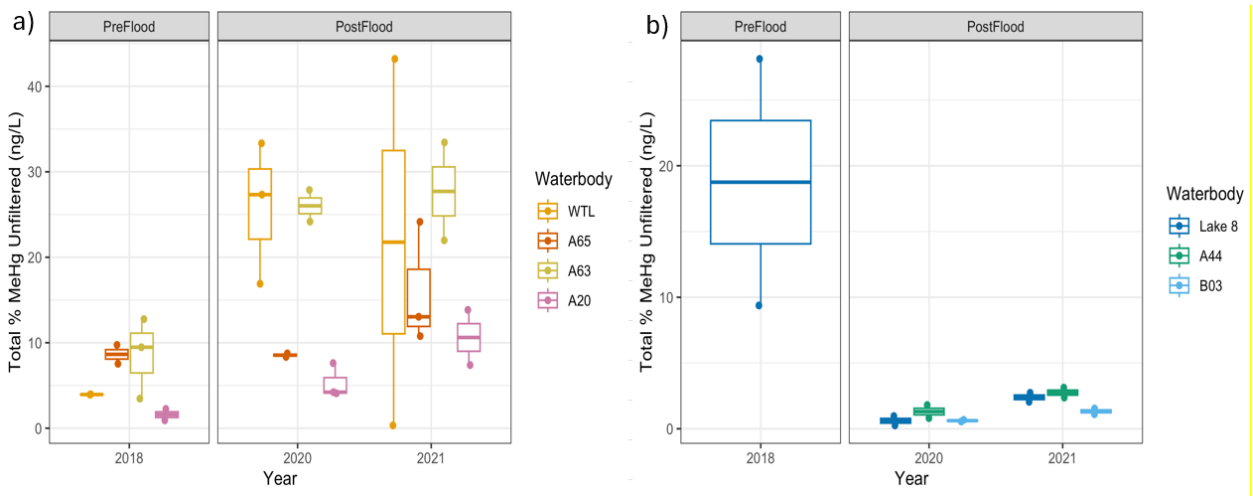


Figure A3.5: *Total aqueous methyl-mercury (MeHg) percent (%) concentrations (ng/L) in unfiltered water chemistry samples collected at flooded lakes (a) and reference lakes (b) during pre-flood (2018) and post-flood (2020 and 2021) years. Box plots indicate the mean, 25th, and 75th percentiles, minimum and maximum values with 1.5x the interquartile range. Individual mean values are plotted. Mercury data from 2019 was contaminated, therefore it was not used in these analyses.*

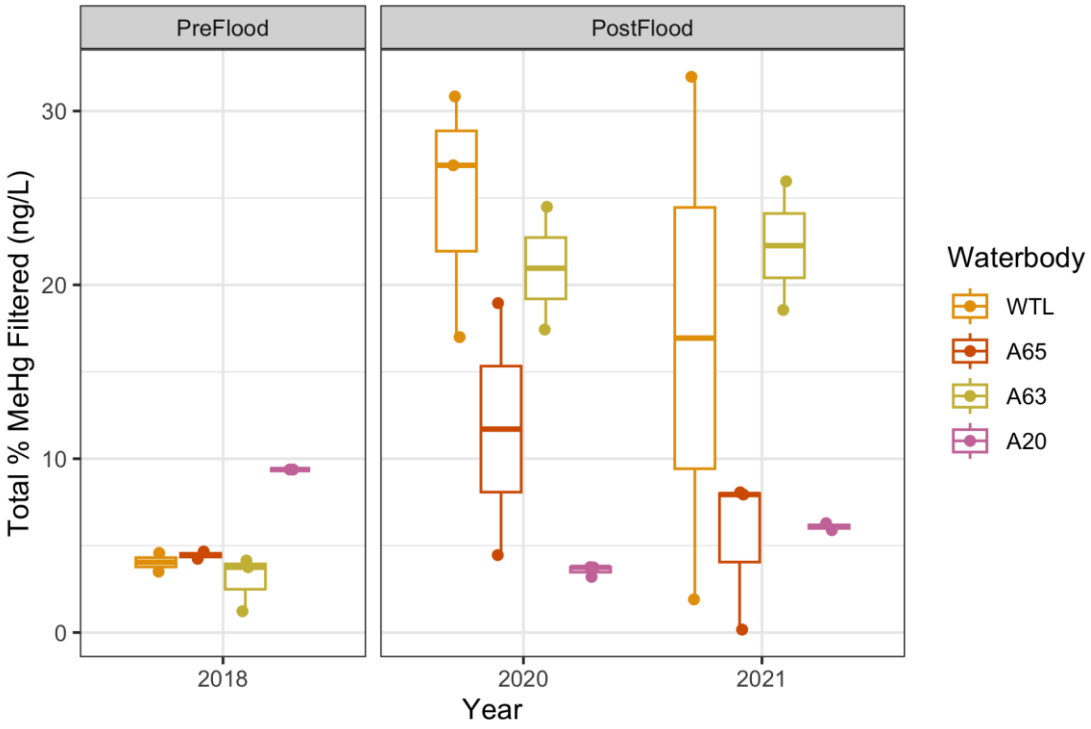


Figure A3.6: *Total aqueous methyl-mercury (MeHg) percent (%) concentrations (ng/L) in filtered water chemistry samples collected at flooded lakes during pre-flood (2018) and post-flood (2020 and 2021) years. Box plots indicate the mean, 25th, and 75th percentiles, minimum and maximum values with 1.5x the interquartile range. Individual mean values are plotted. Mercury data from 2019 was contaminated, therefore it was not used in these analyses.*

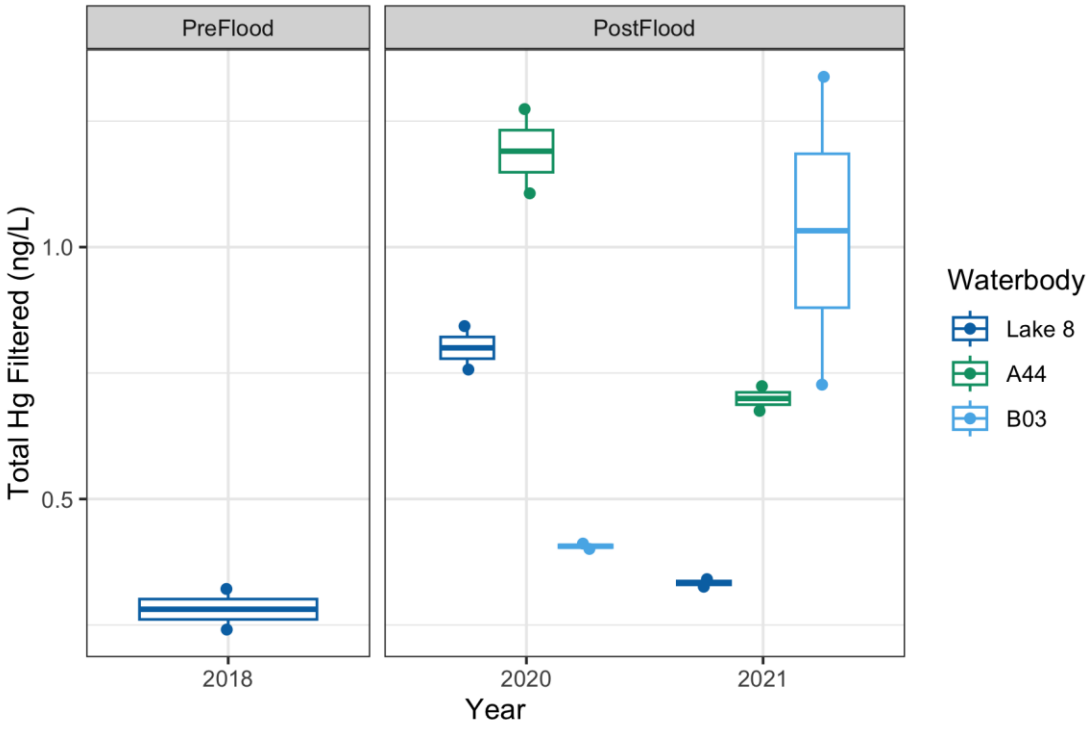


Figure A3.7: *Total aqueous mercury (Hg) concentrations (ng/L) in filtered water chemistry samples collected at reference lakes during pre-flood (2018) and post-flood (2020 and 2021) years. Box plots indicate the mean, 25th, and 75th percentiles, minimum and maximum values with 1.5x the interquartile range. Individual mean values are plotted. Mercury data from 2019 was contaminated, therefore it was not used in these analyses.*

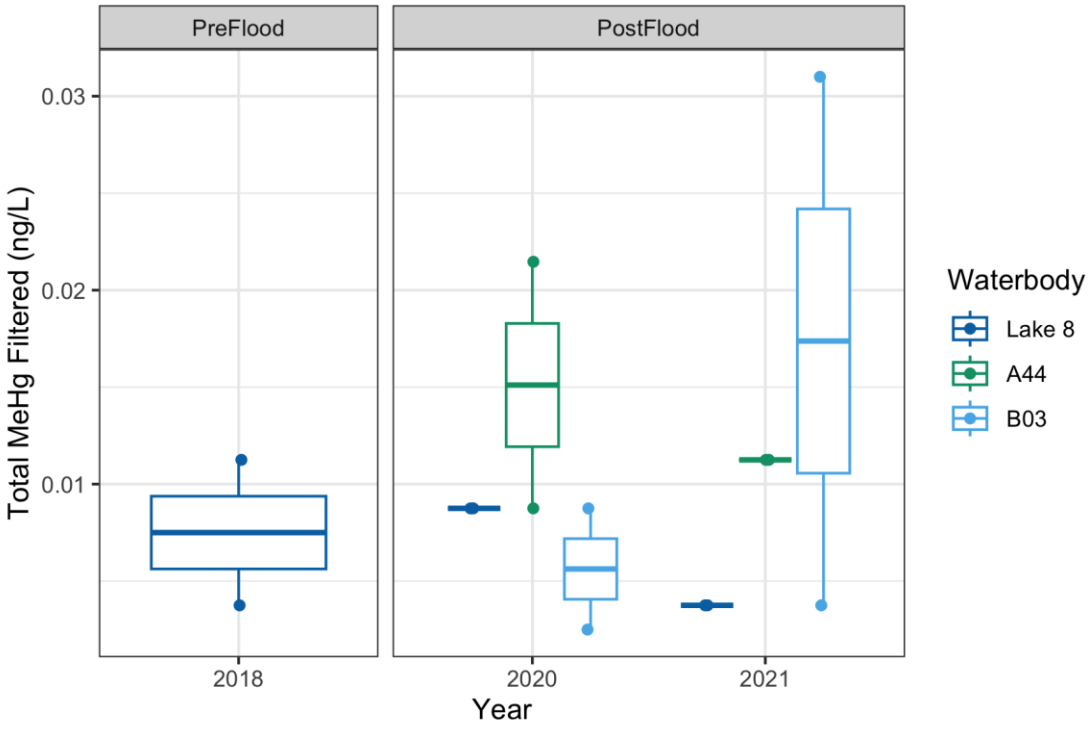


Figure A3.8: *Total aqueous methyl-mercury (MeHg) concentrations (ng/L) in filtered water chemistry samples collected at reference lakes during pre-flood (2018) and post-flood (2020 and 2021) years. Box plots indicate the mean, 25th, and 75th percentiles, minimum and maximum values with 1.5x the interquartile range. Individual mean values are plotted. Mercury data from 2019 was contaminated, therefore it was not used in these analyses.*

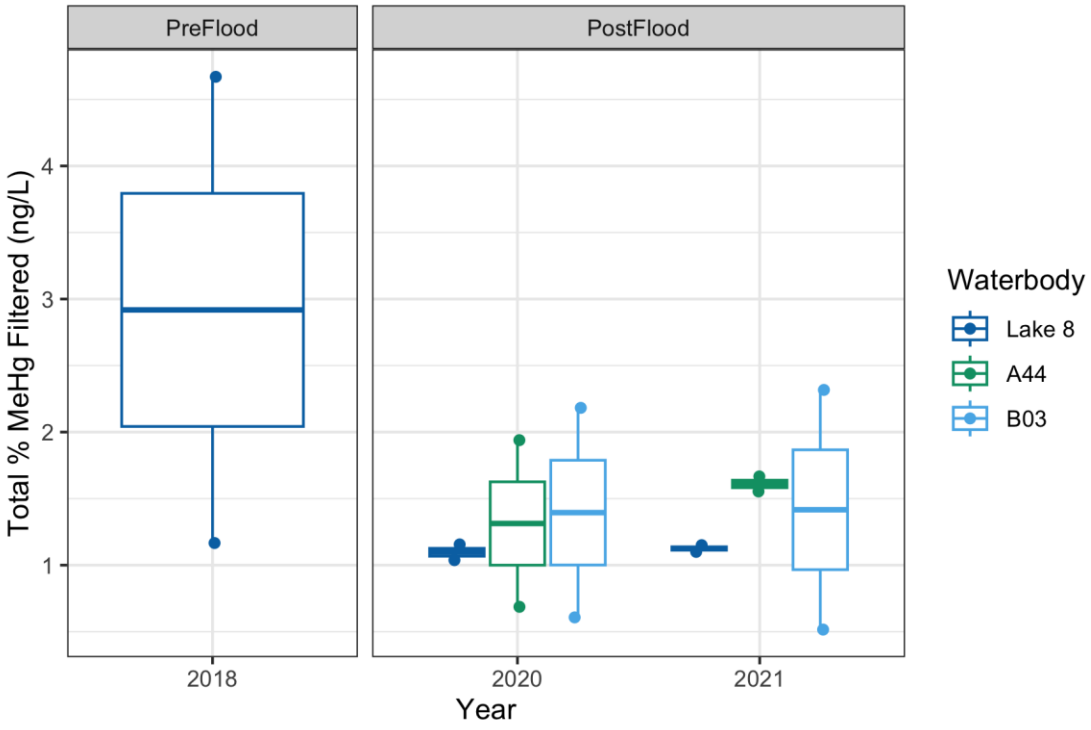


Figure A3.9: *Total aqueous methyl-mercury (MeHg) percent (%) concentrations (ng/L) in filtered water chemistry samples collected at reference lakes during pre-flood (2018) and post-flood (2020 and 2021) years. Box plots indicate the mean, 25th, and 75th percentiles, minimum and maximum values with 1.5x the interquartile range. Individual mean values are plotted. Mercury data from 2019 was contaminated, therefore it was not used in these analyses.*

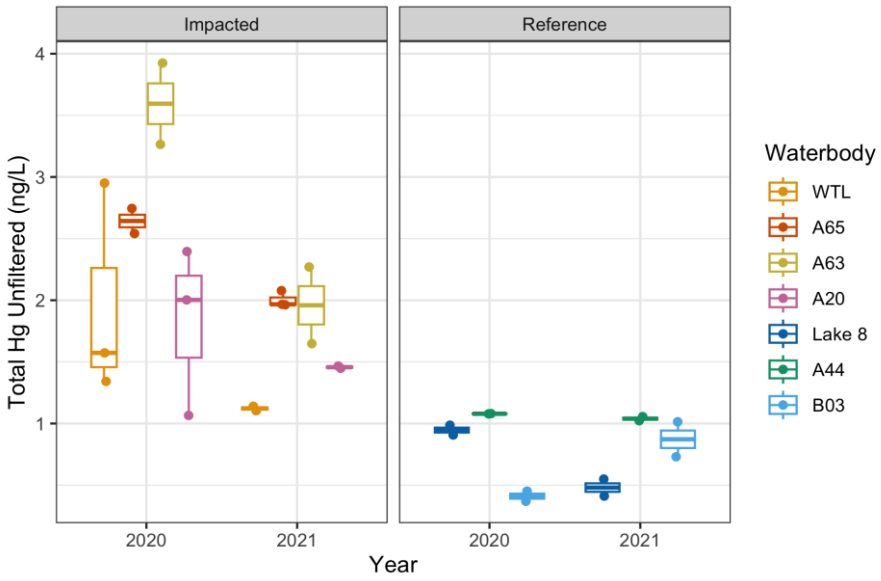


Figure A3.10: *Total aqueous mercury (Hg) concentrations (ng/L) in unfiltered water chemistry samples collected at reference and impacted (flooded) lakes during post-flood (2020 and 2021) years. Box plots indicate the mean, 25th, and 75th percentiles, minimum and maximum values with 1.5x the interquartile range. Individual mean values are plotted. Mercury data from 2019 was contaminated, therefore it was not used in these analyses.*

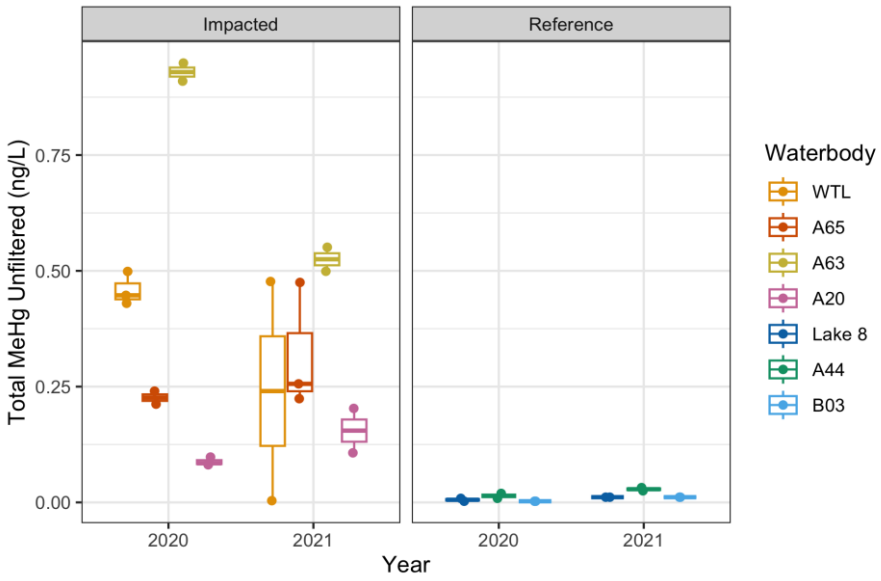


Figure A3.11: *Total aqueous methyl-mercury (MeHg) concentrations (ng/L) in unfiltered water chemistry samples collected at reference and flooded (impacted) lakes during post-flood (2020 and 2021) years. Box plots indicate the mean, 25th, and 75th percentiles, minimum and maximum values with 1.5x the interquartile range. Individual mean values are plotted. Mercury data from 2019 was contaminated, therefore it was not used in these analyses.*

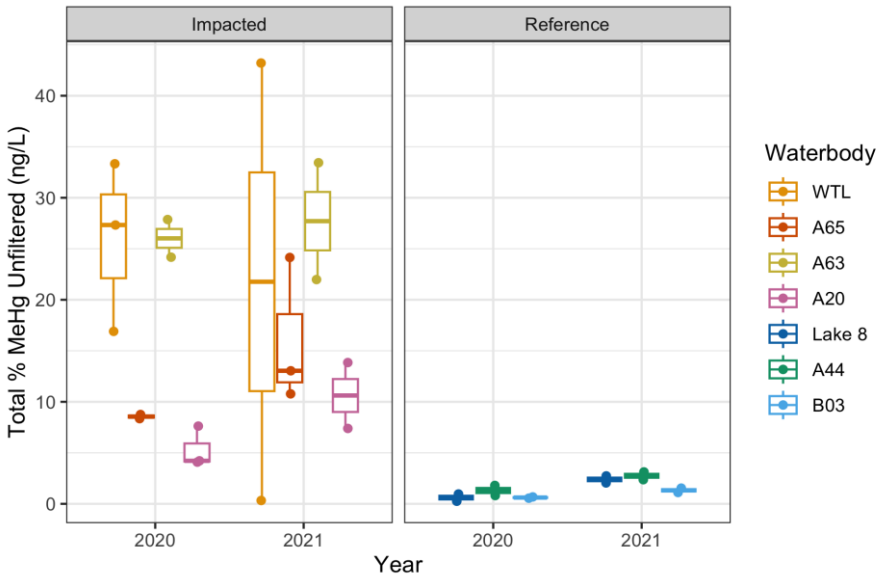


Figure A3.12: *Total aqueous methyl-mercury (MeHg) percent (%) concentrations (ng/L) in unfiltered water chemistry samples collected at reference and flooded (impacted) lakes during post-flood (2020 and 2021) years. Box plots indicate the mean, 25th, and 75th percentiles, minimum and maximum values with 1.5x the interquartile range. Individual mean values are plotted. Mercury data from 2019 was contaminated, therefore it was not used in these analyses.*

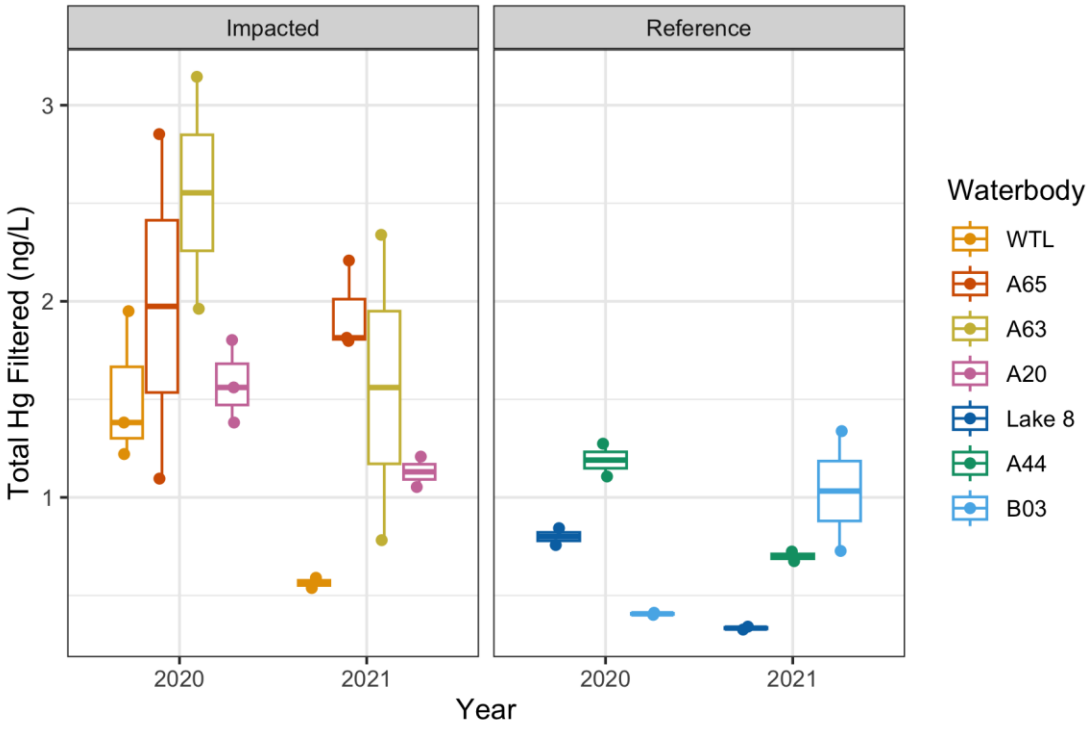


Figure A3.13: *Total aqueous mercury (Hg) concentrations (ng/L) in filtered water chemistry samples collected at reference and impacted (flooded) lakes during post-flood (2020 and 2021) years. Box plots indicate the mean, 25th, and 75th percentiles, minimum and maximum values with 1.5x the interquartile range. Individual mean values are plotted. Mercury data from 2019 was contaminated, therefore it was not used in these analyses.*

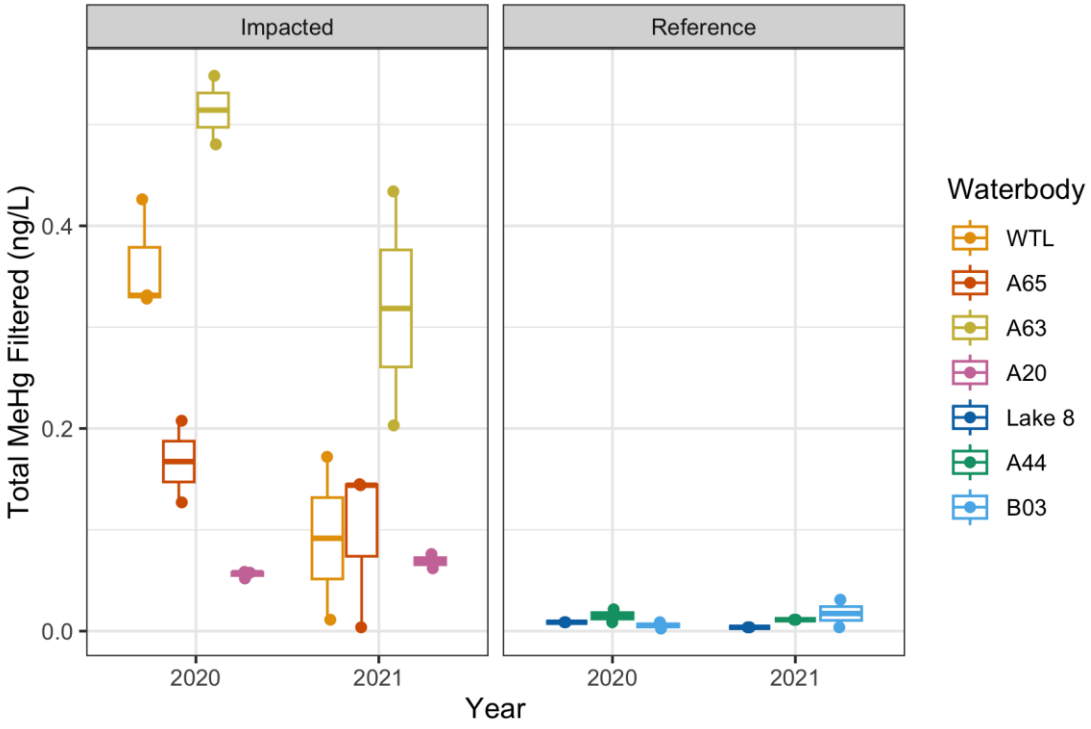


Figure A3.14: *Total aqueous methyl-mercury (MeHg) concentrations (ng/L) in filtered water chemistry samples collected at reference and flooded (impacted) lakes during post-flood (2020 and 2021) years. Box plots indicate the mean, 25th, and 75th percentiles, minimum and maximum values with 1.5x the interquartile range. Individual mean values are plotted. Mercury data from 2019 was contaminated, therefore it was not used in these analyses.*

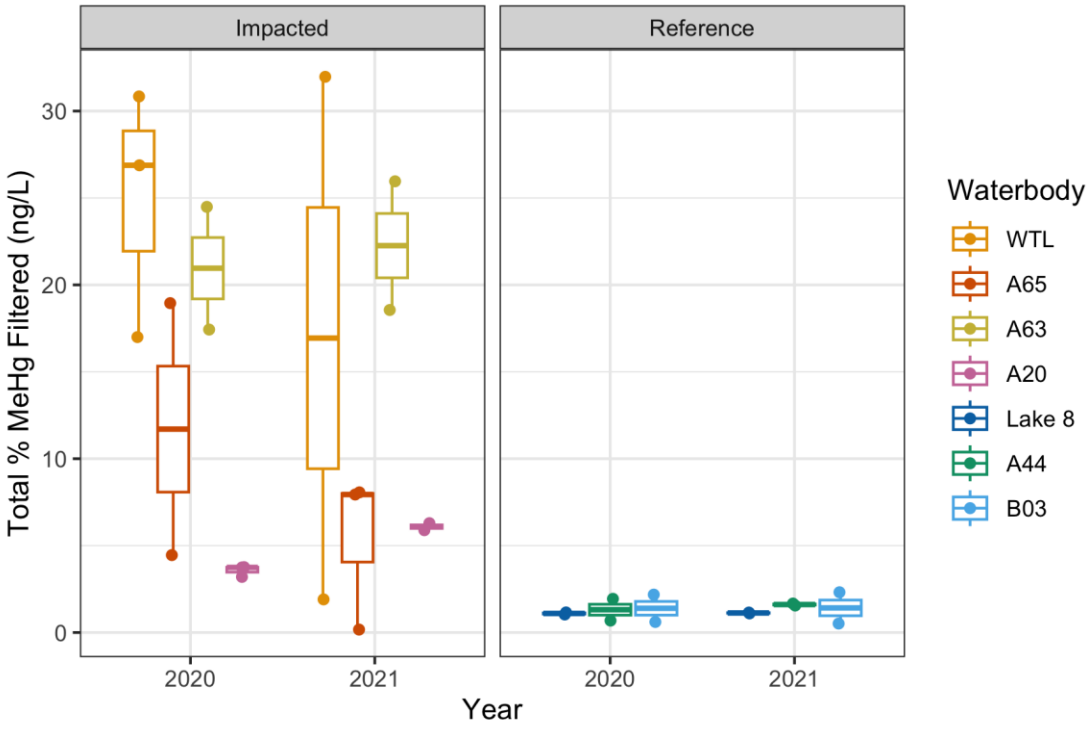


Figure A3.15: *Total aqueous methyl-mercury (MeHg) percent (%) concentrations (ng/L) in filtered water chemistry samples collected at reference and flooded (impacted) lakes during post-flood (2020 and 2021) years. Box plots indicate the mean, 25th, and 75th percentiles, minimum and maximum values with 1.5x the interquartile range. Individual mean values are plotted. Mercury data from 2019 was contaminated, therefore it was not used in these analyses.*

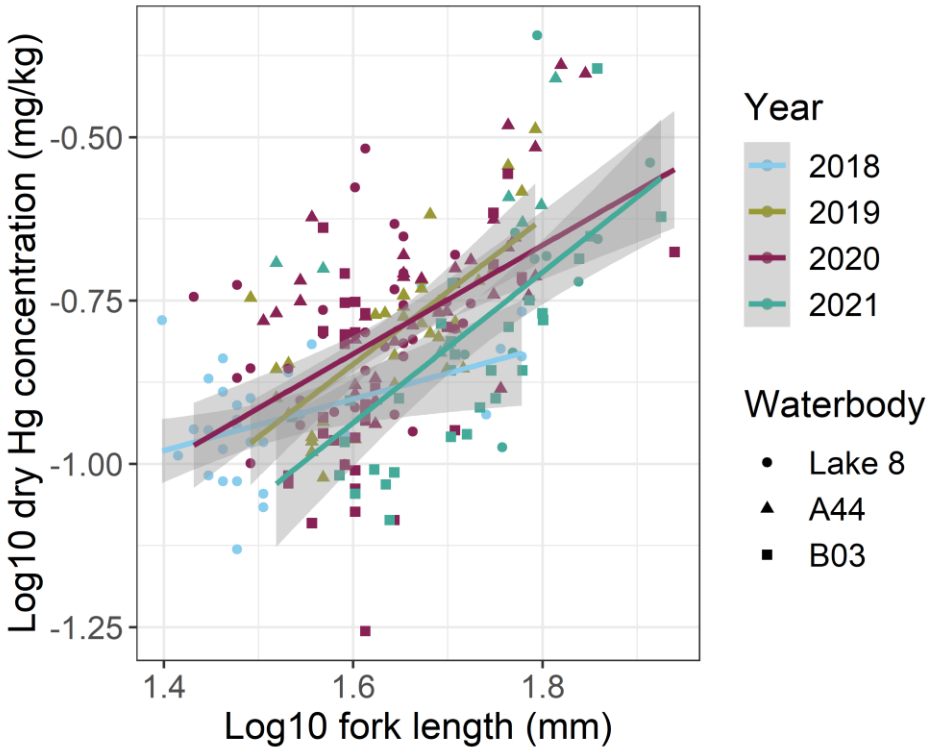


Figure A3.16: *Log $_{10}$ dry mercury (Hg) compared to fork length for Slimy Sculpin at reference lakes from 2018 to 2021. All individual data points are plotted. (Note: one Slimy Sculpin outlier with very low Hg concentration was removed from Lake B03, 2021).*

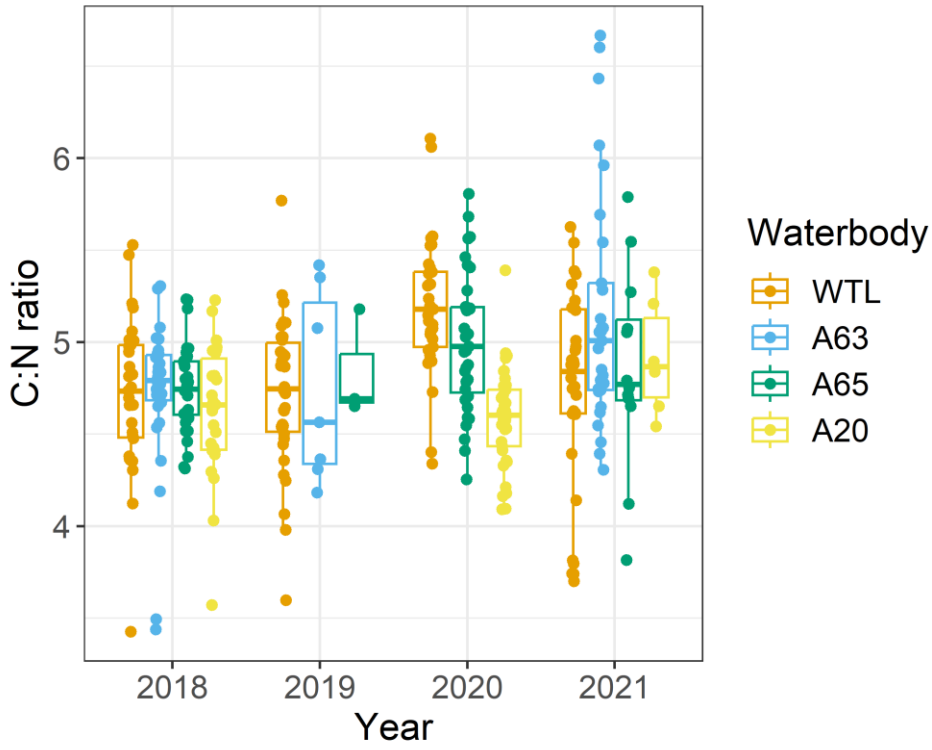


Figure A3.17: *C:N ratio for Slimy Sculpin between 2018 to 2021 at flooded lakes. Boxplots indicate the median, 25th and 75th percentiles, and minimum and maximum values within 1.5x the interquartile range. All individual data points are plotted.*

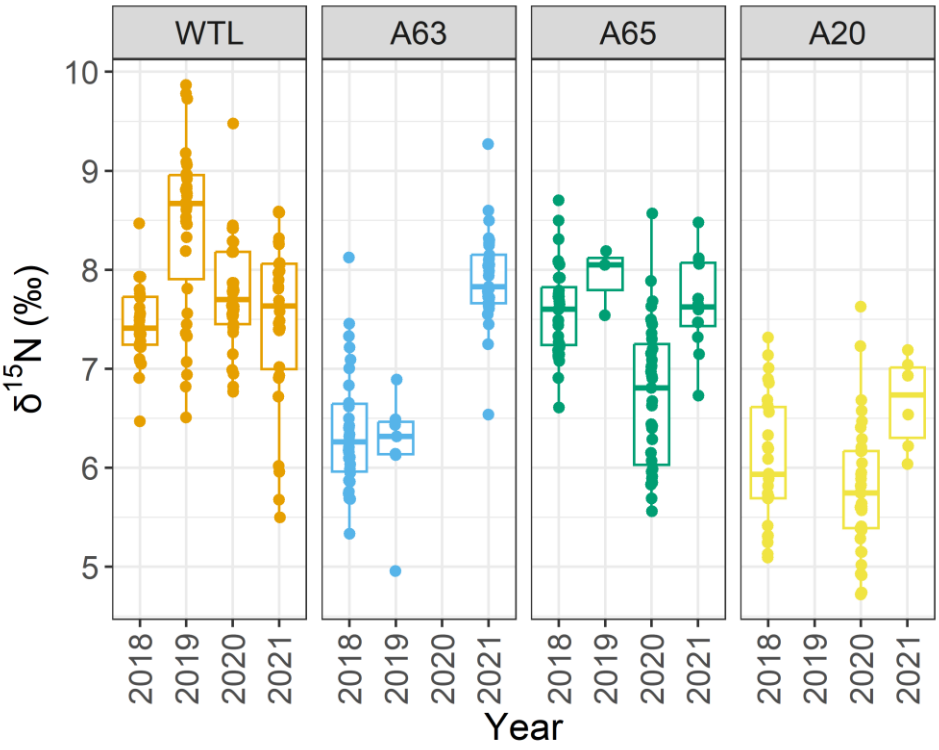


Figure A3.18: *$\delta^{15}N$ for Slimy Sculpin between 2018 and 2021 at flooded lakes. Boxplots indicate the median, 25th and 75th percentiles, and minimum and maximum values within 1.5x the interquartile range. All individual data points are plotted.*

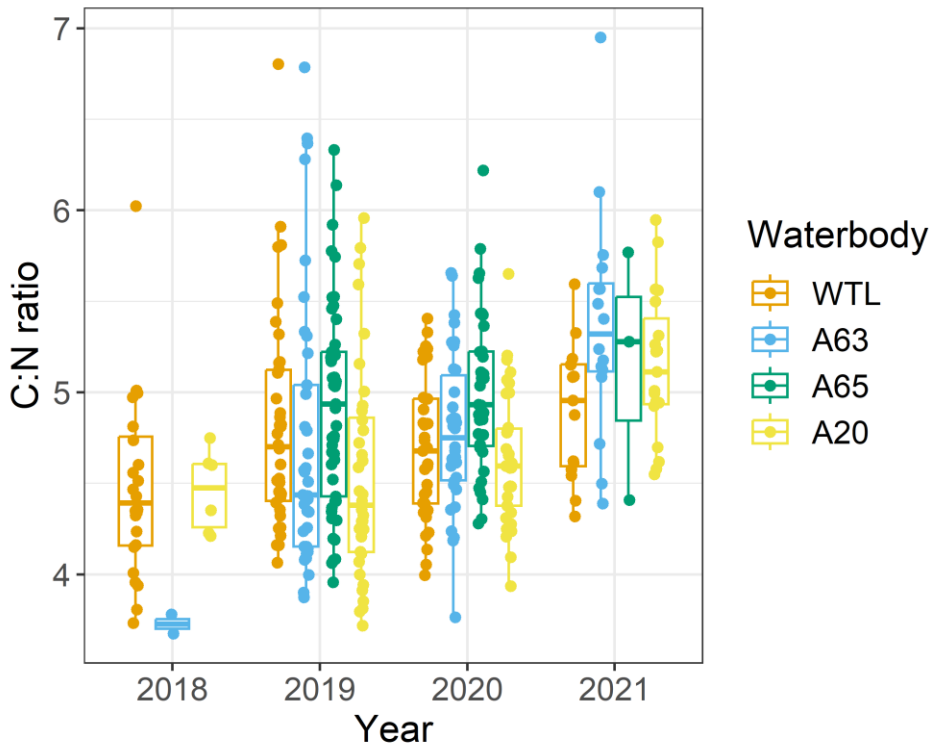


Figure A3.19: *C:N ratio for Ninespine Stickleback between 2018 and 2021 at flooded lakes. Boxplots indicate the median, 25th and 75th percentiles, and minimum and maximum values within 1.5x the interquartile range. All individual data points are plotted.*

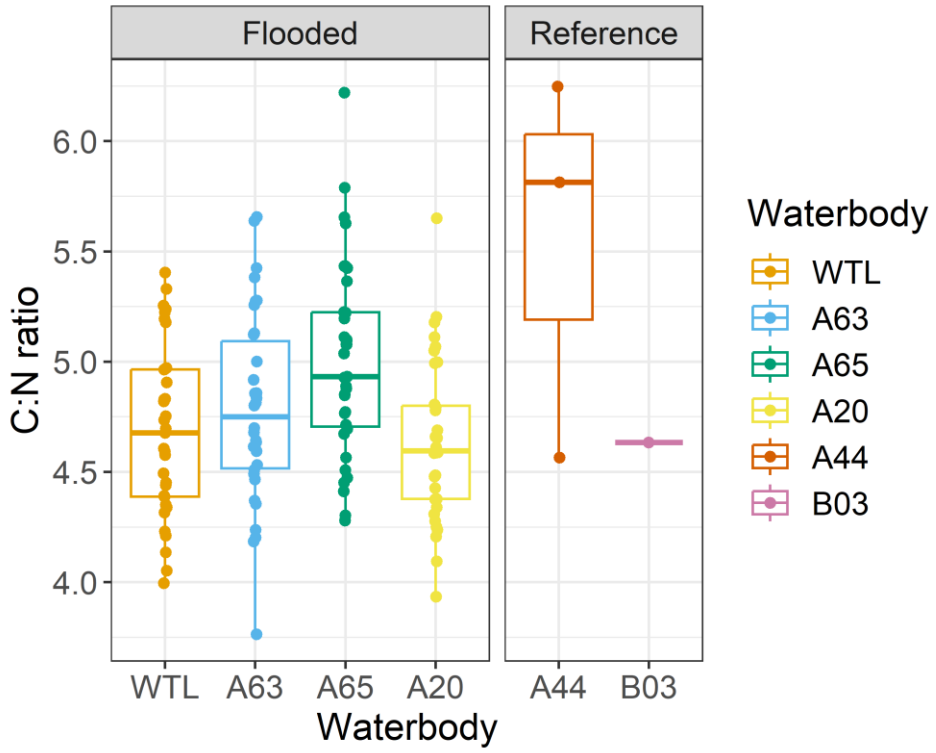


Figure A3.20: *C:N ratio for Ninespine Stickleback at flooded and reference lakes in 2020. Boxplots indicate the median, 25th and 75th percentiles, and minimum and maximum values within 1.5x the interquartile range. All individual data points are plotted.*

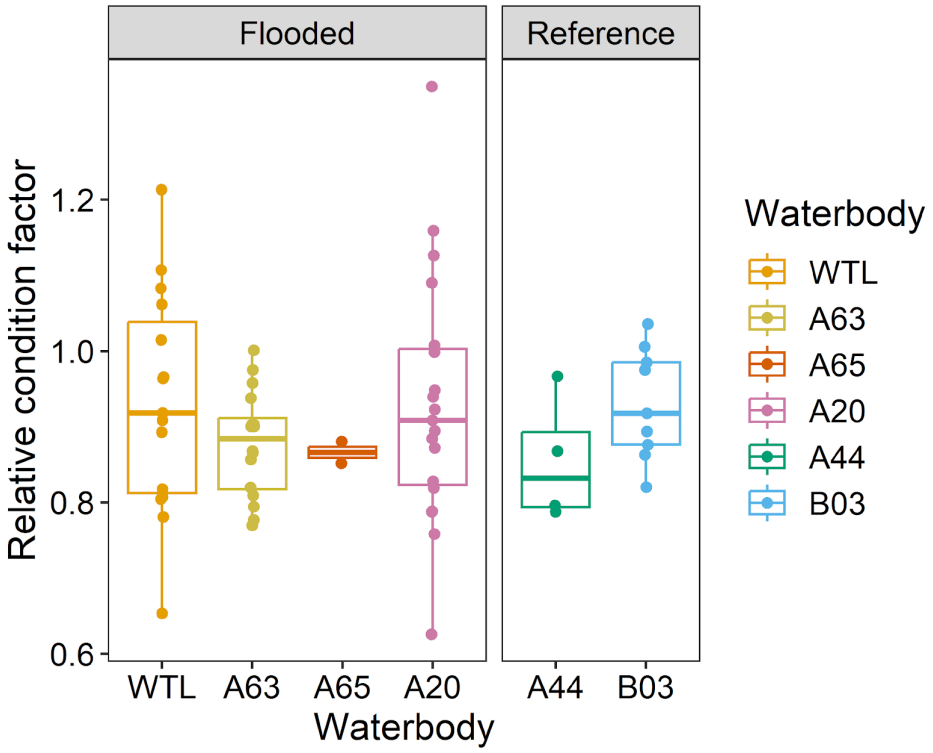


Figure A3.21: *Relative condition for Ninespine Stickleback at flooded and reference lakes in 2021. Boxplots indicate the median, 25th and 75th percentiles, and minimum and maximum values within 1.5x the interquartile range. All individual data points are plotted.*

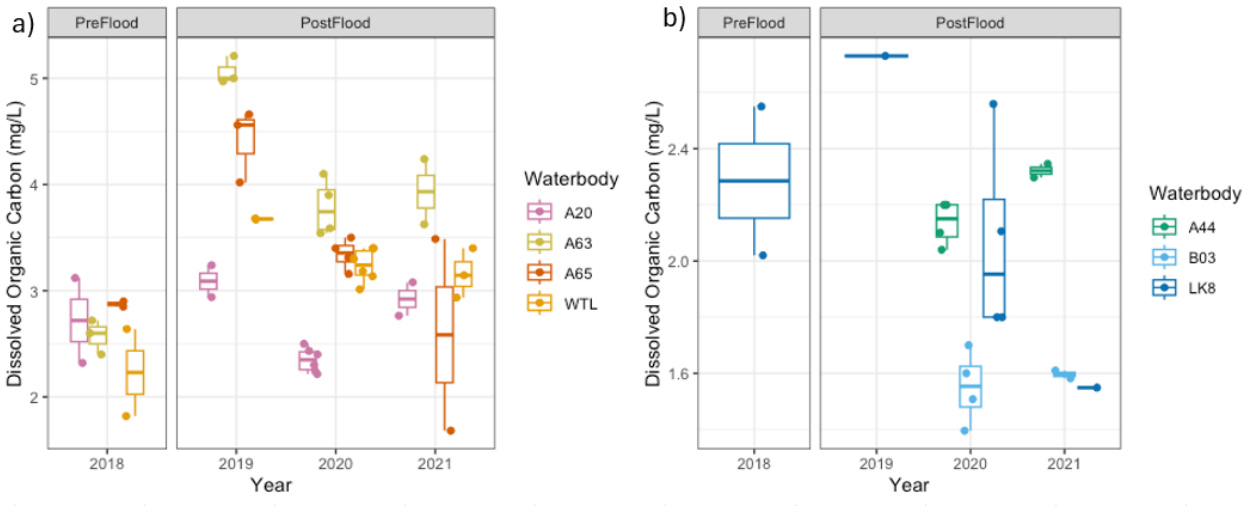


Figure A3.22: *Total dissolved organic carbon (DOC) concentrations (mg/L) in water chemistry samples collected at flooded lakes (a) and reference lakes (b) during pre-flood (2018) and post-flood (2020 and 20212) years. Box plots indicate the mean, 25th, and 75th percentiles, minimum and maximum values with 1.5x the interquartile range. Individual mean values are plotted.*

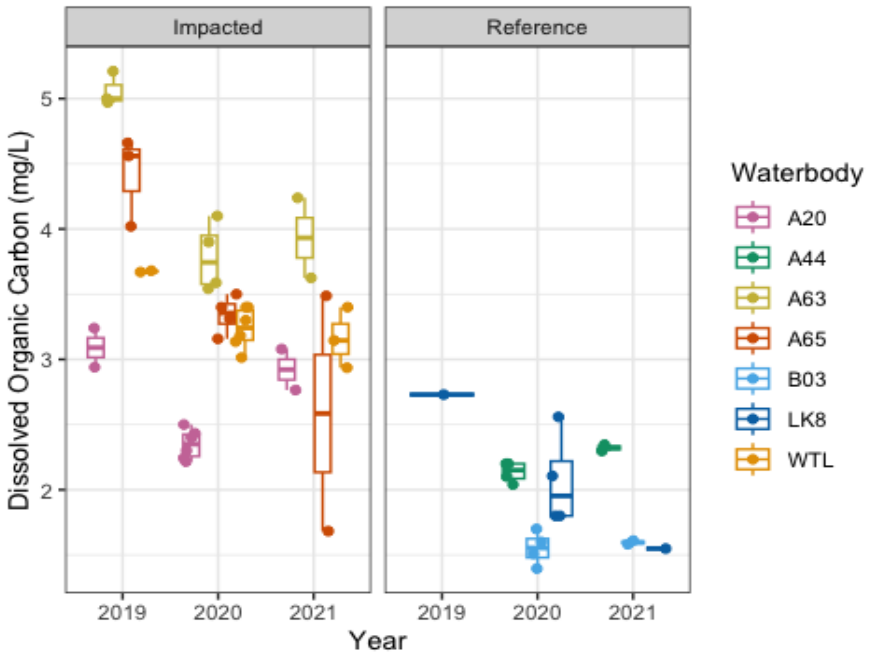


Figure A3.23: *Dissolved organic carbon (DOC) concentrations (mg/L) in water chemistry samples collected at reference and impacted (flooded) lakes during post-flood (2019, 2020, and 2021) years. Box plots indicate the mean, 25th, and 75th percentiles, minimum and maximum values with 1.5x the interquartile range. Individual mean values are plotted.*

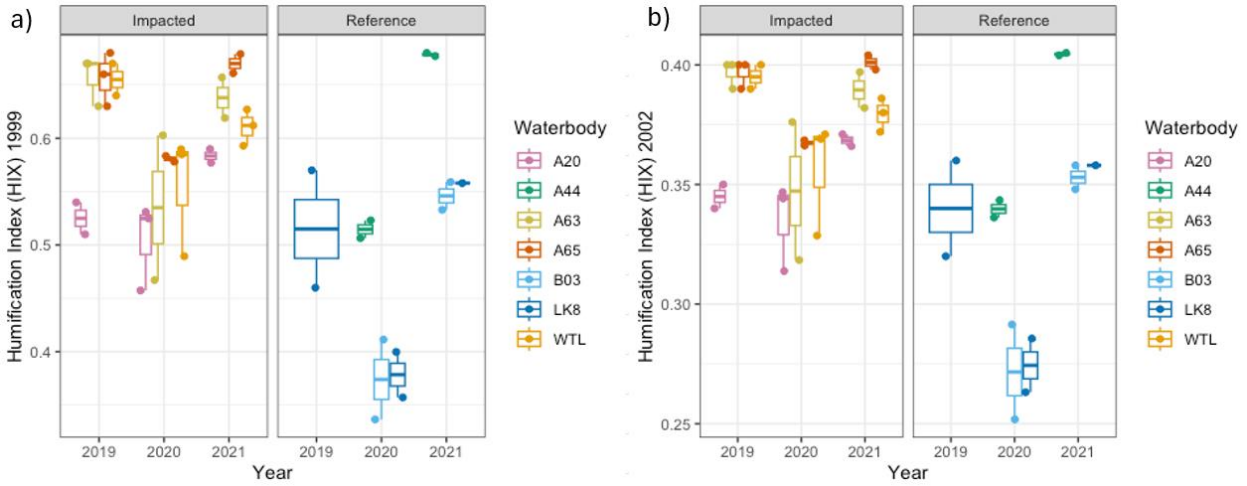


Figure A3.24: *Humification Index (HIX) 1999 (a) and 2002 (b) in water chemistry samples collected at reference and impacted (flooded) lakes during post-flood (2019, 2020, and 2021) years. Box plots indicate the mean, 25th, and 75th percentiles, minimum and maximum values with 1.5x the interquartile range. Individual mean values are plotted.*

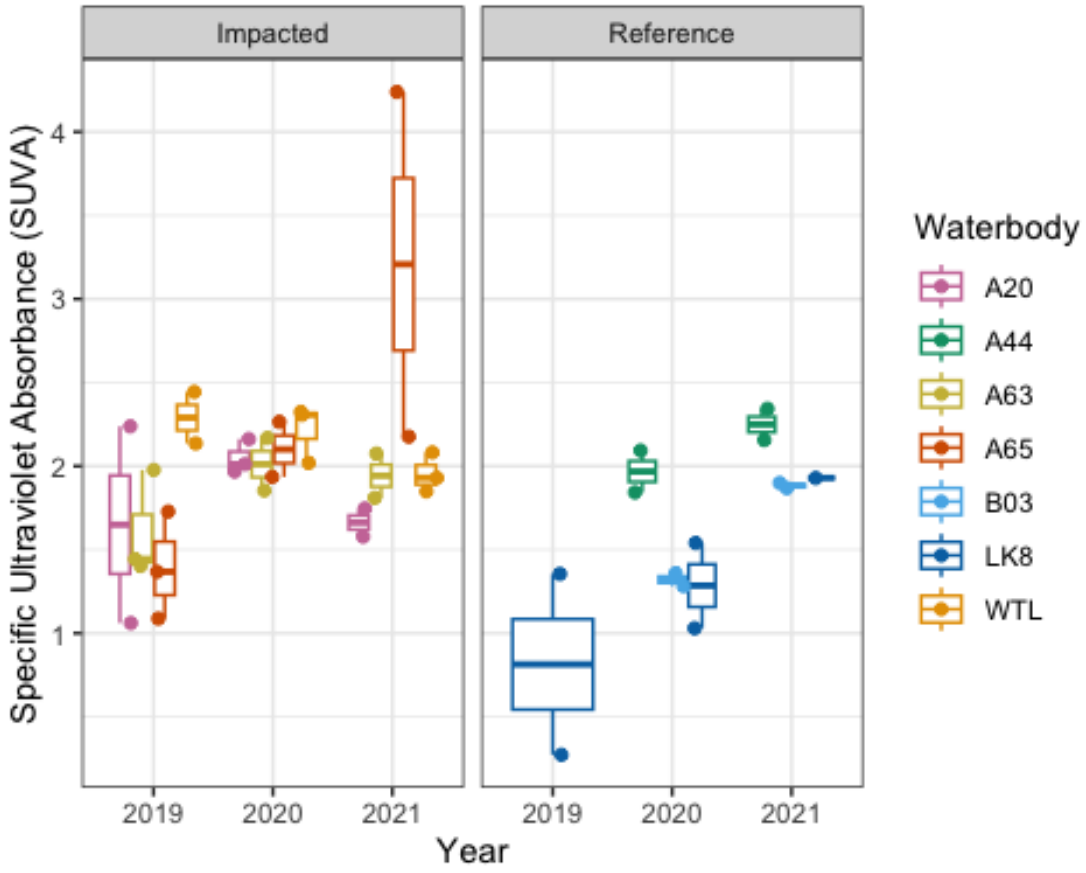


Figure A3.25: *Specific Ultraviolet Absorbance (SUVA) in water chemistry samples collected at reference and impacted (flooded) lakes during post-flood (2019, 2020, and 2021) years. Box plots indicate the mean, 25th, and 75th percentiles, minimum and maximum values with 1.5x the interquartile range. Individual mean values are plotted.*

Appendix A: Tables

Table A2.1: ***The Presence and Absence of Fish Species in each Study Lake between 2018 and 2021. "Y" and green shading indicate the fish species was present. "N" and red indicate the fish species was no present. Data was obtained from C.Portt 2018 and 2019 and Agnico Eagle Mines Ltd in 2023.***

Type	Waterbody	Fish Species					
		Slimy Sculpin (*Cottus cognatus*)	**Ninespine Stickleback (*Pungitius pungitius*)**	**Arctic Char (*Salvelinus alpinus*)**	**Lake Trout (*Salvelinus namaycush*)**	**Round Whitefish (*Prosopium cylindraceum*)**	**Burbot (*Lota lota*)**
Flooded	Whale Tail Lake	Y	Y	Y	Y	Y	Y
	Lake A65	Y	Y	N	Y	Y	N
	Lake A63	Y	Y	Y	Y	Y	N
	Lake A20	Y	Y	Y	Y	Y	N
Reference	Lake 8	Y	Y	Y	Y	N	N
	Lake A44	Y	Y	N	Y	N	N
	Lake B03	Y	Y	Y	Y	N	Y

Table A2.2: Backpack electrofishing catch records for Slimy Sculpin (Cottus cognatus) collected from 2018 to 2021 at flooded lakes (WTL, A63, A65, A20) and reference lakes (LK8, A44, B03). CPUE = catch per unit effort. "-" indicates no available data.

Waterbody	Year	Station ID	Start Date	End Date	Start Time	End Time	Time (Hours)	Pass #	Effort (Seconds)	Slimy Sculpin (SLSC)	
										# Captured	CPUE
WTL	2018	WTL-EF01-2018	26-Jul-2018	26-Jul-2018	09:36	09:50	0.23	1	1596	30	1.13
		WTL-EF02-2018	26-Jul-2018	26-Jul-2018	10:26	10:45	0.32	1	567	9	0.952
		WTL-EF03-2018	26-Jul-2018	26-Jul-2018	10:51	11:03	0.20	1	399.8	9	1.35
		WTL-EF04-2018	26-Jul-2018	26-Jul-2018	11:14	11:53	0.65	1	1102	9	0.490
		WTL-EF05-2018	27-Jul-2018	27-Jul-2018	14:54	15:34	0.67	1	940	7	0.447
		WTL-EF08-2018	28-Jul-2018	28-Jul-2018	08:32	09:29	0.95	1	1994.2	33	0.993
		WTL-EF09-2018	28-Jul-2018	28-Jul-2018	09:51	10:38	0.78	1	1244.9	23	1.11
		WTL-EF10-2018	30-Jul-2018	30-Jul-2018	13:53	14:35	0.70	1	1124	31	1.65
	2019	WTL-EF01-2019	20-Aug-2019	20-Aug-2019	13:05	13:51	0.77	1	1156	11	0.571
		WTL-EF02-2019	20-Aug-2019	20-Aug-2019	14:09	14:52	0.72	2	1386	18	0.779
		WTL-EF03-2019	24-Aug-2019	24-Aug-2019	08:05	08:10	0.08	1	153	3	1.18
	2020	WTL-EF01-2020	26-Aug-20	26-Aug-2020	13:22	13:56	0.57	1	929	5	0.323
		WTL-EF02-2020	26-Aug-20	26-Aug-2020	13:56	14:45	0.82	2	1599	28	1.05
	2021	-	-	-	-	-	-	-	3393	32	0.566
A63	2018	A63-EF01-2018	30-Jul-2018	30-Jul-2018	07:45	08:14	0.48	1	700	16	1.37
		A63-EF02-2018	30-Jul-2018	30-Jul-2018	08:20	08:50	0.50	1	733	29	2.37
		A63-EF03-2018	30-Jul-2018	30-Jul-2018	09:07	09:18	0.18	1	104	1	0.577
		A63-EF04-2018	30-Jul-2018	30-Jul-2018	09:25	09:30	0.08	1	158	7	2.66
		A63-EF05-2018	30-Jul-2018	30-Jul-2018	09:42	10:12	0.50	1	969	31	1.92
	2019	A63-EF01-2019	21-Aug-2019	21-Aug-2019	10:45	11:25	0.67	1	1109	1	0.0541
		A63-EF02-2019	21-Aug-2019	21-Aug-2019	09:10	10:21	1.18	1	1933	6	0.186
	2021	-	-	-	-	-	-	-	2488	29	0.699
A65	2018	A65-EF01-2018	31-Jul-2018	31-Jul-2018	07:40	08:50	1.17	1	1658	29	1.05
		A65-EF02-2018	31-Jul-2018	31-Jul-2018	09:07	09:41	0.57	1	-	23	-
		A65-EF03-2018	31-Jul-2018	31-Jul-2018	09:47	10:35	0.80	1	-	31	-
	2019	A65-EF01-2019	19-Aug-2019	19-Aug-2019	13:00	14:10	1.17	1	2238	2	0.0536
		A65-EF02-2019	19-Aug-2019	19-Aug-2019	14:13	15:21	1.13	2	-	1	-
	2020	A65-EF01-2020	27-Aug-20	27-Aug-2020	10:31	11:39	1.13	1	2024	35	1.04
	2021	-	-	-	-	-	-	-	3210	12	0.224

Table A2.2: Backpack electrofishing catch records for Slimy Sculpin (Cottus cognatus) collected from 2018 to 2021 at flooded lakes (WTL, A63, A65, A20) and reference lakes (LK8, A44, B03). CPUE = catch per unit effort. "-" indicates no available data.

Waterbody	Year	Station ID	Start Date	End Date	Start Time	End Time	Time (Hours)	Pass #	Effort (Seconds)	Slimy Sculpin (SLSC)	
										# Captured	CPUE
A20	2018	A20-EF01-2018	31-Jul-2018	31-Jul-2018	13:45	14:16	0.52	1	966	8	0.497
		A20-EF02-2018	31-Jul-2018	31-Jul-2018	14:34	15:02	0.47	1	798	8	0.602
		A20-EF03-2018	31-Jul-2018	31-Jul-2018	15:50	16:25	0.58	1	934	17	1.09
		A20-EF04-2018	31-Jul-2018	31-Jul-2018	16:48	17:00	0.20	1	-	1	-
		A20-EF05-2018	31-Jul-2018	31-Jul-2018	17:28	17:43	0.25	1	790	3	0.228
		A20-EF06-2018	31-Jul-2018	31-Jul-2018	17:52	18:15	0.38	1	694	3	0.259
		A20-EF07-2018	01-Aug-2018	1-Aug-2018	08:02	08:30	0.47	1	617	3	0.292
		A20-EF08-2018	01-Aug-2018	1-Aug-2018	09:02	09:18	0.27	1	402	6	0.896
		A20-EF09-2018	01-Aug-2018	1-Aug-2018	09:27	09:53	0.43	1	722	12	0.997
		A20-EF09-2018	01-Aug-2018	1-Aug-2018		10:43	10.72	2	543	3	0.331
		A20-EF11-2018	01-Aug-2018	1-Aug-2018	13:34	14:08	0.57	1	1025	10	0.585
		A20-EF10-2018	01-Aug-2018	1-Aug-2018	11:44	11:58	0.23	1	553	1	0.108
	2020	A20-EF01-2020	27-Aug-20	27-Aug-2020	13:29	14:19	0.83	1	1493	8	0.322
		A20-EF02-2020	27-Aug-20	27-Aug-2020	14:28	15:05	0.62	2	1168	29	1.49
	2021	-	-	-	-	-	-	-	5985	6	0.0602
LK8	2018	LK8-EF01-2018	02-Aug-2018	2-Aug-2018	10:40	11:30	0.83	1	1408	15	0.639
		LK8-EF02-2018	02-Aug-2018	2-Aug-2018	13:13	14:42	1.48	1	2738	37	0.811
		LK8-EF03-2018	02-Aug-2018	2-Aug-2018	14:55	15:30	0.58	1	1040	31	1.79
		LK8-EF04-2018	02-Aug-2018	2-Aug-2018	15:43	16:07	0.40	1	683	17	1.49
	2020	LK8-EF01-2020	23-Aug-20	23-Aug-2020	13:47	15:13	1.43	1	2338	53	1.36
		LK8-EF02-2020	23-Aug-20	23-Aug-2020	15:19	15:30	0.18	2	329	2	0.365
		LK8-EF03-2020	24-Aug-20	24-Aug-2020	08:04	08:15	0.18	3	425	2	0.282
		LK8-EF04-2020	24-Aug-20	24-Aug-2020	08:23	09:37	1.23	4	2646	45	1.02
	2021	-	-	-	-	-	-	-	5058	10	0.119
A44	2019	A44-EF01-2019	18-Aug-2019	18-Aug-2019	09:15	10:30	1.25	1	2158	34	0.945
	2020	A44-EF01-2020	29-Aug-20	29-Aug-2020	08:47	10:23	1.60	1	2488	30	0.724
		A44-EF02-2020	29-Aug-20	29-Aug-2020	10:33	10:42	0.15	2	233	4	1.03
	2021	-	-	-	-	-	-	-	4448	8	0.108
B03	2020	B03-EF01-2020	29-Aug-20	29-Aug-2020	14:50	15:22	0.53	1	826	34	2.47
	2021	-	-	-	-	-	-	-	4315	30	0.417

Table A2.3: Backpack electrofishing catch records for Ninespine Stickleback (Pungitius pungitius) collected from 2018 to 2021 at flooded lakes (WTL, A63, A65, A20) and reference lakes (LK8, A44, B03). CPUE = catch per unit effort. "-" indicates no available data.

Waterbody	Year	Station ID	Start Date	End Date	Start Time	End Time	Time (Hours)	Effort (Seconds)	Ninespine Stickleback (NNST)	
									# Captured	CPUE
WTL	2018	WTL-EF01-2018	26-Jul-2018	26-Jul-2018	09:36	09:50	0.23	1596	1	0.0376
		WTL-EF02-2018	26-Jul-2018	26-Jul-2018	10:26	10:45	0.32	567	4	0.423
		WTL-EF04-2018	26-Jul-2018	26-Jul-2018	11:14	11:53	0.65	1102	9	0.490
		WTL-EF06-2018	27-Jul-2018	27-Jul-2018	16:10	18:05	1.92	3517.9	38	0.648
		WTL-EF07-2018	27-Jul-2018	27-Jul-2018	18:12	18:32	0.33	523.9	1	0.115
		WTL-EF08-2018	28-Jul-2018	28-Jul-2018	08:32	09:29	0.95	1994.2	1	0.0301
	2019	WTL-EF01-2019	20-Aug-2019	20-Aug-2019	13:05	13:51	0.77	1156	26	1.35
		WTL-EF02-2019	20-Aug-2019	20-Aug-2019	14:09	14:52	0.72	1386	30	1.30
	2020	WTL-EF01-2020	26-Aug-20	26-Aug-2020	13:22	13:56	0.57	929	33	2.13
		WTL-EF02-2020	26-Aug-20	26-Aug-2020	13:56	14:45	0.82	1599	96	3.60
	2021	-	-	-	-	-	-	3393	15	0.265
A63	2018	A63-EF01-2018	30-Jul-2018	30-Jul-2018	07:45	08:14	0.48	700	1	0.0857
		A63-EF02-2018	30-Jul-2018	30-Jul-2018	08:20	08:50	0.50	733	1	0.0819
	2019	A63-EF01-2019	21-Aug-2019	21-Aug-2019	10:45	11:25	0.67	1109	12	0.649
		A63-EF02-2019	21-Aug-2019	21-Aug-2019	09:10	10:21	1.18	1933	24	0.745
	2020	A63-EF01-2020	26-Aug-20	26-Aug-2020	11:49	12:20	0.52	665	41	3.70
		A63-EF02-2020	26-Aug-20	26-Aug-2020	12:26	12:35	0.15	309	29	5.63
	2021	-	-	-	-	-	-	2488	16	0.386
A20	2018	A20-EF02-2018	31-Jul-2018	31-Jul-2018	14:34	15:02	0.47	798	3	0.226
	2019	A20-EF01-2019	21-Aug-2019	21-Aug-2019	12:31	14:44	2.22	2307	35	0.910
	2020	A20-EF01-2020	27-Aug-20	27-Aug-2020	13:29	14:19	0.83	1493	45	1.81
		A20-EF02-2020	27-Aug-20	27-Aug-2020	14:28	15:05	0.62	1168	62	3.18
	2021	-	-	-	-	-	-	5985	19	0.190
A65	2019	A65-EF01-2019	19-Aug-2019	19-Aug-2019	13:00	14:10	1.17	2238	12	0.322
		A65-EF02-2019	19-Aug-2019	19-Aug-2019	14:13	15:21	1.13	-	37	-
	2020	A65-EF01-2020	27-Aug-20	27-Aug-2020	10:31	11:39	1.13	2024	35	1.04
	2021	-	-	-	-	-	-	3210	3	0.0561

Table A2.3: Backpack electrofishing catch records for Ninespine Stickleback (Pungitius pungitius) collected from 2018 to 2021 at flooded lakes (WTL, A63, A65, A20) and reference lakes (LK8, A44, B03). CPUE = catch per unit effort. "-" indicates no available data.

Waterbody	Year	Station ID	Start Date	End Date	Start Time	End Time	Time (Hours)	Effort (Seconds)	Ninespine Stickleback (NNST)	
									# Captured	CPUE
A44	2019	A44-EF01-2019	18-Aug-2019	18-Aug-2019	09:15	10:30	1.25	2158	2	0.0556
	2020	A44-EF01-2020	29-Aug-20	29-Aug-2020	08:47	10:23	1.60	2488	3	0.0724
		A44-EF02-2020	29-Aug-20	29-Aug-2020	10:33	10:42	0.15	233	5	1.29
	2021	-	-	-	-	-	-	4448	4	0.0540
B03	2020	B03-EF01-2020	29-Aug-20	29-Aug-2020	14:50	15:22	0.53	826	1	0.0727
	2021	-	-	-	-	-	-	4315	9	0.125

Table A2.4: Laboratory Results for all Slimy Sculpin (Cottus cognatus; SLSC) and Ninespine Stickleback (Pungitius pungitius; NNST) laboratory results from Biotron Laboratory, the University of Waterloo Environmental Isotope Laboratory, and AAE Tech Incorporated. These results include total Hg concentrations with all sample quality assurance and quality control (QA/QC) in accordance with international standards. Stable isotopes from fish tissue are presented as percent (%) carbon (C) and nitrogren (N), as well as with per mil (‰) for delta values of each of these. Age estimates were made using extracted otoliths. mm = millimeters, g = grams, mg/kg = milligrams per killogram, THg = total mercury, MDL = method detection limit, MRL= method reporting limit , DUP = duplicate, C = carbon, N = nitrogren, NA = no available data.

Sample Year	Fish Species Code	Lake Name	Fork Length (mm)	Wet Weight (g)	THg WW (mg/kg)	MDL (ng)	MRL (ng)	IPR avg (%)	%C	%N	δ13C	δ15N	DUP %C	DUP %N	DUP δ13C	DUP δ15N	Age Estimate
2018	NNST	WTL	55.0	1.20	0.097	0.0689	0.207	97.0	33.9	8.91	-25.8	9.67	NA	NA	NA	NA	0
2018	NNST	WTL	38.0	0.400	0.0470	0.0727	0.218	103	44.3	11.2	-24.4	8.59	NA	NA	NA	NA	0
2018	NNST	WTL	42.0	0.600	0.0408	0.0689	0.207	98.0	49.2	10.7	-24.0	8.94	NA	NA	NA	NA	0
2018	NNST	WTL	38.0	0.400	0.0499	0.0727	0.218	103	46.9	10.8	-26.8	8.48	NA	NA	NA	NA	0
2018	NNST	WTL	56.0	1.40	0.0518	0.0689	0.207	97.0	41.2	8.56	-26.9	9.95	NA	NA	NA	NA	0
2018	NNST	WTL	44.0	0.500	0.0390	0.0689	0.207	98.0	47.9	11.5	-25.8	9.25	NA	NA	NA	NA	0
2018	NNST	WTL	45.0	0.600	0.0679	0.0727	0.218	103	37.7	10.1	-25.6	8.75	NA	NA	NA	NA	0
2018	NNST	WTL	34.0	0.300	0.0508	0.0727	0.218	103	41.9	10.6	-24.4	9.32	NA	NA	NA	NA	0
2018	NNST	WTL	48.0	0.700	0.0412	0.0727	0.218	103	49.3	11.9	-24.7	8.69	NA	NA	NA	NA	0
2018	NNST	WTL	40.0	0.600	0.0408	0.0689	0.207	98.0	49.4	11.7	-26.3	9.45	NA	NA	NA	NA	0
2018	NNST	WTL	42.0	0.500	0.0424	0.0689	0.207	98.0	46.2	11.5	-24.5	8.53	NA	NA	NA	NA	0
2018	NNST	WTL	41.0	0.600	0.0578	0.0727	0.218	103	45.2	10.4	-25.7	8.98	NA	NA	NA	NA	0
2018	NNST	WTL	46.0	0.600	0.0368	0.0727	0.218	103	47.8	10.5	-24.1	8.33	NA	NA	NA	NA	0
2018	NNST	WTL	41.0	0.400	0.0437	0.0689	0.207	98.0	51.5	11.5	-24.8	8.40	NA	NA	NA	NA	0
2018	NNST	WTL	44.0	0.500	0.0471	0.0689	0.207	98.0	44.9	10.3	-25.0	9.01	NA	NA	NA	NA	0
2018	NNST	WTL	45.0	0.500	0.0480	0.0689	0.207	98.0	52.6	11.6	-27.2	6.98	NA	NA	NA	NA	0
2018	NNST	WTL	69.0	2.60	0.0565	0.0689	0.207	97.0	38.8	8.93	-24.4	9.01	NA	NA	NA	NA	0
2018	NNST	WTL	47.0	0.800	0.0377	0.0689	0.207	98.0	48.8	10.3	-24.6	8.90	NA	NA	NA	NA	0
2018	NNST	WTL	49.0	1.10	NA	NA	NA	NA	NA	NA	NA	NA	NA	NA	NA	NA	NA
2018	NNST	WTL	43.0	0.500	0.0341	0.0727	0.218	103	49.3	11.1	-23.8	8.74	NA	NA	NA	NA	0
2018	NNST	WTL	48.0	0.700	0.0338	0.0689	0.207	98.0	49.0	9.79	-24.4	8.83	NA	NA	NA	NA	0
2018	NNST	WTL	47.0	0.800	0.0327	0.0689	0.207	98.0	41.9	8.39	-24.8	9.06	53.3	10.9	-24.7	9.19	0
2018	NNST	WTL	47.0	0.700	0.0333	0.0689	0.207	98.0	45.4	9.13	-23.9	9.07	NA	NA	NA	NA	0
2018	NNST	WTL	52.0	1.00	0.0367	0.0689	0.207	97.0	46.0	9.18	-25.4	9.04	NA	NA	NA	NA	0
2018	NNST	WTL	55.0	1.00	0.0743	0.0689	0.207	98.0	55.4	9.20	-30.7	7.43	NA	NA	NA	NA	0
2018	SLSC	WTL	30.0	0.100	0.0302	0.0689	0.207	98.0	43.7	10.0	-22.1	7.36	NA	NA	NA	NA	0
2018	NNST	MMT	54.0	1.00	0.0241	0.0689	0.207	97.0	44.1	8.46	-26.3	8.48	NA	NA	NA	NA	0
2018	NNST	MMT	49.0	0.700	0.0255	0.0727	0.218	103	56.7	12.6	-26.5	8.83	NA	NA	NA	NA	0
2018	NNST	MMT	55.0	0.900	0.0313	0.0689	0.207	97.0	40.8	8.47	-25.9	8.70	NA	NA	NA	NA	0
2018	SLSC	MMT	62.0	2.60	0.0533	0.0689	0.207	97.0	33.4	7.90	-21.9	7.48	NA	NA	NA	NA	3
2018	SLSC	MMT	36.0	0.400	0.0269	0.0727	0.218	103	53.9	11.5	-23.7	6.65	55.4	12.2	-23.6	7.09	0
2018	SLSC	MMT	30.0	0.200	0.0323	0.0727	0.218	103	47.0	10.5	-23.7	7.71	NA	NA	NA	NA	0

Table A2.4: Laboratory Results for all Slimy Sculpin (Cottus cognatus; SLSC) and Ninespine Stickleback (Pungitius pungitius; NNST) laboratory results from Biotron Laboratory, the University of Waterloo Environmental Isotope Laboratory, and AAE Tech Incorporated. These results include total Hg concentrations with all sample quality assurance and quality control (QA/QC) in accordance with international standards. Stable isotopes from fish tissue are presented as percent (%) carbon (C) and nitrogren (N), as well as with per mil (‰) for delta values of each of these. Age estimates were made using extracted otoliths. mm = millimeters, g = grams, mg/kg = milligrams per killogram, THg = total mercury, MDL = method detection limit, MRL= method reporting limit , DUP = duplicate, C = carbon, N = nitrogren, NA = no available data.

Sample Year	Fish Species Code	Lake Name	Fork Length (mm)	Wet Weight (g)	THg WW (mg/kg)	MDL (ng)	MRL (ng)	IPR avg (%)	%C	%N	δ13C	δ15N	DUP %C	DUP %N	DUP δ13C	DUP δ15N	Age Estimate
2018	NNST	MMT	55.0	1.40	0.0434	0.0689	0.207	97.0	34.8	6.52	-24.1	8.14	NA	NA	NA	NA	0
2018	SLSC	MMT	45.0	0.900	0.0305	0.0689	0.207	97.0	37.5	8.01	-22.7	7.43	51.7	10.9	-22.8	7.44	1
2018	SLSC	MMT	47.0	0.900	0.0286	0.0689	0.207	98.0	52.2	9.29	-21.4	6.99	NA	NA	NA	NA	2
2018	SLSC	MMT	33.0	0.300	0.0263	0.0727	0.218	103	54.2	10.1	-23.4	6.28	NA	NA	NA	NA	0
2018	SLSC	MMT	48.0	1.00	0.0274	0.0689	0.207	98.0	46.5	9.39	-22.2	6.91	NA	NA	NA	NA	1
2018	SLSC	MMT	46.0	0.900	0.0280	0.0689	0.207	98.0	57.1	10.9	-21.7	6.84	NA	NA	NA	NA	1
2018	SLSC	MMT	47.0	1.00	0.0467	0.0689	0.207	98.0	46.1	9.66	-22.3	7.55	NA	NA	NA	NA	2
2018	SLSC	MMT	29.0	0.300	0.0376	0.0727	0.218	103	52.0	11.1	-23.6	6.51	NA	NA	NA	NA	0
2018	SLSC	MMT	52.0	1.40	0.0313	0.0689	0.207	97.0	32.4	5.29	-23.4	6.66	NA	NA	NA	NA	1
2018	SLSC	MMT	44.0	0.700	0.0358	0.0689	0.207	98.0	40.4	7.99	-22.0	7.31	NA	NA	NA	NA	0
2018	SLSC	MMT	39.0	0.500	0.0652	0.0689	0.207	98.0	49.7	9.43	-22.8	6.86	NA	NA	NA	NA	0
2018	SLSC	MMT	38.0	0.500	0.0274	0.0689	0.207	98.0	48.5	10.1	-23.2	7.17	50.4	10.5	-23.1	7.14	1
2018	SLSC	MMT	35.0	0.400	0.0262	0.0689	0.207	98.0	49.1	9.86	-22.7	7.04	NA	NA	NA	NA	0
2018	SLSC	MMT	32.0	0.300	0.0323	0.0727	0.218	103	45.7	9.76	-23.6	7.19	NA	NA	NA	NA	0
2018	SLSC	MMT	39.0	0.500	0.0262	0.0689	0.207	97.0	35.8	6.83	-23.8	7.06	NA	NA	NA	NA	0
2018	SLSC	MMT	36.0	0.400	0.0263	0.0689	0.207	98.0	54.1	10.7	-23.3	7.16	NA	NA	NA	NA	0
2018	SLSC	MMT	30.0	0.200	0.0273	0.0689	0.207	98.0	47.2	9.60	-21.4	6.59	NA	NA	NA	NA	0
2018	SLSC	MMT	31.0	0.200	0.0345	0.0689	0.207	98.0	48.4	9.50	-22.4	6.53	NA	NA	NA	NA	0
2018	NNST	A63	58.0	1.30	0.0784	0.0689	0.207	99.0	45.0	11.9	-21.8	7.87	NA	NA	NA	NA	0
2018	NNST	A63	45.0	0.600	0.133	0.0689	0.207	99.0	43.1	11.7	-24.1	9.00	NA	NA	NA	NA	0
2018	SLSC	A63	47.0	0.900	0.0482	0.0689	0.207	99.0	47.0	9.84	-22.4	7.00	NA	NA	NA	NA	2
2018	SLSC	A63	60.0	1.30	0.0853	0.0689	0.207	99.0	42.4	12.3	-20.1	7.09	NA	NA	NA	NA	1
2018	SLSC	A63	54.0	1.30	0.0337	0.0689	0.207	99.0	51.5	11.1	-22.7	6.66	NA	NA	NA	NA	1
2018	SLSC	A63	34.0	0.300	0.0307	0.0689	0.207	99.0	50.7	10.2	-24.4	8.13	NA	NA	NA	NA	0
2018	SLSC	A63	57.0	1.20	0.110	0.0689	0.207	99.0	36.2	10.4	-19.7	7.33	NA	NA	NA	NA	3
2018	SLSC	A63	49.0	1.00	0.0326	0.0689	0.207	99.0	46.3	9.11	-21.4	6.32	NA	NA	NA	NA	1
2018	SLSC	A63	51.0	1.00	0.0394	0.0689	0.207	99.0	54.2	11.0	-22.1	6.83	NA	NA	NA	NA	1
2018	SLSC	A63	43.0	0.600	0.0497	0.0689	0.207	99.0	46.2	9.20	-22.8	6.21	50.5	10.7	-22.6	6.70	1
2018	SLSC	A63	60.0	1.90	0.0500	0.0689	0.207	99.0	53.0	11.1	-22.2	7.22	NA	NA	NA	NA	3
2018	SLSC	A63	30.0	0.200	0.0383	0.0689	0.207	99.0	50.1	10.4	-22.6	5.86	NA	NA	NA	NA	0
2018	SLSC	A63	50.0	0.500	0.0455	0.0689	0.207	99.0	46.3	9.70	-23.1	6.50	NA	NA	NA	NA	1

Table A2.4: Laboratory Results for all Slimy Sculpin (Cottus cognatus; SLSC) and Ninespine Stickleback (Pungitius pungitius; NNST) laboratory results from Biotron Laboratory, the University of Waterloo Environmental Isotope Laboratory, and AAE Tech Incorporated. These results include total Hg concentrations with all sample quality assurance and quality control (QA/QC) in accordance with international standards. Stable isotopes from fish tissue are presented as percent (%) carbon (C) and nitrogren (N), as well as with per mil (‰) for delta values of each of these. Age estimates were made using extracted otoliths. mm = millimeters, g = grams, mg/kg = milligrams per killogram, THg = total mercury, MDL = method detection limit, MRL= method reporting limit , DUP = duplicate, C = carbon, N = nitrogren, NA = no available data.

Sample Year	Fish Species Code	Lake Name	Fork Length (mm)	Wet Weight (g)	THg WW (mg/kg)	MDL (ng)	MRL (ng)	IPR avg (%)	%C	%N	δ13C	δ15N	DUP %C	DUP %N	DUP δ13C	DUP δ15N	Age Estimate
2018	SLSC	A63	65.0	2.60	0.0513	0.0689	0.207	99.0	53.3	12.2	-23.6	7.46	NA	NA	NA	NA	2
2018	SLSC	A63	36.0	0.400	0.0263	0.0689	0.207	99.0	49.8	10.5	-22.2	5.87	NA	NA	NA	NA	0
2018	SLSC	A63	59.0	2.00	0.0431	0.0689	0.207	99.0	48.8	10.1	-21.8	6.62	NA	NA	NA	NA	1
2018	SLSC	A63	46.0	1.10	0.0387	0.0689	0.207	99.0	51.3	10.4	-22.2	6.34	NA	NA	NA	NA	1
2018	SLSC	A63	54.0	1.40	0.0473	0.0689	0.207	99.0	47.8	10.2	-21.4	6.16	NA	NA	NA	NA	1
2018	SLSC	A63	47.0	1.00	0.0324	0.0689	0.207	99.0	50.0	11.0	-20.7	6.18	NA	NA	NA	NA	1
2018	SLSC	A63	45.0	0.900	0.0353	0.0689	0.207	99.0	51.4	10.2	-21.3	6.42	48.9	9.63	-21.4	6.46	2
2018	SLSC	A63	31.0	0.300	0.0297	0.0689	0.207	99.0	51.6	10.8	-20.0	5.95	NA	NA	NA	NA	0
2018	SLSC	A63	38.0	0.500	0.0298	0.0689	0.207	99.0	48.5	9.16	-22.5	5.74	NA	NA	NA	NA	0
2018	SLSC	A63	48.0	0.900	0.0356	0.0689	0.207	99.0	54.0	11.2	-22.2	5.99	NA	NA	NA	NA	1
2018	SLSC	A63	55.0	1.60	0.0377	0.0689	0.207	99.0	47.6	9.84	-21.5	6.11	NA	NA	NA	NA	1
2018	SLSC	A63	52.0	1.20	0.0343	0.0689	0.207	99.0	52.7	11.2	-21.3	6.04	NA	NA	NA	NA	2
2018	SLSC	A63	47.0	0.900	0.0343	0.0689	0.207	99.0	55.2	11.4	-21.0	5.69	NA	NA	NA	NA	2
2018	SLSC	A63	37.0	0.500	0.0261	0.0689	0.207	99.0	54.0	11.1	-22.4	5.76	NA	NA	NA	NA	0
2018	SLSC	A63	35.0	0.300	0.0340	0.0689	0.207	99.0	52.2	12.5	-21.2	6.40	NA	NA	NA	NA	0
2018	SLSC	A63	45.0	0.800	0.0407	0.0689	0.207	99.0	48.2	9.08	-22.0	6.10	NA	NA	NA	NA	0
2018	SLSC	A63	37.0	0.500	0.0292	0.0689	0.207	99.0	51.2	10.9	-21.2	5.33	47.8	10.3	-21.2	5.36	1
2018	SLSC	A63	48.0	1.00	0.0315	0.0689	0.207	99.0	57.1	11.6	-21.8	6.32	NA	NA	NA	NA	1
2018	SLSC	A63	34.0	0.300	0.0291	0.0689	0.207	99.0	44.5	9.81	-20.5	5.69	NA	NA	NA	NA	0
2018	SLSC	WTL	59.0	2.10	0.0343	0.0689	0.207	97.0	38.5	7.68	-23.1	7.05	NA	NA	NA	NA	2
2018	SLSC	WTL	47.0	0.900	0.0385	0.0689	0.207	98.0	48.7	9.38	-23.6	7.93	NA	NA	NA	NA	1
2018	SLSC	WTL	45.0	0.800	0.0325	0.0689	0.207	97.0	45.0	9.33	-23.0	7.43	NA	NA	NA	NA	1
2018	SLSC	WTL	37.0	0.400	0.0374	0.0727	0.218	103	46.4	9.26	-25.4	7.52	NA	NA	NA	NA	0
2018	SLSC	WTL	30.0	0.300	0.0297	0.0727	0.218	103	41.7	8.76	-23.1	6.47	NA	NA	NA	NA	0
2018	SLSC	WTL	44.0	0.700	0.0308	0.0689	0.207	98.0	47.8	10.9	-22.2	7.80	NA	NA	NA	NA	1
2018	SLSC	WTL	43.0	0.800	0.0314	0.0689	0.207	98.0	42.9	9.83	-21.5	7.39	NA	NA	NA	NA	1
2018	SLSC	WTL	42.0	0.600	0.0308	0.0689	0.207	97.0	37.1	8.28	-22.1	7.55	NA	NA	NA	NA	1
2018	SLSC	WTL	72.0	2.30	0.102	0.0689	0.207	97.0	41.8	12.2	-24.0	7.93	NA	NA	NA	NA	3
2018	SLSC	WTL	43.0	0.600	0.0295	0.0689	0.207	98.0	50.2	11.0	-21.2	7.10	NA	NA	NA	NA	0
2018	SLSC	WTL	35.0	0.300	0.0358	0.0727	0.218	103	50.1	10.4	-23.5	7.39	NA	NA	NA	NA	0
2018	SLSC	WTL	39.0	0.200	0.0311	0.0689	0.207	98.0	45.9	11.1	-22.6	7.35	NA	NA	NA	NA	NA

Table A2.4: Laboratory Results for all Slimy Sculpin (Cottus cognatus; SLSC) and Ninespine Stickleback (Pungitius pungitius; NNST) laboratory results from Biotron Laboratory, the University of Waterloo Environmental Isotope Laboratory, and AAE Tech Incorporated. These results include total Hg concentrations with all sample quality assurance and quality control (QA/QC) in accordance with international standards. Stable isotopes from fish tissue are presented as percent (%) carbon (C) and nitrogren (N), as well as with per mil (‰) for delta values of each of these. Age estimates were made using extracted otoliths. mm = millimeters, g = grams, mg/kg = milligrams per killogram, THg = total mercury, MDL = method detection limit, MRL= method reporting limit , DUP = duplicate, C = carbon, N = nitrogren, NA = no available data.

Sample Year	Fish Species Code	Lake Name	Fork Length (mm)	Wet Weight (g)	THg WW (mg/kg)	MDL (ng)	MRL (ng)	IPR avg (%)	%C	%N	δ13C	δ15N	DUP %C	DUP %N	DUP δ13C	DUP δ15N	Age Estimate
2018	SLSC	WTL	53.0	1.40	0.0429	0.0689	0.207	98.0	55.9	11.2	-23.2	7.62	51.2	10.2	-23.1	7.50	1
2018	SLSC	WTL	34.0	0.400	0.0360	0.0727	0.218	103	52.5	10.4	-25.1	7.56	NA	NA	NA	NA	0
2018	SLSC	WTL	56.0	2.00	0.0368	0.0689	0.207	97.0	50.0	9.14	-24.1	7.49	NA	NA	NA	NA	1
2018	SLSC	WTL	63.0	2.50	0.0385	0.0689	0.207	97.0	44.9	8.61	-25.9	8.47	NA	NA	NA	NA	2
2018	SLSC	WTL	51.0	1.40	0.0337	0.0689	0.207	97.0	40.4	7.31	-23.6	7.08	NA	NA	NA	NA	1
2018	SLSC	WTL	36.0	0.500	0.0272	0.0689	0.207	98.0	53.4	11.3	-23.5	7.28	NA	NA	NA	NA	1
2018	SLSC	WTL	31.0	0.400	0.0283	0.0689	0.207	98.0	45.5	9.19	-23.5	6.91	NA	NA	NA	NA	0
2018	SLSC	WTL	32.0	0.300	0.0296	0.0727	0.218	103	46.9	10.1	-21.4	7.24	NA	NA	NA	NA	0
2018	SLSC	WTL	32.0	0.300	0.0321	0.0689	0.207	98.0	50.7	11.8	-23.7	7.73	NA	NA	NA	NA	0
2018	SLSC	WTL	32.0	0.400	0.0362	0.0689	0.207	98.0	40.2	8.55	-24.5	7.35	NA	NA	NA	NA	0
2018	SLSC	WTL	42.0	0.700	0.0336	0.0689	0.207	98.0	50.5	10.7	-23.7	7.73	NA	NA	NA	NA	0
2018	SLSC	WTL	29.0	0.200	0.0264	0.0689	0.207	97.0	38.0	8.43	-22.4	7.80	NA	NA	NA	NA	0
2018	SLSC	WTL	38.0	0.500	0.0278	0.0689	0.207	98.0	38.9	8.35	-23.2	7.25	NA	NA	NA	NA	0
2018	SLSC	WTL	34.0	0.300	0.0263	0.0689	0.207	98.0	42.8	9.54	-23.2	7.23	NA	NA	NA	NA	0
2018	SLSC	WTL	37.0	0.400	0.0243	0.0689	0.207	98.0	44.8	10.2	-23.2	7.72	NA	NA	NA	NA	0
2018	SLSC	WTL	34.0	0.400	0.0253	0.0689	0.207	98.0	50.1	10.1	-23.9	7.76	NA	NA	NA	NA	0
2018	SLSC	WTL	36.0	0.400	0.0268	0.0689	0.207	98.0	50.8	10.4	-23.1	7.22	47.1	8.65	-23.6	7.22	0
2018	SLSC	A65	36.0	0.400	0.0397	0.0727	0.218	103	49.7	11.0	-23.4	7.92	47.5	10.2	-23.4	8.03	0
2018	SLSC	A65	43.0	0.600	0.0256	0.0689	0.207	99.0	49.8	11.4	-22.4	7.48	NA	NA	NA	NA	1
2018	SLSC	A65	44.0	0.700	0.0276	0.0689	0.207	97.0	39.8	8.44	-22.6	7.73	46.7	10.0	-22.6	7.93	0
2018	SLSC	A65	39.0	0.600	0.0311	0.0727	0.218	103	54.6	11.2	-23.1	7.14	NA	NA	NA	NA	0
2018	SLSC	A65	39.0	0.500	0.0327	0.0689	0.207	99.0	49.8	10.5	-22.5	8.70	NA	NA	NA	NA	0
2018	SLSC	A65	38.0	0.400	0.0297	0.0727	0.218	103	57.8	12.0	-23.0	7.60	NA	NA	NA	NA	0
2018	SLSC	A65	33.0	0.300	0.0333	0.0727	0.218	103	50.4	11.0	-21.1	6.91	NA	NA	NA	NA	0
2018	SLSC	A65	46.0	1.00	0.0418	0.0689	0.207	99.0	48.2	9.86	-22.6	7.73	NA	NA	NA	NA	1
2018	SLSC	A65	44.0	0.700	0.0363	0.0689	0.207	99.0	54.8	11.8	-22.4	7.14	NA	NA	NA	NA	1
2018	SLSC	A65	57.0	1.70	0.0406	0.0689	0.207	97.0	51.5	9.85	-22.6	8.08	NA	NA	NA	NA	1
2018	SLSC	A65	72.0	3.60	0.0609	0.0689	0.207	99.0	45.2	9.44	-22.4	7.76	NA	NA	NA	NA	3
2018	SLSC	A65	74.0	3.70	0.0760	0.0689	0.207	97.0	44.2	10.2	-22.5	8.09	NA	NA	NA	NA	3
2018	SLSC	A65	45.0	0.900	0.0326	0.0689	0.207	99.0	51.4	9.92	-21.1	7.12	NA	NA	NA	NA	1
2018	SLSC	A65	54.0	1.70	0.0346	0.0689	0.207	99.0	49.7	10.1	-23.1	7.68	NA	NA	NA	NA	2

Table A2.4: Laboratory Results for all Slimy Sculpin (Cottus cognatus; SLSC) and Ninespine Stickleback (Pungitius pungitius; NNST) laboratory results from Biotron Laboratory, the University of Waterloo Environmental Isotope Laboratory, and AAE Tech Incorporated. These results include total Hg concentrations with all sample quality assurance and quality control (QA/QC) in accordance with international standards. Stable isotopes from fish tissue are presented as percent (%) carbon (C) and nitrogren (N), as well as with per mil (‰) for delta values of each of these. Age estimates were made using extracted otoliths. mm = millimeters, g = grams, mg/kg = milligrams per killogram, THg = total mercury, MDL = method detection limit, MRL= method reporting limit , DUP = duplicate, C = carbon, N = nitrogren, NA = no available data.

Sample Year	Fish Species Code	Lake Name	Fork Length (mm)	Wet Weight (g)	THg WW (mg/kg)	MDL (ng)	MRL (ng)	IPR avg (%)	%C	%N	δ13C	δ15N	DUP %C	DUP %N	DUP δ13C	DUP δ15N	Age Estimate
2018	SLSC	A65	54.0	1.50	0.0386	0.0689	0.207	97.0	46.4	9.79	-20.4	7.76	NA	NA	NA	NA	1
2018	SLSC	A65	45.0	1.00	0.0347	0.0689	0.207	99.0	47.2	10.4	-21.8	7.19	46.5	9.50	-22.4	7.29	2
2018	SLSC	A65	65.0	2.90	0.0368	0.0689	0.207	97.0	49.5	10.1	-24.4	8.50	NA	NA	NA	NA	2
2018	SLSC	A65	63.0	2.30	0.0448	0.0689	0.207	99.0	47.4	9.85	-23.0	8.05	NA	NA	NA	NA	2
2018	SLSC	A65	39.0	0.500	0.0274	0.0689	0.207	99.0	50.0	10.8	-22.0	7.44	NA	NA	NA	NA	1
2018	SLSC	A65	38.0	0.500	0.0384	0.0689	0.207	99.0	46.4	10.7	-20.9	7.08	NA	NA	NA	NA	1
2018	SLSC	A65	60.0	2.20	0.0395	0.0689	0.207	99.0	59.1	12.8	-22.4	7.61	NA	NA	NA	NA	3
2018	SLSC	A65	54.0	1.40	0.0346	0.0689	0.207	99.0	52.7	10.6	-23.0	7.65	NA	NA	NA	NA	1
2018	SLSC	A65	41.0	0.700	0.0304	0.0689	0.207	97.0	46.4	9.53	-23.3	8.31	NA	NA	NA	NA	0
2018	SLSC	A65	39.0	0.600	0.0302	0.0689	0.207	99.0	52.3	10.5	-22.8	7.33	NA	NA	NA	NA	0
2018	SLSC	A65	50.0	1.40	0.0389	0.0689	0.207	97.0	37.4	7.57	-22.4	7.44	NA	NA	NA	NA	2
2018	SLSC	A65	42.0	0.700	0.0282	0.0689	0.207	99.0	47.3	9.93	-22.7	7.49	NA	NA	NA	NA	1
2018	SLSC	A65	35.0	0.400	0.0211	0.0689	0.207	99.0	50.6	11.0	-18.8	6.61	NA	NA	NA	NA	1
2018	SLSC	A65	38.0	0.500	0.0253	0.0689	0.207	99.0	54.9	10.5	-22.5	7.27	NA	NA	NA	NA	0
2018	SLSC	A65	38.0	0.500	0.0237	0.0689	0.207	99.0	54.3	12.2	-22.8	7.25	NA	NA	NA	NA	1
2018	SLSC	A65	36.0	0.400	0.0255	0.0689	0.207	99.0	46.8	10.1	-21.9	7.22	NA	NA	NA	NA	1
2018	SLSC	A65	37.0	0.500	0.0351	0.0727	0.218	103	52.3	11.3	-23.1	7.79	NA	NA	NA	NA	0
2018	NNST	A20	59.0	1.60	0.0484	0.0689	0.207	97.0	29.6	6.43	-24.7	8.59	NA	NA	NA	NA	0
2018	NNST	A20	56.0	1.10	0.0662	0.0689	0.207	97.0	40.3	9.53	-22.3	8.32	NA	NA	NA	NA	0
2018	NNST	A20	56.0	1.10	0.0537	0.0689	0.207	99.0	54.0	11.4	-24.6	8.73	NA	NA	NA	NA	0
2018	NNST	A20	58.0	1.30	0.0736	0.0689	0.207	99.0	45.4	10.8	-24.6	8.52	NA	NA	NA	NA	0
2018	NNST	A20	45.0	0.600	0.0314	0.0727	0.218	103	44.3	9.62	-24.6	8.52	NA	NA	NA	NA	0
2018	NNST	A20	42.0	0.500	0.0350	0.0727	0.218	103	43.6	10.0	-25.4	8.23	NA	NA	NA	NA	0
2018	SLSC	A20	32.0	0.300	0.0415	0.0689	0.207	99.0	45.7	9.20	-21.5	7.32	NA	NA	NA	NA	0
2018	SLSC	A20	43.0	0.700	0.0205	0.0689	0.207	97.0	51.5	10.4	-17.9	5.93	NA	NA	NA	NA	1
2018	SLSC	A20	44.0	0.700	0.0198	0.0689	0.207	99.0	48.0	9.67	-19.0	5.31	NA	NA	NA	NA	1
2018	SLSC	A20	29.0	0.200	0.0406	0.0727	0.218	103	48.6	11.1	-21.0	6.63	NA	NA	NA	NA	0
2018	SLSC	A20	52.0	1.30	0.0272	0.0689	0.207	99.0	48.2	10.0	-19.3	5.13	53.9	11.2	-19.4	5.36	1
2018	SLSC	A20	57.0	1.70	0.0491	0.0689	0.207	97.0	42.1	8.40	-19.5	7.14	49.6	10.2	-19.5	6.99	1
2018	SLSC	A20	49.0	1.20	0.0320	0.0689	0.207	99.0	47.5	9.87	-19.1	5.69	NA	NA	NA	NA	1
2018	SLSC	A20	43.0	0.800	0.0201	0.0689	0.207	99.0	56.8	11.5	-17.7	5.10	NA	NA	NA	NA	1

Table A2.4: Laboratory Results for all Slimy Sculpin (Cottus cognatus; SLSC) and Ninespine Stickleback (Pungitius pungitius; NNST) laboratory results from Biotron Laboratory, the University of Waterloo Environmental Isotope Laboratory, and AAE Tech Incorporated. These results include total Hg concentrations with all sample quality assurance and quality control (QA/QC) in accordance with international standards. Stable isotopes from fish tissue are presented as percent (%) carbon (C) and nitrogren (N), as well as with per mil (‰) for delta values of each of these. Age estimates were made using extracted otoliths. mm = millimeters, g = grams, mg/kg = milligrams per killogram, THg = total mercury, MDL = method detection limit, MRL= method reporting limit , DUP = duplicate, C = carbon, N = nitrogren, NA = no available data.

Sample Year	Fish Species Code	Lake Name	Fork Length (mm)	Wet Weight (g)	THg WW (mg/kg)	MDL (ng)	MRL (ng)	IPR avg (%)	%C	%N	δ13C	δ15N	DUP %C	DUP %N	DUP δ13C	DUP δ15N	Age Estimate
2018	SLSC	A20	61.0	3.30	0.0491	0.0689	0.207	99.0	47.4	10.5	-19.6	6.20	NA	NA	NA	NA	4
2018	SLSC	A20	47.0	1.10	0.0272	0.0689	0.207	97.0	40.5	7.84	-20.6	5.94	NA	NA	NA	NA	1
2018	SLSC	A20	45.0	0.700	0.0257	0.0689	0.207	97.0	44.7	10.0	-18.9	6.21	NA	NA	NA	NA	1
2018	SLSC	A20	47.0	0.900	0.0297	0.0689	0.207	99.0	49.7	10.5	-19.6	5.69	NA	NA	NA	NA	1
2018	SLSC	A20	44.0	0.700	0.0190	0.0689	0.207	99.0	50.3	10.9	-17.5	5.41	NA	NA	NA	NA	1
2018	SLSC	A20	28.0	0.200	0.0248	0.0689	0.207	97.0	35.0	8.21	-19.5	6.90	NA	NA	NA	NA	0
2018	SLSC	A20	30.0	0.300	0.0407	0.0727	0.218	103	52.2	11.2	-22.1	7.01	NA	NA	NA	NA	0
2018	SLSC	A20	57.0	1.90	0.0333	0.0689	0.207	99.0	47.1	10.1	-20.2	5.82	NA	NA	NA	NA	2
2018	SLSC	A20	31.0	0.300	0.0275	0.0689	0.207	99.0	45.1	10.5	-19.0	6.69	NA	NA	NA	NA	0
2018	SLSC	A20	29.0	0.200	0.0207	0.0689	0.207	99.0	40.8	9.26	-20.8	5.32	NA	NA	NA	NA	0
2018	SLSC	A20	32.0	0.300	0.0302	0.0727	0.218	103	43.2	9.25	-21.1	6.86	NA	NA	NA	NA	0
2018	SLSC	A20	30.0	0.200	0.0167	0.0689	0.207	99.0	47.4	10.4	-20.5	5.25	NA	NA	NA	NA	0
2018	SLSC	A20	34.0	0.300	0.0232	0.0727	0.218	103	49.3	11.1	-18.8	5.89	51.2	11.4	-19.0	6.47	0
2018	SLSC	A20	35.0	0.300	0.0237	0.0689	0.207	99.0	50.1	10.4	-20.5	5.71	52.2	11.4	-20.4	5.69	0
2018	SLSC	A20	27.0	0.200	0.0316	0.0689	0.207	99.0	44.4	10.1	-21.9	6.56	NA	NA	NA	NA	0
2018	SLSC	A20	33.0	0.200	0.0263	0.0727	0.218	103	47.6	11.8	-19.7	6.33	NA	NA	NA	NA	0
2018	SLSC	A20	63.0	2.30	0.0414	0.0689	0.207	97.0	45.1	8.63	-19.5	5.74	NA	NA	NA	NA	2
2018	SLSC	A20	52.0	1.20	0.0665	0.0689	0.207	99.0	43.2	12.1	-19.5	6.09	NA	NA	NA	NA	2
2018	SLSC	Lake 8	60.0	2.00	0.0292	0.0689	0.207	98.0	53.4	12.6	-23.7	7.27	NA	NA	NA	NA	3
2018	SLSC	Lake 8	60.0	2.40	0.0341	0.0689	0.207	97.0	39.0	7.76	-22.8	7.13	NA	NA	NA	NA	2
2018	SLSC	Lake 8	47.0	0.800	0.0377	0.0689	0.207	97.0	38.2	8.80	-23.0	7.16	NA	NA	NA	NA	1
2018	SLSC	Lake 8	34.0	0.300	0.0276	0.0689	0.207	98.0	52.4	12.3	-23.0	7.22	NA	NA	NA	NA	0
2018	SLSC	Lake 8	30.0	0.300	0.0234	0.0727	0.218	103	51.0	11.9	-24.0	7.22	NA	NA	NA	NA	0
2018	SLSC	Lake 8	29.0	0.300	0.0211	0.0727	0.218	103	43.9	9.88	-22.4	6.56	NA	NA	NA	NA	0
2018	SLSC	Lake 8	39.0	0.500	0.0221	0.0689	0.207	98.0	46.7	10.9	-21.1	7.26	NA	NA	NA	NA	1
2018	SLSC	Lake 8	30.0	0.200	0.0148	0.0689	0.207	98.0	42.0	10.0	-21.5	7.57	NA	NA	NA	NA	0
2018	SLSC	Lake 8	27.0	0.200	0.0305	0.0727	0.218	103	43.6	9.96	-22.0	6.87	NA	NA	NA	NA	0
2018	SLSC	Lake 8	32.0	0.200	0.0179	0.0689	0.207	98.0	52.6	12.4	-22.7	6.90	NA	NA	NA	NA	0
2018	SLSC	Lake 8	28.0	0.200	0.0225	0.0727	0.218	103	42.3	10.2	-20.0	6.21	NA	NA	NA	NA	0
2018	SLSC	Lake 8	28.0	0.200	0.0192	0.0689	0.207	98.0	47.2	10.4	-23.9	6.52	NA	NA	NA	NA	0
2018	SLSC	Lake 8	32.0	0.300	0.0172	0.0727	0.218	103	55.3	11.2	-21.5	7.89	NA	NA	NA	NA	0

Table A2.4: Laboratory Results for all Slimy Sculpin (Cottus cognatus; SLSC) and Ninespine Stickleback (Pungitius pungitius; NNST) laboratory results from Biotron Laboratory, the University of Waterloo Environmental Isotope Laboratory, and AAE Tech Incorporated. These results include total Hg concentrations with all sample quality assurance and quality control (QA/QC) in accordance with international standards. Stable isotopes from fish tissue are presented as percent (%) carbon (C) and nitrogren (N), as well as with per mil (‰) for delta values of each of these. Age estimates were made using extracted otoliths. mm = millimeters, g = grams, mg/kg = milligrams per killogram, THg = total mercury, MDL = method detection limit, MRL= method reporting limit , DUP = duplicate, C = carbon, N = nitrogren, NA = no available data.

Sample Year	Fish Species Code	Lake Name	Fork Length (mm)	Wet Weight (g)	THg WW (mg/kg)	MDL (ng)	MRL (ng)	IPR avg (%)	%C	%N	δ13C	δ15N	DUP %C	DUP %N	DUP δ13C	DUP δ15N	Age Estimate
2018	SLSC	Lake 8	26.0	0.200	0.0205	0.0689	0.207	97.0	36.3	8.68	-23.4	7.44	NA	NA	NA	NA	0
2018	SLSC	Lake 8	29.0	0.300	0.0188	0.0689	0.207	98.0	49.9	11.2	-23.1	7.02	NA	NA	NA	NA	0
2018	SLSC	Lake 8	29.0	0.300	0.0258	0.0689	0.207	98.0	47.8	10.9	-25.0	7.67	NA	NA	NA	NA	0
2018	SLSC	Lake 8	27.0	0.200	0.0226	0.0689	0.207	97.0	36.1	8.26	-23.5	7.35	NA	NA	NA	NA	0
2018	SLSC	Lake 8	31.0	0.200	0.0216	0.0689	0.207	98.0	41.5	8.98	-23.5	6.84	NA	NA	NA	NA	0
2018	SLSC	Lake 8	35.0	0.300	0.0237	0.0689	0.207	98.0	46.7	10.7	-24.1	7.81	46.1	10.2	-24.2	7.24	0
2018	SLSC	Lake 8	28.0	0.200	0.0270	0.0689	0.207	98.0	50.7	12.6	-24.4	7.53	NA	NA	NA	NA	0
2018	SLSC	Lake 8	25.0	0.100	0.0331	0.0689	0.207	97.0	49.1	12.1	-27.0	8.33	NA	NA	NA	NA	0
2018	SLSC	Lake 8	32.0	0.300	0.0216	0.0689	0.207	98.0	47.7	11.5	-23.0	6.76	NA	NA	NA	NA	0
2018	SLSC	Lake 8	30.0	0.200	0.0246	0.0689	0.207	98.0	42.4	9.73	-25.1	8.06	NA	NA	NA	NA	0
2018	SLSC	Lake 8	30.0	0.200	0.0188	0.0689	0.207	98.0	46.1	10.8	-21.7	6.26	NA	NA	NA	NA	0
2018	SLSC	Lake 8	29.0	0.300	0.0290	0.0689	0.207	98.0	45.4	10.5	-23.4	5.78	NA	NA	NA	NA	0
2018	SLSC	Lake 8	28.0	0.200	0.0193	0.0689	0.207	98.0	47.0	11.0	-22.9	7.48	NA	NA	NA	NA	0
2018	SLSC	Lake 8	55.0	1.60	0.0239	0.0689	0.207	97.0	39.7	8.27	-21.9	6.63	35.1	7.51	-21.8	6.48	2
2018	SLSC	Lake 8	30.0	0.300	0.0228	0.0689	0.207	98.0	47.5	11.8	-23.5	7.85	NA	NA	NA	NA	0
2018	SLSC	Lake 8	31.0	0.300	0.0251	0.0689	0.207	98.0	45.5	10.4	-24.7	7.77	NA	NA	NA	NA	0
2018	SLSC	Lake 8	39.0	0.200	0.0201	0.0689	0.207	97.0	39.3	9.23	-22.2	6.78	NA	NA	NA	NA	0
2018	SLSC	Lake 8	57.0	1.70	0.0301	0.0689	0.207	97.0	36.4	7.98	-23.4	7.46	NA	NA	NA	NA	1
2019	SLSC	A44	36.0	0.320	0.0216	0.0727	0.218	103	51.8	12.5	-20.3	6.51	NA	NA	NA	NA	0
2019	SLSC	A44	45.0	0.600	0.0336	0.0689	0.207	97.0	33.9	7.97	-20.6	7.50	NA	NA	NA	NA	1
2019	SLSC	A44	47.0	0.740	0.0381	0.0689	0.207	97.0	39.2	8.76	-20.0	7.83	NA	NA	NA	NA	1
2019	SLSC	A44	45.0	0.740	0.0362	0.0667	0.200	98.0	42.3	9.82	-21.8	7.06	NA	NA	NA	NA	2
2019	SLSC	A44	34.0	0.300	0.0285	0.0727	0.218	103	49.1	12.3	-22.2	6.63	NA	NA	NA	NA	0
2019	SLSC	A44	47.0	0.680	0.0328	0.0667	0.200	98.0	41.1	10.1	-21.7	7.37	NA	NA	NA	NA	2
2019	SLSC	A44	34.0	0.310	0.0238	0.0667	0.200	98.0	46.0	11.0	-22.6	7.10	NA	NA	NA	NA	1
2019	SLSC	A44	31.0	0.200	0.0359	0.0727	0.218	103	45.3	11.0	-22.4	6.96	NA	NA	NA	NA	0
2019	SLSC	A44	33.0	0.270	0.0279	0.0727	0.218	103	49.3	12.2	-23.3	7.48	NA	NA	NA	NA	0
2019	SLSC	A44	36.0	0.350	0.0220	0.0667	0.200	98.0	53.1	11.0	-23.8	7.71	NA	NA	NA	NA	1
2019	SLSC	A44	60.0	1.79	0.0522	0.0667	0.200	98.0	49.7	12.5	-20.4	7.21	NA	NA	NA	NA	3
2019	SLSC	A44	50.0	1.10	0.0279	0.0667	0.200	98.0	46.2	10.4	-20.9	7.81	NA	NA	NA	NA	1
2019	SLSC	A44	44.0	0.740	0.0293	0.0667	0.200	98.0	46.1	11.5	-22.0	6.73	NA	NA	NA	NA	2

Table A2.4: Laboratory Results for all Slimy Sculpin (Cottus cognatus; SLSC) and Ninespine Stickleback (Pungitius pungitius; NNST) laboratory results from Biotron Laboratory, the University of Waterloo Environmental Isotope Laboratory, and AAE Tech Incorporated. These results include total Hg concentrations with all sample quality assurance and quality control (QA/QC) in accordance with international standards. Stable isotopes from fish tissue are presented as percent (%) carbon (C) and nitrogren (N), as well as with per mil (‰) for delta values of each of these. Age estimates were made using extracted otoliths. mm = millimeters, g = grams, mg/kg = milligrams per killogram, THg = total mercury, MDL = method detection limit, MRL= method reporting limit , DUP = duplicate, C = carbon, N = nitrogren, NA = no available data.

Sample Year	Fish Species Code	Lake Name	Fork Length (mm)	Wet Weight (g)	THg WW (mg/kg)	MDL (ng)	MRL (ng)	IPR avg (%)	%C	%N	δ13C	δ15N	DUP %C	DUP %N	DUP δ13C	DUP δ15N	Age Estimate
2019	SLSC	A44	48.0	1.00	0.0317	0.0667	0.200	98.0	56.4	11.7	-21.8	7.28	NA	NA	NA	NA	2
2019	SLSC	A44	49.0	0.910	0.0343	0.0689	0.207	97.0	41.9	8.80	-21.1	7.53	NA	NA	NA	NA	1
2019	SLSC	A44	45.0	0.630	0.0348	0.0667	0.200	98.0	46.9	11.2	-20.7	7.57	NA	NA	NA	NA	1
2019	SLSC	A44	42.0	0.630	0.0338	0.0667	0.200	98.0	46.8	9.89	-20.0	7.04	49.9	10.2	-20.0	7.02	1
2019	SLSC	A44	51.0	1.01	0.0330	0.0667	0.200	98.0	38.4	9.38	-20.9	7.02	NA	NA	NA	NA	2
2019	SLSC	A44	58.0	1.80	0.0573	0.0689	0.207	97.0	41.1	9.67	-19.7	7.78	NA	NA	NA	NA	3
2019	SLSC	A44	36.0	0.370	0.0208	0.0667	0.200	98.0	50.1	10.2	-20.9	7.06	NA	NA	NA	NA	1
2019	SLSC	A44	49.0	0.990	0.0312	0.0667	0.200	98.0	49.8	9.11	-20.1	8.02	NA	NA	NA	NA	2
2019	SLSC	A44	37.0	0.350	0.0232	0.0727	0.218	103	48.2	11.5	-19.2	6.36	NA	NA	NA	NA	0
2019	SLSC	A44	48.0	0.790	0.0482	0.0667	0.200	98.0	46.4	10.6	-21.7	7.83	NA	NA	NA	NA	2
2019	SLSC	A44	54.0	1.29	0.0381	0.0667	0.200	98.0	55.0	11.0	-21.6	7.42	NA	NA	NA	NA	2
2019	SLSC	A44	45.0	0.880	0.0363	0.0667	0.200	98.0	51.8	10.9	-19.0	8.23	NA	NA	NA	NA	1
2019	SLSC	A44	37.0	0.390	0.0191	0.0667	0.200	98.0	50.3	12.7	-20.4	6.73	NA	NA	NA	NA	0
2019	SLSC	A44	62.0	1.83	0.0651	0.0667	0.200	98.0	40.9	9.51	-20.6	7.41	NA	NA	NA	NA	2
2019	SLSC	A44	52.0	1.07	0.0281	0.0689	0.207	97.0	42.3	9.27	-21.6	7.05	NA	NA	NA	NA	1
2019	SLSC	A44	43.0	0.710	0.0340	0.0689	0.207	97.0	39.4	9.35	-18.1	7.68	NA	NA	NA	NA	1
2019	SLSC	A44	47.0	0.810	0.0371	0.0667	0.200	98.0	52.3	11.7	-21.4	7.23	NA	NA	NA	NA	2
2019	SLSC	A44	56.0	1.39	0.0398	0.0667	0.200	98.0	46.3	11.2	-19.4	7.41	49.6	10.9	-20.0	7.44	2
2019	SLSC	A44	40.0	0.430	0.0217	0.0689	0.207	97.0	39.2	8.66	-19.4	8.23	50.7	11.8	-19.3	8.36	0
2019	SLSC	A44	51.0	1.07	0.0322	0.0667	0.200	98.0	48.5	10.9	-20.2	6.75	NA	NA	NA	NA	2
2019	SLSC	A44	44.0	0.750	0.0265	0.0667	0.200	98.0	44.0	9.36	-20.5	7.20	NA	NA	NA	NA	2
2019	SLSC	A44	33.0	0.280	0.0252	0.0667	0.200	98.0	43.0	9.83	-20.5	6.69	NA	NA	NA	NA	0
2019	NNST	A65	31.0	0.220	0.0267	0.0727	0.218	103	49.9	11.3	-25.2	6.91	NA	NA	NA	NA	0
2019	NNST	A65	27.0	0.180	0.0332	0.0689	0.207	97.0	46.4	11.1	-26.3	7.29	NA	NA	NA	NA	0
2019	NNST	A65	35.0	0.270	0.0320	0.0727	0.218	103	53.6	11.6	-26.8	7.63	NA	NA	NA	NA	0
2019	NNST	A65	52.0	0.880	0.0362	0.0689	0.207	99.0	53.2	11.2	-26.6	9.46	NA	NA	NA	NA	0
2019	NNST	A65	71.0	2.82	0.118	0.0689	0.207	97.0	41.1	8.09	-24.0	9.64	NA	NA	NA	NA	1
2019	NNST	A65	54.0	1.03	0.0311	0.0689	0.207	97.0	50.6	9.69	-26.2	9.44	NA	NA	NA	NA	0
2019	NNST	A65	48.0	1.28	0.0397	0.0689	0.207	99.0	53.3	8.42	-27.4	8.91	NA	NA	NA	NA	0
2019	NNST	A65	48.0	0.790	0.0463	0.0727	0.218	103	51.2	10.4	-25.9	7.92	NA	NA	NA	NA	0
2019	NNST	A65	42.0	0.570	0.0377	0.0727	0.218	103	49.3	10.7	-26.6	8.55	NA	NA	NA	NA	0

Table A2.4: Laboratory Results for all Slimy Sculpin (Cottus cognatus; SLSC) and Ninespine Stickleback (Pungitius pungitius; NNST) laboratory results from Biotron Laboratory, the University of Waterloo Environmental Isotope Laboratory, and AAE Tech Incorporated. These results include total Hg concentrations with all sample quality assurance and quality control (QA/QC) in accordance with international standards. Stable isotopes from fish tissue are presented as percent (%) carbon (C) and nitrogren (N), as well as with per mil (‰) for delta values of each of these. Age estimates were made using extracted otoliths. mm = millimeters, g = grams, mg/kg = milligrams per killogram, THg = total mercury, MDL = method detection limit, MRL= method reporting limit , DUP = duplicate, C = carbon, N = nitrogren, NA = no available data.

Sample Year	Fish Species Code	Lake Name	Fork Length (mm)	Wet Weight (g)	THg WW (mg/kg)	MDL (ng)	MRL (ng)	IPR avg (%)	%C	%N	δ13C	δ15N	DUP %C	DUP %N	DUP δ13C	DUP δ15N	Age Estimate
2019	NNST	A65	64.0	1.84	0.0775	0.0689	0.207	97.0	50.8	8.27	-25.7	9.81	NA	NA	NA	NA	0
2019	NNST	A65	26.0	0.130	0.0280	0.0689	0.207	97.0	44.0	10.5	-24.7	6.34	NA	NA	NA	NA	0
2019	NNST	A65	47.0	0.850	0.0373	0.0689	0.207	99.0	55.3	11.0	-25.7	8.32	NA	NA	NA	NA	0
2019	SLSC	A65	54.0	1.34	0.0430	0.0689	0.207	97.0	46.2	9.93	-23.8	7.54	NA	NA	NA	NA	1
2019	SLSC	A65	64.0	2.25	0.0394	0.0689	0.207	97.0	46.6	9.00	-23.5	8.19	NA	NA	NA	NA	2
2019	NNST	A65	31.0	0.180	0.0246	0.0689	0.207	99.0	46.7	10.9	-24.9	6.67	NA	NA	NA	NA	0
2019	NNST	A65	57.0	1.31	0.0307	0.0689	0.207	97.0	51.8	9.99	-25.9	9.17	NA	NA	NA	NA	0
2019	NNST	A65	28.0	0.170	0.0262	0.0689	0.207	99.0	49.6	11.2	-25.8	6.34	NA	NA	NA	NA	0
2019	NNST	A65	50.0	1.11	0.0471	0.0689	0.207	99.0	51.8	10.9	-25.2	7.95	NA	NA	NA	NA	0
2019	NNST	A65	55.0	1.24	0.0425	0.0689	0.207	99.0	55.8	11.1	-25.4	9.26	46.2	9.17	-25.3	9.30	0
2019	NNST	A65	25.0	0.120	0.0365	0.0689	0.207	97.0	41.4	10.1	-24.5	6.51	NA	NA	NA	NA	0
2019	NNST	A65	29.0	0.140	0.0273	0.0689	0.207	99.0	47.2	11.6	-23.8	6.78	NA	NA	NA	NA	0
2019	NNST	A65	50.0	0.650	0.0451	0.0689	0.207	99.0	48.4	9.36	-27.9	8.60	NA	NA	NA	NA	0
2019	NNST	A65	55.0	1.41	0.0450	0.0689	0.207	99.0	46.3	9.10	-26.6	8.90	NA	NA	NA	NA	0
2019	NNST	A65	63.0	2.02	0.0806	0.0689	0.207	97.0	54.3	9.17	-24.2	9.90	41.1	7.04	-24.1	9.71	0
2019	NNST	A65	25.0	0.120	0.0317	0.0689	0.207	99.0	49.9	12.2	-23.5	7.39	NA	NA	NA	NA	0
2019	NNST	A65	54.0	1.25	0.0356	0.0689	0.207	99.0	53.3	9.87	-25.6	8.16	NA	NA	NA	NA	0
2019	NNST	A65	56.0	1.51	0.0459	0.0689	0.207	97.0	57.9	10.6	-26.9	9.47	NA	NA	NA	NA	0
2019	NNST	A65	53.0	1.28	0.0414	0.0689	0.207	99.0	55.5	11.0	-28.1	9.34	NA	NA	NA	NA	0
2019	NNST	A65	56.0	1.25	0.0363	0.0689	0.207	97.0	52.4	9.48	-26.0	8.99	NA	NA	NA	NA	0
2019	NNST	A65	54.0	1.25	0.0390	0.0689	0.207	99.0	56.8	10.4	-25.9	8.70	NA	NA	NA	NA	0
2019	NNST	A65	54.0	1.20	0.0379	0.0689	0.207	97.0	49.0	9.44	-26.6	8.42	NA	NA	NA	NA	0
2019	NNST	A65	53.0	1.17	0.0406	0.0689	0.207	97.0	46.3	9.83	-24.3	7.88	NA	NA	NA	NA	0
2019	NNST	A65	33.0	0.240	0.0303	0.0727	0.218	103	51.9	12.0	-25.8	7.52	NA	NA	NA	NA	0
2019	NNST	A65	55.0	1.33	0.0400	0.0689	0.207	97.0	52.4	9.48	-25.6	9.19	NA	NA	NA	NA	0
2019	NNST	A65	51.0	0.820	0.0458	0.0689	0.207	99.0	42.8	8.68	-26.2	8.75	NA	NA	NA	NA	0
2019	NNST	A65	59.0	1.51	0.0330	0.0689	0.207	97.0	47.7	8.31	-25.3	9.15	NA	NA	NA	NA	0
2019	NNST	A65	47.0	0.880	0.0403	0.0727	0.218	103	50.0	11.1	-25.7	8.46	NA	NA	NA	NA	0
2019	NNST	A65	54.0	0.930	0.0319	0.0689	0.207	99.0	51.9	10.8	-26.3	8.90	NA	NA	NA	NA	0
2019	NNST	A65	47.0	0.860	0.0346	0.0689	0.207	99.0	45.7	8.68	-25.4	8.60	55.3	10.7	-25.3	8.98	0
2019	NNST	A65	32.0	0.260	0.0275	0.0727	0.218	103	52.6	11.9	-26.0	6.85	NA	NA	NA	NA	0

Table A2.4: Laboratory Results for all Slimy Sculpin (Cottus cognatus; SLSC) and Ninespine Stickleback (Pungitius pungitius; NNST) laboratory results from Biotron Laboratory, the University of Waterloo Environmental Isotope Laboratory, and AAE Tech Incorporated. These results include total Hg concentrations with all sample quality assurance and quality control (QA/QC) in accordance with international standards. Stable isotopes from fish tissue are presented as percent (%) carbon (C) and nitrogren (N), as well as with per mil (‰) for delta values of each of these. Age estimates were made using extracted otoliths. mm = millimeters, g = grams, mg/kg = milligrams per killogram, THg = total mercury, MDL = method detection limit, MRL= method reporting limit , DUP = duplicate, C = carbon, N = nitrogren, NA = no available data.

Sample Year	Fish Species Code	Lake Name	Fork Length (mm)	Wet Weight (g)	THg WW (mg/kg)	MDL (ng)	MRL (ng)	IPR avg (%)	%C	%N	δ13C	δ15N	DUP %C	DUP %N	DUP δ13C	DUP δ15N	Age Estimate
2019	NNST	A65	43.0	0.670	0.0342	0.0727	0.218	103	51.6	10.9	-26.3	8.29	NA	NA	NA	NA	0
2019	NNST	A65	45.0	0.850	0.0364	0.0727	0.218	103	52.7	12.1	-25.5	8.27	NA	NA	NA	NA	0
2019	NNST	A65	50.0	1.09	0.0352	0.0689	0.207	97.0	46.8	8.97	-26.8	8.98	NA	NA	NA	NA	0
2019	NNST	A65	50.0	1.08	0.0494	0.0689	0.207	99.0	50.4	9.69	-27.2	8.69	NA	NA	NA	NA	0
2019	NNST	A65	58.0	1.43	0.0469	0.0689	0.207	97.0	50.8	8.79	-26.6	9.38	NA	NA	NA	NA	0
2019	NNST	A65	55.0	1.26	0.0462	0.0689	0.207	99.0	46.7	8.95	-26.2	8.75	NA	NA	NA	NA	0
2019	NNST	A65	47.0	0.890	0.0326	0.0689	0.207	99.0	57.0	11.3	-26.9	8.06	NA	NA	NA	NA	0
2019	NNST	A65	23.0	0.120	0.0288	0.0689	0.207	97.0	41.2	10.4	-23.0	8.31	NA	NA	NA	NA	NA
2019	NNST	A65	30.0	0.190	0.0357	0.0727	0.218	103	49.4	11.3	-25.3	6.40	51.7	12.2	-25.1	6.41	0
2019	NNST	A65	44.0	0.630	0.0376	0.0689	0.207	99.0	52.3	11.2	-25.8	8.24	NA	NA	NA	NA	0
2019	NNST	A65	59.0	1.92	0.0845	0.0689	0.207	97.0	43.8	9.40	-23.7	8.69	45.1	9.51	-23.8	8.29	1
2019	SLSC	A65	62.0	2.28	0.0494	0.0689	0.207	97.0	43.1	9.19	-23.4	8.05	NA	NA	NA	NA	3
2019	NNST	WTL	55.0	1.63	0.0263	0.0689	0.207	97.0	55.6	9.41	-27.0	10.6	NA	NA	NA	NA	0
2019	NNST	WTL	31.0	0.220	0.0522	0.0727	0.218	103	52.7	12.1	-26.0	7.85	NA	NA	NA	NA	NA
2019	NNST	WTL	60.0	1.98	0.0437	0.0689	0.207	97.0	44.3	8.23	-26.8	10.1	NA	NA	NA	NA	0
2019	NNST	WTL	29.0	0.160	0.0224	0.0689	0.207	98.0	47.7	9.61	-26.8	6.48	NA	NA	NA	NA	0
2019	NNST	WTL	59.0	2.35	0.0419	0.0689	0.207	98.0	54.6	8.03	-25.9	7.77	52.1	8.04	-25.7	7.70	1
2019	NNST	WTL	61.0	3.13	0.0520	0.0689	0.207	97.0	49.1	8.45	-25.8	8.96	NA	NA	NA	NA	1
2019	NNST	WTL	55.0	1.46	0.0518	0.0689	0.207	98.0	52.9	9.64	-27.3	10.5	NA	NA	NA	NA	0
2019	NNST	WTL	53.0	1.18	0.0333	0.0689	0.207	98.0	51.8	9.73	-25.1	10.1	NA	NA	NA	NA	0
2019	NNST	WTL	53.0	1.64	0.0485	0.0689	0.207	98.0	49.0	9.55	-24.0	10.2	NA	NA	NA	NA	0
2019	NNST	WTL	21.0	0.0700	0.0238	0.0689	0.207	97.0	48.3	11.4	-24.1	8.04	NA	NA	NA	NA	0
2019	NNST	WTL	22.0	0.110	0.0364	0.0689	0.207	98.0	48.1	11.3	-25.8	7.41	NA	NA	NA	NA	0
2019	NNST	WTL	32.0	0.210	0.0309	0.0727	0.218	103	52.1	11.5	-27.7	7.12	NA	NA	NA	NA	0
2019	NNST	WTL	32.0	0.280	0.0280	0.0689	0.207	98.0	41.9	9.28	-28.6	7.31	NA	NA	NA	NA	0
2019	NNST	WTL	25.0	0.140	0.0314	0.0727	0.218	103	50.6	11.5	-26.0	7.18	NA	NA	NA	NA	0
2019	NNST	WTL	21.0	0.0700	0.0206	0.0689	0.207	98.0	46.0	11.1	-25.5	7.27	NA	NA	NA	NA	NA
2019	NNST	WTL	54.0	1.29	0.0274	0.0689	0.207	98.0	48.6	9.51	-27.2	10.3	NA	NA	NA	NA	0
2019	NNST	WTL	32.0	0.240	0.0271	0.0689	0.207	98.0	41.9	9.70	-27.6	8.29	NA	NA	NA	NA	0
2019	NNST	WTL	54.0	1.86	0.0522	0.0689	0.207	98.0	46.3	9.47	-25.4	9.21	NA	NA	NA	NA	0
2019	NNST	WTL	25.0	0.140	0.0227	0.0689	0.207	97.0	54.9	13.0	-24.3	9.08	NA	NA	NA	NA	0

Table A2.4: Laboratory Results for all Slimy Sculpin (Cottus cognatus; SLSC) and Ninespine Stickleback (Pungitius pungitius; NNST) laboratory results from Biotron Laboratory, the University of Waterloo Environmental Isotope Laboratory, and AAE Tech Incorporated. These results include total Hg concentrations with all sample quality assurance and quality control (QA/QC) in accordance with international standards. Stable isotopes from fish tissue are presented as percent (%) carbon (C) and nitrogren (N), as well as with per mil (‰) for delta values of each of these. Age estimates were made using extracted otoliths. mm = millimeters, g = grams, mg/kg = milligrams per killogram, THg = total mercury, MDL = method detection limit, MRL= method reporting limit , DUP = duplicate, C = carbon, N = nitrogren, NA = no available data.

Sample Year	Fish Species Code	Lake Name	Fork Length (mm)	Wet Weight (g)	THg WW (mg/kg)	MDL (ng)	MRL (ng)	IPR avg (%)	%C	%N	δ13C	δ15N	DUP %C	DUP %N	DUP δ13C	DUP δ15N	Age Estimate
2019	NNST	WTL	42.0	0.700	0.0444	0.0727	0.218	103	51.4	9.94	-25.5	8.45	NA	NA	NA	NA	0
2019	NNST	WTL	31.0	0.230	0.0393	0.0689	0.207	98.0	44.0	9.13	-28.6	8.57	51.5	10.5	-28.7	8.81	0
2019	NNST	WTL	35.0	0.310	0.0296	0.0689	0.207	98.0	48.2	9.90	-30.3	8.75	NA	NA	NA	NA	0
2019	NNST	WTL	34.0	0.290	0.0227	0.0727	0.218	103	52.2	11.1	-28.0	8.27	NA	NA	NA	NA	0
2019	NNST	WTL	26.0	0.160	0.0243	0.0689	0.207	98.0	53.6	12.1	-23.9	8.58	NA	NA	NA	NA	0
2019	NNST	WTL	30.0	0.190	0.0266	0.0689	0.207	98.0	45.8	10.3	-26.8	8.51	NA	NA	NA	NA	0
2019	NNST	WTL	28.0	0.160	0.0229	0.0689	0.207	97.0	43.8	10.5	-22.6	8.40	NA	NA	NA	NA	0
2019	SLSC	WTL	73.0	4.21	0.0298	0.0689	0.207	97.0	46.8	9.34	-25.3	9.73	NA	NA	NA	NA	3
2019	SLSC	WTL	57.0	1.81	0.0298	0.0689	0.207	98.0	56.0	11.4	-26.8	8.61	NA	NA	NA	NA	1
2019	SLSC	WTL	36.0	0.470	0.0539	0.0727	0.218	103	53.7	11.0	-26.5	8.19	NA	NA	NA	NA	0
2019	SLSC	WTL	32.0	0.320	0.0223	0.0727	0.218	103	52.9	11.8	-23.2	8.75	NA	NA	NA	NA	0
2019	SLSC	WTL	38.0	0.500	0.0276	0.0727	0.218	103	52.2	11.3	-27.3	8.68	NA	NA	NA	NA	0
2019	SLSC	WTL	39.0	0.620	0.0218	0.0689	0.207	98.0	45.4	10.1	-27.9	9.87	NA	NA	NA	NA	0
2019	SLSC	WTL	51.0	1.38	0.0232	0.0689	0.207	97.0	51.9	12.2	-26.2	9.78	NA	NA	NA	NA	1
2019	SLSC	WTL	39.0	0.690	0.0346	0.0689	0.207	98.0	56.4	11.1	-21.9	8.96	NA	NA	NA	NA	1
2019	SLSC	WTL	37.0	0.450	0.0390	0.0727	0.218	103	52.1	11.2	-26.2	7.33	NA	NA	NA	NA	0
2019	SLSC	WTL	39.0	0.580	0.0349	0.0689	0.207	98.0	53.1	11.9	-27.7	8.82	NA	NA	NA	NA	0
2019	SLSC	WTL	34.0	0.380	0.112	0.0727	0.218	103	53.6	11.8	-28.1	7.81	55.2	11.4	-28.4	7.87	0
2019	NNST	WTL	36.0	0.270	0.0302	0.0689	0.207	98.0	49.3	11.1	-25.2	9.23	NA	NA	NA	NA	0
2019	NNST	WTL	27.0	0.160	0.0224	0.0689	0.207	98.0	47.2	11.6	-23.3	10.0	NA	NA	NA	NA	0
2019	NNST	WTL	32.0	0.200	0.0330	0.0689	0.207	98.0	45.4	10.9	-25.8	8.07	43.2	10.4	-25.6	7.55	0
2019	NNST	WTL	33.0	0.230	0.0383	0.0689	0.207	98.0	47.0	10.4	-27.4	8.78	NA	NA	NA	NA	0
2019	NNST	WTL	32.0	0.210	0.0489	0.0689	0.207	98.0	47.4	10.3	-27.9	8.30	NA	NA	NA	NA	0
2019	NNST	WTL	32.0	0.210	0.0174	0.0689	0.207	98.0	48.8	10.4	-23.6	8.14	NA	NA	NA	NA	0
2019	NNST	WTL	36.0	0.290	0.0170	0.0689	0.207	98.0	52.9	11.0	-25.9	7.59	NA	NA	NA	NA	0
2019	NNST	WTL	59.0	1.66	0.0192	0.0689	0.207	98.0	52.4	9.04	-30.5	10.9	NA	NA	NA	NA	0
2019	NNST	WTL	29.0	0.150	0.0233	0.0689	0.207	98.0	50.2	10.4	-25.8	7.70	NA	NA	NA	NA	0
2019	NNST	WTL	69.0	2.48	0.0585	0.0689	0.207	97.0	47.0	9.10	-23.6	10.3	NA	NA	NA	NA	0
2019	NNST	WTL	50.0	0.760	0.0367	0.0689	0.207	97.0	46.3	9.69	-24.3	10.0	49.0	10.4	-24.3	10.3	0
2019	SLSC	WTL	38.0	0.450	0.0341	0.0689	0.207	98.0	44.8	9.68	-28.2	8.95	NA	NA	NA	NA	0
2019	SLSC	WTL	47.0	0.890	0.0338	0.0689	0.207	98.0	52.1	10.2	-22.4	9.18	NA	NA	NA	NA	1

Table A2.4: Laboratory Results for all Slimy Sculpin (Cottus cognatus; SLSC) and Ninespine Stickleback (Pungitius pungitius; NNST) laboratory results from Biotron Laboratory, the University of Waterloo Environmental Isotope Laboratory, and AAE Tech Incorporated. These results include total Hg concentrations with all sample quality assurance and quality control (QA/QC) in accordance with international standards. Stable isotopes from fish tissue are presented as percent (%) carbon (C) and nitrogren (N), as well as with per mil (‰) for delta values of each of these. Age estimates were made using extracted otoliths. mm = millimeters, g = grams, mg/kg = milligrams per killogram, THg = total mercury, MDL = method detection limit, MRL= method reporting limit , DUP = duplicate, C = carbon, N = nitrogren, NA = no available data.

Sample Year	Fish Species Code	Lake Name	Fork Length (mm)	Wet Weight (g)	THg WW (mg/kg)	MDL (ng)	MRL (ng)	IPR avg (%)	%C	%N	δ13C	δ15N	DUP %C	DUP %N	DUP δ13C	DUP δ15N	Age Estimate
2019	SLSC	WTL	49.0	0.970	0.0357	0.0689	0.207	97.0	49.4	10.5	-24.6	9.09	NA	NA	NA	NA	1
2019	SLSC	WTL	55.0	1.59	0.0339	0.0689	0.207	97.0	50.6	10.4	-26.5	8.49	NA	NA	NA	NA	2
2019	SLSC	WTL	66.0	2.62	0.0208	0.0689	0.207	98.0	46.0	9.29	-25.7	8.33	NA	NA	NA	NA	1
2019	SLSC	WTL	60.0	2.12	0.0263	0.0689	0.207	97.0	49.2	8.53	-26.8	7.56	NA	NA	NA	NA	1
2019	SLSC	WTL	67.0	2.27	0.0472	0.0689	0.207	97.0	37.8	10.5	-22.8	8.97	NA	NA	NA	NA	3
2019	SLSC	WTL	45.0	0.690	0.0262	0.0689	0.207	97.0	43.3	8.85	-20.8	8.92	NA	NA	NA	NA	1
2019	SLSC	WTL	36.0	0.380	0.0188	0.0689	0.207	98.0	52.4	12.0	-26.5	8.46	51.2	11.9	-26.6	8.72	0
2019	SLSC	WTL	57.0	0.890	0.0374	0.0689	0.207	98.0	53.0	10.8	-26.0	7.45	NA	NA	NA	NA	2
2019	SLSC	WTL	39.0	0.640	0.0759	0.0689	0.207	98.0	50.8	9.95	-25.8	6.82	NA	NA	NA	NA	0
2019	SLSC	WTL	44.0	0.700	0.0325	0.0689	0.207	98.0	50.4	11.1	-21.2	8.53	NA	NA	NA	NA	1
2019	SLSC	WTL	36.0	0.490	0.0224	0.0689	0.207	98.0	42.9	10.0	-26.1	8.64	NA	NA	NA	NA	0
2019	SLSC	WTL	45.0	0.650	0.0311	0.0689	0.207	98.0	46.0	11.3	-23.7	8.96	NA	NA	NA	NA	1
2019	SLSC	WTL	55.0	1.53	0.0327	0.0689	0.207	98.0	41.5	8.73	-25.8	8.84	NA	NA	NA	NA	1
2019	SLSC	WTL	40.0	0.590	0.0157	0.0689	0.207	97.0	59.2	11.4	-26.6	6.51	NA	NA	NA	NA	0
2019	SLSC	WTL	58.0	1.77	0.0282	0.0689	0.207	98.0	47.0	9.65	-27.1	8.66	NA	NA	NA	NA	2
2019	SLSC	WTL	41.0	0.630	0.0191	0.0689	0.207	98.0	46.7	10.3	-24.1	6.94	NA	NA	NA	NA	0
2019	SLSC	WTL	69.0	3.47	0.0421	0.0689	0.207	97.0	46.5	9.82	-25.6	8.81	NA	NA	NA	NA	3
2019	SLSC	WTL	38.0	0.470	0.0166	0.0689	0.207	98.0	49.7	9.45	-26.3	7.07	NA	NA	NA	NA	0
2019	NNST	WTL	37.0	0.400	0.0301	0.0727	0.218	103	51.7	11.6	-28.7	10.3	NA	NA	NA	NA	0
2019	SLSC	A63	47.0	1.23	0.0318	0.0689	0.207	99.0	54.2	10.1	-25.6	6.32	NA	NA	NA	NA	1
2019	SLSC	A63	35.0	0.430	0.0361	0.0689	0.207	99.0	48.8	11.3	-24.2	6.13	NA	NA	NA	NA	0
2019	SLSC	A63	57.0	2.22	0.0475	0.0689	0.207	99.0	59.3	10.9	-24.9	6.43	NA	NA	NA	NA	2
2019	SLSC	A63	48.0	1.07	0.0441	0.0689	0.207	99.0	46.6	10.2	-22.3	6.89	NA	NA	NA	NA	2
2019	SLSC	A63	35.0	0.440	0.0385	0.0689	0.207	99.0	48.3	11.6	-25.1	6.14	NA	NA	NA	NA	0
2019	SLSC	A63	39.0	0.640	0.0289	0.0689	0.207	99.0	52.9	10.4	-25.8	4.96	54.4	11.2	-25.4	5.09	1
2019	SLSC	A63	35.0	0.440	0.0366	0.0689	0.207	99.0	53.3	12.2	-26.0	6.49	NA	NA	NA	NA	1
2019	NNST	A63	65.0	1.96	0.0380	0.0689	0.207	99.0	64.2	10.1	-28.4	8.46	NA	NA	NA	NA	0
2019	NNST	A63	57.0	1.85	0.0404	0.0689	0.207	99.0	58.0	9.23	-26.8	7.48	NA	NA	NA	NA	0
2019	NNST	A63	52.0	1.49	0.0365	0.0689	0.207	99.0	56.0	8.25	-29.6	8.03	NA	NA	NA	NA	0
2019	NNST	A63	55.0	1.38	0.0350	0.0825	0.248	101	54.1	9.79	-29.3	8.76	NA	NA	NA	NA	0
2019	NNST	A63	58.0	1.57	0.0348	0.0825	0.248	101	57.7	9.03	-28.1	8.63	NA	NA	NA	NA	0

Table A2.4: Laboratory Results for all Slimy Sculpin (Cottus cognatus; SLSC) and Ninespine Stickleback (Pungitius pungitius; NNST) laboratory results from Biotron Laboratory, the University of Waterloo Environmental Isotope Laboratory, and AAE Tech Incorporated. These results include total Hg concentrations with all sample quality assurance and quality control (QA/QC) in accordance with international standards. Stable isotopes from fish tissue are presented as percent (%) carbon (C) and nitrogren (N), as well as with per mil (‰) for delta values of each of these. Age estimates were made using extracted otoliths. mm = millimeters, g = grams, mg/kg = milligrams per killogram, THg = total mercury, MDL = method detection limit, MRL= method reporting limit , DUP = duplicate, C = carbon, N = nitrogren, NA = no available data.

Sample Year	Fish Species Code	Lake Name	Fork Length (mm)	Wet Weight (g)	THg WW (mg/kg)	MDL (ng)	MRL (ng)	IPR avg (%)	%C	%N	δ13C	δ15N	DUP %C	DUP %N	DUP δ13C	DUP δ15N	Age Estimate
2019	NNST	A63	51.0	1.33	0.0399	0.0825	0.248	101	54.4	10.2	-27.3	7.97	NA	NA	NA	NA	0
2019	NNST	A63	29.0	0.230	0.0337	0.0825	0.248	101	51.1	11.1	-26.6	6.29	NA	NA	NA	NA	0
2019	NNST	A63	26.0	0.150	0.0447	0.0825	0.248	101	46.7	12.0	-25.6	6.02	NA	NA	NA	NA	0
2019	NNST	A63	27.0	0.210	0.0425	0.0825	0.248	101	53.7	10.8	-27.7	5.70	50.5	10.8	-27.2	5.78	0
2019	NNST	A63	19.0	0.0700	0.0594	0.0689	0.207	99.0	44.3	11.4	-26.5	5.50	NA	NA	NA	NA	0
2019	NNST	A63	34.0	0.300	0.0360	0.0825	0.248	101	52.6	9.18	-29.0	7.02	NA	NA	NA	NA	0
2019	NNST	A63	29.0	0.180	0.0469	0.0825	0.248	101	47.2	11.1	-26.8	7.47	NA	NA	NA	NA	0
2019	NNST	A63	34.0	0.300	0.0321	0.0825	0.248	101	55.6	12.7	-27.4	5.77	NA	NA	NA	NA	0
2019	NNST	A63	27.0	0.180	0.0447	0.0689	0.207	99.0	50.0	10.9	-28.1	6.27	NA	NA	NA	NA	0
2019	NNST	A63	27.0	0.150	0.0478	0.0689	0.207	99.0	52.2	11.6	-27.3	5.51	NA	NA	NA	NA	0
2019	NNST	A63	31.0	0.210	0.0463	0.0689	0.207	99.0	46.5	9.66	-27.0	5.52	NA	NA	NA	NA	0
2019	NNST	A63	42.0	0.540	0.0356	0.0689	0.207	99.0	57.9	11.5	-28.1	6.60	NA	NA	NA	NA	0
2019	NNST	A63	31.0	0.270	0.0391	0.0689	0.207	99.0	54.0	11.3	-26.6	6.55	NA	NA	NA	NA	0
2019	NNST	A63	26.0	0.140	0.0453	0.0689	0.207	99.0	46.3	10.9	-27.4	6.33	48.8	12.0	-27.2	5.91	0
2019	NNST	A63	29.0	0.180	0.0501	0.0689	0.207	99.0	52.3	12.0	-27.1	6.54	NA	NA	NA	NA	0
2019	NNST	A63	27.0	0.180	0.0419	0.0689	0.207	99.0	49.9	11.3	-27.9	6.65	NA	NA	NA	NA	0
2019	NNST	A63	29.0	0.190	0.0506	0.0689	0.207	99.0	50.3	11.0	-26.9	5.91	NA	NA	NA	NA	0
2019	NNST	A63	28.0	0.180	0.0446	0.0689	0.207	99.0	48.2	9.24	-27.7	6.26	NA	NA	NA	NA	0
2019	NNST	A63	31.0	0.230	0.0417	0.0689	0.207	99.0	58.5	12.6	-27.9	5.55	NA	NA	NA	NA	0
2019	NNST	A63	28.0	0.150	0.0458	0.0689	0.207	99.0	56.1	13.6	-25.9	6.31	NA	NA	NA	NA	0
2019	NNST	A63	31.0	0.220	0.0493	0.0689	0.207	99.0	50.4	12.2	-27.0	5.96	NA	NA	NA	NA	0
2019	NNST	A63	25.0	0.800	0.0486	0.0689	0.207	99.0	47.4	11.9	-26.9	5.64	NA	NA	NA	NA	0
2019	NNST	A63	32.0	0.240	0.0316	0.0689	0.207	99.0	48.4	10.9	-27.5	6.18	NA	NA	NA	NA	0
2019	NNST	A63	26.0	0.170	0.0484	0.0689	0.207	99.0	51.4	12.6	-26.5	5.29	49.1	12.0	-26.5	5.22	0
2019	NNST	A63	33.0	0.250	0.0356	0.0689	0.207	99.0	45.4	10.9	-26.1	6.58	NA	NA	NA	NA	0
2019	NNST	A63	31.0	0.210	0.0511	0.0689	0.207	99.0	47.1	10.6	-27.1	6.64	NA	NA	NA	NA	0
2019	NNST	A63	32.0	0.240	0.0408	0.0689	0.207	99.0	52.7	9.93	-28.2	6.35	NA	NA	NA	NA	0
2019	NNST	A63	26.0	0.130	0.0610	0.0689	0.207	99.0	49.0	11.8	-27.1	6.04	NA	NA	NA	NA	0
2019	NNST	A63	29.0	0.220	0.0506	0.0689	0.207	99.0	52.0	12.7	-27.2	6.69	NA	NA	NA	NA	0
2019	NNST	A63	31.0	0.200	0.0474	0.0689	0.207	99.0	48.5	11.1	-28.4	6.61	NA	NA	NA	NA	0
2019	NNST	A63	30.0	0.240	0.0415	0.0689	0.207	99.0	50.2	12.3	-27.5	6.71	NA	NA	NA	NA	0

Table A2.4: Laboratory Results for all Slimy Sculpin (Cottus cognatus; SLSC) and Ninespine Stickleback (Pungitius pungitius; NNST) laboratory results from Biotron Laboratory, the University of Waterloo Environmental Isotope Laboratory, and AAE Tech Incorporated. These results include total Hg concentrations with all sample quality assurance and quality control (QA/QC) in accordance with international standards. Stable isotopes from fish tissue are presented as percent (%) carbon (C) and nitrogren (N), as well as with per mil (‰) for delta values of each of these. Age estimates were made using extracted otoliths. mm = millimeters, g = grams, mg/kg = milligrams per killogram, THg = total mercury, MDL = method detection limit, MRL= method reporting limit , DUP = duplicate, C = carbon, N = nitrogren, NA = no available data.

Sample Year	Fish Species Code	Lake Name	Fork Length (mm)	Wet Weight (g)	THg WW (mg/kg)	MDL (ng)	MRL (ng)	IPR avg (%)	%C	%N	δ13C	δ15N	DUP %C	DUP %N	DUP δ13C	DUP δ15N	Age Estimate
2019	NNST	A63	24.0	0.120	0.0517	0.0689	0.207	99.0	49.1	11.8	-27.3	5.58	NA	NA	NA	NA	0
2019	NNST	A20	51.0	0.900	0.0514	0.0689	0.207	99.0	51.9	9.10	-24.5	8.68	NA	NA	NA	NA	0
2019	NNST	A20	45.0	0.780	0.0392	0.0727	0.218	103	44.2	8.84	-25.1	7.57	NA	NA	NA	NA	0
2019	NNST	A20	44.0	0.520	0.0393	0.0727	0.218	103	48.5	10.1	-24.9	7.57	NA	NA	NA	NA	0
2019	NNST	A20	43.0	0.530	0.0408	0.0727	0.218	103	51.0	10.5	-24.5	7.01	NA	NA	NA	NA	0
2019	NNST	A20	53.0	1.08	0.0398	0.0689	0.207	99.0	58.6	10.1	-25.7	8.68	NA	NA	NA	NA	0
2019	NNST	A20	57.0	1.23	0.0408	0.0689	0.207	99.0	54.7	11.2	-24.6	8.37	51.2	10.0	-24.9	8.63	0
2019	NNST	A20	34.0	0.270	0.0362	0.0689	0.207	99.0	55.6	12.5	-24.0	7.51	NA	NA	NA	NA	0
2019	NNST	A20	38.0	0.310	0.0491	0.0727	0.218	103	47.8	10.4	-29.4	6.69	NA	NA	NA	NA	0
2019	NNST	A20	32.0	0.160	0.0239	0.0689	0.207	99.0	49.8	10.5	-25.6	6.15	NA	NA	NA	NA	0
2019	NNST	A20	50.0	0.780	0.0465	0.0689	0.207	99.0	51.8	10.5	-26.4	8.37	NA	NA	NA	NA	0
2019	NNST	A20	60.0	1.40	0.0314	0.0689	0.207	97.0	48.7	8.18	-27.8	9.01	NA	NA	NA	NA	0
2019	NNST	A20	53.0	1.29	0.0842	0.0689	0.207	97.0	44.4	10.8	-24.6	9.00	NA	NA	NA	NA	0
2019	NNST	A20	64.0	1.60	0.0936	0.0689	0.207	97.0	47.4	9.19	-24.5	9.42	NA	NA	NA	NA	0
2019	NNST	A20	32.0	0.210	0.0295	0.0689	0.207	99.0	48.6	13.1	-22.1	5.87	NA	NA	NA	NA	0
2019	NNST	A20	33.0	0.230	0.0363	0.0727	0.218	103	50.1	10.8	-27.6	6.39	NA	NA	NA	NA	0
2019	NNST	A20	28.0	0.130	0.0292	0.0689	0.207	99.0	51.7	13.1	-24.3	5.72	NA	NA	NA	NA	0
2019	NNST	A20	29.0	0.170	0.0276	0.0689	0.207	99.0	51.1	11.7	-24.1	6.15	NA	NA	NA	NA	0
2019	NNST	A20	50.0	0.860	0.0373	0.0689	0.207	99.0	57.0	10.2	-26.3	8.28	NA	NA	NA	NA	0
2019	NNST	A20	48.0	0.780	0.0538	0.0727	0.218	103	51.4	9.65	-24.9	8.18	NA	NA	NA	NA	0
2019	NNST	A20	33.0	0.200	0.0303	0.0689	0.207	99.0	49.3	11.6	-24.5	6.56	NA	NA	NA	NA	0
2019	NNST	A20	29.0	0.140	0.0314	0.0689	0.207	99.0	54.9	12.8	-24.9	6.51	NA	NA	NA	NA	0
2019	NNST	A20	28.0	0.150	0.0342	0.0689	0.207	99.0	52.5	12.2	-23.8	6.83	51.4	12.9	-23.5	6.99	0
2019	NNST	A20	43.0	0.510	0.0421	0.0727	0.218	103	48.1	11.3	-23.9	7.20	NA	NA	NA	NA	0
2019	NNST	A20	28.0	0.130	0.0294	0.0689	0.207	99.0	49.9	13.2	-22.4	6.49	NA	NA	NA	NA	0
2019	NNST	A20	24.0	0.110	0.0405	0.0689	0.207	97.0	43.6	10.6	-22.6	6.64	NA	NA	NA	NA	0
2019	NNST	A20	25.0	0.100	0.0291	0.0689	0.207	97.0	42.5	10.6	-24.3	5.35	NA	NA	NA	NA	0
2019	NNST	A20	27.0	0.130	0.0195	0.0689	0.207	97.0	40.6	9.97	-22.0	6.47	NA	NA	NA	NA	0
2019	NNST	A20	30.0	0.140	0.0268	0.0689	0.207	97.0	42.2	10.9	-23.2	6.61	NA	NA	NA	NA	0
2019	NNST	A20	30.0	0.180	0.0241	0.0689	0.207	99.0	49.5	11.8	-24.8	6.37	NA	NA	NA	NA	0
2019	NNST	A20	28.0	0.140	0.0410	0.0689	0.207	99.0	48.5	10.4	-25.6	6.38	NA	NA	NA	NA	0

Table A2.4: Laboratory Results for all Slimy Sculpin (Cottus cognatus; SLSC) and Ninespine Stickleback (Pungitius pungitius; NNST) laboratory results from Biotron Laboratory, the University of Waterloo Environmental Isotope Laboratory, and AAE Tech Incorporated. These results include total Hg concentrations with all sample quality assurance and quality control (QA/QC) in accordance with international standards. Stable isotopes from fish tissue are presented as percent (%) carbon (C) and nitrogren (N), as well as with per mil (‰) for delta values of each of these. Age estimates were made using extracted otoliths. mm = millimeters, g = grams, mg/kg = milligrams per killogram, THg = total mercury, MDL = method detection limit, MRL= method reporting limit , DUP = duplicate, C = carbon, N = nitrogren, NA = no available data.

Sample Year	Fish Species Code	Lake Name	Fork Length (mm)	Wet Weight (g)	THg WW (mg/kg)	MDL (ng)	MRL (ng)	IPR avg (%)	%C	%N	δ13C	δ15N	DUP %C	DUP %N	DUP δ13C	DUP δ15N	Age Estimate
2019	NNST	A20	24.0	0.0800	0.0256	0.0689	0.207	97.0	40.5	10.4	-22.7	6.29	NA	NA	NA	NA	0
2019	NNST	A20	28.0	0.120	0.0246	0.0689	0.207	99.0	44.3	11.6	-22.4	6.07	NA	NA	NA	NA	0
2019	NNST	A20	35.0	0.240	0.0333	0.0727	0.218	103	49.8	11.2	-27.1	5.98	51.3	11.6	-27.0	6.20	0
2019	NNST	A20	35.0	0.290	0.0439	0.0689	0.207	99.0	51.2	12.1	-23.5	7.27	NA	NA	NA	NA	0
2019	NNST	A20	36.0	0.320	0.0409	0.0727	0.218	103	48.4	11.0	-25.5	7.17	NA	NA	NA	NA	0
2019	NNST	A20	31.0	0.250	0.0483	0.0727	0.218	103	48.9	11.3	-24.2	7.35	NA	NA	NA	NA	0
2019	SLSC	MMT	55.0	1.63	0.0326	0.0689	0.207	97.0	41.5	7.82	-22.9	7.99	NA	NA	NA	NA	2
2019	SLSC	MMT	45.0	0.790	0.0415	0.0689	0.207	97.0	47.6	10.3	-23.1	8.17	NA	NA	NA	NA	1
2019	SLSC	MMT	63.0	1.86	0.0732	0.0689	0.207	97.0	47.1	11.3	-21.4	7.55	47.2	11.3	-21.4	7.56	4
2019	SLSC	MMT	49.0	1.03	0.0303	0.0689	0.207	98.0	47.6	9.63	-22.7	7.91	45.4	9.95	-22.4	8.13	2
2019	SLSC	MMT	36.0	0.420	0.0303	0.0727	0.218	103	49.7	12.0	-20.0	7.83	NA	NA	NA	NA	0
2019	SLSC	MMT	56.0	1.67	0.0351	0.0689	0.207	98.0	42.9	9.36	-23.8	7.97	NA	NA	NA	NA	2
2019	SLSC	MMT	39.0	0.490	0.0193	0.0689	0.207	98.0	43.1	9.45	-19.9	8.50	NA	NA	NA	NA	1
2019	SLSC	MMT	38.0	0.450	0.0282	0.0727	0.218	103	45.7	11.2	-22.0	8.29	NA	NA	NA	NA	0
2019	SLSC	MMT	40.0	0.510	0.0263	0.0689	0.207	98.0	49.3	11.0	-22.8	8.62	NA	NA	NA	NA	1
2019	SLSC	MMT	36.0	0.370	0.0383	0.0727	0.218	103	49.2	12.0	-21.9	8.07	NA	NA	NA	NA	0
2019	SLSC	MMT	52.0	1.46	0.0360	0.0689	0.207	98.0	52.2	10.1	-22.5	7.55	NA	NA	NA	NA	1
2019	SLSC	MMT	59.0	1.48	0.0300	0.0689	0.207	98.0	41.6	8.47	-23.5	7.86	NA	NA	NA	NA	2
2019	SLSC	MMT	58.0	1.41	0.0389	0.0689	0.207	98.0	44.7	9.04	-18.6	7.39	NA	NA	NA	NA	2
2019	SLSC	MMT	47.0	0.850	0.0246	0.0689	0.207	98.0	51.8	12.4	-21.5	8.29	NA	NA	NA	NA	2
2019	SLSC	MMT	83.0	5.25	0.0481	0.0689	0.207	97.0	40.2	7.83	-22.8	7.96	NA	NA	NA	NA	4
2019	SLSC	MMT	55.0	1.45	0.0389	0.0689	0.207	98.0	46.1	10.2	-19.7	7.82	NA	NA	NA	NA	2
2019	SLSC	MMT	56.0	1.58	0.0319	0.0689	0.207	98.0	47.2	10.1	-22.3	7.56	NA	NA	NA	NA	2
2019	SLSC	MMT	58.0	1.78	0.0414	0.0689	0.207	98.0	44.4	9.07	-23.0	7.70	48.2	8.77	-23.6	7.85	2
2019	SLSC	MMT	57.0	1.47	0.0382	0.0689	0.207	98.0	46.0	8.92	-23.4	8.06	NA	NA	NA	NA	2
2019	SLSC	MMT	57.0	1.84	0.0348	0.0689	0.207	98.0	41.1	8.60	-21.9	8.35	NA	NA	NA	NA	2
2019	SLSC	MMT	49.0	0.990	0.0391	0.0689	0.207	98.0	49.5	10.2	-22.0	7.95	NA	NA	NA	NA	2
2019	SLSC	MMT	42.0	0.680	0.0316	0.0689	0.207	98.0	40.3	8.85	-20.7	7.24	NA	NA	NA	NA	2
2019	SLSC	MMT	58.0	1.72	0.0296	0.0689	0.207	98.0	49.0	9.88	-22.9	7.53	NA	NA	NA	NA	2
2019	SLSC	MMT	50.0	1.06	0.0360	0.0689	0.207	97.0	43.9	9.33	-22.3	8.33	NA	NA	NA	NA	1
2019	SLSC	MMT	54.0	1.27	0.0462	0.0689	0.207	98.0	55.6	12.3	-23.0	7.61	NA	NA	NA	NA	2

Table A2.4: Laboratory Results for all Slimy Sculpin (Cottus cognatus; SLSC) and Ninespine Stickleback (Pungitius pungitius; NNST) laboratory results from Biotron Laboratory, the University of Waterloo Environmental Isotope Laboratory, and AAE Tech Incorporated. These results include total Hg concentrations with all sample quality assurance and quality control (QA/QC) in accordance with international standards. Stable isotopes from fish tissue are presented as percent (%) carbon (C) and nitrogren (N), as well as with per mil (‰) for delta values of each of these. Age estimates were made using extracted otoliths. mm = millimeters, g = grams, mg/kg = milligrams per killogram, THg = total mercury, MDL = method detection limit, MRL= method reporting limit , DUP = duplicate, C = carbon, N = nitrogren, NA = no available data.

Sample Year	Fish Species Code	Lake Name	Fork Length (mm)	Wet Weight (g)	THg WW (mg/kg)	MDL (ng)	MRL (ng)	IPR avg (%)	%C	%N	δ13C	δ15N	DUP %C	DUP %N	DUP δ13C	DUP δ15N	Age Estimate
2019	SLSC	MMT	59.0	1.82	0.0392	0.0689	0.207	98.0	56.5	12.2	-22.4	7.98	NA	NA	NA	NA	2
2019	SLSC	MMT	59.0	1.59	0.0520	0.0689	0.207	98.0	50.3	12.7	-19.7	7.20	NA	NA	NA	NA	2
2019	SLSC	MMT	54.0	1.49	0.0335	0.0689	0.207	98.0	55.5	11.6	-22.5	7.99	NA	NA	NA	NA	2
2019	SLSC	MMT	48.0	0.910	0.0343	0.0689	0.207	98.0	49.8	10.9	-22.5	8.37	52.9	12.5	-22.2	8.47	2
2019	SLSC	MMT	41.0	0.560	0.0276	0.0689	0.207	98.0	52.5	12.2	-22.3	8.93	NA	NA	NA	NA	0
2019	SLSC	MMT	49.0	0.910	0.0395	0.0689	0.207	98.0	51.9	9.16	-21.7	7.62	NA	NA	NA	NA	2
2019	SLSC	MMT	51.0	1.48	0.0476	0.0689	0.207	98.0	55.6	11.4	-23.3	8.04	NA	NA	NA	NA	2
2019	SLSC	MMT	51.0	1.16	0.0519	0.0689	0.207	98.0	48.6	10.8	-21.5	8.34	NA	NA	NA	NA	2
2019	SLSC	MMT	39.0	0.420	0.0374	0.0727	0.218	103	54.2	12.0	-22.4	7.99	NA	NA	NA	NA	0
2019	SLSC	MMT	60.0	1.83	0.0271	0.0689	0.207	97.0	49.4	10.6	-21.9	7.66	NA	NA	NA	NA	2
2019	SLSC	MMT	40.0	0.450	0.0317	0.0727	0.218	103	48.5	11.0	-22.5	7.63	NA	NA	NA	NA	0
2019	NNST	MMT	43.0	0.510	0.0275	0.0727	0.218	103	54.6	10.0	-26.5	9.77	NA	NA	NA	NA	0
2019	NNST	MMT	49.0	0.760	0.0355	0.0727	0.218	103	49.7	9.07	-25.9	9.33	NA	NA	NA	NA	NA
2019	NNST	MMT	59.0	1.27	0.0249	0.0689	0.207	97.0	45.8	8.11	-27.6	10.2	NA	NA	NA	NA	0
2019	NNST	MMT	57.0	1.52	0.0482	0.0689	0.207	97.0	49.3	9.54	-27.1	10.1	NA	NA	NA	NA	0
2019	NNST	MMT	54.0	1.21	0.0352	0.0689	0.207	98.0	62.5	9.65	-28.0	11.4	NA	NA	NA	NA	0
2019	NNST	MMT	52.0	0.860	0.0241	0.0689	0.207	97.0	47.2	9.12	-26.3	9.98	NA	NA	NA	NA	NA
2019	NNST	MMT	54.0	1.27	0.0455	0.0689	0.207	97.0	46.1	8.80	-25.7	10.0	NA	NA	NA	NA	0
2019	SLSC	WTL	69.0	2.93	0.0452	0.0689	0.207	98.0	50.6	10.1	-25.4	7.36	NA	NA	NA	NA	3
2019	SLSC	WTL	66.0	2.53	0.131	0.0689	0.207	97.0	44.2	11.1	-23.9	8.77	NA	NA	NA	NA	3
2019	SLSC	WTL	54.0	1.46	0.0500	0.0689	0.207	98.0	44.1	8.77	-27.5	9.06	NA	NA	NA	NA	2
2020	SLSC	MMT	40.0	0.536	0.0217	0.0689	0.207	98.0	59.9	11.9	-20.4	7.10	NA	NA	NA	NA	0
2020	SLSC	MMT	37.0	0.417	0.0239	0.0727	0.218	103	52.5	11.3	-19.6	8.02	48.7	10.0	-19.7	7.45	0
2020	SLSC	MMT	49.0	1.13	0.0251	0.0689	0.207	98.0	47.9	9.56	-20.5	7.61	NA	NA	NA	NA	1
2020	SLSC	MMT	40.0	0.559	0.0159	0.0689	0.207	98.0	52.0	10.1	-19.4	7.67	51.1	10.2	-19.3	7.63	1
2020	SLSC	MMT	51.0	1.18	0.0620	0.0689	0.207	98.0	41.5	8.65	-23.6	7.97	NA	NA	NA	NA	1
2020	NNST	MMT	30.0	0.193	0.0217	0.0727	0.218	103	52.6	10.7	-24.5	6.86	NA	NA	NA	NA	0
2020	NNST	MMT	40.0	0.440	0.0225	0.0727	0.218	103	48.9	11.2	-23.7	7.69	NA	NA	NA	NA	0
2020	SLSC	MMT	55.0	1.22	0.0292	0.0689	0.207	98.0	47.8	10.4	-22.0	8.52	NA	NA	NA	NA	1
2020	SLSC	MMT	52.0	1.09	0.0265	0.0689	0.207	98.0	47.8	10.0	-21.5	8.73	NA	NA	NA	NA	1
2020	SLSC	MMT	51.0	0.999	0.0329	0.0689	0.207	98.0	44.5	8.71	-23.2	7.85	NA	NA	NA	NA	1

Table A2.4: Laboratory Results for all Slimy Sculpin (Cottus cognatus; SLSC) and Ninespine Stickleback (Pungitius pungitius; NNST) laboratory results from Biotron Laboratory, the University of Waterloo Environmental Isotope Laboratory, and AAE Tech Incorporated. These results include total Hg concentrations with all sample quality assurance and quality control (QA/QC) in accordance with international standards. Stable isotopes from fish tissue are presented as percent (%) carbon (C) and nitrogren (N), as well as with per mil (‰) for delta values of each of these. Age estimates were made using extracted otoliths. mm = millimeters, g = grams, mg/kg = milligrams per killogram, THg = total mercury, MDL = method detection limit, MRL= method reporting limit , DUP = duplicate, C = carbon, N = nitrogren, NA = no available data.

Sample Year	Fish Species Code	Lake Name	Fork Length (mm)	Wet Weight (g)	THg WW (mg/kg)	MDL (ng)	MRL (ng)	IPR avg (%)	%C	%N	δ13C	δ15N	DUP %C	DUP %N	DUP δ13C	DUP δ15N	Age Estimate
2020	SLSC	MMT	60.0	1.99	0.0396	0.0689	0.207	97.0	45.2	10.4	-21.0	8.23	NA	NA	NA	NA	2
2020	SLSC	MMT	59.0	1.49	0.0282	0.0689	0.207	98.0	41.4	9.82	-23.4	9.90	NA	NA	NA	NA	1
2020	SLSC	MMT	51.0	0.984	0.0313	0.0689	0.207	98.0	44.2	9.13	-21.8	8.34	NA	NA	NA	NA	1
2020	SLSC	MMT	46.0	0.740	0.0249	0.0689	0.207	98.0	46.1	10.2	-20.0	8.72	NA	NA	NA	NA	1
2020	SLSC	MMT	65.0	1.87	0.0665	0.0689	0.207	97.0	53.6	12.7	-21.4	8.85	45.2	10.5	-21.5	8.83	2
2020	SLSC	MMT	46.0	0.859	0.0291	0.0689	0.207	98.0	46.1	10.3	-22.1	9.51	NA	NA	NA	NA	1
2020	SLSC	MMT	53.0	1.35	0.0380	0.0689	0.207	97.0	49.5	9.58	-21.0	8.45	NA	NA	NA	NA	2
2020	SLSC	MMT	37.0	0.362	0.0235	0.0727	0.218	103	52.8	10.9	-20.8	7.84	NA	NA	NA	NA	0
2020	SLSC	MMT	51.0	1.21	0.0246	0.0689	0.207	98.0	51.7	9.62	-20.6	8.00	NA	NA	NA	NA	1
2020	SLSC	MMT	67.0	2.14	0.0743	0.0689	0.207	97.0	46.8	12.7	-18.7	8.21	NA	NA	NA	NA	2
2020	SLSC	MMT	38.0	0.445	0.0553	0.0727	0.218	103	50.4	10.7	-24.6	6.66	NA	NA	NA	NA	0
2020	SLSC	MMT	54.0	1.18	0.0585	0.0689	0.207	98.0	48.9	9.64	-25.1	8.53	51.4	10.1	-25.3	8.27	1
2020	SLSC	MMT	49.0	0.855	0.0296	0.0689	0.207	98.0	41.6	8.85	-19.9	8.33	NA	NA	NA	NA	1
2020	SLSC	MMT	40.0	0.483	0.0247	0.0689	0.207	98.0	44.2	9.11	-20.2	9.51	NA	NA	NA	NA	0
2020	SLSC	MMT	51.0	1.20	0.0620	0.0689	0.207	98.0	51.6	9.63	-24.5	7.33	NA	NA	NA	NA	1
2020	SLSC	MMT	61.0	1.93	0.0492	0.0689	0.207	98.0	44.7	9.59	-22.4	8.17	NA	NA	NA	NA	3
2020	SLSC	MMT	44.0	0.636	0.0426	0.0689	0.207	98.0	49.4	10.2	-21.8	9.18	NA	NA	NA	NA	0
2020	SLSC	MMT	47.0	0.887	0.0272	0.0689	0.207	98.0	49.0	9.56	-21.6	7.81	NA	NA	NA	NA	1
2020	SLSC	MMT	64.0	1.84	0.0560	0.0689	0.207	98.0	47.3	9.70	-21.7	8.97	NA	NA	NA	NA	2
2020	SLSC	MMT	43.0	0.570	0.0313	0.0689	0.207	97.0	52.6	11.0	-19.5	9.01	NA	NA	NA	NA	0
2020	SLSC	MMT	55.0	1.39	0.0333	0.0689	0.207	98.0	55.9	11.2	-21.4	9.00	NA	NA	NA	NA	2
2020	SLSC	MMT	40.0	0.427	0.0188	0.0689	0.207	98.0	51.0	10.9	-22.5	8.39	NA	NA	NA	NA	0
2020	SLSC	MMT	38.0	0.457	0.0192	0.0727	0.218	103	52.7	10.9	-18.3	7.44	NA	NA	NA	NA	0
2020	SLSC	MMT	35.0	0.363	0.0211	0.0727	0.218	103	49.0	11.5	-20.9	7.21	NA	NA	NA	NA	0
2020	SLSC	MMT	37.0	0.394	0.0194	0.0689	0.207	98.0	42.4	9.28	-20.2	8.14	48.1	10.7	-20.2	8.12	1
2020	NNST	MMT	34.0	0.252	0.0196	0.0727	0.218	103	50.3	10.8	-26.5	7.72	49.3	11.1	-26.2	7.65	0
2020	NNST	MMT	57.0	1.70	0.0678	0.0689	0.207	97.0	46.5	8.16	-26.7	9.89	NA	NA	NA	NA	0
2020	NNST	MMT	57.0	1.12	0.0592	0.0689	0.207	98.0	47.5	6.96	-26.8	10.2	NA	NA	NA	NA	1
2020	NNST	MMT	60.0	1.54	0.0323	0.0689	0.207	97.0	49.8	8.54	-27.9	9.60	NA	NA	NA	NA	0
2020	NNST	MMT	60.0	1.66	0.0583	0.0689	0.207	97.0	49.1	8.24	-27.3	10.5	NA	NA	NA	NA	0
2020	NNST	MMT	55.0	1.10	0.0291	0.0689	0.207	97.0	50.2	9.06	-27.1	8.92	NA	NA	NA	NA	0

Table A2.4: Laboratory Results for all Slimy Sculpin (Cottus cognatus; SLSC) and Ninespine Stickleback (Pungitius pungitius; NNST) laboratory results from Biotron Laboratory, the University of Waterloo Environmental Isotope Laboratory, and AAE Tech Incorporated. These results include total Hg concentrations with all sample quality assurance and quality control (QA/QC) in accordance with international standards. Stable isotopes from fish tissue are presented as percent (%) carbon (C) and nitrogren (N), as well as with per mil (‰) for delta values of each of these. Age estimates were made using extracted otoliths. mm = millimeters, g = grams, mg/kg = milligrams per killogram, THg = total mercury, MDL = method detection limit, MRL= method reporting limit , DUP = duplicate, C = carbon, N = nitrogren, NA = no available data.

Sample Year	Fish Species Code	Lake Name	Fork Length (mm)	Wet Weight (g)	THg WW (mg/kg)	MDL (ng)	MRL (ng)	IPR avg (%)	%C	%N	δ13C	δ15N	DUP %C	DUP %N	DUP δ13C	DUP δ15N	Age Estimate
2020	SLSC	Lake 8	46.0	0.735	0.0310	0.0689	0.207	98.0	50.2	12.1	-20.3	7.80	NA	NA	NA	NA	1
2020	SLSC	Lake 8	50.0	1.17	0.0354	0.0689	0.207	97.0	45.0	9.86	-21.4	6.88	NA	NA	NA	NA	3
2020	SLSC	Lake 8	35.0	0.389	0.0229	0.0727	0.218	103	44.2	9.96	-17.3	6.09	NA	NA	NA	NA	0
2020	SLSC	Lake 8	30.0	0.289	0.0375	0.0689	0.207	98.0	43.7	11.2	-21.8	7.58	NA	NA	NA	NA	0
2020	SLSC	Lake 8	37.0	0.557	0.0317	0.0689	0.207	98.0	55.5	10.9	-22.7	7.36	NA	NA	NA	NA	0
2020	SLSC	Lake 8	46.0	1.05	0.0225	0.0689	0.207	98.0	53.4	10.8	-21.0	6.88	NA	NA	NA	NA	1
2020	SLSC	Lake 8	45.0	0.598	0.0350	0.0689	0.207	97.0	50.7	12.1	-19.6	6.20	NA	NA	NA	NA	1
2020	SLSC	Lake 8	51.0	1.14	0.0323	0.0689	0.207	97.0	46.7	11.1	-20.3	7.41	NA	NA	NA	NA	3
2020	SLSC	Lake 8	34.0	0.287	0.0280	0.0727	0.218	103	44.0	11.9	-21.6	6.37	NA	NA	NA	NA	0
2020	SLSC	Lake 8	45.0	0.630	0.0307	0.0689	0.207	98.0	46.5	11.6	-23.4	8.25	NA	NA	NA	NA	1
2020	SLSC	Lake 8	40.0	0.533	0.0529	0.0689	0.207	98.0	45.6	11.3	-26.2	8.50	NA	NA	NA	NA	1
2020	SLSC	Lake 8	40.0	0.514	0.0243	0.0689	0.207	97.0	39.0	9.34	-18.2	5.56	NA	NA	NA	NA	1
2020	SLSC	Lake 8	60.0	1.77	0.0380	0.0689	0.207	97.0	49.4	10.8	-25.1	8.41	NA	NA	NA	NA	2
2020	SLSC	Lake 8	44.0	0.675	0.0467	0.0689	0.207	98.0	48.4	12.4	-22.8	7.71	NA	NA	NA	NA	1
2020	SLSC	Lake 8	31.0	0.271	0.0200	0.0727	0.218	103	44.0	11.6	-17.8	6.12	NA	NA	NA	NA	0
2020	SLSC	Lake 8	41.0	0.567	0.0277	0.0689	0.207	98.0	44.6	11.2	-19.4	6.73	NA	NA	NA	NA	1
2020	SLSC	Lake 8	38.0	0.440	0.0240	0.0689	0.207	98.0	45.8	11.0	-17.9	5.57	44.1	10.8	-17.7	5.61	2
2020	SLSC	Lake 8	27.0	0.215	0.0361	0.0727	0.218	103	48.8	12.6	-21.1	7.21	NA	NA	NA	NA	0
2020	SLSC	Lake 8	44.0	0.675	0.0370	0.0689	0.207	98.0	50.3	13.1	-22.7	7.74	NA	NA	NA	NA	1
2020	SLSC	Lake 8	41.0	0.579	0.0608	0.0689	0.207	98.0	48.8	12.6	-22.2	7.88	NA	NA	NA	NA	1
2020	SLSC	Lake 8	53.0	1.16	0.0352	0.0689	0.207	97.0	45.2	11.3	-19.9	7.11	43.4	10.6	-20.0	6.89	2
2020	SLSC	Lake 8	51.0	1.01	0.0418	0.0689	0.207	98.0	47.6	11.8	-22.6	7.61	NA	NA	NA	NA	2
2020	SLSC	Lake 8	52.0	1.02	0.0328	0.0689	0.207	98.0	49.7	12.0	-23.2	7.81	NA	NA	NA	NA	3
2020	SLSC	Lake 8	39.0	0.506	0.0200	0.0689	0.207	98.0	48.8	11.8	-17.3	5.69	NA	NA	NA	NA	1
2020	SLSC	Lake 8	44.0	0.731	0.0238	0.0689	0.207	98.0	43.2	10.3	-20.6	6.59	NA	NA	NA	NA	1
2020	SLSC	Lake 8	45.0	0.726	0.0447	0.0689	0.207	98.0	46.3	11.7	-22.4	7.50	NA	NA	NA	NA	2
2020	SLSC	Lake 8	41.0	0.598	0.0318	0.0689	0.207	98.0	48.1	10.6	-21.4	6.69	NA	NA	NA	NA	1
2020	SLSC	Lake 8	30.0	0.266	0.0271	0.0727	0.218	103	47.6	11.7	-18.8	6.78	45.5	11.3	-18.8	6.73	0
2020	SLSC	Lake 8	45.0	0.732	0.0391	0.0689	0.207	98.0	44.8	11.6	-22.7	7.46	NA	NA	NA	NA	1
2020	SLSC	Lake 8	35.0	0.341	0.0250	0.0689	0.207	98.0	43.7	10.6	-19.8	7.21	47.9	12.1	-19.6	7.12	0
2020	SLSC	Lake 8	43.0	0.541	0.0302	0.0689	0.207	98.0	48.6	10.7	-20.8	6.93	NA	NA	NA	NA	1

Table A2.4: Laboratory Results for all Slimy Sculpin (Cottus cognatus; SLSC) and Ninespine Stickleback (Pungitius pungitius; NNST) laboratory results from Biotron Laboratory, the University of Waterloo Environmental Isotope Laboratory, and AAE Tech Incorporated. These results include total Hg concentrations with all sample quality assurance and quality control (QA/QC) in accordance with international standards. Stable isotopes from fish tissue are presented as percent (%) carbon (C) and nitrogren (N), as well as with per mil (‰) for delta values of each of these. Age estimates were made using extracted otoliths. mm = millimeters, g = grams, mg/kg = milligrams per killogram, THg = total mercury, MDL = method detection limit, MRL= method reporting limit , DUP = duplicate, C = carbon, N = nitrogren, NA = no available data.

Sample Year	Fish Species Code	Lake Name	Fork Length (mm)	Wet Weight (g)	THg WW (mg/kg)	MDL (ng)	MRL (ng)	IPR avg (%)	%C	%N	δ13C	δ15N	DUP %C	DUP %N	DUP δ13C	DUP δ15N	Age Estimate
2020	SLSC	Lake 8	31.0	0.262	0.0279	0.0689	0.207	98.0	47.3	11.3	-18.6	6.02	NA	NA	NA	NA	0
2020	SLSC	Lake 8	45.0	0.689	0.0293	0.0689	0.207	98.0	48.8	11.8	-21.3	6.61	NA	NA	NA	NA	1
2020	SLSC	Lake 8	37.0	0.567	0.0344	0.0689	0.207	98.0	49.7	12.1	-20.9	6.59	NA	NA	NA	NA	1
2020	NNST	MMT	41.0	0.446	0.0211	0.0727	0.218	103	50.8	10.0	-26.2	8.17	NA	NA	NA	NA	0
2020	NNST	WTL	40.0	0.545	0.305	0.0689	0.207	98.0	37.4	7.74	-30.4	8.40	NA	NA	NA	NA	0
2020	NNST	WTL	38.0	0.342	0.312	0.0727	0.218	103	46.8	9.84	-30.6	8.68	NA	NA	NA	NA	0
2020	NNST	WTL	38.0	0.361	0.237	0.0689	0.207	98.0	45.9	10.5	-30.5	8.49	NA	NA	NA	NA	0
2020	NNST	WTL	40.0	0.522	0.291	0.0689	0.207	98.0	56.6	10.8	-30.8	8.33	NA	NA	NA	NA	0
2020	NNST	WTL	36.0	0.293	0.314	0.0727	0.218	103	45.8	10.0	-30.0	8.62	NA	NA	NA	NA	0
2020	NNST	WTL	39.0	0.432	0.305	0.0727	0.218	103	49.0	10.2	-29.5	8.32	NA	NA	NA	NA	0
2020	NNST	WTL	24.0	0.109	0.311	0.0689	0.207	97.0	48.0	11.8	-27.2	7.89	NA	NA	NA	NA	0
2020	NNST	WTL	29.0	0.189	0.316	0.0689	0.207	97.0	42.7	9.85	-28.4	7.95	NA	NA	NA	NA	0
2020	NNST	WTL	35.0	0.290	0.156	0.0689	0.207	98.0	43.6	9.21	-25.5	9.45	NA	NA	NA	NA	0
2020	NNST	WTL	36.0	0.300	0.275	0.0689	0.207	98.0	51.4	10.6	-29.1	8.20	NA	NA	NA	NA	0
2020	NNST	WTL	34.0	0.235	0.297	0.0689	0.207	98.0	49.3	9.91	-29.5	7.61	46.3	9.53	-29.4	7.72	0
2020	NNST	WTL	26.0	0.169	0.250	0.0689	0.207	98.0	45.5	10.8	-29.8	7.76	NA	NA	NA	NA	0
2020	NNST	WTL	37.0	0.434	0.165	0.0689	0.207	98.0	44.0	9.80	-26.7	9.20	NA	NA	NA	NA	0
2020	NNST	WTL	26.0	0.139	0.146	0.0689	0.207	98.0	50.4	12.6	-23.8	9.73	NA	NA	NA	NA	0
2020	NNST	WTL	25.0	0.132	0.354	0.0689	0.207	97.0	52.3	11.9	-26.9	8.16	NA	NA	NA	NA	0
2020	NNST	WTL	45.0	0.618	0.332	0.0727	0.218	103	46.3	10.1	-30.3	8.87	NA	NA	NA	NA	0
2020	NNST	WTL	41.0	0.415	0.265	0.0727	0.218	103	50.1	10.2	-30.2	8.25	NA	NA	NA	NA	0
2020	NNST	WTL	47.0	0.666	0.275	0.0727	0.218	103	51.7	9.87	-31.4	9.23	NA	NA	NA	NA	0
2020	NNST	WTL	44.0	0.535	0.256	0.0689	0.207	98.0	53.2	10.1	-30.6	8.65	NA	NA	NA	NA	0
2020	NNST	WTL	44.0	0.561	0.315	0.0727	0.218	103	56.7	10.6	-31.3	7.80	NA	NA	NA	NA	0
2020	NNST	WTL	42.0	0.544	0.322	0.0727	0.218	103	50.8	9.81	-31.2	8.02	NA	NA	NA	NA	0
2020	NNST	WTL	31.0	0.222	0.278	0.0727	0.218	103	51.6	12.3	-28.9	8.28	52.5	10.9	-29.6	7.67	0
2020	NNST	WTL	51.0	0.928	0.221	0.0689	0.207	97.0	47.1	8.71	-31.7	9.66	NA	NA	NA	NA	0
2020	NNST	WTL	45.0	0.585	0.281	0.0689	0.207	98.0	49.5	9.97	-30.5	8.76	NA	NA	NA	NA	0
2020	NNST	WTL	44.0	0.551	0.237	0.0689	0.207	98.0	39.0	8.47	-30.8	8.74	NA	NA	NA	NA	0
2020	NNST	WTL	43.0	0.510	0.244	0.0689	0.207	98.0	51.1	11.5	-30.0	8.80	NA	NA	NA	NA	0
2020	NNST	WTL	32.0	0.226	0.348	0.0689	0.207	98.0	47.0	11.4	-29.4	7.41	NA	NA	NA	NA	0

Table A2.4: Laboratory Results for all Slimy Sculpin (Cottus cognatus; SLSC) and Ninespine Stickleback (Pungitius pungitius; NNST) laboratory results from Biotron Laboratory, the University of Waterloo Environmental Isotope Laboratory, and AAE Tech Incorporated. These results include total Hg concentrations with all sample quality assurance and quality control (QA/QC) in accordance with international standards. Stable isotopes from fish tissue are presented as percent (%) carbon (C) and nitrogren (N), as well as with per mil (‰) for delta values of each of these. Age estimates were made using extracted otoliths. mm = millimeters, g = grams, mg/kg = milligrams per killogram, THg = total mercury, MDL = method detection limit, MRL= method reporting limit , DUP = duplicate, C = carbon, N = nitrogren, NA = no available data.

Sample Year	Fish Species Code	Lake Name	Fork Length (mm)	Wet Weight (g)	THg WW (mg/kg)	MDL (ng)	MRL (ng)	IPR avg (%)	%C	%N	δ13C	δ15N	DUP %C	DUP %N	DUP δ13C	DUP δ15N	Age Estimate
2020	NNST	WTL	40.0	0.413	0.267	0.0689	0.207	98.0	54.5	11.7	-30.3	8.61	NA	NA	NA	NA	0
2020	NNST	WTL	40.0	0.441	0.228	0.0689	0.207	98.0	43.9	8.45	-30.8	8.37	51.0	10.1	-30.6	8.58	0
2020	NNST	WTL	44.0	0.533	0.279	0.0689	0.207	98.0	48.7	10.9	-28.4	8.83	NA	NA	NA	NA	0
2020	NNST	WTL	32.0	0.223	0.225	0.0689	0.207	98.0	47.7	11.0	-29.5	7.96	NA	NA	NA	NA	NA
2020	NNST	WTL	34.0	0.299	0.211	0.0727	0.218	103	51.1	11.6	-26.6	10.1	NA	NA	NA	NA	0
2020	NNST	WTL	36.0	0.400	0.281	0.0689	0.207	98.0	41.2	8.77	-30.2	8.01	NA	NA	NA	NA	0
2020	SLSC	WTL	45.0	0.937	0.212	0.0689	0.207	97.0	46.1	9.11	-28.3	8.42	NA	NA	NA	NA	1
2020	SLSC	WTL	45.0	0.740	0.268	0.0689	0.207	98.0	49.9	9.83	-28.0	7.45	NA	NA	NA	NA	0
2020	SLSC	WTL	54.0	1.45	0.142	0.0689	0.207	98.0	48.1	9.29	-29.0	6.77	NA	NA	NA	NA	1
2020	SLSC	WTL	65.0	2.47	0.179	0.0689	0.207	97.0	46.6	9.37	-25.4	7.79	NA	NA	NA	NA	3
2020	SLSC	WTL	42.0	0.710	0.0883	0.0689	0.207	98.0	50.8	10.1	-28.5	7.15	NA	NA	NA	NA	2
2020	SLSC	WTL	58.0	2.01	0.165	0.0689	0.207	97.0	45.2	8.79	-28.2	7.55	NA	NA	NA	NA	1
2020	SLSC	WTL	53.0	1.23	0.217	0.0689	0.207	98.0	47.4	9.68	-28.4	8.42	NA	NA	NA	NA	1
2020	SLSC	WTL	54.0	1.57	0.207	0.0689	0.207	98.0	53.0	9.53	-29.6	7.54	NA	NA	NA	NA	1
2020	SLSC	WTL	47.0	1.19	0.211	0.0689	0.207	98.0	48.5	8.98	-28.7	7.42	NA	NA	NA	NA	1
2020	SLSC	WTL	53.0	1.47	0.183	0.0689	0.207	98.0	55.7	11.4	-28.4	7.60	47.9	10.5	-28.0	7.56	2
2020	SLSC	WTL	45.0	0.812	0.216	0.0689	0.207	97.0	41.9	7.78	-28.1	7.87	NA	NA	NA	NA	1
2020	SLSC	WTL	37.0	0.515	0.279	0.0727	0.218	103	59.1	10.7	-28.0	7.79	NA	NA	NA	NA	0
2020	SLSC	WTL	47.0	0.952	0.228	0.0689	0.207	98.0	49.3	8.13	-28.3	6.82	NA	NA	NA	NA	0
2020	SLSC	WTL	54.0	1.63	0.203	0.0689	0.207	98.0	50.0	10.2	-28.6	7.63	NA	NA	NA	NA	1
2020	SLSC	WTL	69.0	2.70	0.250	0.0689	0.207	97.0	50.1	11.4	-25.0	9.48	NA	NA	NA	NA	3
2020	SLSC	WTL	60.0	2.31	0.180	0.0689	0.207	97.0	51.5	9.31	-31.2	7.87	62.0	10.9	-28.9	7.91	3
2020	SLSC	WTL	64.0	2.35	0.154	0.0689	0.207	98.0	40.4	7.89	-29.7	7.59	NA	NA	NA	NA	1
2020	SLSC	WTL	59.0	2.12	0.179	0.0689	0.207	98.0	51.2	9.18	-28.3	8.19	NA	NA	NA	NA	1
2020	SLSC	WTL	61.0	2.10	0.162	0.0689	0.207	98.0	51.9	10.5	-28.9	6.99	NA	NA	NA	NA	1
2020	SLSC	WTL	65.0	2.62	0.251	0.0689	0.207	98.0	47.2	9.99	-26.7	8.28	NA	NA	NA	NA	2
2020	SLSC	WTL	61.0	1.96	0.211	0.0689	0.207	98.0	44.7	8.61	-29.3	7.77	NA	NA	NA	NA	2
2020	SLSC	WTL	47.0	0.866	0.260	0.0689	0.207	98.0	44.6	8.52	-28.9	7.64	NA	NA	NA	NA	1
2020	SLSC	WTL	66.0	2.62	0.189	0.0689	0.207	98.0	39.2	9.02	-26.4	8.18	NA	NA	NA	NA	2
2020	SLSC	WTL	52.0	1.28	0.210	0.0689	0.207	97.0	43.6	8.55	-28.3	8.29	NA	NA	NA	NA	1
2020	SLSC	WTL	45.0	0.833	0.227	0.0689	0.207	98.0	47.4	9.56	-27.8	7.70	58.4	9.35	-28.7	7.77	1

Table A2.4: Laboratory Results for all Slimy Sculpin (Cottus cognatus; SLSC) and Ninespine Stickleback (Pungitius pungitius; NNST) laboratory results from Biotron Laboratory, the University of Waterloo Environmental Isotope Laboratory, and AAE Tech Incorporated. These results include total Hg concentrations with all sample quality assurance and quality control (QA/QC) in accordance with international standards. Stable isotopes from fish tissue are presented as percent (%) carbon (C) and nitrogren (N), as well as with per mil (‰) for delta values of each of these. Age estimates were made using extracted otoliths. mm = millimeters, g = grams, mg/kg = milligrams per killogram, THg = total mercury, MDL = method detection limit, MRL= method reporting limit , DUP = duplicate, C = carbon, N = nitrogren, NA = no available data.

Sample Year	Fish Species Code	Lake Name	Fork Length (mm)	Wet Weight (g)	THg WW (mg/kg)	MDL (ng)	MRL (ng)	IPR avg (%)	%C	%N	δ13C	δ15N	DUP %C	DUP %N	DUP δ13C	DUP δ15N	Age Estimate
2020	SLSC	WTL	40.0	0.580	0.206	0.0727	0.218	103	53.0	9.87	-27.9	7.37	NA	NA	NA	NA	0
2020	SLSC	WTL	54.0	1.54	0.155	0.0689	0.207	98.0	48.7	7.97	-31.1	6.95	NA	NA	NA	NA	1
2020	SLSC	WTL	71.0	3.25	0.170	0.0689	0.207	97.0	45.8	8.45	-28.1	8.45	NA	NA	NA	NA	2
2020	SLSC	WTL	61.0	2.19	0.195	0.0689	0.207	98.0	45.6	9.05	-28.5	7.42	NA	NA	NA	NA	2
2020	SLSC	WTL	45.0	0.794	0.251	0.0689	0.207	98.0	46.0	8.66	-28.6	7.78	NA	NA	NA	NA	0
2020	SLSC	WTL	45.0	0.709	0.276	0.0727	0.218	103	52.6	10.1	-28.3	7.82	NA	NA	NA	NA	0
2020	SLSC	WTL	43.0	0.636	0.248	0.0727	0.218	103	55.2	10.4	-27.9	7.53	NA	NA	NA	NA	0
2020	SLSC	WTL	41.0	0.590	0.296	0.0727	0.218	103	51.5	9.70	-28.1	8.18	NA	NA	NA	NA	0
2020	NNST	A20	36.0	0.299	0.0713	0.0689	0.207	99.0	52.9	11.0	-27.4	6.85	NA	NA	NA	NA	0
2020	NNST	A20	44.0	0.580	0.113	0.0727	0.218	103	48.2	9.65	-28.5	7.02	NA	NA	NA	NA	0
2020	NNST	A20	37.0	0.342	0.242	0.0689	0.207	99.0	42.4	9.84	-25.6	6.34	NA	NA	NA	NA	0
2020	NNST	A20	30.0	0.190	0.0436	0.0689	0.207	99.0	47.5	11.2	-26.3	6.49	NA	NA	NA	NA	0
2020	NNST	A20	38.0	0.364	0.108	0.0689	0.207	99.0	46.7	9.96	-27.7	6.88	NA	NA	NA	NA	0
2020	NNST	A20	44.0	0.592	0.154	0.0689	0.207	99.0	52.3	10.1	-27.2	6.33	49.1	10.0	-26.9	6.42	0
2020	NNST	A20	32.0	0.214	0.0646	0.0727	0.218	103	50.1	11.2	-27.3	7.06	NA	NA	NA	NA	0
2020	NNST	A20	31.0	0.224	0.0787	0.0727	0.218	103	49.3	11.0	-26.8	7.18	NA	NA	NA	NA	0
2020	NNST	A20	40.0	0.358	0.169	0.0689	0.207	99.0	53.3	11.6	-26.8	6.79	NA	NA	NA	NA	0
2020	NNST	A20	41.0	0.462	0.286	0.0727	0.218	103	50.3	9.93	-27.7	7.25	53.6	10.4	-27.8	7.36	0
2020	NNST	A20	31.0	0.211	0.0777	0.0689	0.207	99.0	47.2	10.2	-26.2	6.67	NA	NA	NA	NA	0
2020	NNST	A20	29.0	0.156	0.193	0.0689	0.207	97.0	50.6	11.4	-26.3	5.81	NA	NA	NA	NA	0
2020	NNST	A20	36.0	0.280	0.127	0.0689	0.207	99.0	50.4	10.5	-25.5	6.74	NA	NA	NA	NA	0
2020	NNST	A20	40.0	0.401	0.291	0.0689	0.207	99.0	53.1	10.4	-29.7	7.19	NA	NA	NA	NA	0
2020	NNST	A20	36.0	0.344	0.144	0.0689	0.207	99.0	47.2	10.8	-25.6	6.52	NA	NA	NA	NA	0
2020	NNST	A20	32.0	0.242	0.160	0.0689	0.207	99.0	52.9	12.6	-26.2	6.07	NA	NA	NA	NA	0
2020	NNST	A20	44.0	0.543	0.0917	0.0689	0.207	99.0	51.0	11.0	-28.0	7.32	NA	NA	NA	NA	0
2020	NNST	A20	35.0	0.281	0.463	0.0727	0.218	103	47.4	10.9	-28.9	7.36	NA	NA	NA	NA	0
2020	NNST	A20	36.0	0.302	0.197	0.0689	0.207	99.0	48.6	10.4	-27.8	6.96	NA	NA	NA	NA	0
2020	NNST	A20	37.0	0.348	0.241	0.0727	0.218	103	49.8	10.4	-27.4	6.63	NA	NA	NA	NA	0
2020	NNST	A20	35.0	0.256	0.111	0.0689	0.207	99.0	49.1	11.5	-25.9	7.16	NA	NA	NA	NA	0
2020	NNST	A20	35.0	0.260	0.0603	0.0689	0.207	99.0	42.6	9.72	-27.1	6.98	46.3	10.5	-27.1	6.84	0
2020	NNST	A20	59.0	1.15	0.0852	0.0689	0.207	97.0	47.4	10.3	-28.0	8.65	NA	NA	NA	NA	0

Table A2.4: Laboratory Results for all Slimy Sculpin (Cottus cognatus; SLSC) and Ninespine Stickleback (Pungitius pungitius; NNST) laboratory results from Biotron Laboratory, the University of Waterloo Environmental Isotope Laboratory, and AAE Tech Incorporated. These results include total Hg concentrations with all sample quality assurance and quality control (QA/QC) in accordance with international standards. Stable isotopes from fish tissue are presented as percent (%) carbon (C) and nitrogren (N), as well as with per mil (‰) for delta values of each of these. Age estimates were made using extracted otoliths. mm = millimeters, g = grams, mg/kg = milligrams per killogram, THg = total mercury, MDL = method detection limit, MRL= method reporting limit , DUP = duplicate, C = carbon, N = nitrogren, NA = no available data.

Sample Year	Fish Species Code	Lake Name	Fork Length (mm)	Wet Weight (g)	THg WW (mg/kg)	MDL (ng)	MRL (ng)	IPR avg (%)	%C	%N	δ13C	δ15N	DUP %C	DUP %N	DUP δ13C	DUP δ15N	Age Estimate
2020	NNST	A20	42.0	0.547	0.0860	0.0727	0.218	103	51.5	9.11	-29.4	7.59	NA	NA	NA	NA	0
2020	NNST	A20	37.0	0.331	0.0443	0.0689	0.207	99.0	45.0	8.90	-28.7	7.45	NA	NA	NA	NA	0
2020	NNST	A20	40.0	0.426	0.196	0.0727	0.218	103	46.9	10.2	-25.9	6.61	NA	NA	NA	NA	0
2020	NNST	A20	36.0	0.278	0.130	0.0689	0.207	99.0	51.4	12.6	-26.0	6.88	NA	NA	NA	NA	0
2020	NNST	A20	50.0	0.782	0.124	0.0689	0.207	97.0	51.3	9.85	-29.4	7.77	NA	NA	NA	NA	0
2020	NNST	A20	43.0	0.442	0.117	0.0727	0.218	103	49.3	10.7	-28.2	7.36	NA	NA	NA	NA	0
2020	NNST	A20	39.0	0.334	0.207	0.0727	0.218	103	51.5	11.2	-27.4	6.27	NA	NA	NA	NA	0
2020	NNST	A20	29.0	0.199	0.117	0.0689	0.207	99.0	50.0	12.7	-25.6	6.24	NA	NA	NA	NA	0
2020	NNST	A20	35.0	0.297	0.0950	0.0689	0.207	99.0	47.3	9.47	-30.0	8.24	NA	NA	NA	NA	0
2020	NNST	A20	34.0	0.229	0.129	0.0689	0.207	99.0	52.3	11.4	-26.9	6.62	NA	NA	NA	NA	0
2020	NNST	A20	34.0	0.266	0.162	0.0689	0.207	99.0	41.7	9.81	-27.0	6.99	NA	NA	NA	NA	0
2020	NNST	A20	37.0	0.308	0.203	0.0689	0.207	99.0	46.5	10.4	-26.2	6.64	NA	NA	NA	NA	0
2020	SLSC	A20	39.0	0.463	0.0846	0.0689	0.207	99.0	47.4	10.4	-24.6	5.75	NA	NA	NA	NA	1
2020	SLSC	A20	44.0	0.743	0.197	0.0689	0.207	99.0	39.9	8.67	-25.4	5.89	NA	NA	NA	NA	2
2020	SLSC	A20	54.0	1.36	0.116	0.0689	0.207	99.0	53.0	11.1	-25.1	5.82	45.9	9.86	-24.9	5.76	1
2020	SLSC	A20	48.0	0.926	0.110	0.0689	0.207	99.0	43.9	9.23	-23.3	6.17	NA	NA	NA	NA	1
2020	SLSC	A20	46.0	0.797	0.112	0.0689	0.207	99.0	51.8	11.3	-25.0	6.29	NA	NA	NA	NA	1
2020	SLSC	A20	40.0	0.499	0.105	0.0689	0.207	99.0	46.4	9.40	-24.1	5.15	NA	NA	NA	NA	0
2020	SLSC	A20	37.0	0.463	0.176	0.0727	0.218	103	49.8	10.6	-24.2	5.75	NA	NA	NA	NA	0
2020	SLSC	A20	36.0	0.364	0.0514	0.0727	0.218	103	46.8	10.8	-24.1	5.15	NA	NA	NA	NA	0
2020	SLSC	A20	35.0	0.351	0.114	0.0727	0.218	103	46.0	10.1	-24.7	4.93	NA	NA	NA	NA	0
2020	SLSC	A20	37.0	0.437	0.0827	0.0689	0.207	99.0	44.9	9.81	-23.7	5.82	NA	NA	NA	NA	0
2020	SLSC	A20	37.0	0.422	0.0549	0.0689	0.207	99.0	52.2	11.3	-21.8	4.72	NA	NA	NA	NA	0
2020	SLSC	A20	35.0	0.332	0.0602	0.0689	0.207	99.0	52.2	11.0	-23.6	5.94	NA	NA	NA	NA	1
2020	SLSC	A20	38.0	0.438	0.144	0.0689	0.207	99.0	56.3	11.6	-24.5	4.92	NA	NA	NA	NA	0
2020	SLSC	A20	44.0	0.766	0.108	0.0689	0.207	99.0	43.6	9.34	-23.9	6.69	NA	NA	NA	NA	1
2020	SLSC	A20	53.0	1.31	0.0919	0.0689	0.207	97.0	51.9	9.63	-25.9	6.47	NA	NA	NA	NA	2
2020	SLSC	A20	36.0	0.410	0.0770	0.0689	0.207	99.0	53.2	12.1	-23.6	6.21	NA	NA	NA	NA	0
2020	SLSC	A20	31.0	0.326	0.0712	0.0727	0.218	103	48.5	10.5	-22.3	5.39	49.9	11.4	-22.0	5.23	0
2020	SLSC	A20	40.0	0.549	0.152	0.0689	0.207	97.0	50.3	10.7	-25.1	6.17	NA	NA	NA	NA	1
2020	SLSC	A20	68.0	2.72	0.117	0.0689	0.207	97.0	48.3	10.4	-24.1	7.63	NA	NA	NA	NA	3

Table A2.4: Laboratory Results for all Slimy Sculpin (Cottus cognatus; SLSC) and Ninespine Stickleback (Pungitius pungitius; NNST) laboratory results from Biotron Laboratory, the University of Waterloo Environmental Isotope Laboratory, and AAE Tech Incorporated. These results include total Hg concentrations with all sample quality assurance and quality control (QA/QC) in accordance with international standards. Stable isotopes from fish tissue are presented as percent (%) carbon (C) and nitrogren (N), as well as with per mil (‰) for delta values of each of these. Age estimates were made using extracted otoliths. mm = millimeters, g = grams, mg/kg = milligrams per killogram, THg = total mercury, MDL = method detection limit, MRL= method reporting limit , DUP = duplicate, C = carbon, N = nitrogren, NA = no available data.

Sample Year	Fish Species Code	Lake Name	Fork Length (mm)	Wet Weight (g)	THg WW (mg/kg)	MDL (ng)	MRL (ng)	IPR avg (%)	%C	%N	δ13C	δ15N	DUP %C	DUP %N	DUP δ13C	DUP δ15N	Age Estimate
2020	SLSC	A20	35.0	0.430	0.133	0.0689	0.207	99.0	51.1	11.8	-24.0	5.41	44.8	10.4	-23.8	5.44	0
2020	SLSC	A20	45.0	0.775	0.0587	0.0689	0.207	97.0	45.8	9.31	-23.3	6.05	NA	NA	NA	NA	1
2020	SLSC	A20	47.0	1.02	0.112	0.0689	0.207	99.0	55.2	11.2	-24.7	5.61	NA	NA	NA	NA	1
2020	SLSC	A20	32.0	0.346	0.0549	0.0727	0.218	103	46.0	11.2	-21.2	4.74	NA	NA	NA	NA	0
2020	SLSC	A20	43.0	0.664	0.0501	0.0689	0.207	99.0	50.4	10.9	-21.5	5.57	NA	NA	NA	NA	1
2020	SLSC	A20	55.0	1.77	0.0600	0.0689	0.207	97.0	44.1	9.11	-22.9	5.95	46.6	9.88	-23.0	5.96	4
2020	SLSC	A20	39.0	0.493	0.0412	0.0689	0.207	99.0	48.9	10.8	-22.7	5.29	NA	NA	NA	NA	0
2020	SLSC	A20	40.0	0.484	0.0645	0.0689	0.207	99.0	47.4	9.88	-24.8	5.82	NA	NA	NA	NA	0
2020	SLSC	A20	38.0	0.522	0.0854	0.0689	0.207	99.0	49.1	11.0	-23.2	5.64	NA	NA	NA	NA	0
2020	SLSC	A20	36.0	0.400	0.106	0.0689	0.207	99.0	45.3	10.8	-26.0	5.61	NA	NA	NA	NA	0
2020	SLSC	A20	43.0	0.630	0.112	0.0689	0.207	99.0	46.3	10.6	-23.9	5.63	NA	NA	NA	NA	1
2020	SLSC	A20	49.0	1.09	0.097	0.0689	0.207	97.0	47.5	10.2	-24.5	6.41	NA	NA	NA	NA	NA
2020	SLSC	A20	56.0	1.54	0.0789	0.0689	0.207	99.0	48.7	11.0	-23.4	6.58	NA	NA	NA	NA	3
2020	SLSC	A20	40.0	0.576	0.0664	0.0689	0.207	99.0	58.4	12.4	-23.4	5.37	NA	NA	NA	NA	0
2020	SLSC	A20	38.0	0.466	0.0474	0.0689	0.207	99.0	49.3	11.8	-24.5	7.23	50.4	12.3	-24.5	7.41	0
2020	SLSC	A20	34.0	0.447	0.128	0.0689	0.207	99.0	48.1	10.6	-24.5	5.02	NA	NA	NA	NA	0
2020	SLSC	A20	47.0	0.952	0.104	0.0689	0.207	99.0	51.7	12.6	-22.8	5.60	NA	NA	NA	NA	1
2020	SLSC	A20	38.0	0.430	0.0771	0.0689	0.207	99.0	43.7	10.4	-24.2	5.59	NA	NA	NA	NA	0
2020	NNST	A65	59.0	1.81	0.127	0.0825	0.248	101	42.1	8.07	-26.5	8.43	NA	NA	NA	NA	0
2020	NNST	A65	45.0	0.583	0.108	0.0825	0.248	101	42.0	8.04	-29.3	8.04	NA	NA	NA	NA	0
2020	NNST	A65	46.0	0.673	0.129	0.0825	0.248	101	44.3	9.13	-28.0	8.18	NA	NA	NA	NA	0
2020	NNST	A65	35.0	0.336	0.214	0.0727	0.218	103	53.7	11.9	-28.5	7.28	NA	NA	NA	NA	0
2020	NNST	A65	51.0	0.989	0.146	0.0825	0.248	101	52.0	9.70	-29.6	8.26	NA	NA	NA	NA	0
2020	NNST	A65	38.0	0.385	0.0796	0.0727	0.218	103	50.8	10.4	-26.8	7.45	NA	NA	NA	NA	0
2020	NNST	A65	39.0	0.478	0.0598	0.0825	0.248	101	44.3	8.69	-26.8	7.31	NA	NA	NA	NA	0
2020	NNST	A65	36.0	0.406	0.100	0.0825	0.248	101	49.7	10.6	-27.1	7.76	NA	NA	NA	NA	0
2020	NNST	A65	36.0	0.395	0.119	0.0727	0.218	103	52.9	10.4	-26.7	7.18	NA	NA	NA	NA	0
2020	NNST	A65	46.0	0.810	0.144	0.0727	0.218	103	53.3	9.81	-28.2	7.38	NA	NA	NA	NA	0
2020	NNST	A65	39.0	0.457	0.127	0.0825	0.248	101	51.1	8.84	-30.6	8.60	49.3	8.16	-31.0	8.36	0
2020	NNST	A65	33.0	0.264	0.253	0.0727	0.218	103	51.2	10.9	-29.5	7.96	NA	NA	NA	NA	0
2020	NNST	A65	41.0	0.504	0.315	0.0825	0.248	101	48.3	10.1	-30.3	8.82	NA	NA	NA	NA	0

Table A2.4: Laboratory Results for all Slimy Sculpin (Cottus cognatus; SLSC) and Ninespine Stickleback (Pungitius pungitius; NNST) laboratory results from Biotron Laboratory, the University of Waterloo Environmental Isotope Laboratory, and AAE Tech Incorporated. These results include total Hg concentrations with all sample quality assurance and quality control (QA/QC) in accordance with international standards. Stable isotopes from fish tissue are presented as percent (%) carbon (C) and nitrogren (N), as well as with per mil (‰) for delta values of each of these. Age estimates were made using extracted otoliths. mm = millimeters, g = grams, mg/kg = milligrams per killogram, THg = total mercury, MDL = method detection limit, MRL= method reporting limit , DUP = duplicate, C = carbon, N = nitrogren, NA = no available data.

Sample Year	Fish Species Code	Lake Name	Fork Length (mm)	Wet Weight (g)	THg WW (mg/kg)	MDL (ng)	MRL (ng)	IPR avg (%)	%C	%N	δ13C	δ15N	DUP %C	DUP %N	DUP δ13C	DUP δ15N	Age Estimate
2020	NNST	A65	42.0	0.520	0.108	0.0825	0.248	101	48.4	8.91	-29.8	7.44	NA	NA	NA	NA	0
2020	NNST	A65	45.0	0.582	0.179	0.0727	0.218	103	48.9	9.91	-28.8	7.46	NA	NA	NA	NA	0
2020	NNST	A65	38.0	0.440	0.245	0.0825	0.248	101	46.5	10.5	-29.2	7.82	NA	NA	NA	NA	0
2020	NNST	A65	43.0	0.569	0.292	0.0727	0.218	103	51.8	9.55	-30.5	8.40	NA	NA	NA	NA	NA
2020	NNST	A65	39.0	0.494	0.276	0.0825	0.248	101	47.9	10.1	-30.0	8.14	NA	NA	NA	NA	0
2020	NNST	A65	46.0	0.669	0.148	0.0825	0.248	101	48.9	8.68	-30.1	8.21	NA	NA	NA	NA	0
2020	NNST	A65	39.0	0.471	0.224	0.0825	0.248	101	53.3	11.0	-30.2	7.98	NA	NA	NA	NA	0
2020	NNST	A65	40.0	0.411	0.183	0.0825	0.248	101	41.0	7.25	-30.2	7.06	NA	NA	NA	NA	0
2020	NNST	A65	32.0	0.270	0.108	0.0825	0.248	101	56.2	11.2	-27.5	7.15	NA	NA	NA	NA	0
2020	NNST	A65	38.0	0.472	0.140	0.0825	0.248	101	56.9	9.15	-30.8	8.28	NA	NA	NA	NA	0
2020	NNST	A65	35.0	0.265	0.200	0.0825	0.248	101	49.8	10.2	-28.6	8.27	47.0	11.8	-27.3	8.46	0
2020	NNST	A65	30.0	0.224	0.232	0.0689	0.207	97.0	47.0	10.5	-28.3	8.13	NA	NA	NA	NA	0
2020	NNST	A65	40.0	0.404	0.175	0.0825	0.248	101	46.0	8.86	-28.7	7.96	NA	NA	NA	NA	0
2020	NNST	A65	38.0	0.366	0.133	0.0825	0.248	101	47.5	9.36	-29.2	7.46	NA	NA	NA	NA	0
2020	NNST	A65	36.0	0.295	0.0626	0.0825	0.248	101	48.2	9.79	-27.2	8.74	NA	NA	NA	NA	0
2020	NNST	A65	38.0	0.396	0.141	0.0825	0.248	101	47.5	10.2	-27.7	7.80	NA	NA	NA	NA	0
2020	NNST	A65	39.0	0.415	0.0923	0.0825	0.248	101	49.6	9.71	-28.6	8.26	NA	NA	NA	NA	0
2020	NNST	A65	42.0	0.452	0.150	0.0727	0.218	103	50.2	11.0	-26.1	7.47	NA	NA	NA	NA	0
2020	NNST	A65	41.0	0.405	0.142	0.0727	0.218	103	54.6	10.7	-28.8	8.06	52.2	10.1	-29.0	7.97	0
2020	NNST	A65	35.0	0.389	0.216	0.0825	0.248	101	42.8	9.62	-27.9	7.74	NA	NA	NA	NA	0
2020	NNST	A65	31.0	0.195	0.097	0.0727	0.218	103	49.5	11.5	-25.9	8.35	NA	NA	NA	NA	NA
2020	NNST	A65	32.0	0.270	0.0697	0.0825	0.248	101	44.0	10.3	-24.8	7.48	NA	NA	NA	NA	0
2020	SLSC	A65	23.0	0.150	0.0892	0.0689	0.207	97.0	41.7	9.17	-24.3	7.02	NA	NA	NA	NA	0
2020	SLSC	A65	27.0	0.236	0.110	0.0825	0.248	101	51.3	10.9	-27.4	7.63	NA	NA	NA	NA	0
2020	SLSC	A65	27.0	0.240	0.128	0.0825	0.248	101	52.5	10.5	-27.1	7.36	NA	NA	NA	NA	0
2020	SLSC	A65	26.0	0.199	0.0673	0.0689	0.207	97.0	45.1	10.2	-20.9	5.85	NA	NA	NA	NA	0
2020	SLSC	A65	26.0	0.205	0.095	0.0825	0.248	101	50.7	10.2	-24.0	5.96	45.2	8.45	-24.3	5.79	0
2020	SLSC	A65	26.0	0.193	0.109	0.0825	0.248	101	54.3	10.8	-25.8	5.99	NA	NA	NA	NA	0
2020	SLSC	A65	23.0	0.121	0.0878	0.0825	0.248	101	48.7	10.9	-24.4	5.89	NA	NA	NA	NA	0
2020	SLSC	A65	25.0	0.172	0.0886	0.0689	0.207	97.0	47.2	10.3	-23.3	5.83	NA	NA	NA	NA	0
2020	SLSC	A65	25.0	0.169	0.100	0.0825	0.248	101	46.2	9.63	-25.0	5.69	NA	NA	NA	NA	0

Table A2.4: Laboratory Results for all Slimy Sculpin (Cottus cognatus; SLSC) and Ninespine Stickleback (Pungitius pungitius; NNST) laboratory results from Biotron Laboratory, the University of Waterloo Environmental Isotope Laboratory, and AAE Tech Incorporated. These results include total Hg concentrations with all sample quality assurance and quality control (QA/QC) in accordance with international standards. Stable isotopes from fish tissue are presented as percent (%) carbon (C) and nitrogren (N), as well as with per mil (‰) for delta values of each of these. Age estimates were made using extracted otoliths. mm = millimeters, g = grams, mg/kg = milligrams per killogram, THg = total mercury, MDL = method detection limit, MRL= method reporting limit , DUP = duplicate, C = carbon, N = nitrogren, NA = no available data.

Sample Year	Fish Species Code	Lake Name	Fork Length (mm)	Wet Weight (g)	THg WW (mg/kg)	MDL (ng)	MRL (ng)	IPR avg (%)	%C	%N	δ13C	δ15N	DUP %C	DUP %N	DUP δ13C	DUP δ15N	Age Estimate
2020	SLSC	A65	42.0	0.884	0.128	0.0727	0.218	103	53.2	10.3	-26.1	6.44	NA	NA	NA	NA	0
2020	SLSC	A65	47.0	1.10	0.0852	0.0825	0.248	101	50.2	10.5	-23.6	5.85	NA	NA	NA	NA	1
2020	SLSC	A65	49.0	1.26	0.115	0.0825	0.248	101	49.0	9.46	-27.5	7.68	NA	NA	NA	NA	2
2020	SLSC	A65	44.0	0.801	0.132	0.0727	0.218	103	55.5	9.56	-28.3	6.07	NA	NA	NA	NA	0
2020	SLSC	A65	42.0	0.868	0.122	0.0727	0.218	103	57.3	10.5	-26.3	7.45	NA	NA	NA	NA	1
2020	SLSC	A65	26.0	0.208	0.0869	0.0825	0.248	101	49.4	10.8	-23.1	5.91	NA	NA	NA	NA	0
2020	SLSC	A65	45.0	1.03	0.127	0.0727	0.218	103	50.1	9.65	-27.6	7.30	NA	NA	NA	NA	1
2020	SLSC	A65	47.0	0.924	0.129	0.0825	0.248	101	49.4	10.2	-25.7	6.97	NA	NA	NA	NA	1
2020	SLSC	A65	47.0	0.985	0.108	0.0825	0.248	101	48.5	9.37	-27.7	6.81	NA	NA	NA	NA	1
2020	SLSC	A65	51.0	1.19	0.144	0.0689	0.207	97.0	46.8	8.23	-28.4	6.63	NA	NA	NA	NA	2
2020	SLSC	A65	54.0	1.67	0.108	0.0825	0.248	101	53.3	9.85	-27.6	6.29	NA	NA	NA	NA	1
2020	SLSC	A65	54.0	1.93	0.133	0.0689	0.207	97.0	44.0	7.89	-28.0	7.09	NA	NA	NA	NA	1
2020	SLSC	A65	61.0	2.41	0.129	0.0825	0.248	101	54.2	10.7	-27.8	7.15	53.1	10.5	-27.8	7.13	1
2020	SLSC	A65	57.0	2.13	0.114	0.0825	0.248	101	48.2	9.13	-27.4	6.91	NA	NA	NA	NA	1
2020	SLSC	A65	45.0	1.15	0.143	0.0825	0.248	101	50.2	9.67	-26.8	6.68	NA	NA	NA	NA	1
2020	SLSC	A65	70.0	2.76	0.117	0.0825	0.248	101	44.7	10.5	-24.7	7.50	NA	NA	NA	NA	3
2020	SLSC	A65	47.0	1.02	0.109	0.0825	0.248	101	51.8	10.2	-27.9	6.40	NA	NA	NA	NA	1
2020	SLSC	A65	48.0	0.992	0.139	0.0825	0.248	101	50.1	9.01	-28.2	6.15	NA	NA	NA	NA	1
2020	SLSC	A65	51.0	1.38	0.124	0.0825	0.248	101	59.2	10.9	-28.0	6.42	NA	NA	NA	NA	1
2020	SLSC	A65	66.0	2.90	0.101	0.0689	0.207	97.0	49.5	10.2	-25.5	8.57	NA	NA	NA	NA	NA
2020	SLSC	A65	64.0	2.35	0.110	0.0825	0.248	101	37.7	8.12	-25.1	7.46	NA	NA	NA	NA	2
2020	SLSC	A65	45.0	0.764	0.121	0.0727	0.218	103	50.5	10.4	-26.3	7.20	NA	NA	NA	NA	1
2020	SLSC	A65	62.0	2.24	0.104	0.0825	0.248	101	53.1	11.2	-26.2	6.92	NA	NA	NA	NA	1
2020	SLSC	A65	24.0	0.180	0.151	0.0689	0.207	97.0	49.1	10.5	-25.6	5.56	NA	NA	NA	NA	0
2020	SLSC	A65	60.0	2.16	0.115	0.0689	0.207	97.0	40.0	7.72	-27.7	7.03	51.8	10.8	-27.5	7.31	2
2020	SLSC	A65	62.0	2.14	0.108	0.0689	0.207	97.0	48.6	9.80	-25.5	7.89	NA	NA	NA	NA	2
2020	SLSC	A44	51.0	1.04	0.0398	0.0667	0.200	98.0	45.1	10.2	-20.1	7.36	NA	NA	NA	NA	2
2020	SLSC	A44	58.0	1.48	0.0429	0.0667	0.200	98.0	41.9	9.64	-21.2	7.72	NA	NA	NA	NA	2
2020	SLSC	A44	42.0	0.516	0.0249	0.0689	0.207	97.0	45.8	9.94	-20.9	6.08	NA	NA	NA	NA	2
2020	SLSC	A44	53.0	1.17	0.0410	0.0689	0.207	97.0	49.1	11.5	-21.6	7.69	NA	NA	NA	NA	1
2020	SLSC	A44	49.0	0.873	0.0353	0.0667	0.200	98.0	50.7	11.9	-20.1	7.65	NA	NA	NA	NA	1

Table A2.4: Laboratory Results for all Slimy Sculpin (Cottus cognatus; SLSC) and Ninespine Stickleback (Pungitius pungitius; NNST) laboratory results from Biotron Laboratory, the University of Waterloo Environmental Isotope Laboratory, and AAE Tech Incorporated. These results include total Hg concentrations with all sample quality assurance and quality control (QA/QC) in accordance with international standards. Stable isotopes from fish tissue are presented as percent (%) carbon (C) and nitrogren (N), as well as with per mil (‰) for delta values of each of these. Age estimates were made using extracted otoliths. mm = millimeters, g = grams, mg/kg = milligrams per killogram, THg = total mercury, MDL = method detection limit, MRL= method reporting limit , DUP = duplicate, C = carbon, N = nitrogren, NA = no available data.

Sample Year	Fish Species Code	Lake Name	Fork Length (mm)	Wet Weight (g)	THg WW (mg/kg)	MDL (ng)	MRL (ng)	IPR avg (%)	%C	%N	δ13C	δ15N	DUP %C	DUP %N	DUP δ13C	DUP δ15N	Age Estimate
2020	SLSC	A44	70.0	2.53	0.0792	0.0689	0.207	97.0	43.0	11.1	-20.8	8.87	NA	NA	NA	NA	4
2020	SLSC	A44	47.0	0.757	0.0384	0.0689	0.207	97.0	49.8	10.9	-20.0	8.01	NA	NA	NA	NA	1
2020	SLSC	A44	46.0	0.818	0.0326	0.0667	0.200	98.0	51.4	11.6	-21.0	7.15	NA	NA	NA	NA	1
2020	SLSC	A44	33.0	0.333	0.0340	0.0727	0.218	103	47.9	12.3	-19.1	6.58	NA	NA	NA	NA	0
2020	SLSC	A44	59.0	1.71	0.0444	0.0667	0.200	98.0	50.4	10.9	-20.8	7.48	NA	NA	NA	NA	2
2020	SLSC	A44	56.0	1.57	0.0363	0.0667	0.200	98.0	53.4	11.6	-20.8	6.36	NA	NA	NA	NA	3
2020	SLSC	A44	41.0	0.577	0.0336	0.0667	0.200	98.0	51.8	12.0	-20.7	6.88	45.4	8.70	-21.7	6.75	1
2020	SLSC	A44	42.0	0.559	0.0270	0.0667	0.200	98.0	49.8	10.5	-21.3	8.43	NA	NA	NA	NA	1
2020	SLSC	A44	62.0	2.01	0.0387	0.0667	0.200	98.0	48.8	10.8	-19.8	8.64	NA	NA	NA	NA	2
2020	SLSC	A44	61.0	1.72	0.0362	0.0667	0.200	98.0	42.8	9.79	-18.3	8.38	NA	NA	NA	NA	3
2020	SLSC	A44	62.0	2.00	0.0611	0.0689	0.207	97.0	45.1	11.0	-20.6	7.64	NA	NA	NA	NA	3
2020	SLSC	A44	57.0	1.63	0.0261	0.0667	0.200	98.0	43.4	9.92	-19.6	8.15	NA	NA	NA	NA	1
2020	SLSC	A44	36.0	0.375	0.0477	0.0727	0.218	103	52.2	11.8	-21.2	6.48	NA	NA	NA	NA	0
2020	SLSC	A44	66.0	2.01	0.0815	0.0689	0.207	97.0	44.9	11.3	-20.2	7.74	NA	NA	NA	NA	3
2020	SLSC	A44	58.0	1.51	0.0659	0.0689	0.207	97.0	52.8	11.9	-20.6	8.03	NA	NA	NA	NA	3
2020	SLSC	A44	45.0	0.683	0.0386	0.0667	0.200	98.0	50.3	10.7	-20.4	6.64	NA	NA	NA	NA	1
2020	SLSC	A44	40.0	0.488	0.0256	0.0667	0.200	98.0	51.3	12.2	-21.4	7.66	NA	NA	NA	NA	0
2020	SLSC	A44	40.0	0.516	0.0311	0.0689	0.207	97.0	43.4	10.3	-20.8	6.93	NA	NA	NA	NA	0
2020	SLSC	A44	32.0	0.448	0.0331	0.0727	0.218	103	49.2	11.4	-20.8	6.50	NA	NA	NA	NA	0
2020	SLSC	A44	50.0	0.980	0.0342	0.0689	0.207	97.0	45.7	9.67	-21.8	7.72	38.2	7.99	-21.8	7.80	1
2020	SLSC	A44	44.0	0.726	0.0308	0.0667	0.200	98.0	47.2	10.0	-21.2	6.94	NA	NA	NA	NA	1
2020	SLSC	A44	35.0	0.391	0.0355	0.0727	0.218	103	49.3	11.7	-21.0	7.01	54.0	12.7	-20.9	6.98	0
2020	SLSC	A44	42.0	0.617	0.0230	0.0667	0.200	98.0	34.4	5.53	-18.9	6.95	NA	NA	NA	NA	1
2020	SLSC	A44	45.0	0.773	0.0391	0.0667	0.200	98.0	46.3	10.1	-20.1	7.45	NA	NA	NA	NA	1
2020	SLSC	A44	49.0	0.924	0.0341	0.0667	0.200	98.0	56.2	10.9	-20.4	6.92	47.3	10.9	-19.6	7.19	1
2020	SLSC	A44	40.0	0.571	0.0264	0.0667	0.200	98.0	44.5	10.6	-21.0	6.57	NA	NA	NA	NA	1
2020	SLSC	A44	45.0	0.792	0.0417	0.0667	0.200	98.0	45.2	8.70	-22.1	7.30	NA	NA	NA	NA	1
2020	SLSC	A44	35.0	0.344	0.0382	0.0727	0.218	103	48.0	10.1	-20.5	5.95	NA	NA	NA	NA	0
2020	SLSC	A44	56.0	1.43	0.0473	0.0667	0.200	98.0	45.5	11.9	-22.3	6.35	NA	NA	NA	NA	2
2020	NNST	A44	59.0	1.33	0.0388	0.0689	0.207	97.0	49.2	7.87	-27.8	9.17	NA	NA	NA	NA	0
2020	NNST	A44	61.0	1.18	0.0395	0.0689	0.207	97.0	47.6	8.19	-29.6	9.58	NA	NA	NA	NA	0

Table A2.4: Laboratory Results for all Slimy Sculpin (Cottus cognatus; SLSC) and Ninespine Stickleback (Pungitius pungitius; NNST) laboratory results from Biotron Laboratory, the University of Waterloo Environmental Isotope Laboratory, and AAE Tech Incorporated. These results include total Hg concentrations with all sample quality assurance and quality control (QA/QC) in accordance with international standards. Stable isotopes from fish tissue are presented as percent (%) carbon (C) and nitrogren (N), as well as with per mil (‰) for delta values of each of these. Age estimates were made using extracted otoliths. mm = millimeters, g = grams, mg/kg = milligrams per killogram, THg = total mercury, MDL = method detection limit, MRL= method reporting limit , DUP = duplicate, C = carbon, N = nitrogren, NA = no available data.

Sample Year	Fish Species Code	Lake Name	Fork Length (mm)	Wet Weight (g)	THg WW (mg/kg)	MDL (ng)	MRL (ng)	IPR avg (%)	%C	%N	δ13C	δ15N	DUP %C	DUP %N	DUP δ13C	DUP δ15N	Age Estimate
2020	NNST	A44	45.0	0.522	0.0379	0.0727	0.218	103	49.7	10.9	-27.2	8.78	NA	NA	NA	NA	0
2020	SLSC	B03	34.0	0.343	0.0192	0.0727	0.218	103	50.5	11.4	-19.0	4.72	NA	NA	NA	NA	0
2020	SLSC	B03	41.0	0.547	0.0233	0.0667	0.200	98.0	50.4	12.5	-19.7	5.95	NA	NA	NA	NA	1
2020	SLSC	B03	37.0	0.418	0.0223	0.0727	0.218	103	47.4	11.9	-21.9	6.75	NA	NA	NA	NA	0
2020	SLSC	B03	39.0	0.510	0.0305	0.0667	0.200	98.0	41.0	9.16	-21.7	7.91	NA	NA	NA	NA	1
2020	SLSC	B03	41.0	0.636	0.0238	0.0667	0.200	98.0	46.7	11.3	-23.2	7.13	NA	NA	NA	NA	1
2020	SLSC	B03	39.0	0.455	0.0391	0.0727	0.218	103	49.3	10.6	-22.7	6.53	NA	NA	NA	NA	0
2020	SLSC	B03	37.0	0.381	0.0236	0.0667	0.200	98.0	51.3	13.7	-21.9	6.67	NA	NA	NA	NA	1
2020	SLSC	B03	51.0	1.08	0.0378	0.0667	0.200	98.0	45.8	10.0	-23.5	6.66	NA	NA	NA	NA	1
2020	SLSC	B03	56.0	1.47	0.0484	0.0667	0.200	98.0	40.4	7.32	-21.7	6.95	NA	NA	NA	NA	2
2020	SLSC	B03	36.0	0.481	0.0162	0.0667	0.200	98.0	57.7	14.5	-22.5	7.35	46.6	11.2	-22.7	7.26	0
2020	SLSC	B03	39.0	0.487	0.0353	0.0667	0.200	98.0	48.6	10.3	-23.6	6.26	NA	NA	NA	NA	1
2020	SLSC	B03	40.0	0.509	0.0183	0.0667	0.200	98.0	49.4	12.5	-21.6	6.64	NA	NA	NA	NA	1
2020	SLSC	B03	42.0	0.591	0.0261	0.0667	0.200	98.0	50.1	11.7	-21.6	6.30	NA	NA	NA	NA	1
2020	SLSC	B03	58.0	1.63	0.0556	0.0689	0.207	97.0	45.3	10.9	-20.8	7.31	NA	NA	NA	NA	3
2020	SLSC	B03	44.0	0.605	0.0164	0.0689	0.207	97.0	41.7	9.07	-22.8	7.82	NA	NA	NA	NA	1
2020	SLSC	B03	41.0	0.603	0.0111	0.0667	0.200	98.0	39.7	9.59	-22.6	6.99	NA	NA	NA	NA	1
2020	SLSC	B03	56.0	1.45	0.0404	0.0689	0.207	97.0	42.8	8.90	-23.7	7.10	NA	NA	NA	NA	3
2020	SLSC	B03	51.0	1.08	0.0225	0.0667	0.200	98.0	48.6	10.1	-22.3	7.27	NA	NA	NA	NA	1
2020	SLSC	B03	40.0	0.510	0.0169	0.0667	0.200	98.0	44.2	10.6	-23.5	7.72	NA	NA	NA	NA	1
2020	SLSC	B03	37.0	0.525	0.0319	0.0667	0.200	98.0	42.9	10.6	-23.4	6.46	NA	NA	NA	NA	1
2020	SLSC	B03	34.0	0.362	0.0187	0.0667	0.200	98.0	43.6	10.8	-19.0	5.62	NA	NA	NA	NA	0
2020	SLSC	B03	40.0	0.542	0.0318	0.0667	0.200	98.0	55.1	12.3	-24.2	6.45	NA	NA	NA	NA	0
2020	SLSC	B03	38.0	0.511	0.0217	0.0727	0.218	103	50.0	11.0	-20.2	5.73	NA	NA	NA	NA	0
2020	SLSC	B03	37.0	0.529	0.0460	0.0727	0.218	103	47.9	11.0	-20.2	5.53	NA	NA	NA	NA	0
2020	SLSC	B03	60.0	1.95	0.0385	0.0689	0.207	97.0	45.2	9.42	-21.6	6.95	NA	NA	NA	NA	3
2020	SLSC	B03	40.0	0.515	0.0195	0.0667	0.200	98.0	45.0	11.1	-24.8	7.28	49.9	12.7	-24.8	7.23	1
2020	SLSC	B03	40.0	0.515	0.0354	0.0667	0.200	98.0	45.4	10.4	-21.9	5.96	NA	NA	NA	NA	1
2020	SLSC	B03	50.0	1.01	0.0323	0.0689	0.207	97.0	44.1	10.1	-21.6	6.56	NA	NA	NA	NA	1
2020	SLSC	B03	40.0	0.479	0.0219	0.0667	0.200	98.0	54.9	13.3	-22.1	6.84	NA	NA	NA	NA	1
2020	SLSC	B03	39.0	0.503	0.0316	0.0667	0.200	98.0	50.2	11.4	-23.0	6.48	NA	NA	NA	NA	1

Table A2.4: Laboratory Results for all Slimy Sculpin (Cottus cognatus; SLSC) and Ninespine Stickleback (Pungitius pungitius; NNST) laboratory results from Biotron Laboratory, the University of Waterloo Environmental Isotope Laboratory, and AAE Tech Incorporated. These results include total Hg concentrations with all sample quality assurance and quality control (QA/QC) in accordance with international standards. Stable isotopes from fish tissue are presented as percent (%) carbon (C) and nitrogren (N), as well as with per mil (‰) for delta values of each of these. Age estimates were made using extracted otoliths. mm = millimeters, g = grams, mg/kg = milligrams per killogram, THg = total mercury, MDL = method detection limit, MRL= method reporting limit , DUP = duplicate, C = carbon, N = nitrogren, NA = no available data.

Sample Year	Fish Species Code	Lake Name	Fork Length (mm)	Wet Weight (g)	THg WW (mg/kg)	MDL (ng)	MRL (ng)	IPR avg (%)	%C	%N	δ13C	δ15N	DUP %C	DUP %N	DUP δ13C	DUP δ15N	Age Estimate
2020	SLSC	B03	41.0	0.526	0.0340	0.0689	0.207	97.0	47.2	11.7	-23.0	6.91	NA	NA	NA	NA	1
2020	SLSC	B03	39.0	0.468	0.0199	0.0667	0.200	98.0	52.6	11.9	-22.6	6.75	NA	NA	NA	NA	1
2020	SLSC	B03	41.0	0.578	0.0247	0.0667	0.200	98.0	44.0	8.06	-21.6	5.66	NA	NA	NA	NA	0
2020	SLSC	B03	87.0	6.62	0.0422	0.0689	0.207	97.0	43.6	8.72	-26.5	7.73	51.3	10.6	-26.3	7.37	4
2020	NNST	B03	45.0	0.595	0.0165	0.0727	0.218	103	49.6	10.7	-28.1	8.33	51.5	9.67	-28.9	8.53	0
2021	SLSC	A20	61.9	2.00	0.134	0.0825	0.248	101	53.3	9.90	-25.7	6.54	NA	NA	NA	NA	1
2021	SLSC	A20	45.2	0.700	0.099	0.0825	0.248	101	46.0	9.39	-22.8	7.19	NA	NA	NA	NA	1
2021	SLSC	A20	44.8	0.600	0.0801	0.0825	0.248	101	43.5	9.35	-21.8	6.22	NA	NA	NA	NA	1
2021	SLSC	A20	33.8	0.300	0.133	0.0825	0.248	101	49.5	10.2	-23.9	7.04	NA	NA	NA	NA	0
2021	SLSC	A20	33.2	0.200	0.110	0.0825	0.248	101	47.6	10.5	-23.1	6.93	NA	NA	NA	NA	0
2021	NNST	A20	67.1	2.60	0.180	0.0825	0.248	101	54.0	9.27	-27.8	8.77	NA	NA	NA	NA	0
2021	NNST	A20	61.3	1.40	0.416	0.0825	0.248	101	40.8	8.83	-27.0	9.34	NA	NA	NA	NA	0
2021	NNST	A20	52.8	0.900	0.210	0.0825	0.248	101	53.5	10.2	-27.4	8.77	55.4	10.8	-27.2	8.69	0
2021	NNST	A20	59.1	1.10	0.130	0.0825	0.248	101	51.0	10.2	-27.2	8.84	NA	NA	NA	NA	0
2021	NNST	A20	45.5	0.400	0.171	0.0825	0.248	101	50.3	10.2	-28.1	9.02	NA	NA	NA	NA	0
2021	NNST	A20	65.2	2.00	0.218	0.0825	0.248	101	49.6	10.8	-27.2	9.26	NA	NA	NA	NA	1
2021	NNST	A20	55.1	1.20	0.223	0.0825	0.248	101	50.2	11.0	-26.9	8.87	NA	NA	NA	NA	0
2021	NNST	A20	55.9	1.00	0.136	0.0825	0.248	101	48.8	8.78	-27.5	8.69	NA	NA	NA	NA	0
2021	NNST	A20	52.3	1.10	0.182	0.0825	0.248	101	52.2	10.6	-27.6	9.10	NA	NA	NA	NA	0
2021	NNST	A20	53.3	1.00	0.129	0.0825	0.248	101	43.1	8.18	-26.3	8.55	NA	NA	NA	NA	0
2021	NNST	A20	45.4	0.500	0.162	0.0825	0.248	101	51.8	10.5	-26.6	8.80	NA	NA	NA	NA	0
2021	NNST	A20	62.6	1.20	0.298	0.0825	0.248	101	50.2	9.01	-26.9	9.19	NA	NA	NA	NA	0
2021	NNST	A20	55.1	1.00	0.432	0.0825	0.248	101	46.1	9.82	-27.0	8.88	48.6	9.30	-27.3	8.72	0
2021	NNST	A20	55.4	1.00	0.144	0.0825	0.248	101	53.2	10.0	-27.6	9.39	NA	NA	NA	NA	0
2021	NNST	A20	65.2	1.40	0.172	0.0825	0.248	101	36.0	7.04	-27.0	8.43	NA	NA	NA	NA	0
2021	NNST	A20	60.7	1.20	0.221	0.0825	0.248	101	54.7	10.5	-27.0	8.61	NA	NA	NA	NA	0
2021	NNST	A20	61.0	1.30	0.162	0.0825	0.248	101	50.6	10.1	-26.4	9.44	NA	NA	NA	NA	0
2021	NNST	A20	52.3	0.900	0.211	0.0825	0.248	101	37.1	6.23	-27.4	8.24	NA	NA	NA	NA	0
2021	NNST	A20	51.2	0.900	0.180	0.0825	0.248	101	52.2	9.49	-27.7	7.92	NA	NA	NA	NA	0
2021	SLSC	A20	49.1	0.900	0.0812	0.0825	0.248	101	50.8	9.76	-23.3	6.04	NA	NA	NA	NA	1
2021	SLSC	A65	71.0	3.30	0.120	0.0825	0.248	101	53.1	11.2	-24.3	7.32	NA	NA	NA	NA	3

Table A2.4: Laboratory Results for all Slimy Sculpin (Cottus cognatus; SLSC) and Ninespine Stickleback (Pungitius pungitius; NNST) laboratory results from Biotron Laboratory, the University of Waterloo Environmental Isotope Laboratory, and AAE Tech Incorporated. These results include total Hg concentrations with all sample quality assurance and quality control (QA/QC) in accordance with international standards. Stable isotopes from fish tissue are presented as percent (%) carbon (C) and nitrogren (N), as well as with per mil (‰) for delta values of each of these. Age estimates were made using extracted otoliths. mm = millimeters, g = grams, mg/kg = milligrams per killogram, THg = total mercury, MDL = method detection limit, MRL= method reporting limit , DUP = duplicate, C = carbon, N = nitrogren, NA = no available data.

Sample Year	Fish Species Code	Lake Name	Fork Length (mm)	Wet Weight (g)	THg WW (mg/kg)	MDL (ng)	MRL (ng)	IPR avg (%)	%C	%N	δ13C	δ15N	DUP %C	DUP %N	DUP δ13C	DUP δ15N	Age Estimate
2021	SLSC	A65	44.9	0.600	0.099	0.0825	0.248	101	54.6	10.8	-26.5	8.48	NA	NA	NA	NA	0
2021	SLSC	A65	62.8	1.80	0.162	0.0825	0.248	101	49.7	8.96	-24.1	7.47	52.4	11.0	-23.7	7.87	2
2021	SLSC	A65	77.3	3.80	0.286	0.0825	0.248	101	45.4	11.0	-24.8	8.12	NA	NA	NA	NA	3
2021	SLSC	A65	74.0	3.60	0.199	0.0825	0.248	101	49.5	9.39	-25.6	7.47	NA	NA	NA	NA	2
2021	SLSC	A65	82.1	4.20	0.106	0.0825	0.248	101	43.1	11.3	-20.7	8.06	NA	NA	NA	NA	3
2021	SLSC	A65	44.9	0.700	0.172	0.0825	0.248	101	51.0	11.0	-26.4	7.60	NA	NA	NA	NA	0
2021	SLSC	A65	40.0	0.600	0.216	0.0825	0.248	101	45.6	8.99	-27.4	7.15	NA	NA	NA	NA	0
2021	SLSC	A65	61.0	1.60	0.105	0.0825	0.248	101	45.0	9.40	-23.5	7.65	NA	NA	NA	NA	1
2021	SLSC	A65	47.1	0.700	0.183	0.0825	0.248	101	47.1	8.13	-27.5	8.10	NA	NA	NA	NA	0
2021	SLSC	A65	53.1	1.10	0.123	0.0825	0.248	101	56.9	12.1	-25.9	6.73	NA	NA	NA	NA	1
2021	SLSC	A65	42.1	0.600	0.120	0.0825	0.248	101	46.0	9.75	-26.1	7.71	NA	NA	NA	NA	0
2021	NNST	A65	59.4	1.20	0.180	0.0825	0.248	101	42.7	7.40	-27.2	8.91	NA	NA	NA	NA	0
2021	NNST	A65	60.1	1.20	0.283	0.0689	0.207	95.0	49.3	9.34	-27.5	9.03	53.3	8.81	-28.0	9.24	0
2021	NNST	A65	NA	NA	0.513	0.0825	0.248	101	43.7	9.92	-28.8	10.2	NA	NA	NA	NA	0
2021	SLSC	A44	37.0	0.300	0.0399	0.0825	0.248	101	51.0	11.4	-22.6	7.11	NA	NA	NA	NA	0
2021	SLSC	A44	62.9	1.80	0.0499	0.0825	0.248	101	54.0	11.3	-20.5	6.15	NA	NA	NA	NA	0
2021	SLSC	A44	65.1	1.90	0.0777	0.0825	0.248	101	46.1	9.59	-20.8	7.01	NA	NA	NA	NA	0
2021	SLSC	A44	60.1	1.60	0.0469	0.0825	0.248	101	49.8	10.1	-21.2	6.65	NA	NA	NA	NA	2
2021	SLSC	A44	33.0	0.200	0.0406	0.0825	0.248	101	48.7	10.6	-21.9	7.26	NA	NA	NA	NA	0
2021	SLSC	WTL	81.0	5.00	0.403	0.0825	0.248	101	59.7	11.4	-27.3	7.69	NA	NA	NA	NA	3
2021	SLSC	WTL	89.9	6.80	0.342	0.0825	0.248	101	52.9	11.0	-28.0	8.59	NA	NA	NA	NA	3
2021	SLSC	WTL	65.0	2.30	0.422	0.0689	0.207	95.0	54.4	11.0	-29.3	7.41	NA	NA	NA	NA	3
2021	SLSC	WTL	81.1	3.30	0.419	0.0825	0.248	101	47.5	12.7	-23.7	8.26	NA	NA	NA	NA	3
2021	SLSC	WTL	59.5	1.60	0.320	0.0825	0.248	101	32.6	7.41	-27.7	8.32	NA	NA	NA	NA	2
2021	SLSC	WTL	88.2	4.60	0.401	0.0825	0.248	101	50.0	13.1	-24.3	8.06	45.1	11.4	-24.6	8.47	3
2021	SLSC	WTL	62.7	1.70	0.367	0.0825	0.248	101	53.2	10.9	-30.0	7.39	54.8	9.55	-31.2	7.38	1
2021	SLSC	WTL	66.1	2.30	0.296	0.0825	0.248	101	59.3	10.5	-29.0	7.48	NA	NA	NA	NA	2
2021	SLSC	WTL	59.3	1.80	0.276	0.0825	0.248	101	49.8	10.6	-26.8	8.28	50.4	12.1	-26.4	8.33	2
2021	SLSC	WTL	60.2	1.70	0.338	0.0825	0.248	101	44.5	8.59	-29.2	7.46	NA	NA	NA	NA	1
2021	SLSC	WTL	51.6	1.00	0.478	0.0825	0.248	101	45.2	9.26	-28.0	8.58	NA	NA	NA	NA	1
2021	SLSC	WTL	38.7	0.400	0.377	0.0825	0.248	101	45.1	8.49	-30.2	7.40	NA	NA	NA	NA	0

Table A2.4: Laboratory Results for all Slimy Sculpin (Cottus cognatus; SLSC) and Ninespine Stickleback (Pungitius pungitius; NNST) laboratory results from Biotron Laboratory, the University of Waterloo Environmental Isotope Laboratory, and AAE Tech Incorporated. These results include total Hg concentrations with all sample quality assurance and quality control (QA/QC) in accordance with international standards. Stable isotopes from fish tissue are presented as percent (%) carbon (C) and nitrogren (N), as well as with per mil (‰) for delta values of each of these. Age estimates were made using extracted otoliths. mm = millimeters, g = grams, mg/kg = milligrams per killogram, THg = total mercury, MDL = method detection limit, MRL= method reporting limit , DUP = duplicate, C = carbon, N = nitrogren, NA = no available data.

Sample Year	Fish Species Code	Lake Name	Fork Length (mm)	Wet Weight (g)	THg WW (mg/kg)	MDL (ng)	MRL (ng)	IPR avg (%)	%C	%N	δ13C	δ15N	DUP %C	DUP %N	DUP δ13C	DUP δ15N	Age Estimate
2021	SLSC	WTL	40.8	0.600	0.353	0.0825	0.248	101	41.2	7.65	-31.0	6.92	NA	NA	NA	NA	1
2021	SLSC	WTL	46.8	0.700	0.354	0.0825	0.248	101	51.6	9.87	-29.3	7.97	NA	NA	NA	NA	1
2021	SLSC	WTL	110	14.2	0.164	0.0825	0.248	101	45.3	9.04	-22.3	8.58	NA	NA	NA	NA	5
2021	NNST	WTL	55.1	0.900	0.433	0.0825	0.248	101	40.2	8.78	-27.1	10.9	NA	NA	NA	NA	0
2021	NNST	WTL	54.8	1.20	0.463	0.0825	0.248	101	44.5	8.99	-29.1	10.8	42.2	7.50	-29.6	10.3	0
2021	NNST	WTL	57.5	1.00	0.311	0.0825	0.248	101	46.5	9.15	-28.1	9.94	NA	NA	NA	NA	0
2021	NNST	WTL	57.2	0.800	0.274	0.0825	0.248	101	41.9	9.52	-26.4	10.3	NA	NA	NA	NA	0
2021	NNST	WTL	55.1	1.00	0.434	0.0825	0.248	101	44.7	10.3	-26.8	9.69	NA	NA	NA	NA	0
2021	SLSC	B03	70.9	2.70	0.0446	0.0825	0.248	101	51.1	11.3	-22.9	7.63	NA	NA	NA	NA	2
2021	SLSC	B03	50.5	0.900	0.0309	0.0825	0.248	101	52.9	10.9	-21.2	5.98	NA	NA	NA	NA	1
2021	SLSC	B03	55.7	1.20	0.0277	0.0825	0.248	101	58.7	12.4	-21.3	6.10	NA	NA	NA	NA	1
2021	SLSC	B03	50.5	0.800	0.0221	0.0825	0.248	101	51.9	10.6	-21.4	5.53	NA	NA	NA	NA	1
2021	SLSC	B03	50.7	1.00	0.0377	0.0825	0.248	101	55.8	12.0	-21.7	6.05	NA	NA	NA	NA	0
2021	SLSC	B03	54.2	1.10	0.0245	0.0825	0.248	101	46.5	9.38	-24.4	7.83	NA	NA	NA	NA	1
2021	SLSC	B03	34.3	0.200	0.0235	0.0825	0.248	101	42.2	9.78	-22.4	6.91	43.8	11.1	-22.2	7.41	0
2021	NNST	B03	56.1	1.00	0.0319	0.0825	0.248	101	49.6	9.97	-26.4	8.76	NA	NA	NA	NA	0
2021	NNST	B03	52.8	0.800	0.0258	0.0825	0.248	101	46.3	10.6	-26.0	8.49	NA	NA	NA	NA	0
2021	SLSC	LK8	59.0	1.40	0.0452	0.0825	0.248	101	44.7	8.20	-25.4	6.67	NA	NA	NA	NA	2
2021	SLSC	LK8	68.9	3.00	0.0380	0.0825	0.248	101	48.9	10.3	-22.9	6.70	NA	NA	NA	NA	3
2021	SLSC	LK8	52.2	1.00	0.0294	0.0825	0.248	101	43.8	9.39	-22.5	7.28	NA	NA	NA	NA	2
2021	SLSC	LK8	63.7	1.90	0.0416	0.0825	0.248	101	51.2	10.7	-24.5	7.41	NA	NA	NA	NA	1
2021	SLSC	LK8	82.0	4.60	0.0577	0.0825	0.248	101	52.6	11.0	-23.7	7.49	NA	NA	NA	NA	5
2021	SLSC	LK8	62.3	1.90	0.0907	0.0825	0.248	101	37.6	8.11	-28.6	8.04	NA	NA	NA	NA	2
2021	SLSC	LK8	58.7	1.40	0.0296	0.0825	0.248	101	42.1	10.6	-19.8	7.72	NA	NA	NA	NA	1
2021	SLSC	LK8	72.2	4.10	0.0442	0.0825	0.248	101	40.7	7.82	-21.3	7.28	54.5	11.0	-21.1	7.19	4
2021	SLSC	LK8	61.9	1.90	0.0412	0.0825	0.248	101	54.7	9.82	-23.9	7.74	NA	NA	NA	NA	1
2021	SLSC	LK8	57.2	1.50	0.0212	0.0825	0.248	101	47.7	11.4	-22.5	6.89	NA	NA	NA	NA	2
2021	SLSC	A63	81.0	4.00	0.484	0.0825	0.248	101	41.7	9.69	-25.3	7.63	NA	NA	NA	NA	3
2021	SLSC	A63	81.0	4.20	0.361	0.0825	0.248	101	53.1	10.9	-25.7	8.27	NA	NA	NA	NA	3
2021	SLSC	A63	39.0	0.400	0.378	0.0825	0.248	101	52.9	11.2	-28.9	8.10	NA	NA	NA	NA	0
2021	SLSC	A63	40.2	0.500	0.328	0.0825	0.248	101	45.6	9.63	-27.6	8.05	NA	NA	NA	NA	0

Table A2.4: Laboratory Results for all Slimy Sculpin (Cottus cognatus; SLSC) and Ninespine Stickleback (Pungitius pungitius; NNST) laboratory results from Biotron Laboratory, the University of Waterloo Environmental Isotope Laboratory, and AAE Tech Incorporated. These results include total Hg concentrations with all sample quality assurance and quality control (QA/QC) in accordance with international standards. Stable isotopes from fish tissue are presented as percent (%) carbon (C) and nitrogren (N), as well as with per mil (‰) for delta values of each of these. Age estimates were made using extracted otoliths. mm = millimeters, g = grams, mg/kg = milligrams per killogram, THg = total mercury, MDL = method detection limit, MRL= method reporting limit , DUP = duplicate, C = carbon, N = nitrogren, NA = no available data.

Sample Year	Fish Species Code	Lake Name	Fork Length (mm)	Wet Weight (g)	THg WW (mg/kg)	MDL (ng)	MRL (ng)	IPR avg (%)	%C	%N	δ13C	δ15N	DUP %C	DUP %N	DUP δ13C	DUP δ15N	Age Estimate
2021	SLSC	A63	47.2	0.800	0.336	0.0825	0.248	101	50.8	10.5	-28.0	7.45	NA	NA	NA	NA	0
2021	SLSC	A63	49.9	1.00	0.396	0.0825	0.248	101	34.7	7.89	-28.2	8.04	NA	NA	NA	NA	1
2021	SLSC	A63	40.9	0.600	0.380	0.0825	0.248	101	41.7	8.14	-28.1	7.66	NA	NA	NA	NA	0
2021	SLSC	A63	44.3	0.600	0.267	0.0825	0.248	101	43.1	8.49	-27.1	8.60	NA	NA	NA	NA	0
2021	SLSC	A63	47.2	0.700	0.402	0.0825	0.248	101	52.1	10.9	-29.5	8.32	NA	NA	NA	NA	0
2021	SLSC	A63	40.8	0.600	0.412	0.0825	0.248	101	48.1	9.46	-28.4	8.30	NA	NA	NA	NA	0
2021	SLSC	A63	75.1	3.50	0.394	0.0825	0.248	101	54.2	8.93	-27.3	6.54	NA	NA	NA	NA	2
2021	SLSC	A63	49.1	0.800	0.404	0.0825	0.248	101	46.5	9.20	-28.9	7.71	NA	NA	NA	NA	0
2021	SLSC	A63	43.1	0.500	0.287	0.0825	0.248	101	46.0	9.10	-24.2	7.64	NA	NA	NA	NA	0
2021	SLSC	A63	45.3	0.600	0.344	0.0825	0.248	101	51.2	10.2	-29.3	7.61	NA	NA	NA	NA	0
2021	SLSC	A63	44.4	0.600	0.485	0.0825	0.248	101	47.6	7.99	-30.6	7.78	NA	NA	NA	NA	0
2021	SLSC	A63	43.0	0.700	0.279	0.0825	0.248	101	37.6	5.70	-28.0	7.25	55.0	10.8	-27.0	7.48	0
2021	SLSC	A63	52.9	1.10	0.394	0.0825	0.248	101	49.7	8.96	-29.7	7.81	NA	NA	NA	NA	0
2021	SLSC	A63	48.2	0.800	0.348	0.0825	0.248	101	51.5	8.00	-30.3	8.15	NA	NA	NA	NA	0
2021	SLSC	A63	45.2	0.700	0.316	0.0825	0.248	101	46.7	7.00	-30.1	7.83	NA	NA	NA	NA	0
2021	SLSC	A63	41.2	0.500	0.312	0.0825	0.248	101	50.7	11.4	-28.2	7.73	NA	NA	NA	NA	0
2021	SLSC	A63	45.1	0.700	0.324	0.0825	0.248	101	49.2	10.6	-27.9	7.99	NA	NA	NA	NA	0
2021	SLSC	A63	43.0	0.500	0.358	0.0825	0.248	101	41.6	8.68	-29.0	8.11	NA	NA	NA	NA	0
2021	SLSC	A63	43.6	0.700	0.411	0.0825	0.248	101	46.5	8.79	-28.3	7.55	NA	NA	NA	NA	0
2021	SLSC	A63	44.2	0.700	0.334	0.0825	0.248	101	58.7	10.3	-30.3	7.94	NA	NA	NA	NA	0
2021	SLSC	A63	46.0	0.700	0.207	0.0825	0.248	101	49.0	9.86	-27.4	9.27	NA	NA	NA	NA	0
2021	SLSC	A63	44.9	0.600	0.256	0.0825	0.248	101	42.0	7.89	-27.8	8.50	48.3	9.72	-27.4	8.89	0
2021	SLSC	A63	51.8	1.00	0.345	0.0825	0.248	101	44.5	9.78	-27.6	7.70	NA	NA	NA	NA	0
2021	SLSC	A63	47.2	0.800	0.316	0.0825	0.248	101	47.7	10.3	-27.3	8.25	NA	NA	NA	NA	0
2021	SLSC	A63	48.2	0.700	0.283	0.0825	0.248	101	49.2	10.4	-26.7	7.72	NA	NA	NA	NA	0
2021	NNST	A63	53.4	0.800	0.485	0.0825	0.248	101	37.2	6.77	-30.0	9.93	NA	NA	NA	NA	0
2021	NNST	A63	57.3	1.20	0.408	0.0825	0.248	101	44.6	8.25	-29.5	9.27	NA	NA	NA	NA	0
2021	NNST	A63	58.1	1.20	0.259	0.0825	0.248	101	43.0	7.57	-29.3	9.76	NA	NA	NA	NA	1
2021	NNST	A63	60.2	1.10	0.470	0.0825	0.248	101	52.3	8.58	-29.0	9.00	NA	NA	NA	NA	0
2021	NNST	A63	54.0	0.900	0.283	0.0825	0.248	101	38.8	7.57	-30.0	9.89	NA	NA	NA	NA	0
2021	NNST	A63	57.1	1.10	0.346	0.0825	0.248	101	52.3	9.39	-30.1	8.82	NA	NA	NA	NA	0

Table A2.4: Laboratory Results for all Slimy Sculpin (Cottus cognatus; SLSC) and Ninespine Stickleback (Pungitius pungitius; NNST) laboratory results from Biotron Laboratory, the University of Waterloo Environmental Isotope Laboratory, and AAE Tech Incorporated. These results include total Hg concentrations with all sample quality assurance and quality control (QA/QC) in accordance with international standards. Stable isotopes from fish tissue are presented as percent (%) carbon (C) and nitrogren (N), as well as with per mil (‰) for delta values of each of these. Age estimates were made using extracted otoliths. mm = millimeters, g = grams, mg/kg = milligrams per killogram, THg = total mercury, MDL = method detection limit, MRL= method reporting limit , DUP = duplicate, C = carbon, N = nitrogren, NA = no available data.

Sample Year	Fish Species Code	Lake Name	Fork Length (mm)	Wet Weight (g)	THg WW (mg/kg)	MDL (ng)	MRL (ng)	IPR avg (%)	%C	%N	δ13C	δ15N	DUP %C	DUP %N	DUP δ13C	DUP δ15N	Age Estimate
2021	NNST	A63	50.0	0.800	0.586	0.0825	0.248	101	36.3	7.06	-29.4	10.1	52.4	10.3	-29.5	9.48	0
2021	NNST	A63	57.1	1.10	0.597	0.0825	0.248	101	42.5	7.38	-29.2	9.19	NA	NA	NA	NA	0
2021	NNST	A63	70.5	1.90	0.684	0.0825	0.248	101	45.6	10.4	-27.4	9.21	NA	NA	NA	NA	0
2021	NNST	A63	72.9	2.00	0.634	0.0825	0.248	101	46.4	9.83	-27.7	9.40	NA	NA	NA	NA	0
2021	NNST	A63	57.9	1.10	0.433	0.0825	0.248	101	48.6	9.56	-29.2	9.99	NA	NA	NA	NA	NA
2021	NNST	A63	73.2	1.90	0.416	0.0825	0.248	101	55.2	12.3	-26.8	9.34	NA	NA	NA	NA	0
2021	NNST	A63	51.1	0.800	0.400	0.0825	0.248	101	54.0	9.69	-29.3	9.59	NA	NA	NA	NA	0
2021	NNST	A63	55.3	0.900	0.338	0.0825	0.248	101	41.9	6.03	-31.5	9.30	NA	NA	NA	NA	0
2021	NNST	A63	58.4	1.30	0.346	0.0825	0.248	101	41.4	7.91	-29.7	8.81	NA	NA	NA	NA	0
2021	NNST	A63	51.1	0.800	0.347	0.0825	0.248	101	55.0	10.6	-29.0	10.0	NA	NA	NA	NA	0
2021	SLSC	WTL	68.3	3.30	0.303	0.0825	0.248	101	55.0	11.9	-27.7	7.83	47.9	9.17	-28.4	7.72	2
2021	SLSC	WTL	73.3	3.20	0.490	0.0825	0.248	101	44.2	11.9	-25.2	7.90	NA	NA	NA	NA	2
2021	SLSC	WTL	74.5	2.80	0.655	0.0825	0.248	101	53.2	14.2	-24.9	8.06	NA	NA	NA	NA	2
2021	SLSC	WTL	79.9	3.90	0.468	0.0825	0.248	101	45.7	12.0	-25.3	7.99	NA	NA	NA	NA	2
2021	SLSC	WTL	63.0	2.90	0.285	0.0825	0.248	101	54.7	11.2	-28.3	6.91	NA	NA	NA	NA	1
2021	SLSC	WTL	83.0	3.80	0.390	0.0825	0.248	101	45.0	10.9	-27.9	8.07	NA	NA	NA	NA	2
2021	SLSC	WTL	68.2	2.70	0.295	0.0825	0.248	101	46.3	10.0	-28.7	6.93	NA	NA	NA	NA	1
2021	SLSC	WTL	39.3	0.500	0.273	0.0825	0.248	101	49.9	9.61	-30.1	5.50	NA	NA	NA	NA	0
2021	SLSC	WTL	64.1	2.00	0.350	0.0825	0.248	101	52.7	11.1	-29.0	6.72	NA	NA	NA	NA	1
2021	SLSC	WTL	70.2	3.00	0.294	0.0825	0.248	101	52.9	11.4	-28.2	6.02	NA	NA	NA	NA	2
2021	SLSC	WTL	69.3	3.30	0.300	0.0825	0.248	101	54.5	11.8	-27.8	8.05	47.0	10.1	-27.8	8.22	2
2021	SLSC	WTL	62.5	2.10	0.296	0.0825	0.248	101	58.4	10.5	-29.4	5.68	NA	NA	NA	NA	1
2021	SLSC	WTL	47.2	0.900	0.301	0.0825	0.248	101	51.6	10.5	-28.8	7.41	NA	NA	NA	NA	0
2021	SLSC	WTL	45.1	0.700	0.272	0.0825	0.248	101	49.3	10.7	-29.5	7.02	NA	NA	NA	NA	0
2021	SLSC	WTL	63.9	1.90	0.390	0.0825	0.248	101	54.5	10.2	-29.3	7.81	NA	NA	NA	NA	1
2021	SLSC	WTL	42.1	0.600	0.334	0.0825	0.248	101	48.4	10.2	-29.9	5.96	NA	NA	NA	NA	0
2021	SLSC	WTL	49.8	1.00	0.258	0.0825	0.248	101	41.7	8.38	-29.7	7.58	NA	NA	NA	NA	0
2021	NNST	WTL	53.0	1.00	0.500	0.0825	0.248	101	34.8	6.84	-29.7	9.67	NA	NA	NA	NA	0
2021	NNST	WTL	57.2	1.30	0.357	0.0825	0.248	101	44.2	9.59	-28.5	9.50	NA	NA	NA	NA	1
2021	NNST	WTL	53.1	0.800	0.210	0.0825	0.248	101	49.0	8.75	-26.3	9.00	NA	NA	NA	NA	0
2021	NNST	WTL	62.4	1.40	0.386	0.0825	0.248	101	49.6	9.63	-30.7	9.99	51.7	10.5	-30.5	9.68	0

Table A2.4: Laboratory Results for all Slimy Sculpin (Cottus cognatus; SLSC) and Ninespine Stickleback (Pungitius pungitius; NNST) laboratory results from Biotron Laboratory, the University of Waterloo Environmental Isotope Laboratory, and AAE Tech Incorporated. These results include total Hg concentrations with all sample quality assurance and quality control (QA/QC) in accordance with international standards. Stable isotopes from fish tissue are presented as percent (%) carbon (C) and nitrogren (N), as well as with per mil (‰) for delta values of each of these. Age estimates were made using extracted otoliths. mm = millimeters, g = grams, mg/kg = milligrams per killogram, THg = total mercury, MDL = method detection limit, MRL= method reporting limit , DUP = duplicate, C = carbon, N = nitrogren, NA = no available data.

Sample Year	Fish Species Code	Lake Name	Fork Length (mm)	Wet Weight (g)	THg WW (mg/kg)	MDL (ng)	MRL (ng)	IPR avg (%)	%C	%N	δ13C	δ15N	DUP %C	DUP %N	DUP δ13C	DUP δ15N	Age Estimate
2021	NNST	WTL	43.9	0.700	0.317	0.0825	0.248	101	45.2	8.76	-27.2	9.05	NA	NA	NA	NA	0
2021	NNST	WTL	60.2	1.30	0.239	0.0825	0.248	101	42.4	7.95	-26.1	9.38	NA	NA	NA	NA	0
2021	NNST	WTL	51.8	1.00	0.247	0.0825	0.248	101	55.8	10.8	-25.6	8.93	NA	NA	NA	NA	0
2021	NNST	WTL	56.0	0.900	0.330	0.0689	0.207	95.0	52.8	10.8	-27.5	8.63	NA	NA	NA	NA	0
2021	NNST	WTL	57.5	1.20	0.567	0.0825	0.248	101	49.6	10.7	-30.2	10.2	NA	NA	NA	NA	0
2021	NNST	WTL	74.5	2.50	0.800	0.0825	0.248	101	49.2	10.8	-28.6	9.65	NA	NA	NA	NA	0
2021	NNST	MMT	45.1	0.500	0.0912	0.0825	0.248	101	44.2	8.65	-24.6	9.74	NA	NA	NA	NA	0
2021	NNST	MMT	64.0	1.40	0.0345	0.0825	0.248	101	69.6	13.2	-25.1	10.4	NA	NA	NA	NA	0
2021	NNST	MMT	59.8	1.20	0.0518	0.0825	0.248	101	51.8	9.60	-25.6	9.50	NA	NA	NA	NA	0
2021	NNST	MMT	54.9	0.800	0.0305	0.0825	0.248	101	47.5	8.18	-26.5	10.8	63.3	13.0	-26.0	10.6	0
2021	NNST	MMT	54.2	0.900	0.0353	0.0825	0.248	101	44.7	6.64	-26.8	10.1	NA	NA	NA	NA	0
2021	NNST	MMT	51.6	0.800	0.0400	0.0825	0.248	101	47.3	8.58	-25.2	10.3	NA	NA	NA	NA	0
2021	NNST	MMT	65.3	1.60	0.0568	0.0825	0.248	101	39.0	7.43	-25.1	10.0	NA	NA	NA	NA	0
2021	NNST	MMT	52.8	0.900	0.0373	0.0825	0.248	101	46.5	9.36	-24.7	10.5	NA	NA	NA	NA	0
2021	NNST	MMT	52.1	0.800	0.0344	0.0825	0.248	101	48.3	9.49	-26.0	10.2	NA	NA	NA	NA	0
2021	NNST	MMT	56.3	1.00	0.0622	0.0825	0.248	101	52.3	11.6	-25.5	10.3	NA	NA	NA	NA	0
2021	NNST	MMT	52.1	0.800	0.0296	0.0825	0.248	101	59.2	10.6	-25.5	10.7	NA	NA	NA	NA	0
2021	NNST	MMT	45.2	0.600	0.0371	0.0825	0.248	101	49.7	10.9	-25.2	10.8	NA	NA	NA	NA	0
2021	NNST	MMT	61.9	1.30	0.0301	0.0825	0.248	101	48.2	9.56	-25.2	10.0	NA	NA	NA	NA	0
2021	NNST	MMT	58.1	1.20	0.0518	0.0825	0.248	101	51.1	9.62	-26.5	10.6	46.0	9.37	-26.2	10.7	0
2021	NNST	MMT	54.0	0.900	0.0349	0.0825	0.248	101	52.3	9.30	-25.1	10.4	NA	NA	NA	NA	0
2021	NNST	MMT	48.1	0.600	0.0638	0.0825	0.248	101	52.0	10.2	-25.1	9.86	NA	NA	NA	NA	0
2021	NNST	MMT	54.3	1.00	0.0398	0.0825	0.248	101	57.5	9.71	-25.6	9.56	NA	NA	NA	NA	0
2021	NNST	MMT	57.2	1.10	0.0304	0.0825	0.248	101	51.4	9.53	-25.7	11.5	NA	NA	NA	NA	0
2021	NNST	MMT	53.1	0.900	0.0311	0.0825	0.248	101	49.1	9.26	-25.7	10.7	NA	NA	NA	NA	0
2021	NNST	MMT	58.0	1.10	0.0389	0.0825	0.248	101	51.2	11.2	-24.1	10.1	NA	NA	NA	NA	0
2021	NNST	MMT	52.9	0.900	0.0525	0.0825	0.248	101	57.3	9.16	-26.2	10.2	NA	NA	NA	NA	0
2021	NNST	MMT	63.0	1.50	0.0724	0.0825	0.248	101	34.7	7.51	-23.8	10.2	NA	NA	NA	NA	0
2021	NNST	MMT	51.9	0.700	0.0370	0.0825	0.248	101	51.6	8.55	-25.6	10.1	NA	NA	NA	NA	0
2021	NNST	MMT	57.1	1.00	0.0661	0.0825	0.248	101	52.0	10.1	-24.6	9.60	52.5	10.3	-24.3	9.39	0
2021	NNST	MMT	74.5	2.20	0.0667	0.0825	0.248	101	62.4	9.14	-26.6	10.0	NA	NA	NA	NA	0

Table A2.4: Laboratory Results for all Slimy Sculpin (Cottus cognatus; SLSC) and Ninespine Stickleback (Pungitius pungitius; NNST) laboratory results from Biotron Laboratory, the University of Waterloo Environmental Isotope Laboratory, and AAE Tech Incorporated. These results include total Hg concentrations with all sample quality assurance and quality control (QA/QC) in accordance with international standards. Stable isotopes from fish tissue are presented as percent (%) carbon (C) and nitrogren (N), as well as with per mil (‰) for delta values of each of these. Age estimates were made using extracted otoliths. mm = millimeters, g = grams, mg/kg = milligrams per killogram, THg = total mercury, MDL = method detection limit, MRL= method reporting limit , DUP = duplicate, C = carbon, N = nitrogren, NA = no available data.

Sample Year	Fish Species Code	Lake Name	Fork Length (mm)	Wet Weight (g)	THg WW (mg/kg)	MDL (ng)	MRL (ng)	IPR avg (%)	%C	%N	δ13C	δ15N	DUP %C	DUP %N	DUP δ13C	DUP δ15N	Age Estimate
2021	NNST	MMT	61.3	1.50	0.0446	0.0825	0.248	101	56.5	10.0	-24.6	10.3	NA	NA	NA	NA	0
2021	NNST	MMT	55.2	1.00	0.0259	0.0825	0.248	101	51.9	11.1	-25.3	10.8	NA	NA	NA	NA	0
2021	NNST	MMT	50.9	0.800	0.0427	0.0825	0.248	101	37.9	8.81	-25.0	9.90	NA	NA	NA	NA	0
2021	NNST	MMT	69.6	2.00	0.0698	0.0825	0.248	101	42.9	8.18	-23.9	9.08	NA	NA	NA	NA	0
2021	NNST	MMT	46.2	0.700	0.0332	0.0825	0.248	101	45.7	9.39	-26.2	9.60	NA	NA	NA	NA	0
2021	NNST	MMT	54.4	0.900	0.0374	0.0825	0.248	101	36.8	7.75	-24.5	9.30	NA	NA	NA	NA	0
2021	NNST	MMT	54.0	1.00	0.0418	0.0825	0.248	101	44.6	9.21	-24.7	9.33	NA	NA	NA	NA	0
2021	SLSC	MMT	53.3	1.00	0.0268	0.0825	0.248	101	50.1	11.3	-21.1	8.54	NA	NA	NA	NA	1
2021	SLSC	MMT	49.0	0.800	0.0341	0.0825	0.248	101	46.0	9.36	-22.1	7.47	47.2	9.97	-21.6	7.79	1
2021	SLSC	MMT	65.2	1.80	0.0538	0.0825	0.248	101	46.6	13.1	-17.9	8.09	NA	NA	NA	NA	2
2021	SLSC	MMT	50.1	0.800	0.0361	0.0825	0.248	101	52.9	10.6	-22.2	8.37	NA	NA	NA	NA	1
2021	SLSC	MMT	34.2	0.300	0.0518	0.0825	0.248	101	47.2	9.72	-24.2	8.39	NA	NA	NA	NA	0
2021	SLSC	MMT	52.5	1.10	0.0341	0.0825	0.248	101	54.8	11.8	-22.0	7.29	NA	NA	NA	NA	1
2021	SLSC	MMT	42.0	0.500	0.0406	0.0825	0.248	101	54.6	10.4	-23.4	7.24	NA	NA	NA	NA	0
2021	SLSC	MMT	65.2	2.00	0.0562	0.0825	0.248	101	52.4	11.2	-21.7	7.97	NA	NA	NA	NA	2
2021	SLSC	MMT	58.9	1.50	0.0247	0.0825	0.248	101	49.8	9.84	-22.5	9.47	NA	NA	NA	NA	1
2021	SLSC	MMT	60.9	1.60	0.0356	0.0825	0.248	101	59.6	9.40	-23.2	7.27	NA	NA	NA	NA	1
2021	SLSC	MMT	57.0	1.40	0.0278	0.0825	0.248	101	47.4	9.79	-22.0	7.78	NA	NA	NA	NA	1
2021	SLSC	MMT	65.0	2.20	0.0606	0.0825	0.248	101	49.3	8.36	-23.4	8.69	44.8	8.14	-23.6	8.70	1
2021	SLSC	MMT	64.3	2.00	0.0678	0.0825	0.248	101	64.9	11.3	-21.5	9.03	NA	NA	NA	NA	2
2021	SLSC	MMT	38.2	0.400	0.0281	0.0825	0.248	101	53.4	11.2	-22.3	7.78	NA	NA	NA	NA	0
2021	SLSC	MMT	50.2	0.900	0.0309	0.0825	0.248	101	44.7	8.85	-22.8	7.87	NA	NA	NA	NA	0
2021	SLSC	MMT	61.9	2.10	0.0317	0.0825	0.248	101	50.9	7.85	-23.6	7.93	NA	NA	NA	NA	1
2021	SLSC	MMT	36.0	0.400	0.0300	0.0825	0.248	101	54.0	11.9	-22.3	7.79	NA	NA	NA	NA	0
2021	SLSC	MMT	39.3	0.500	0.0280	0.0825	0.248	101	54.9	10.1	-23.6	7.98	NA	NA	NA	NA	0
2021	SLSC	MMT	74.3	2.90	0.0823	0.0825	0.248	101	47.5	13.2	-20.1	8.44	NA	NA	NA	NA	3
2021	SLSC	MMT	40.1	0.500	0.0284	0.0825	0.248	101	52.1	13.2	-21.8	7.29	NA	NA	NA	NA	0
2021	SLSC	MMT	52.3	1.10	0.0473	0.0825	0.248	101	55.5	8.71	-23.2	8.62	NA	NA	NA	NA	1
2021	SLSC	MMT	39.0	0.400	0.0237	0.0825	0.248	101	45.7	10.1	-23.1	8.23	48.1	10.1	-23.5	7.46	0
2021	SLSC	MMT	63.1	2.10	0.0327	0.0825	0.248	101	59.0	10.1	-23.5	7.99	NA	NA	NA	NA	2
2021	SLSC	MMT	60.0	1.60	0.0498	0.0825	0.248	101	55.0	9.60	-24.1	8.24	NA	NA	NA	NA	1

Table A2.4: Laboratory Results for all Slimy Sculpin (Cottus cognatus; SLSC) and Ninespine Stickleback (Pungitius pungitius; NNST) laboratory results from Biotron Laboratory, the University of Waterloo Environmental Isotope Laboratory, and AAE Tech Incorporated. These results include total Hg concentrations with all sample quality assurance and quality control (QA/QC) in accordance with international standards. Stable isotopes from fish tissue are presented as percent (%) carbon (C) and nitrogren (N), as well as with per mil (‰) for delta values of each of these. Age estimates were made using extracted otoliths. mm = millimeters, g = grams, mg/kg = milligrams per killogram, THg = total mercury, MDL = method detection limit, MRL= method reporting limit , DUP = duplicate, C = carbon, N = nitrogren, NA = no available data.

Sample Year	Fish Species Code	Lake Name	Fork Length (mm)	Wet Weight (g)	THg WW (mg/kg)	MDL (ng)	MRL (ng)	IPR avg (%)	%C	%N	δ13C	δ15N	DUP %C	DUP %N	DUP δ13C	DUP δ15N	Age Estimate
2021	SLSC	MMT	60.9	1.90	0.0297	0.0825	0.248	101	58.0	10.5	-22.2	7.99	NA	NA	NA	NA	2
2021	SLSC	MMT	58.1	1.50	0.0314	0.0825	0.248	101	43.5	11.1	-19.5	8.13	NA	NA	NA	NA	2
2021	SLSC	MMT	39.0	0.500	0.0272	0.0825	0.248	101	50.4	10.2	-23.0	7.86	NA	NA	NA	NA	0
2021	SLSC	MMT	39.9	0.500	0.0418	0.0825	0.248	101	49.7	10.8	-23.3	8.65	NA	NA	NA	NA	0
2021	SLSC	MMT	36.2	0.400	0.0256	0.0825	0.248	101	50.4	11.0	-22.0	7.54	NA	NA	NA	NA	0
2021	SLSC	MMT	40.0	0.400	0.0325	0.0825	0.248	101	50.5	11.2	-23.1	8.57	NA	NA	NA	NA	0
2021	SLSC	MMT	37.2	0.400	0.0377	0.0825	0.248	101	56.6	12.7	-22.6	7.42	NA	NA	NA	NA	0
2021	SLSC	B03	56.3	1.50	0.0252	0.0825	0.248	101	57.2	10.6	-25.8	7.68	49.3	10.2	-25.4	7.62	1
2021	SLSC	B03	60.1	1.70	0.0277	0.0825	0.248	101	60.3	10.3	-22.0	5.84	NA	NA	NA	NA	2
2021	SLSC	B03	39.0	0.500	0.0215	0.0825	0.248	101	50.8	10.2	-23.6	6.32	NA	NA	NA	NA	0
2021	SLSC	B03	84.2	4.80	0.0478	0.0825	0.248	101	60.5	14.0	-22.4	7.59	NA	NA	NA	NA	4
2021	SLSC	B03	44.0	0.600	0.0194	0.0825	0.248	101	51.0	9.80	-22.4	5.78	NA	NA	NA	NA	0
2021	SLSC	B03	41.1	0.500	0.00202	0.0825	0.248	101	56.7	10.0	-24.3	6.67	NA	NA	NA	NA	0
2021	SLSC	B03	38.5	0.400	0.0192	0.0825	0.248	101	56.6	10.4	-22.8	6.12	NA	NA	NA	NA	0
2021	SLSC	B03	41.9	0.500	0.0197	0.0825	0.248	101	43.9	8.96	-21.3	6.03	NA	NA	NA	NA	0
2021	SLSC	B03	63.1	2.30	0.0340	0.0825	0.248	101	51.5	10.1	-22.6	7.12	NA	NA	NA	NA	2
2021	SLSC	B03	39.5	0.400	0.0250	0.0825	0.248	101	45.7	9.17	-23.1	6.19	NA	NA	NA	NA	0
2021	SLSC	B03	69.0	2.90	0.0411	0.0825	0.248	101	53.7	10.6	-22.6	6.69	49.7	9.64	-22.8	6.45	3
2021	SLSC	B03	72.1	2.60	0.0807	0.0825	0.248	101	41.8	11.0	-21.0	7.04	NA	NA	NA	NA	4
2021	SLSC	B03	61.1	1.70	0.0356	0.0825	0.248	101	46.8	9.85	-20.3	6.99	NA	NA	NA	NA	4
2021	SLSC	B03	43.5	0.600	0.0164	0.0825	0.248	101	50.3	9.18	-22.0	6.71	NA	NA	NA	NA	0
2021	SLSC	B03	40.0	0.400	0.0180	0.0825	0.248	101	39.0	8.03	-21.4	5.71	NA	NA	NA	NA	0
2021	SLSC	B03	49.3	0.900	0.0329	0.0825	0.248	101	56.8	12.3	-22.2	6.31	NA	NA	NA	NA	1
2021	SLSC	B03	44.5	0.600	0.0251	0.0825	0.248	101	59.8	13.7	-22.5	6.43	NA	NA	NA	NA	0
2021	SLSC	B03	43.1	0.500	0.0185	0.0825	0.248	101	47.9	9.24	-22.1	5.82	NA	NA	NA	NA	0
2021	SLSC	B03	51.0	1.10	0.0293	0.0825	0.248	101	55.4	10.5	-22.0	6.67	NA	NA	NA	NA	1
2021	SLSC	B03	58.1	1.60	0.0323	0.0825	0.248	101	53.8	10.3	-20.9	6.34	NA	NA	NA	NA	2
2021	SLSC	B03	52.5	1.00	0.0223	0.0825	0.248	101	50.9	8.67	-22.2	6.35	46.5	9.19	-21.7	6.33	1
2021	SLSC	B03	50.5	0.900	0.0279	0.0825	0.248	101	47.5	9.41	-21.5	5.44	NA	NA	NA	NA	1
2021	SLSC	B03	63.2	2.10	0.0331	0.0825	0.248	101	45.3	9.14	-22.7	7.14	NA	NA	NA	NA	3
2021	NNST	B03	56.1	1.20	0.0268	0.0825	0.248	101	56.6	10.1	-27.9	8.64	NA	NA	NA	NA	0

Table A2.4: Laboratory Results for all Slimy Sculpin (Cottus cognatus; SLSC) and Ninespine Stickleback (Pungitius pungitius; NNST) laboratory results from Biotron Laboratory, the University of Waterloo Environmental Isotope Laboratory, and AAE Tech Incorporated. These results include total Hg concentrations with all sample quality assurance and quality control (QA/QC) in accordance with international standards. Stable isotopes from fish tissue are presented as percent (%) carbon (C) and nitrogren (N), as well as with per mil (‰) for delta values of each of these. Age estimates were made using extracted otoliths. mm = millimeters, g = grams, mg/kg = milligrams per killogram, THg = total mercury, MDL = method detection limit, MRL= method reporting limit , DUP = duplicate, C = carbon, N = nitrogren, NA = no available data.

Sample Year	Fish Species Code	Lake Name	Fork Length (mm)	Wet Weight (g)	THg WW (mg/kg)	MDL (ng)	MRL (ng)	IPR avg (%)	%C	%N	δ13C	δ15N	DUP %C	DUP %N	DUP δ13C	DUP δ15N	Age Estimate
2021	NNST	B03	52.9	0.900	0.0439	0.0825	0.248	101	51.6	9.45	-27.9	8.70	NA	NA	NA	NA	0
2021	NNST	B03	58.3	1.30	0.0549	0.0825	0.248	101	59.6	11.6	-28.1	8.90	NA	NA	NA	NA	0
2021	NNST	B03	53.4	0.900	0.0214	0.0825	0.248	101	53.2	9.39	-28.2	8.84	NA	NA	NA	NA	0
2021	NNST	B03	57.3	1.20	0.0324	0.0825	0.248	101	57.1	8.73	-28.6	8.07	NA	NA	NA	NA	0
2021	NNST	B03	55.8	1.00	0.0422	0.0825	0.248	101	47.6	9.46	-27.6	8.26	NA	NA	NA	NA	0
2021	NNST	B03	57.1	1.20	0.0250	0.0825	0.248	101	62.9	12.4	-26.7	8.53	NA	NA	NA	NA	0
2021	SLSC	A44	49.2	0.900	0.0296	0.0825	0.248	101	55.3	12.2	-20.7	6.44	38.0	8.69	-20.4	6.09	1
2021	SLSC	A44	50.1	0.900	0.0303	0.0825	0.248	101	53.4	11.9	-19.6	6.10	NA	NA	NA	NA	1
2021	SLSC	A44	58.1	1.50	0.0512	0.0825	0.248	101	59.5	9.50	-23.9	6.75	NA	NA	NA	NA	2
2021	NNST	A44	68.8	2.00	0.0727	0.0825	0.248	101	56.5	8.78	-28.1	8.59	NA	NA	NA	NA	0
2021	NNST	A44	63.3	1.30	0.0846	0.0825	0.248	101	45.4	6.54	-29.2	9.16	NA	NA	NA	NA	0
2021	NNST	A44	57.9	1.10	0.0443	0.0825	0.248	101	40.9	6.70	-25.8	8.03	NA	NA	NA	NA	0
2021	NNST	A44	51.1	0.700	0.0362	0.0825	0.248	101	55.9	9.35	-27.4	8.63	NA	NA	NA	NA	0
2020	NNST	A63	40.0	0.551	0.286	0.0825	0.248	101	51.2	10.2	-30.6	8.04	NA	NA	NA	NA	0
2020	NNST	A63	49.0	0.828	0.218	0.0825	0.248	101	42.1	8.72	-30.3	8.02	59.5	12.0	-30.5	8.04	0
2020	NNST	A63	36.0	0.313	0.321	0.0825	0.248	101	44.6	9.07	-30.2	7.33	NA	NA	NA	NA	0
2020	NNST	A63	38.0	0.342	0.417	0.0825	0.248	101	52.3	11.3	-29.5	7.32	NA	NA	NA	NA	0
2020	NNST	A63	45.0	0.547	0.278	0.0825	0.248	101	53.2	9.43	-31.3	7.88	NA	NA	NA	NA	0
2020	NNST	A63	34.0	0.295	0.312	0.0825	0.248	101	50.7	11.3	-28.7	8.02	NA	NA	NA	NA	0
2020	NNST	A63	36.0	0.382	0.376	0.0825	0.248	101	46.0	10.5	-29.6	8.03	NA	NA	NA	NA	0
2020	NNST	A63	31.0	0.222	0.424	0.0825	0.248	101	47.5	10.9	-28.9	6.89	NA	NA	NA	NA	0
2020	NNST	A63	35.0	0.264	0.240	0.0825	0.248	101	48.3	10.3	-29.7	8.04	NA	NA	NA	NA	0
2020	NNST	A63	41.0	0.468	0.240	0.0825	0.248	101	43.9	8.09	-30.5	7.15	NA	NA	NA	NA	0
2020	NNST	A63	35.0	0.279	0.276	0.0825	0.248	101	52.6	9.31	-31.0	7.00	NA	NA	NA	NA	0
2020	NNST	A63	42.0	0.410	0.198	0.0825	0.248	101	53.2	10.9	-30.5	9.23	48.6	10.2	-30.4	8.54	0
2020	NNST	A63	36.0	0.318	0.351	0.0825	0.248	101	47.6	9.06	-30.9	7.74	NA	NA	NA	NA	0
2020	NNST	A63	43.0	0.567	0.257	0.0825	0.248	101	51.8	10.8	-30.4	8.01	NA	NA	NA	NA	0
2020	NNST	A63	35.0	0.279	0.342	0.0825	0.248	101	50.6	11.0	-29.8	7.76	NA	NA	NA	NA	0
2020	NNST	A63	41.0	0.471	0.303	0.0825	0.248	101	47.9	10.3	-29.2	7.55	NA	NA	NA	NA	0
2020	NNST	A63	41.0	0.423	0.304	0.0825	0.248	101	46.8	9.99	-29.0	7.48	NA	NA	NA	NA	0
2020	NNST	A63	38.0	0.340	0.290	0.0825	0.248	101	48.3	9.42	-29.0	6.84	NA	NA	NA	NA	0

Table A2.4: Laboratory Results for all Slimy Sculpin (Cottus cognatus; SLSC) and Ninespine Stickleback (Pungitius pungitius; NNST) laboratory results from Biotron Laboratory, the University of Waterloo Environmental Isotope Laboratory, and AAE Tech Incorporated. These results include total Hg concentrations with all sample quality assurance and quality control (QA/QC) in accordance with international standards. Stable isotopes from fish tissue are presented as percent (%) carbon (C) and nitrogren (N), as well as with per mil (‰) for delta values of each of these. Age estimates were made using extracted otoliths. mm = millimeters, g = grams, mg/kg = milligrams per killogram, THg = total mercury, MDL = method detection limit, MRL= method reporting limit , DUP = duplicate, C = carbon, N = nitrogren, NA = no available data.

Sample Year	Fish Species Code	Lake Name	Fork Length (mm)	Wet Weight (g)	THg WW (mg/kg)	MDL (ng)	MRL (ng)	IPR avg (%)	%C	%N	δ13C	δ15N	DUP %C	DUP %N	DUP δ13C	DUP δ15N	Age Estimate
2020	NNST	A63	39.0	0.354	0.193	0.0825	0.248	101	45.5	8.45	-31.0	8.43	NA	NA	NA	NA	0
2020	NNST	A63	36.0	0.331	0.263	0.0825	0.248	101	52.3	11.5	-29.0	7.47	NA	NA	NA	NA	0
2020	NNST	A63	27.0	0.149	0.433	0.0825	0.248	101	46.2	10.3	-28.7	7.45	NA	NA	NA	NA	0
2020	NNST	A63	35.0	0.268	0.265	0.0825	0.248	101	50.3	11.1	-27.8	7.78	48.3	10.6	-27.9	7.73	0
2020	NNST	A63	34.0	0.224	0.221	0.0825	0.248	101	52.4	12.5	-26.6	7.55	NA	NA	NA	NA	0
2020	NNST	A63	26.0	0.103	0.328	0.0825	0.248	101	45.4	12.1	-26.9	6.97	NA	NA	NA	NA	0
2020	NNST	A63	31.0	0.224	0.488	0.0825	0.248	101	44.5	9.25	-29.1	6.73	NA	NA	NA	NA	0
2020	NNST	A63	33.0	0.258	0.319	0.0825	0.248	101	50.2	9.51	-29.2	6.93	NA	NA	NA	NA	0
2020	NNST	A63	35.0	0.327	0.246	0.0825	0.248	101	47.2	9.73	-28.4	7.24	NA	NA	NA	NA	0
2020	NNST	A63	40.0	0.362	0.319	0.0825	0.248	101	50.1	10.9	-29.1	7.15	NA	NA	NA	NA	0
2020	NNST	A63	35.0	0.296	0.372	0.0825	0.248	101	47.5	9.00	-30.5	7.51	NA	NA	NA	NA	0
2020	NNST	A63	41.0	0.414	0.446	0.0825	0.248	101	45.0	9.28	-29.3	7.30	NA	NA	NA	NA	0
2020	NNST	A63	36.0	0.325	0.348	0.0825	0.248	101	49.7	9.70	-30.8	7.68	45.7	8.31	-31.3	7.66	0
2020	NNST	A63	29.0	0.134	0.324	0.0825	0.248	101	48.5	11.5	-28.3	6.75	NA	NA	NA	NA	0
2020	NNST	A63	27.0	0.140	0.514	0.0825	0.248	101	53.9	12.7	-28.2	6.93	NA	NA	NA	NA	0
2020	NNST	A63	25.0	0.149	0.379	0.0825	0.248	101	41.9	9.11	-28.1	6.49	NA	NA	NA	NA	0

Table A2.5: Accuracy of laboratory results for all Slimy Sculpin (Cottus cognatus; SLSC) and Ninespine Stickleback (Pungitius pungitius; NNST) mercury tissue chemistry samples from Biotron Center for Experimental Climate Change Research. CRM = certified reference materials, MS = matrix spike, MSD = matrix spike duplicate, N/A = no available data.

Sample Year	CRM	Recovery CRM (%)	Recovery MS & MSD (%)
2018	N/A	105	99 & 101
2019	N/A	105	99 & 101
2020	N/A	105	99 & 101
2021	DORM-5	107	104 & 104
2018	DORM-5	99	100 & 100
2019	DORM-5	99	100 & 100
2020	DORM-5	99	100 & 100
2018	DORM-5	100	100 & 100
2019	DORM-5	100	100 & 100
2020	DORM-5	100	100 & 100
2018	DORM-5	105	98 & 98
2019	DORM-5	105	98 & 98
2019	DORM-5	96	110 & 112
2020	DORM-5	105	98 & 98
2020	DORM-5	96	110 & 112
2019	DORM-5	91	99 & 98
2020	DORM-5	91	99 & 98

Table A2.6: Precision of laboratory results for Slimy Sculpin (Cottus cognatus; SLSC) and Ninespine Stickleback (Pungitius pungitius; NNST) mercury tissue chemistry from Biotron Center for Experimental Climate Change Research and stable isotope analyses from the Unviersity of Waterloo Environmental Isotope Laboratory. Hg = mercury, RPD = relative percent difference, DUP = duplicate, MS = matrix spike.

Sample Year	Fish Species Code	Hg Analysis RPD in DUP (%)		Hg Analysis RPD in MS (%)		Stable Isotope Analysis RPD (%)	
		Mean	Standard Deviation	Mean	Standard Deviation	Mean	Standard Deviation
2018	NNST	4.72	2.19	1.92	0.810	12.0	12.0
	SLSC	5.47	1.61	1.88	0.636	8.62	7.32
2019	NNST	5.22	1.58	2.01	0.582	8.21	7.38
	SLSC	5.43	1.61	1.75	0.670	6.61	6.75
2020	NNST	4.79	1.99	2.11	0.704	5.28	3.68
	SLSC	5.29	1.62	1.86	0.636	10.8	6.67
2021	NNST	7.36	1.19	1.98	0.124	12.1	11.8
	SLSC	7.91	0.555	1.98	0.0793	12.2	11.0

Table A2.7: Mercury (Hg) and methyl mercury (MeHg) water chemistry laboratory precision and accuracy results from Biotron Center for Experimental Climate Change Research. THg = total mercury, MDL = method detection limit, MRL = method reporting limit, DUP = duplicate, RPD = relative percent difference, IPR = initial precision and recovery, OPR = ongoing precision and recovery, MS = matrix spike, MSD = matrix spike duplicate, SD = standard deviation, NA = no available data.

Sample Year	Sample Identification	THg MDL (ng/L)	THg MRL (ng/L)	THg DUP RPD	THg IPR	THg OPR	THg MS RPD	THg MS DUP RPD	THg Quality Control Sample % Recovery	THg Recovery MS MSD	THg Method Blank	THg IPR SD	MeHg MDL (ng/L)	MeHg MRL (ng/L)	MeHg DUP RPD	MeHg IPR	MeHg OPR	MeHg MS RPD	MeHg MS DUP RPD	MeHg Quality Control Sample % Recovery	MeHg Recovery MS MSD	MeHg Method Blank	MeHg IPR SD
2018	A20-WQ01-2018	0.07	0.22	7	98	109	2	2	100	113, 112	<MDL	NA	0.01	0.02	19	97	98	4	4	77	83, 84	<MDL	NA
2018	A20-WQ02-2018	0.07	0.22	7	98	109	2	2	100	113, 112	<MDL	NA	0.01	0.02	19	97	98	4	4	77	83, 84	<MDL	NA
2018	A63-WQ01-A-2018	0.07	0.22	7	98	109	2	2	100	113, 112	<MDL	NA	0.01	0.02	19	97	98	4	4	77	83, 84	<MDL	NA
2018	A63-WQ01-B-2018	0.07	0.22	7	98	109	2	2	100	113, 112	<MDL	NA	0.01	0.02	19	97	98	4	4	77	83, 84	<MDL	NA
2018	A63-WQ02-2018	0.07	0.22	7	98	109	2	2	100	113, 112	<MDL	NA	0.01	0.02	19	97	98	4	4	77	83, 84	<MDL	NA
2018	A65-WQ01-2018	0.07	0.22	7	98	109	2	2	100	113, 112	<MDL	NA	0.01	0.02	19	97	98	4	4	77	83, 84	<MDL	NA
2018	A65-WQ02-2018	0.07	0.22	7	98	109	2	2	100	113, 112	<MDL	NA	0.01	0.02	19	97	98	4	4	77	83, 84	<MDL	NA
2018	A76-WQ01-2018	0.07	0.22	7	98	109	2	2	100	113, 112	<MDL	NA	0.01	0.02	19	97	98	4	4	77	83, 84	<MDL	NA
2018	A76-WQ02-A-2018	0.07	0.22	7	98	109	2	2	100	113, 112	<MDL	NA	0.01	0.02	19	97	98	4	4	77	83, 84	<MDL	NA
2018	A76-WQ02-B-2018	0.07	0.22	7	98	109	2	2	100	113, 112	<MDL	NA	0.01	0.02	19	97	98	4	4	77	83, 84	<MDL	NA
2018	LK8-WQ01-2018	0.07	0.22	7	98	109	2	2	100	113, 112	<MDL	NA	0.01	0.02	19	97	98	4	4	77	83, 84	<MDL	NA
2018	LK8-WQ02-2018	0.07	0.22	7	98	109	2	2	100	113, 112	<MDL	NA	0.01	0.02	19	97	98	4	4	77	83, 84	<MDL	NA
2018	MMT-WQ01-2018	0.07	0.22	7	98	109	2	2	100	113, 112	<MDL	NA	0.01	0.02	19	97	98	4	4	77	83, 84	<MDL	NA
2018	MMT-WQ02-2018	0.07	0.22	7	98	109	2	2	100	113, 112	<MDL	NA	0.01	0.02	19	97	98	4	4	77	83, 84	<MDL	NA
2018	NEM-WQ01-2018	0.07	0.22	7	98	109	2	2	100	113, 112	<MDL	NA	0.01	0.02	19	97	98	4	4	77	83, 84	<MDL	NA
2018	NEM-WQ02-2018	0.07	0.22	7	98	109	2	2	100	113, 112	<MDL	NA	0.01	0.02	19	97	98	4	4	77	83, 84	<MDL	NA
2018	WTL-WQ01-2018	0.07	0.22	7	98	109	2	2	100	113, 112	<MDL	NA	0.01	0.02	19	97	98	4	4	77	83, 84	<MDL	NA
2018	WTL-WQ02-2018	0.07	0.22	7	98	109	2	2	100	113, 112	<MDL	NA	0.01	0.02	19	97	98	4	4	77	83, 84	<MDL	NA
2019	DS1-WQ01-2019	0.07	0.22	2, 5	98, 97	100, 101	1, 3	1, 3	90, 89	94, 92; 96, 93	<MDL	2, 1	0.01	0.02	11, 4	100, 89	97, 102	100, 3	100, 3	93, 89	100, 100; 90, 93	<MDL	2, 3
2019	DS1-WQ02-2019	0.07	0.22	2, 5	98, 97	100, 101	1, 3	1, 3	90, 89	94, 92; 96, 93	<MDL	2, 1	0.01	0.02	11, 4	100, 89	97, 102	100, 3	100, 3	93, 89	100, 100; 90, 93	<MDL	2, 3
2019	A20-WQ01-2019	0.07	0.22	2, 5	98, 97	100, 101	1, 3	1, 3	90, 89	94, 92; 96, 93	<MDL	2, 1	0.01	0.02	11, 4	100, 89	97, 102	100, 3	100, 3	93, 89	100, 100; 90, 93	<MDL	2, 3
2019	A20-WQ02-2019	0.07	0.22	2, 5	98, 97	100, 101	1, 3	1, 3	90, 89	94, 92; 96, 93	<MDL	2, 1	0.01	0.02	11, 4	100, 89	97, 102	100, 3	100, 3	93, 89	100, 100; 90, 93	<MDL	2, 3
2019	A63-WQ01-2019	0.07	0.22	5	97	101	3	3	89	96, 93	<MDL	1	0.01	0.02	4	89	102	3	3	89	90, 93	<MDL	3
2019	A63-WQ02A-2019	0.07	0.22	5	97	101	3	3	89	96, 93	<MDL	1	0.01	0.02	4	89	102	3	3	89	90, 93	<MDL	3
2019	A63-WQ02B-2019	0.07	0.22	5	97	101	3	3	89	96, 93	<MDL	1	0.01	0.02	4	89	102	3	3	89	90, 93	<MDL	3
2019	A65-WQ01-2019	0.07	0.22	2, 5	98, 97	100, 101	1, 3	1, 3	90, 89	94, 92; 96, 93	<MDL	2, 1	0.01	0.02	11, 4	100, 89	97, 102	100, 3	100, 3	93, 89	100, 100; 90, 93	<MDL	2, 3
2019	A65-WQ02A-2019	0.07	0.22	2, 5	98, 97	100, 101	1, 3	1, 3	90, 89	94, 92; 96, 93	<MDL	2, 1	0.01	0.02	11, 4	100, 89	97, 102	100, 3	100, 3	93, 89	100, 100; 90, 93	<MDL	2, 3
2019	A65-WQ02B-2019	0.07	0.22	2, 5	98, 97	100, 101	1, 3	1, 3	90, 89	94, 92; 96, 93	<MDL	2, 1	0.01	0.02	11, 4	100, 89	97, 102	100, 3	100, 3	93, 89	100, 100; 90, 93	<MDL	2, 3
2019	A76-WQ01-2019	0.07	0.22	2, 5	98, 97	100, 101	1, 3	1, 3	90, 89	94, 92; 96, 93	<MDL	2, 1	0.01	0.02	11, 4	100, 89	97, 102	100, 3	100, 3	93, 89	100, 100; 90, 93	<MDL	2, 3
2019	A76-WQ02-2019	0.07	0.22	2, 5	98, 97	100, 101	1, 3	1, 3	90, 89	94, 92; 96, 93	<MDL	2, 1	0.01	0.02	11, 4	100, 89	97, 102	100, 3	100, 3	93, 89	100, 100; 90, 93	<MDL	2, 3
2019	LK8-WQ01-2019	0.07	0.22	2, 5	98, 97	100, 101	1, 3	1, 3	90, 89	94, 92; 96, 93	<MDL	2, 1	0.01	0.02	11, 4	100, 89	97, 102	100, 3	100, 3	93, 89	100, 100; 90, 93	<MDL	2, 3
2019	LK8-WQ02-2019	0.07	0.22	2, 5	98, 97	100, 101	1, 3	1, 3	90, 89	94, 92; 96, 93	<MDL	2, 1	0.01	0.02	11, 4	100, 89	97, 102	100, 3	100, 3	93, 89	100, 100; 90, 93	<MDL	2, 3
2019	MMT-WQ01-2019	0.07	0.22	2, 5	98, 97	100, 101	1, 3	1, 3	90, 89	94, 92; 96, 93	<MDL	2, 1	0.01	0.02	11, 4	100, 89	97, 102	100, 3	100, 3	93, 89	100, 100; 90, 93	<MDL	2, 3
2019	MMT-WQ02-2019	0.07	0.22	2, 5	98, 97	100, 101	1, 3	1, 3	90, 89	94, 92; 96, 93	<MDL	2, 1	0.01	0.02	11, 4	100, 89	97, 102	100, 3	100, 3	93, 89	100, 100; 90, 93	<MDL	2, 3

Table A2.7: Mercury (Hg) and methyl mercury (MeHg) water chemistry laboratory precision and accuracy results from Biotron Center for Experimental Climate Change Research. THg = total mercury, MDL = method detection limit, MRL = method reporting limit, DUP = duplicate, RPD = relative percent difference, IPR = initial precision and recovery, OPR = ongoing precision and recovery, MS = matrix spike, MSD = matrix spike duplicate, SD = standard deviation, NA = no available data.

Sample Year	Sample Identification	THg MDL (ng/L)	THg MRL (ng/L)	THg DUP RPD	THg IPR	THg OPR	THg MS RPD	THg MS DUP RPD	THg Quality Control Sample % Recovery	THg Recovery MS MSD	THg Method Blank	THg IPR SD	MeHg MDL (ng/L)	MeHg MRL (ng/L)	MeHg DUP RPD	MeHg IPR	MeHg OPR	MeHg MS RPD	MeHg MS DUP RPD	MeHg Quality Control Sample % Recovery	MeHg Recovery MS MSD	MeHg Method Blank	MeHg IPR SD
2019	WTL-WQ01-2019	0.07	0.22	2, 5	98, 97	100, 101	1, 3	1, 3	90, 89	94, 92; 96, 93	<MDL	2, 1	0.01	0.02	11, 4	100, 89	97, 102	100, 3	100, 3	93, 89	100, 100; 90, 93	<MDL	2, 3
2019	WTL-WQ02-2019	0.07	0.22	2, 5	98, 97	100, 101	1, 3	1, 3	90, 89	94, 92; 96, 93	<MDL	2, 1	0.01	0.02	11, 4	100, 89	97, 102	100, 3	100, 3	93, 89	100, 100; 90, 93	<MDL	2, 3
2020	DS1-WQ01-2020	0.06	0.17	8	100	100	4	4	107	94, 95	<MDL	1	0.006	0.004	5	98	106	2	2	96	111, 111	<MDL	2
2020	DS1-WQ02-2020	0.06	0.17	8	100	100	4	4	107	94, 95	<MDL	1	0.006	0.018	5	98	106	2	2	96	111, 111	<MDL	2
2020	A20-WQ01A-2020	0.06	0.17	8	100	100	4	4	107	94, 95	<MDL	1	0.006	0.018	5	98	106	2	2	96	111, 111	<MDL	2
2020	A20-WQ01B-2020	0.06	0.17	8	100	100	4	4	107	94, 95	<MDL	1	0.006	0.018	5	98	106	2	2	96	111, 111	<MDL	2
2020	A20-WQ02-2020	0.06	0.17	8	100	100	4	4	107	94, 95	<MDL	1	0.006	0.018	5	98	106	2	2	96	111, 111	<MDL	2
2020	A63-WQ01-2020	0.04	0.02	7	102	94	5	5	91	103, 104	<MDL	2	0.006	0.018	2	102	105	1	1	105	109, 107	<MDL	5
2020	A63-WQ02-2020	0.04	0.02	7	102	94	5	5	91	103, 104	<MDL	2	0.006	0.018	2	102	105	1	1	105	109, 107	<MDL	5
2020	A44-WQ01-2020	0.04	0.02	7	102	94	5	5	91	103, 104	<MDL	2	0.006	0.018	2	102	105	1	1	105	109, 107	<MDL	5
2020	A44-WQ02-2020	0.04	0.02	7	102	94	5	5	91	103, 104	<MDL	2	0.006	0.018	2	102	105	1	1	105	109, 107	<MDL	5
2020	A65-WQ01-2020	0.06	0.17	8	100	100	4	4	107	94, 95	<MDL	1	0.006	0.018	5	98	106	2	2	96	111, 111	<MDL	2
2020	A65-WQ02-2020	0.06	0.17	8	100	100	4	4	107	94, 95	<MDL	1	0.006	0.018	5	98	106	2	2	96	111, 111	<MDL	2
2020	A76-WQ01-2020	0.06	0.17	8	100	100	4	4	107	94, 95	<MDL	1	0.006	0.018	5	98	106	2	2	96	111, 111	<MDL	2
2020	A76-WQ02-2020	0.06	0.17	8	100	100	4	4	107	94, 95	<MDL	1	0.006	0.018	5	98	106	2	2	96	111, 111	<MDL	2
2020	LK1-23	0.06	0.17	8	100	100	4	4	107	94, 95	<MDL	1	0.006	0.018	5	98	106	2	2	96	111, 111	<MDL	2
2020	LK1-24	0.06	0.17	8	100	100	4	4	107	94, 95	<MDL	1	0.006	0.018	5	98	106	2	2	96	111, 111	<MDL	2
2020	LK8-WQ01-2020	0.06	0.17	8	100	100	4	4	107	94, 95	<MDL	1	0.006	0.018	5	98	106	2	2	96	111, 111	<MDL	2
2020	LK8-WQ02-2020	0.06	0.17	8	100	100	4	4	107	94, 95	<MDL	1	0.006	0.018	5	98	106	2	2	96	111, 111	<MDL	2
2020	B3-WQ01	0.06	0.17	8	100	100	4	4	107	94, 95	<MDL	1	0.006	0.018	5	98	106	2	2	96	111, 111	<MDL	2
2020	B3-WQ02	0.06	0.17	8	100	100	4	4	107	94, 95	<MDL	1	0.006	0.018	5	98	106	2	2	96	111, 111	<MDL	2
2020	INUG-124	0.06	0.17	8	100	100	4	4	107	94, 95	<MDL	1	0.006	0.018	5	98	106	2	2	96	111, 111	<MDL	2
2020	INUG-125	0.06	0.17	8	100	100	4	4	107	94, 95	<MDL	1	0.006	0.018	5	98	106	2	2	96	111, 111	<MDL	2
2020	MMT-WQ01-2020	0.06	0.17	8	100	100	4	4	107	94, 95	<MDL	1	0.006	0.018	5	98	106	2	2	96	111, 111	<MDL	2
2020	MMT-WQ02-2020	0.06	0.17	8	100	100	4	4	107	94, 95	<MDL	1	0.006	0.018	5	98	106	2	2	96	111, 111	<MDL	2
2020	NEM-WQ01-2020	0.04	0.02	7	102	94	5	5	91	103, 104	<MDL	2	0.006	0.018	2	102	105	1	1	105	109, 107	<MDL	5
2020	NEM-WQ02-2020	0.04	0.02	7	102	94	5	5	91	103, 104	<MDL	2	0.006	0.018	2	102	105	1	1	105	109, 107	<MDL	5
2020	PDL-89	0.06	0.17	8	100	100	4	4	107	94, 95	<MDL	1	0.006	0.018	5	98	106	2	2	96	111, 111	<MDL	2
2020	PDL-90	0.06	0.17	8	100	100	4	4	107	94, 95	<MDL	1	0.006	0.018	5	98	106	2	2	96	111, 111	<MDL	2
2020	WTL-WQ01A-2020	0.06	0.17	8	100	100	4	4	107	94, 95	<MDL	1	0.006	0.018	5	98	106	2	2	96	111, 111	<MDL	2
2020	WTL-WQ01B-2020	0.06	0.17	8	100	100	4	4	107	94, 95	<MDL	1	0.006	0.018	5	98	106	2	2	96	111, 111	<MDL	2
2020	WTL-WQ02-2020	0.06	0.17	8	100	100	4	4	107	94, 95	<MDL	1	0.006	0.018	5	98	106	2	2	96	111, 111	<MDL	2
2021	A20-WQ01-2021	0.06	0.17	4	102	105	1	1	101	102, 102	<MDL	3	0.01	0.02	8	100	97	4	4	103	106, 106	<MDL	4
2021	A20-WQ02-2021	0.06	0.17	4	102	105	1	1	101	102, 102	<MDL	3	0.01	0.02	8	100	97	4	4	103	106, 106	<MDL	4
2021	A63-WQ01-2021	0.06	0.17	4	102	105	1	1	101	102, 102	<MDL	3	0.01	0.02	8	100	97	4	4	103	106, 106	<MDL	4
2021	A63-WQ02-2021	0.06	0.17	4	102	105	1	1	101	102, 102	<MDL	3	0.01	0.02	8	100	97	4	4	103	106, 106	<MDL	4
2021	A44-WQ01-2021	0.06	0.17	4	102	105	1	1	101	102, 102	<MDL	3	0.01	0.02	8	100	97	4	4	103	106, 106	<MDL	4
2021	A44-WQ02-2021	0.06	0.17	4	102	105	1	1	101	102, 102	<MDL	3	0.01	0.02	8	100	97	4	4	103	106, 106	<MDL	4
2021	A44-BLANK-2021	0.06	0.17	4	102	105	1	1	101	102, 102	<MDL	3	0.01	0.02	8	100	97	4	4	103	106, 106	<MDL	4
2021	A65-WQ01-2021	0.06	0.17	4	102	105	1	1	101	102, 102	<MDL	3	0.01	0.02	8	100	97	4	4	103	106, 106	<MDL	4
2021	A65-WQ02-2021	0.06	0.17	4	102	105	1	1	101	102, 102	<MDL	3	0.01	0.02	8	100	97	4	4	103	106, 106	<MDL	4
2021	A65-WQ02-2021-A	0.06	0.17	4	102	105	1	1	101	102, 102	<MDL	3	0.01	0.02	8	100	97	4	4	103	106, 106	<MDL	4
2021	A65-WQ02-2021-B	0.06	0.17	4	102	105	1	1	101	102, 102	<MDL	3	0.01	0.02	8	100	97	4	4	103	106, 106	<MDL	4
2021	D01-WQ01-2021	0.06	0.17	4	102	105	1	1	101	102, 102	<MDL	3	0.01	0.02	8	100	97	4	4	103	106, 106	<MDL	4
2021	D01-WQ02-2021	0.06	0.17	4	102	105	1	1	101	102, 102	<MDL	3	0.01	0.02	8	100	97	4	4	103	106, 106	<MDL	4

Table A2.7: Mercury (Hg) and methyl mercury (MeHg) water chemistry laboratory precision and accuracy results from Biotron Center for Experimental Climate Change Research. THg = total mercury, MDL = method detection limit, MRL = method reporting limit, DUP = duplicate, RPD = relative percent difference, IPR = initial precision and recovery, OPR = ongoing precision and recovery, MS = matrix spike, MSD = matrix spike duplicate, SD = standard deviation, NA = no available data.

Sample Year	Sample Identification	THg MDL (ng/L)	THg MRL (ng/L)	THg DUP RPD	THg IPR	THg OPR	THg MS RPD	THg MS DUP RPD	THg Quality Control Sample % Recovery	THg Recovery MS MSD	THg Method Blank	THg IPR SD	MeHg MDL (ng/L)	MeHg MRL (ng/L)	MeHg DUP RPD	MeHg IPR	MeHg OPR	MeHg MS RPD	MeHg MS DUP RPD	MeHg Quality Control Sample % Recovery	MeHg Recovery MS MSD	MeHg Method Blank	MeHg IPR SD
2021	LAKE8-WQ01-2021	0.06	0.17	4	102	105	1	1	101	102, 102	<MDL	3	0.01	0.02	8	100	97	4	4	103	106, 106	<MDL	4
2021	LAKE8-WQ02-2021	0.06	0.17	4	102	105	1	1	101	102, 102	<MDL	3	0.01	0.02	8	100	97	4	4	103	106, 106	<MDL	4
2021	B03-WQ01-2021	0.06	0.17	4	102	105	1	1	101	102, 102	<MDL	3	0.01	0.02	8	100	97	4	4	103	106, 106	<MDL	4
2021	B03-WQ02-2021	0.06	0.17	4	102	105	1	1	101	102, 102	<MDL	3	0.01	0.02	8	100	97	4	4	103	106, 106	<MDL	4
2021	MMT-WQ01-2021	0.06	0.17	4	102	105	1	1	101	102, 102	<MDL	3	0.01	0.02	8	100	97	4	4	103	106, 106	<MDL	4
2021	MMT-WQ02-2021	0.06	0.17	4	102	105	1	1	101	102, 102	<MDL	3	0.01	0.02	8	100	97	4	4	103	106, 106	<MDL	4
2021	MMT-BLANK-2021	0.06	0.17	4	102	105	1	1	101	102, 102	<MDL	3	0.01	0.02	8	100	97	4	4	103	106, 106	<MDL	4
2021	WTL-WQ01-2021	0.06	0.17	4	102	105	1	1	101	102, 102	<MDL	3	0.01	0.02	8	100	97	4	4	103	106, 106	<MDL	4
2021	WTL-WQ02-2021	0.06	0.17	4	102	105	1	1	101	102, 102	<MDL	3	0.01	0.02	8	100	97	4	4	103	106, 106	<MDL	4

Table A2.8: ***Summary of statistical models used to determine differences between flooded and reference lakes and between pre-flood (2018 and 2019) and post-flood (2020 and 2021) years. "SLSC" = Slimy =Sculpin (Cottus cognatus). "NSSB" = Ninespine Stickleback (Pungitius pungitius). "LMEM" = linear mixed effects model. "ANCOVA" = analysis of covariance. "FL" = fork length. "Hg" = mercury. "NA" = not applicable. 1|waterbody/year is equivalent to 1|waterbody + 1|waterbody:year. It is the random variation in intercept for each waterbody as well as each waterbody:year interaction.***

Endpoint	Fish Species	Waterbody Exposue Type	Years	Model Type	Response (Dependent) Variable	Fixed Effect	Random Effects
Mercury	SLSC	Flooded	2018-2021	LMEM	log10 dry Hg concentration	year* $\log_{10}$ FL	1| waterbody/year
	NSSB	Flooded	2018-2021	LMEM	log10 dry Hg concentration	year+$\log_{10}$FL	1 + $\log_{10}$ FL |year:waterbody
	SLSC	Reference	2018-2021	LMEM	log10 dry Hg concentration	year* $\log_{10}$ FL	1| waterbody
	SLSC	Flooded+Reference	2018	Linear Model (ANCOVA)	log10 dry Hg concentration	waterbody + $\log_{10}$FL	NA
	SLSC	Flooded+Reference	2019	Linear Model (ANCOVA)	log10 dry Hg concentration	waterbody + $\log_{10}$FL	NA
	SLSC	Flooded+Reference	2020	LMEM	log10 dry Hg concentration	exposure*$\log_{10}$FL	1| waterbody
	SLSC	Flooded+Reference	2021	LMEM	log10 dry Hg concentration	exposure*$\log_{10}$FL	1| waterbody
	NSSB	Flooded+Reference	2020	LMEM	log10 dry Hg concentration	exposure+$\log_{10}$FL	1| waterbody
	NSSB	Flooded+Reference	2021	LMEM	log10 dry Hg concentration	exposure+$\log_{10}$FL	1| waterbody
Relative Condition	SLSC	Flooded	2018-2021	LMEM	relative condition	year* $\log_{10}$ FL	1| waterbody:year
	NSSB	Flooded+Reference	2018-2021	LMEM	relative condition	year* $\log_{10}$ FL	1| waterbody:year
	SLSC	Reference	2018-2021	Linear Model (ANCOVA)	relative condition	year* $\log_{10}$ FL	NA
	SLSC	Flooded+Reference	2018	Linear Model (ANCOVA)	relative condition	waterbody + $\log_{10}$FL	NA
	SLSC	Flooded+Reference	2019	Linear Model (ANCOVA)	relative condition	waterbody + $\log_{10}$FL	NA
	SLSC	Flooded+Reference	2020	LMEM	relative condition	exposure+$\log_{10}$FL	1| waterbody
	SLSC	Flooded+Reference	2021	Linear Model (ANCOVA)	relative condition	exposure+$\log_{10}$FL	NA
	NSSB	Flooded+Reference	2020	LMEM	relative condition	exposure+$\log_{10}$FL	1| waterbody
	NSSB	Flooded+Reference	2021	Linear Model (ANCOVA)	relative condition	exposure+$\log_{10}$FL	NA
C:N Ratio	SLSC	Flooded	2018-2021	LMEM	C:N	year* $\log_{10}$ FL	1| waterbody:year
	NSSB	Flooded	2018-2021	LMEM	C:N	year* $\log_{10}$ FL	1| waterbody:year
	SLSC	Reference	2018-2021	LMEM	C:N	year+$\log_{10}$FL	1 | year:waterbody
	SLSC	Flooded+Reference	2018	Linear Model (ANCOVA)	C:N	waterbody + $\log_{10}$FL	NA
	SLSC	Flooded+Reference	2019	Linear Model (ANCOVA)	C:N	waterbody + $\log_{10}$FL	NA
	SLSC	Flooded+Reference	2020	LMEM	C:N	exposure+$\log_{10}$FL	1 + $\log_{10}$FL | waterbody
	SLSC	Flooded+Reference	2021	LMEM	C:N	exposure+$\log_{10}$FL	1| waterbody
	NSSB	Flooded+Reference	2020	LMEM	C:N	exposure*$\log_{10}$FL	1| waterbody
	NSSB	Flooded+Reference	2021	LMEM	C:N	exposure*$\log_{10}$FL	1| waterbody

Table A2.8: ***Summary of statistical models used to determine differences between flooded and reference lakes and between pre-flood (2018 and 2019) and post-flood (2020 and 2021) years. "SLSC" = Slimy =Sculpin (Cottus cognatus). "NSSB" = Ninespine Stickleback (Pungitius pungitius). "LMEM" = linear mixed effects model. "ANCOVA" = analysis of covariance. "FL" = fork length. "Hg" = mercury. "NA" = not applicable. 1|waterbody/year is equivalent to 1|waterbody + 1|waterbody:year. It is the random variation in intercept for each waterbody as well as each waterbody:year interaction.***

Endpoint	Fish Species	Waterbody Exposue Type	Years	Model Type	Response (Dependent) Variable	Fixed Effect	Random Effects
$\delta^{13}C$	SLSC	Flooded	2018-2021	LMEM	$\delta^{13}C$	year* $\log_{10}$ FL	1| waterbody/year
	NSSB	Flooded	2018-2021	LMEM	$\delta^{13}C$	year* $\log_{10}$ FL	1| waterbody/year
	SLSC	Reference	2018-2021	LMEM	$\delta^{13}C$	year* $\log_{10}$ FL	1 | year:waterbody
	SLSC	Flooded+Reference	2018	Linear Model (ANCOVA)	$\delta^{13}C$	waterbody * $\log_{10}$FL	NA
	SLSC	Flooded+Reference	2019	Linear Model (ANCOVA)	$\delta^{13}C$	waterbody + $\log_{10}$FL	NA
	SLSC	Flooded+Reference	2020	LMEM	$\delta^{13}C$	exposure+$\log_{10}$FL	1| waterbody
	SLSC	Flooded+Reference	2021	LMEM	$\delta^{13}C$	exposure*$\log_{10}$FL	1| waterbody
	NSSB	Flooded+Reference	2020	LMEM	$\delta^{13}C$	exposure+$\log_{10}$FL	1| waterbody
	NSSB	Flooded+Reference	2021	LMEM	$\delta^{13}C$	exposure+$\log_{10}$FL	1| waterbody
$\delta^{15}N$	SLSC	Flooded+Reference (each lake individually analysed)	2018-2021	Linear Model (ANCOVA)	$\delta^{15}N$	year* $\log_{10}$ FL	NA
	NSSB	Flooded+Reference (each lake individually analysed)	2018-2021	Linear Model (ANCOVA)	$\delta^{15}N$	year* $\log_{10}$ FL	NA

Table A3.1: Mercury concentrations (unfiltered) in water chemistry samples collected from flooded (A20, A63, A65, WTL) and reference (A44, B03, LK8) lakes between 2018 and 2021. Hg = mercury, MeHg = methryl mercury, NA = no available data.

Year	Date (Day-Month-Year)	Lake	Parameter (ng/L)		
			Total Hg	MeHg	% MeHg
2018	17-08-18	A20	0.498	0.0113	2.26
	17-08-18		0.407	0.00375	0.922
	20-08-18	A63	0.319	0.0302	9.48
	20-08-18		0.325	0.0113	3.46
	20-08-18		0.385	0.0492	12.8
	20-08-18	A65	0.364	0.0275	7.54
	20-08-18		0.361	0.0352	9.75
	16-08-18	WTL	0.287	0.0113	3.93
	16-08-18		0.284	0.0113	3.97
	21-08-18	LK8	0.0400	0.00375	9.38
	21-08-18		0.0400	0.0113	28.1
2019	16-08-19	A20	NA	0.0304	NA
	16-08-19		NA	0.0230	NA
	19-08-19	A63	NA	0.357	NA
	19-08-19		NA	0.162	NA
	19-08-19		NA	0.125	NA
	19-08-19	A65	NA	0.0834	NA
	19-08-19		NA	0.0602	NA
	19-08-19		NA	0.0592	NA
	18-08-19	WTL	NA	0.0663	NA
	18-08-19		NA	0.0798	NA
	16-08-19	LK8	NA	0.0323	NA
	16-08-19		NA	0.0113	NA

Table A3.1: Mercury concentrations (unfiltered) in water chemistry samples collected from flooded (A20, A63, A65, WTL) and reference (A44, B03, LK8) lakes between 2018 and 2021. Hg = mercury, MeHg = methryl mercury, NA = no available data.

Year	Date (Day-Month-Year)	Lake	Parameter (ng/L)		
			Total Hg	MeHg	% MeHg
2020	14-08-20	A20	1.07	0.0812	7.62
	14-08-20		2.40	0.0979	4.09
	14-08-20		2.00	0.0845	4.22
	12-08-20	A63	3.26	0.910	27.9
	12-08-20		3.92	0.949	24.2
	12-08-20	A65	2.74	0.240	8.76
	12-08-20		2.54	0.212	8.35
	12-08-20	WTL	1.57	0.430	27.3
	12-08-20		1.34	0.447	33.3
	12-08-20		2.95	0.499	16.9
	29-08-20	A44	1.08	0.0195	1.80
	29-08-20		1.08	0.00875	0.810
	29-08-20	B03	0.369	0.0025	0.677
	29-08-20		0.451	0.0025	0.554
	23-08-20	LK8	0.986	0.0025	0.254
	23-08-20		0.907	0.00875	0.965
2021	10-08-21	A20	1.47	0.203	13.8
	10-08-21		1.45	0.107	7.39
	16-08-21	A63	1.65	0.551	33.4
	16-08-21		2.27	0.499	22.0
	11-08-21	A65	2.08	0.224	10.8
	12-08-21		1.96	0.256	13.0
	12-08-21		1.97	0.475	24.1
	11-08-21	WTL	1.10	0.477	43.2
	16-08-21		1.14	0.00375	0.329

Table A3.1: Mercury concentrations (unfiltered) in water chemistry samples collected from flooded (A20, A63, A65, WTL) and reference (A44, B03, LK8) lakes between 2018 and 2021. Hg = mercury, MeHg = methryl mercury, NA = no available data.

Year	Date (Day-Month-Year)	Lake	Parameter (ng/L)		
			Total Hg	MeHg	% MeHg
2021	13-08-21	A44	1.06	0.025	2.37
	13-08-21		1.02	0.032	3.13
	14-08-21	B03	0.730	0.0113	1.54
	14-08-21		1.01	0.0113	1.11
	15-08-21	LK8	0.411	0.0113	2.74
	15-08-21		0.549	0.0113	2.05

Table A3.2: ***Summary statistics for dry mercury concentration (mg/kg) in muscle rissue of Slimy Sculpin (Cottus cognatus; SLSC) and Ninespine Stickleback (Pungitius pungitius; NNST) collected at flooded (WTL, A63, A65, A20) and reference (LK8, B03, A44) lakes between 2018 to 2021. "n" = number of observations. "NA" = no data available. Shading indicates post-flooding years of the study.***

Fish Species	Year	Waterbody	n	Mean	Minimum	Maximum	Standard Deviaiton	Standard Error
SLSC	2018	WTL	30	0.171	0.121	0.511	0.0681	0.0124
		A63	30	0.205	0.131	0.548	0.0863	0.0157
		A65	34	0.179	0.106	0.380	0.0516	0.00885
		A20	26	0.155	0.0837	0.333	0.0582	0.0114
		Lake 8	31	0.120	0.0740	0.188	0.0267	0.00479
	2019	WTL	34	0.189	0.0790	0.656	0.123	0.0211
		A63	7	0.188	0.144	0.238	0.0325	0.0123
		A65	3	0.220	0.197	0.247	0.0253	0.0146
		A44	35	0.166	0.0953	0.325	0.0506	0.00855
	2020	WTL	33	1.04	0.442	1.48	0.225	0.0393
		A65	35	0.569	0.336	0.754	0.0956	0.0162
		A20	37	0.473	0.206	0.984	0.182	0.0299
		Lake 8	34	0.164	0.100	0.304	0.0452	0.00776
		A44	34	0.198	0.115	0.408	0.0690	0.0118
		B03	34	0.144	0.0554	0.278	0.0528	0.00905
	2021	WTL	32	1.76	0.818	3.28	0.447	0.0791
		A63	29	1.75	1.03	2.43	0.317	0.0589
		A65	12	0.788	0.496	1.43	0.283	0.0817
		A20	6	0.531	0.400	0.668	0.119	0.0486
		Lake 8	10	0.219	0.106	0.453	0.0965	0.0305
		A44	8	0.229	0.148	0.389	0.0764	0.0270
		B03	30	0.144	0.0100	0.403	0.0672	0.0123

Table A3.2: ***Summary statistics for dry mercury concentration (mg/kg) in muscle rissue of Slimy Sculpin (Cottus cognatus; SLSC) and Ninespine Stickleback (Pungitius pungitius; NNST) collected at flooded (WTL, A63, A65, A20) and reference (LK8, B03, A44) lakes between 2018 to 2021. "n" = number of observations. "NA" = no data available. Shading indicates post-flooding years of the study.***

Fish Species	Year	Waterbody	n	Mean	Minimum	Maximum	Standard Deviaiton	Standard Error
NNST	2018	WTL	25	0.238	0.164	0.484	0.0747	NA
		A63	2	0.528	0.392	0.663	0.192	0.135
		A20	6	0.257	0.157	0.368	0.0835	0.0341
	2019	WTL	38	0.165	0.0850	0.293	0.0573	0.00929
		A63	37	0.218	0.158	0.305	0.0355	0.00584
		A65	49	0.205	0.123	0.590	0.0837	0.0120
		A20	36	0.194	0.0980	0.468	0.0748	0.0125
	2020	WTL	33	1.35	0.731	1.77	0.259	0.0451
		A63	34	1.60	0.963	2.57	0.401	0.0688
		A65	35	0.791	0.299	1.57	0.333	0.0562
		A20	35	0.740	0.218	2.32	0.423	0.0716
		A44	3	0.194	0.190	0.198	0.00425	0.00246
		B03	1	0.0826	0.0826	0.0826	NA	NA
	2021	WTL	15	1.96	1.05	4.00	0.764	0.197
		A63	16	2.20	1.30	3.42	0.637	0.159
		A65	3	1.63	0.900	2.56	0.852	0.492
		A20	19	1.05	0.644	2.16	0.430	0.0987
		A44	4	0.297	0.181	0.423	0.115	0.0573
		B03	9	0.169	0.107	0.274	0.0549	0.0183

Table A3.3: ***Lake-specific analyses of covariance (ANCOVA) results for the covariate δ¹⁵N ratios in Slimy Sculpin and Ninespine Stickleback fish tissue collected from flooded lakes between 2018 and 2021. FL = Fork Length, NA = not available.***

Variable	Ninespine Stickleback				Slimy Sculpin			
	Sum of Squares	Degrees of Freedom	F-Value	Pr(>F)	Sum of Squares	Degrees of Freedom	F-Value	Pr(>F)
A20								
(Intercept)	0.101587995	1	0.495696984	0.483255891	3.749482904	1	12.44113323	0.00078968
year	2.441784529	3	3.97154941	0.010512375	7.732984546	2	12.82938121	2.12E-05
$\log_{10}$(FL)	3.301186422	1	16.10808591	0.00012541	0.063515524	1	0.21075042	0.647759915
year:$\log_{10}$(FL)	2.371514916	3	3.857256262	0.012096371	7.275199054	2	12.06989377	3.65E-05
Residuals	18.0346943	88	NA	NA	18.98680921	63	NA	NA
A63								
(Intercept)	2.613337367	1	11.99713312	0.000854188	2.299838255	1	8.114420672	0.00600708
year	6.180722862	3	9.45801537	1.99E-05	3.3132202	2	5.844946362	0.004795121
$\log_{10}$(FL)	0.038652356	1	0.177442632	0.674695975	0.460441051	1	1.624554413	0.207372102
year:$\log_{10}$(FL)	5.300076616	3	8.110411551	8.68E-05	2.294918535	2	4.048531318	0.022422609
Residuals	17.64424256	81	NA	NA	17.00556341	60	NA	NA
A65								
(Intercept)	0.00367368	1	0.015239508	0.902061656	6.069110517	1	22.37420228	9.65E-06
year	2.901065535	2	6.017237387	0.003677714	11.97457929	3	14.71504259	1.06E-07
$\log_{10}$(FL)	0.012964989	1	0.053782595	0.817199533	6.402042539	1	23.60157957	5.89E-06
year:$\log_{10}$(FL)	2.975417507	2	6.171454332	0.003217048	NA	NA	NA	NA
Residuals	19.28503297	80	NA	NA	21.42913186	79	NA	NA
WTL								
(Intercept)	1.672089617	1	2.990629385	0.086686405	6.703641104	1	15.8226227	0.000117511
year	3.289878785	3	1.961379755	0.12430816	24.08339842	3	18.94803738	3.52E-10
$\log_{10}$(FL)	19.9689266	1	35.71558491	3.17E-08	6.501594598	1	15.34573177	0.000147001
Residuals	58.70650861	105	NA	NA	52.53563284	124	NA	NA

Table A3.4: Summary of pairwise difference contrasts for covariates of mercury concentrations in Slimy Sculpin (Cottus cognatus; SLSC) and Ninespine Stickleback (Pungitius pungitius; NNST). Flooded lakes include WTL, A63, A65, and A20. Reference lakes include A44, B03, and LK8.

Covariate	Fish Species	Exposure Type	Fork Length	Contrast Years		Estimate	Standard Error	Degrees of Freedom	T-Ratio	P-Value
Relative Condition	NNST	Flooded	50	2018	2019	-0.149	0.0674	13.4	-2.22	0.168
			50	2018	2020	0.0661	0.0710	16.5	0.930	0.789
			50	2018	2021	0.116	0.0752	18.7	1.55	0.430
			50	2019	2020	0.216	0.0595	13.4	3.62	0.0138
			50	2019	2021	0.266	0.0645	16.1	4.12	0.00393
			50	2020	2021	0.0504	0.0682	20.2	0.739	0.880
	SLSC		48	2018	2019	-0.0611	0.0598	11.16	-1.023	0.7401
			48	2018	2020	-0.0464	0.0529	8.18	-0.876	0.8169
			48	2018	2021	0.1724	0.0518	9.85	3.327	0.0332
			48	2019	2020	0.0148	0.0624	10.36	0.236	0.9951
			48	2019	2021	0.2335	0.0615	12.14	3.8	0.0115
			48	2020	2021	0.2188	0.0548	9.12	3.991	0.0134
	SLSC	Reference	48	2018	2019	0.0746	0.0522	208	1.43	0.4821
			48	2018	2020	0.0422	0.0476	208	0.887	0.8115
			48	2018	2021	0.1769	0.0504	208	3.511	0.0031
			48	2019	2020	-0.0324	0.0306	208	-1.058	0.7155
			48	2019	2021	0.1023	0.0348	208	2.936	0.0192
			48	2020	2021	0.1347	0.0275	208	4.899	<.0001
$\delta^{13}C$	SLSC	Flooded	48	2018	2019	2.03	0.624	7.78	3.249	0.0482
			48	2018	2020	4.68	0.564	5.82	8.309	0.0008
			48	2018	2021	4.91	0.531	6.73	9.261	0.0002
			48	2019	2020	2.66	0.678	7.21	3.917	0.0221
			48	2019	2021	2.89	0.633	8.13	4.563	0.0077
			48	2020	2021	0.23	0.585	6.6	0.393	0.9777

Table A3.4: Summary of pairwise difference contrasts for covariates of mercury concentrations in Slimy Sculpin (Cottus cognatus; SLSC) and Ninespine Stickleback (Pungitius pungitius; NNST). Flooded lakes include WTL, A63, A65, and A20. Reference lakes include A44, B03, and LK8.

Covariate	Fish Species	Exposure Type	Fork Length	Contrast Years		Estimate	Standard Error	Degrees of Freedom	T-Ratio	P-Value
δ13C	NNST	Flooded	50	2018	2019	1.81	0.559	10.21	3.239	0.0368
			50	2018	2020	5.43	0.588	12.63	9.232	<.0001
			50	2018	2021	3.61	0.605	13.80	5.976	0.0002
			50	2019	2020	3.62	0.474	9.71	7.648	0.0001
			50	2019	2021	1.80	0.51	12.09	3.535	0.0184
			50	2020	2021	-1.82	0.542	15.45	-3.355	0.0196
	SLSC	Reference	48	2018	2019	-2.033	1.43	4.16	-1.422	0.5473
			48	2018	2020	-1.239	1.188	4.46	-1.043	0.7358
			48	2018	2021	-0.260	1.21	4.76	-0.215	0.996
			48	2019	2020	0.794	1.127	3.62	0.704	0.8904
			48	2019	2021	1.773	1.151	3.89	1.541	0.4967
			48	2020	2021	0.979	0.831	4.2	1.178	0.668
C:N	SLSC	Flooded	48	2018	2019	-0.0409	0.142	11.06	-0.289	0.9912
			48	2018	2020	-0.231	0.121	7.85	-1.905	0.2995
			48	2018	2021	-0.2718	0.121	9.98	-2.242	0.1773
			48	2019	2020	-0.1901	0.147	10.09	-1.295	0.5861
			48	2019	2021	-0.2309	0.147	12.19	-1.573	0.428
			48	2020	2021	-0.0408	0.127	8.99	-0.321	0.9878
	NNST		50	2018	2019	-0.8775	0.17	13.6	-5.162	0.0008
			50	2018	2020	-0.8451	0.179	16.6	-4.731	0.0011
			50	2018	2021	-0.8923	0.186	18.7	-4.786	0.0007
			50	2019	2020	0.0325	0.15	13.4	0.217	0.9962
			50	2019	2021	-0.0148	0.159	15.9	-0.093	0.9997
			50	2020	2021	-0.0473	0.168	19.9	-0.281	0.992

Table A3.4: Summary of pairwise difference contrasts for covariates of mercury concentrations in Slimy Sculpin (Cottus cognatus; SLSC) and Ninespine Stickleback (Pungitius pungitius; NNST). Flooded lakes include WTL, A63, A65, and A20. Reference lakes include A44, B03, and LK8.

Covariate	Fish Species	Exposure Type	Fork Length	Contrast Years		Estimate	Standard Error	Degrees of Freedom	T-Ratio	P-Value
Age-at-Length	SLSC	Flooded	48	2018	2019	0.000104	0.0436	11.14	0.002	1
			48	2018	2020	0.018979	0.0385	8.15	0.493	0.9584
			48	2018	2021	0.150662	0.0377	9.85	3.995	0.0117
			48	2019	2020	0.018874	0.0455	10.34	0.415	0.975
			48	2019	2021	0.150558	0.0448	12.13	3.357	0.0251
			48	2020	2021	0.131683	0.0399	9.11	3.302	0.0376
		Reference	48	2018	2019	-0.0733	0.0392	131	-1.872	0.245
			48	2018	2020	-0.0267	0.029	187	-0.920	0.794
			48	2018	2021	0.1269	0.0362	187	3.509	0.0031
			48	2019	2020	0.0466	0.0269	164	1.733	0.310
			48	2019	2021	0.2002	0.0333	147	6.010	<.0001
			48	2020	2021	0.1536	0.0223	210	6.886	<.0001

Table A3.5: Summary of estimated marginal means for covariates of mercury concentrations in Slimy Sculpin (Cottus cognatus; SLSC) and Ninespine Stickleback (Pungitius pungitius; NNST). Flooded lakes include WTL, A63, A65, and A20. Reference lakes include A44, B03, and LK8.

Covariate	Fish Species	Exposure Type	Year	Fork Length	Estimated Marginal Mean	Standard Error	Degrees of Freedom	Lower Confidence Level	Upper Confidence Level
Relative Condition	NNST	Flooded	2018	50	1.03	0.055	16	0.916	1.15
			2019	50	1.18	0.0391	9.97	1.09	1.27
			2020	50	0.966	0.0449	17.4	0.871	1.06
			2021	50	0.916	0.0513	22.7	0.81	1.02
	SLSC		2018	48	1.078	0.0352	8.73	0.998	1.158
			2019	48	1.139	0.0483	12.94	1.035	1.244
			2020	48	1.124	0.0395	7.78	1.033	1.216
			2021	48	0.906	0.038	11.00	0.822	0.989
	SLSC	Reference	2018	48	1.022	0.045	208	0.933	1.11
			2019	48	0.947	0.0264	208	0.895	1.00
			2020	48	0.98	0.0155	208	0.949	1.01
			2021	48	0.845	0.0227	208	0.800	0.89
$\delta^{13}C$	SLSC	Flooded	2018	48	-21.8	0.981	3.61	-24.6	-18.9
			2019	48	-23.8	1.044	4.49	-26.6	-21.0
			2020	48	-26.5	1.008	3.97	-29.3	-23.7
			2021	48	-26.7	0.991	3.74	-29.5	-23.9
	NNST		2018	50	-24.6	0.622	8.82	-26.0	-23.2
			2019	50	-26.4	0.517	5.08	-27.7	-25.1
			2020	50	-30	0.549	6.47	-31.4	-28.7
			2021	50	-28.2	0.58	7.81	-29.6	-26.9
	SLSC	Reference	2018	48	-22.7	1.045	4.75	-25.5	-20.0
			2019	48	-20.7	0.976	3.61	-23.5	-17.9

Table A3.5: ***Summary of estimated marginal means for covariates of mercury concentrations in Slimy Sculpin (Cottus cognatus; SLSC) and Ninespine Stickleback (Pungitius pungitius; NNST). Flooded lakes include WTL, A63, A65, and A20. Reference lakes include A44, B03, and LK8.***

Covariate	Fish Species	Exposure Type	Year	Fork Length	Estimated Marginal Mean	Standard Error	Degrees of Freedom	Lower Confidence Level	Upper Confidence Level
$\delta^{13}C$	SLSC	Reference	2020	48	-21.5	0.564	3.64	-23.1	-19.9
			2021	48	-22.5	0.61	4.78	-24.1	-20.9
C:N	SLSC	Flooded	2018	48	4.72	0.0813	8.61	4.53	4.90
			2019	48	4.76	0.116	12.73	4.51	5.01
			2020	48	4.95	0.0900	7.3	4.74	5.16
			2021	48	4.99	0.0899	11.39	4.79	5.19
	NNST		2018	50	4.36	0.1384	16.3	4.07	4.66
			2019	50	5.24	0.0987	10.1	5.02	5.46
			2020	50	5.21	0.1129	17.2	4.97	5.45
			2021	50	5.26	0.1249	22.5	5.00	5.52
Age-at-Length	SLSC	Flooded	2018	48	1.001	0.118	8.7	0.75	1.288
			2019	48	1.001	0.1625	12.91	0.679	1.385
			2020	48	0.916	0.1266	7.75	0.643	1.233
			2021	48	0.415	0.0902	11.02	0.229	0.628
		Reference	2018	48	1.18	0.173	9.29	0.712	1.78
			2019	48	1.58	0.189	6.31	1.01	2.32
			2020	48	1.32	0.122	2.39	0.621	2.32
			2021	48	0.63	0.1	4.14	0.259	1.11